UNIVERSITÀ DEGLI STUDI DI CASSINO E
DEL LAZIO MERIDIONALE

Ph.D. course in
Methods, Models and Technologies for Engineering

Curriculum: Civil and Environmental Engineering

XXXIV cycle

Remediation of PAH-contaminated marine sediments through sustainable techniques

SSD: ICAR/03

Course Coordinator
Prof. Fabrizio Marignetti

Ph.D. Student
Francesco Bianco

Supervisors
Prof. Marco Race
Prof. Giovanni Esposito

ACKNOWLEDGEMENTS

This doctoral scholarship was co–funded by the Italian Ministry of University and Research (MUR) and the Erasmus Mundus Joint Doctorate Program ETeCoS^3 (Environmental Technologies for Contaminated Solids, Soils, and Sediments) [grant agreement FPA number 2010–0009].

ABSTRACT

The issue of polycyclic aromatic hydrocarbons (PAHs) is widespread in marine environments involving ecological systems and human health. At the same time, research on eco–friendly alternatives for the treatment of PAH–contaminated marine sediments and their reuse after remediation must be stepped up. For this purpose, this doctoral thesis firstly examined technical, economic and energy aspects to evaluate the most sustainable technology for removing phenanthrene (PHE) from marine sediments. Anaerobic bioremediation, sediment washing (SW) and thermal desorption were conducted under low liquid phase (i.e. 60% and solid–to–liquid ratio of 1:3) and low temperature (i.e. 200°C), whose resulted in a PHE removal of 68, 97 and 88%, respectively. On the other hand, the bioremediation exhibited the lowest cost (i.e. 228 €·m^{-3}) and a similar energy input (i.e. 16 kWh·m^{-3}) to SW due to a significant energy gain from the biogas produced during anaerobic digestion.

Therefore, the use of digestate and organic fraction of municipal solid waste (OFMSW) was subsequently proposed as novel biostimulation amendments for improving the anaerobic bioremediation. A nutrient solution was also supplemented in some experiments to enhance the biostimulation yields. The simultaneous addition of OFMSW and nutrients increased the total PAH removal up to 55% and led to the highest biohydrogen and biomethane production of 80 and 140 mL·g VS^{-1}, respectively, indicating that bioenergy can be further recovered during PAH degradation by enhancing the sustainability of the entire process.

Afterwards, the present thesis work focused on the treatment of spent SW solutions, since SW has proven to be the most effective remediation approach for PAH–polluted sediments, but still raises waste handling concerns due to a considerable amount of effluents generated downstream of the SW process. The biological treatment of a PHE– and ethanol (EtOH)–containing spent SW solution was initially investigated as a highly–efficient, inexpensive and environmentally–friendly strategy. The experimental activity was conducted in a fed–batch bioreactor by evaluating several PHE concentrations (i.e. 20–140 mg·L^{-1}) within six successive cycles under aerobic conditions. A PHE biodegradation up to 91% following a first–order kinetic model was achieved by an enriched PHE–degrading consortium mainly composed of

Proteobacteria and *Bacteroidota* phyla, after a proper supplementation of nutrients (i.e. nitrogen and phosphorous). A techno–economic evaluation was carried out particularly considering EtOH recovery as a resource to be reused in SW treatment units, thus reducing the total cost of the whole remediation process by approximately 50%.

Finally, this thesis assessed both the PHE desorption from sediments using Tween® 80 (TW80) as extracting agent and the treatment of the resulting spent SW solution in a novel biochar (BC) immobilized–cell bioreactor. The SW process reached a PHE removal of up to about 91% using a surfactant solution containing 10,800 $mg \cdot L^{-1}$ of TW80, and the generated amount of spent PHE–polluted SW solution can be controlled by keeping a solid to liquid ratio up to 1:4. A PHE degradation of up to 96% was subsequently achieved after 43 days of continuous reactor operation, aerobically treating the TW80 solution with a hydraulic retention time of 3.5 days. *Brevundimonas*, *Chryseobacterium*, *Dysgonomonas*, *Nubsella*, and both uncultured *Weeksellaceae* and *Xanthobacteraceae* genera were mainly involved in PHE biodegradation. A rough economic study showed a total cost of 342.60 $€ \cdot ton^{-1}$ of sediment, including the SW operations, TW80 and BC supply and the biological treatment of the SW solution.

TABLE OF CONTENTS

LIST OF FIGURES

LIST OF TABLES

INTRODUCTION

Polycyclic aromatic hydrocarbons (PAHs) are recognized as priority pollutants by several organizations such as the US Environmental Protection Agency (US EPA) and International Agency for Research on Cancer (IARC) due to their toxic, carcinogenic, genotoxic, mutagenic, teratogenic and recalcitrant properties [1–4]. Pyrogenic (e.g. industrial activities, fires, volcanic eruptions) and petrogenic (e.g. crude oil seepage, biomass decomposition) processes are the main PAH emission sources [5]. Pyrogenic PAHs can be adsorbed onto atmospheric particulate matter and subsequently enter into water bodies after their deposition, whereas petrogenic PAHs can be instantly released into the environment [6].

Afterwards, PAHs can accumulate into environmental sinks such as sediments by persisting over time due to their recalcitrant properties and, for such reason, PAHs are considered persistent organic pollutants [7,8]. Also, the presence of organic matter in the sediments can even increase PAH persistence in the aquatic ecosystem, in which the adsorption mechanism can be guided by the attractive forces of van der Waals, intermolecular interactions and exchange of electrical charges by limiting the natural attenuation phenomena [9]. Indeed, natural transformation processes such as photo–oxidation and abiotic degradation are not adequate to contain this type of pollution.

Thus, PAH concentrations are significant in marine sediments and can reach an average of 200 mg kg^{-1} in industrialized and densely populated areas [10]. Since sediment dredging is needed to facilitate the navigation of deep hull ships, the large amount of adsorbed PAHs onto sediments raises waste management concerns [11]. A remediation process is, therefore, necessary to limit PAH pollution and its harmful effects on the environment and humans by encouraging the reuse of remediated sediments following the national legislations. Thus, several technologies, i.e. thermal, biological and physical–chemical, can be employed to remediate polluted matrices [12].

Thermal treatments such as thermal desorption can be affordable to perform quick sediment remediation with a high PAH removal efficiency [13]. Thermal desorption consists in the use of temperature up to 600 °C to allow PAH desorption from contaminated sediments with the following treatment of gas stream through

destructive or recovery strategies [14]. However, the presence of pollutants characterized by a high–boiling point such as is coupled with the increase of energy required for thermal desorption. Thus, a low–temperature thermal desorption (i.e. 200 °C) has been here evaluated also aimed at avoiding the PAH isomerization phenomenon (i.e. the release of more reactive compounds) [15]. Notwithstanding, plant growth and microbial population can significantly change in thermally–treated sediments compared to the untreated matrix.

Bioremediation is an environmental–friendly solution involving microorganisms to biologically degrade PAHs from polluted sediments [16]. Bioremediation can take place via biostimulation when organic amendments (e.g. compost) or nutrients (e.g. nitrogen, phosphorus) are added to the sediment to enhance PAH degradation [17]. Bioaugmentation can be alternatively performed by inoculating engineered autochthonous or allochthonous bacteria (e.g. *Pseudomonas* and *Rhodococcus* strains) to the contaminated sediment to improve PAH removal [18]. Biostimulation and bioaugmentation techniques have largely been employed under aerobic conditions for remediating PAH–containing sediments [19] and alternatively been carried out under anaerobic and anoxic conditions in the present work by comparing methanogenic, nitrate– and sulfate–reducing conditions in order to evaluate the possibility of producing bioenergy (e.g. biomethane) during bioremediation. Also, digestate and the organic fraction of municipal solid waste have been used in this work for the first time as extra–organic and microbial sources to remediate PAH–contaminated marine sediments. However, PAH bioavailability, which indicates the PAH portion available for biological transformation, can represent a limiting factor for sediment bioremediation [20].

Physical–chemical technologies can cope with this issue by also acting on the non–bioavailable fraction of PAHs. Among the physical–chemical approaches, sediment washing represents a well–established technique due to its operational simpleness, cheapness and high effectiveness [21]. Sediment washing consists in the employment of extracting agents (e.g. solvents, surfactants) to enhance PAH desorption from the solid matrix to the aqueous phase by decreasing their octanol–water partition coefficient [22]. The effectiveness of various extracting agents such as acetone, 1–pentanol and 2–propanol has been ascertained for PAH desorption during sediment washing [23]. Thus, the deployment of green solvents such as ethanol has been proposed as an attractive alternative to the mentioned solvents, being tolerable for microorganisms present in the sediment [24]. Also, the application of non–ionic surfactants, such as Tween® 80 (TW80), as extracting agents has proven to be an

economic alternative to anionic and cationic surfactants to enhance PAH desorption from soils [25], but has scarcely been examined for sediments. Notwithstanding, low surfactant amounts can be not effective for a complete PAH desorption from the sediment [26] and, therefore, this thesis has emphasized the evaluation of influencing parameters (e.g. TW80 concentration, solid–to–liquid ratio). However, the generation of a considerable amount of spent sediment washing effluents requires further treatment efforts and can limit the use of the sediment washing process.

Among the different technologies available for the treatment of spent sediment washing solutions, biological processes can represent the most cost–effective and eco–friendly approaches [27]. The microbial metabolism can be influenced by several parameters such as PAH concentration, the type of washing agent, the presence of nutrients, the dissolved oxygen level, pH and temperature [16]. The bioreactor configuration can affect PAH removal efficiency as well. So far, PAH biodegradation from sediment washing solutions has largely been investigated in batch flasks, whereas both fed–batch and continuous–flow bioreactor operations here proposed have more considerable margins for interesting scientific implications. Also, the use of immobilized–cell bioreactors can improve the microbial retention developing a biofilm onto supporting media, thus decreasing the hydraulic retention times rather than in suspended–cell bioreactors [28]. The choice of the most appropriate carrier for cell immobilization can play a major role for a proper bioreactor functioning. In this context, the use of carbonaceous amendments (e.g. active carbon) as biocarriers for microbial immobilization in bioreactors treating hydrocarbons–containing streams was previously reported [29]. Specifically, biochar has been proposed in this work as a novel and sustainable biocarrier for cell immobilization being a porous biomaterial rich in nutrients when produced at a pyrolysis temperature below 500 °C.

Also, the application of biochar as an amendment directly in the sediment gives rise to other environmental consequences in a perspective of a circular economy, being biochar thermochemically obtained from pyrolysis of substances regarded as wastes. Previous studies demonstrated the efficiency, cost–effectiveness and eco–friendliness of biochar for treating PAH–polluted solid matrices mainly through adsorption mechanism mostly due to a high carbon content and specific surface area of the adsorbent [30–32]. Thus, biochar can cope with the mentioned drawbacks shown by other remediation techniques. However, the previous reviews did not shed light on the addition of biochar to sediment contaminated by PAHs. Therefore, the existing state of understanding regarding the deployment of biochar for remediating PAH–polluted

sediments was reviewed during the pandemic due to the impossibility to perform lab experiments.

This Ph.D. thesis is composed of six chapters including a preliminary bibliographic study, four research chapters and a literature review chapter followed by a final section addressed to conclusive remarks and future perspectives. The structure of the present thesis is reported as follows:

- chapter 1 is an overview of the literature, focusing on the problem statement of PAH–contaminated marine sediments and the knowledge of available remediation technologies to shed light on what scientific literature lacks;
- chapter 2 compares performances, costs and energy balance of bioremediation under anaerobic and anoxic conditions, sediment washing by using ethanol as a washing agent, and low–temperature thermal desorption as ex–situ techniques for remediating marine sediments contaminated by phenanthrene, here used as the model PAH compound;
- chapter 3 investigates the effect of the addition of digestate and the organic fraction of municipal solid waste on sediment biostimulation by assessing the evolution of total and bioavailable PAH concentrations (i.e. phenanthrene, anthracene, fluoranthene and pyrene) under methanogenic conditions, which have been proven to be particularly cost–effective in the previous chapter due to biogas production aimed at energy recovering;
- chapter 4 evaluates the biological treatment of ethanol– and phenanthrene–containing washing solution, which simulates the results of sediment washing showed in chapter 2, in a fed–batch reactor under aerobic conditions by monitoring the effects of operating parameters such as dissolved organic carbon, nutrients, oxygen level and pH. A techno–economic assessment particularly focused on ethanol recovery for its reuse as a washing agent is carried out as well;
- chapter 5 assess the desorption of phenanthrene from marine sediments using TW80 as extracting agent and the biodegradation of the obtained spent sediment washing solution in a biochar immobilized–cell reactor operated in both batch and continuous–flow modes. The application of biochar for microbial immobilization was identified as a lack of scientific literature after the literature review activity reported in chapter 5. Also, the dominant PHE–degrading bacterial families and genera throughout the bioreactor operation ere determined. A preliminary economic evaluation of the whole

process was carried out to evaluate its possible employment in full–scale applications;

- chapter 6 mainly discusses the mechanisms involved during adsorption, bioremediation, and enhanced persulfate degradation of biochar–amended PAH–polluted sediments through a literature overview;
- a conclusion section highlights the main findings of this doctoral thesis and discusses their relevance to existing literature. Recommendations for future studies are expressed in this chapter.

CHAPTER 1. STATE OF ART

1.1 General properties of PAHs

Polycyclic aromatic hydrocarbons (PAHs) are organic compounds consisting of two or more benzene rings settled in linear, angular, or cluster chains (Figure 1.1). The basic element is the benzene ring, which presents delocalized electrons π that alternate with individual and double bonds. This configuration makes the molecules more chemically stable, and therefore the polarity and the ability to cleave the bonds is reduced [33]. PAHs are listed as low molecular weight (LMW) and high molecular weight (HMW) compounds when formed by 2 or 3 benzene rings (e.g. naphthalene) and more than 3 benzene rings (e.g. benzo[a]pyrene) (Figure 1.1) [34], respectively. US–EPA has recognized 28 PAHs as priority pollutants considering their characteristics of carcinogenicity and toxicity by also including benzo[a]anthracene, benzo[b]fluoranthene, benzo[k]fluoranthene, chrysene, dibenzo[a]anthracene and indeno[1,2,3–c,d]pyrene (Table 1.1) [35].

1.1.1 Physical–chemical properties of PAHs

PAHs show as up colorless, white or yellow–green solids with a pleasant odor [36]. Although their reactivity to electrophilic replacement and oxidation–reduction reactions is influenced by the number of benzene rings and the position of carbon atoms, PAHs can be chemically classified as relatively stable compounds [12,37,38]. In general, PAHs are characterized by low solubility in water (i.e. 0.001–30 $mg \cdot L^{-1}$), high lipophilicity, high boiling (i.e. 100–500 °C) and melting points (i.e. 100–300 °C), and low vapor pressure (i.e. $6.4 \cdot 10^{-12}$–0.085 mm Hg) (Table 1.1). These properties are more pronounced with the increase of PAH molecular weight [3,39].

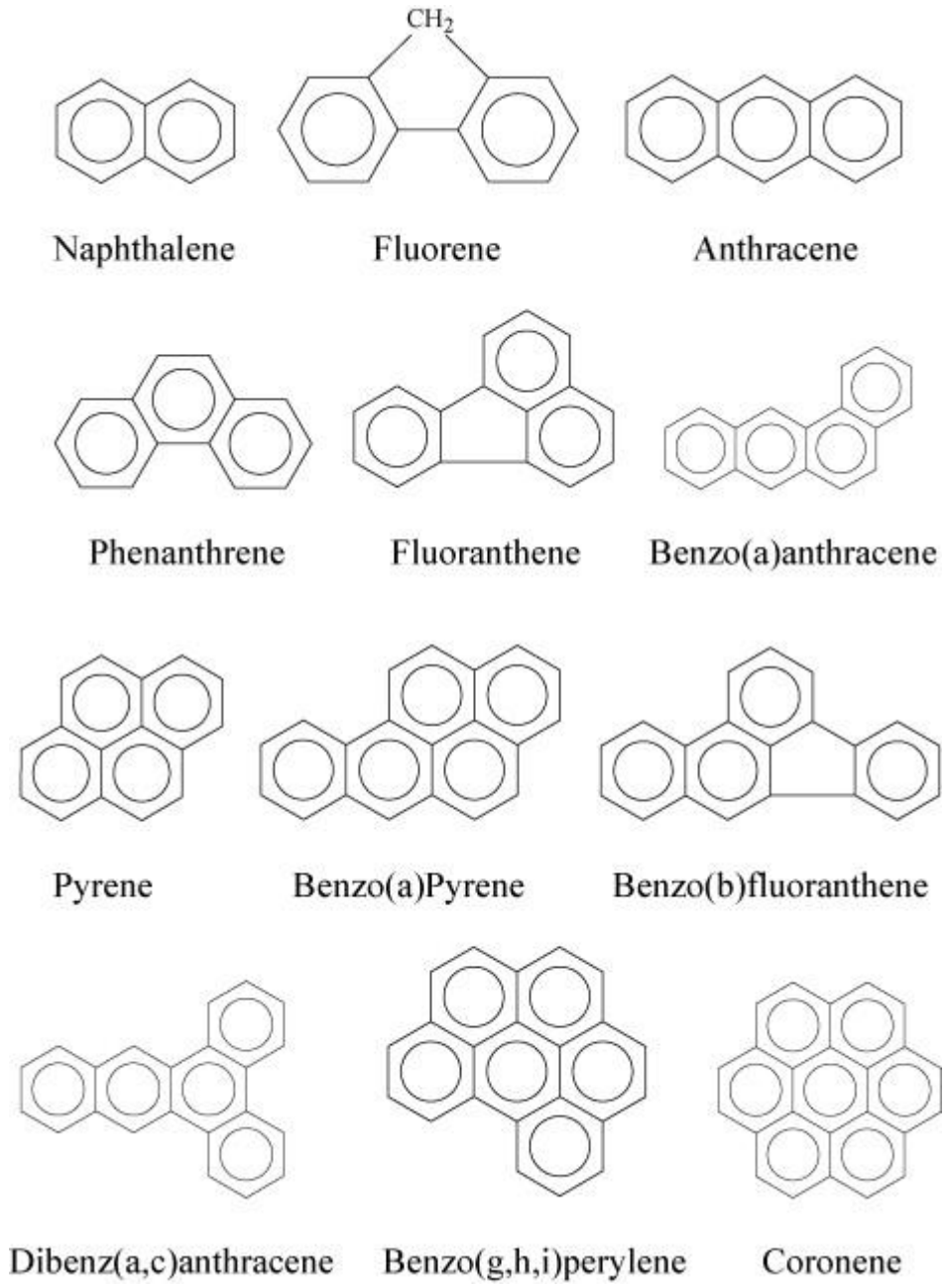

Figure 1.1 – Chemical structure of main polycyclic aromatic hydrocarbons. The figure is taken from Haritash and Kaushik [40].

Table 1.1 – Physical–chemical properties of the 28 priority polycyclic aromatic hydrocarbons [4].

Compounds	Number of rings	Molecular weight [g·mol^{-1}]	Melting point [°C]	Aqueous solubility [mg·L^{-1}]*	Vapor pressure [mm Hg]*
Naphthalene	2	128.174	80	31	0.085
Acenaphthene	3	154.212	93	3.57–3.93	0.0022
Acenaphthylene	3	152.196	89.4	3.93	0.0048
Anthracene	3	178.234	216	0.04	$6.56 \cdot 10^{-6}$
Fluorene	3	166.218	114.8	1.69	$6 \cdot 10^{-4}$
Phenanthrene	3	178.234	99	1.1	$1.21 \cdot 10^{-4}$
Fluoranthene	4	202.25	110.2	0.2–0.26	$9.22 \cdot 10^{-6}$
Pyrene	4	202.25	150.6	0.135	$4.5 \cdot 10^{-6}$
Chrysene/ benzo[a]phenanthrene	4	228.294	255	$2.0 \cdot 10^{-3}$	$6.23 \cdot 10^{-9}$
7,12–Dimethyilbenz[a]anthracene	4	256.348	123	0.061	$6.8 \cdot 10^{-7}$
5–Methylchrysene	4	242.321	117.5	0.062	$5.45 \cdot 10^{-7}$
Benzo[a]pyrene	5	252.309	179	$1.62 \cdot 10^{-3}$	$5.49 \cdot 10^{-9}$
Benzo[j]fluoranthene	5	252.306	165.2	$2.5 \cdot 10^{-9}$	$2.7 \cdot 10^{-8}$
Benzo[a]anthracene	5	252.316	155	$9.4 \cdot 10^{-3}$	$2.1 \cdot 10^{-7}$
Benzo[b]fluoranthene	5	278.354	168.4	0.0015	$5.0 \cdot 10^{-7}$
Benzo[k]fluoranthene	5	252.316	217	0.00076	$9.65 \cdot 10^{-10}$
Dibenz[a,h]anthracene	5	279.342	268	0.00166	$9.55 \cdot 10^{-10}$
Dibenz[a,h]acridine	5	279.342	228	0.159	$7.51 \cdot 10^{-10}$
Dibenz[a,j]acridine	5	279.342	216	0.159	$1.05 \cdot 10^{-9}$
7H–Dibenzo[e,g]carbazole	5	267.331	158	NA	$3.4 \cdot 10^{-9}$
3–Methylcholanthrene	5	268.359	178	$2.8 \cdot 10^{-3}$	$4.3 \cdot 10^{-8}$
Benzo[r,s,t]penaphene	6	302.376	283.6	$7.4 \cdot 10^{-5}$	$1.8 \cdot 10^{-11}$
Dibenzo[a,e]fluoranthene	6	302.368	232	$2.12 \cdot 10^{-4}$	$7.33 \cdot 10^{-11}$
Dibenzo[a,e]pyrene	6	302.368	244.4	$1.6 \cdot 10^{-4}$	$5.2 \cdot 10^{-11}$
Dibenzo[a,h]pyrene	6	302.368	318	$3.5 \cdot 10^{-5}$	$6.4 \cdot 10^{-12}$
Dibenzo[a,l]pyrene	6	302.368	283.6	$7.5 \cdot 10^{-5}$	$2.17 \cdot 10^{-8}$
Indeno[1,2,3–cd]pyrene	6	276.338	164	$6.2 \cdot 10^{-2}$	$1.25 \cdot 10^{-10}$
Benzo[g,h,i]perylene	6	276.338	278.3	$2.6 \cdot 10^{-4}$	$1.0 \cdot 10^{-10}$

NA = not available; * = at 25°C.

The number of benzene rings also affects the hydrophobicity of the PAHs. For example, LMWs are more soluble and volatile compared to HWMs (Table 1.1) [41]. In addition, in the presence of ions in water, the solubility of PAHs is further reduced through the "salting out" effect that is determined by the constant K_s. The "salting out" effect between the organic compound solubility and salt concentration is defined by the empirical relationship as follows:

$$K_s \cdot [salt]_t = log\left(\frac{[C_o]}{[C_{salt}]}\right) \quad \text{(Eq. 1.1)}$$

where Ks ($L \cdot mol^{-1}$ or $kg \cdot mol^{-1}$) is the salting or Setshenow constant, $[salt]_t$ ($mol \cdot L^{-1}$ or $mol \cdot kg^{-1}$) is the concentration of ionic salts, C_0 ($mol \cdot L^{-1}$) is the solubility of PAHs in distilled water and C_{salt} ($mol \cdot L^{-1}$) is the solubility of PAHs in a solution of ionic salts. Therefore, the salting effect is important for the marine environment by influencing the fate and distribution of PAHs in the water systems since the compound hydrophilicity is directly proportional to the constant Ks [42].

However, PAHs are characterized by a high hydrophobicity, which allows their solubilization to organic solvents, and this property is measured with the octanol–water partition ($K_{o/w}$) constant. Octanol is an organic solvent with similar behavior to organic matter, and the partition constant is expressed on a logarithmic basis as follows:

$$log\ K_{o/w} = log \frac{[S_O]}{[S_W]} \quad \text{(Eq. 1.2)}$$

$K_{o/w}$ is the partition constants octanol–water, S_O is the concentration of a solute in a water–saturated octanol phase, S_W is the same concentration in the water phase [43]. Thus, the log $K_{o/w}$, which values are comprised between 3.37 and 6.50 (Table 1.2) for naphthalene and indeno[1,2,3–cd]pyrene, respectively, is inversely proportional to the solubility of PAHs (Table 1.1) [44].

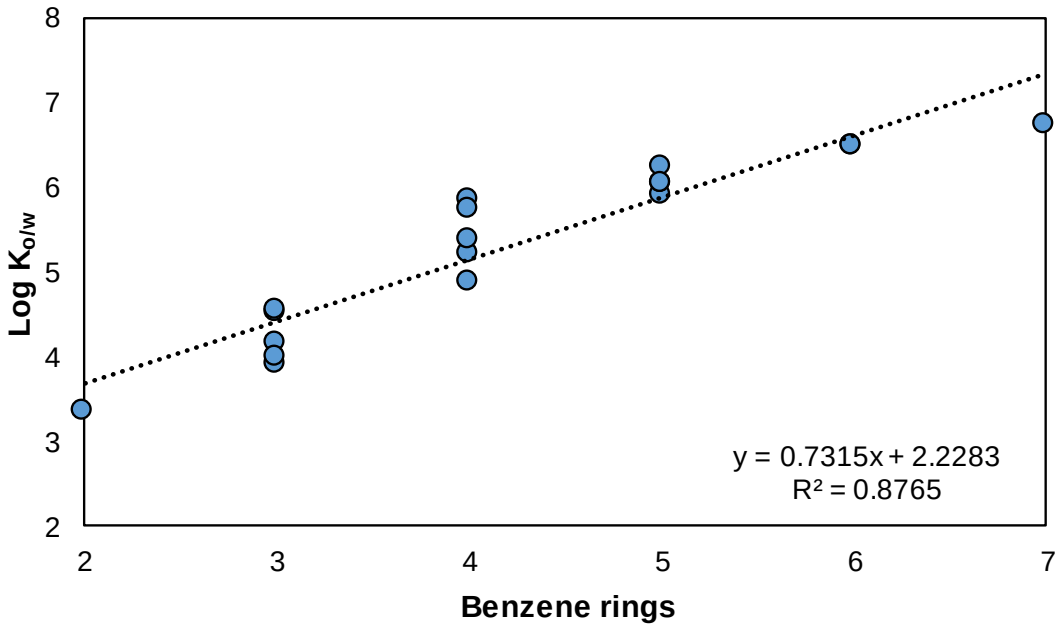

Figure 1.2 – Number of benzene rings vs octanol–water ($K_{o/w}$) constant for polycyclic aromatic hydrocarbons.

Table 1.2 – Octanol–water partition coefficients (log $K_{o/w}$) and Henry's law constant (H) for PAHs and their derivate [44,45].

Compounds	CAS No.	log $K_{o/w}$	*H* [kPa·m^3·mol^{-1}]
Naphthalene	91–20–3	3.37	$4.89 \cdot 10^{-2}$
Anthracene	120–12–7	4.54	$7.30 \cdot 10^{-2}$
Phenanthrene	85–01–8	4.57	$3.98 \cdot 10^{-3}$
Chrysene	218–01–9	5.86	$1.22 \cdot 10^{-5}$
Benz[a]anthracene	56–55–3	5.91	NA
Benzo[a]pyrene	50–32–8	6.04	$3.4 \cdot 10^{-5}$
Acenaphthene	83–32–9	3.92	$1.48 \cdot 10^{-2}$
Fluorene	86–73–7	4.18	$1.01 \cdot 10^{-2}$
Fluoranthene	206–44–0	5.22	$6.5 \cdot 10^{-4}$
Benzo[a]fluorene	238–84–6	5.40	NA
Triphenylene	217–59–4	5.49	NA
Perylene	198–55–0	6.25	$3.00 \cdot 10^{-6}$
1–Methylnaphthalene	90–12–0	3.87	$4.49 \cdot 10^{-2}$
2–Methylnaphthalene	91–57–6	3.86	NA
9–Methylanthracene	779–02–2	5.07	NA
Benzo[b]fluorene	243–17–4	5.75	NA
Benzo[g,h,i]perylene	191–24–2	6.50	$2.70 \cdot 10^{-5}$
Coronene	191–07–1	6.75	NA
Acenaphthylene	208–96–8	4.00	$1.14 \cdot 10^{-3}$
1–Ethylnaphthalene	1127–76–0	4.39	NA
Pyrene	129–00–0	4.88	$1.10 \cdot 10^{-3}$
Naphthacene	92–24–0	5.90	NA
Benzo[b]fluoranthene	205–99–2	6.06	$5.10 \cdot 10^{-5}$
Indeno[1,2,3–c,d]pyrene	193–39–5	6.50	$2.90 \cdot 10^{-5}$

NA = not available; PAHs = polycyclic aromatic hydrocarbons.

In addition, PAH lipophilicity can be positively correlated to the benzene rings of PAHs by a linear regression ($R^2 = 0.88$) between the octanol–water partition constants with and benzene ring number ($y = 0.73x + 2.23$, Figure 1.2), as also showed by Sahu and Pandit [46]. The octanol–water distribution constant inevitably affects the biological and chemical transformations, the distribution of PAHs in the environment, and the mechanisms of adsorption and bioaccumulation. Indeed, PAHs with high log $K_{o/w}$ values (i.e. 5–7) can be easily adsorbed onto sediment particles or bioaccumulated by biota. On the contrary, low log $K_{o/w}$ values (i.e.<5) can enhanced of the transportation phenomena of PAHs [47–49]. These properties are essential for

understanding the different transportation and distribution mechanisms of PAHs into the various ecosystems.

1.1.2 PAH effects on human health

PAHs can exhibit toxic, genotoxic, teratogenic, mutagenic and carcinogenic effects [2,50–53], and therefore, the United States Environmental Protection Agency (US EPA) identified 28 PAHs as priority pollutants in 2008 [54]. Also, the International Agency for Research on Cancer (IARC) recognized some PAHs as possible or likely carcinogens in different groups (Table 1.3) [55]. Indeed, in group 1 are included PAHs considered carcinogenic to humans, group 2A comprises PAHs probably carcinogenic to humans, group 2B groups those possible carcinogenic to humans and in group 3 not classifiable PAHs due to poor evidence about the carcinogenicity to humans [55–57] (Table 1.3).

The 3 main pathways of PAH exposure to humans are inhalation, ingestion and skin contact [58]. For example, due to their lipophilic properties, PAHs can be quickly absorbed by the human body through the gastrointestinal system after the ingestion and subsequently distributed to fatty organs and tissues such as the liver and colon prior to being eventually secreted by urine or feces. Once entering in the human body, PAHs can show their carcinogenicity when are metabolically activated by enzymes such as cytochrome P450 and epoxide hydrolase, which lead to the production of reaction intermediates with carcinogenic properties (i.e. cyclic ethers) after the oxidation of the π–bond of carbon–carbon in the aromatic system (Figure 1.3) [59]. Thus, the living organisms can metabolize the polar compounds (i.e. PAHs) into more hydrosoluble substances, which can be further metabolized. During the metabolization process, the reaction intermediates can interact with biological macromolecules (i.e. DNA, RNA) causing alterations and mutations in the genetic material [60]. Although not all PAHs can generate mutations and carcinomas, those with obvious carcinogenic properties are formed by 5 benzene rings at least such as benzo[a]pyrene (Table 1.3) [61,62].

Table 1.3 − Polycyclic aromatic hydrocarbon (PAH) classification by International Agency for Research on Cancer (IARC) [55–57] *and the toxic equivalent factor (TEF) of PAHs* [63].

PAHs	IARC group	*TEF*
Naphthalene	2B[b]	0.001
Acenaphthene	3[c]	0.001
Acenaphthylene	NA	0.001
Anthracene	3	0.01
Fluorene	3	0.001
Phenanthrene	3	0.001
Fluoranthene	3	0.001
Pyrene	3	0.001
Chrysene	2B	0.001
7,12–Dimethyilbenz(a)anthracene	NA	NA
5–Methylchrysene	2B	NA
Benzo(a)pyrene	1[a]	1
Benzo(j)fluoranthene	2B	NA
Benzo(a)anthracene	2B	1
Benzo(b)fluoranthene	2B	0.1
Benzo(k)fluoranthene	2B	0.1
Dibenz(a,h)anthracene	2A	1
Dibenz(a,h)acridine	2B	NA
Dibenz(a,j)acridine	2B	NA
7H–Dibenzo(e,g)carbazole	2B	NA
3–Methylcholanthrene	NA	NA
Benzo(r,s,t)penaphene	2B	NA
Dibenzo(a,e)fluoranthene	3	NA
Dibenzo(a,e)pyrene	3	NA
Dibenzo(a,h)pyrene	2B	NA
Dibenzo(a,l)pyrene	3	NA
Indeno(1,2,3–cd)pyrene	2B	0.1
Benzo(g,h,i)perylene	3	0.01

a = carcinogenic group; b = probably carcinogenic; c = not classified; NA = not available.

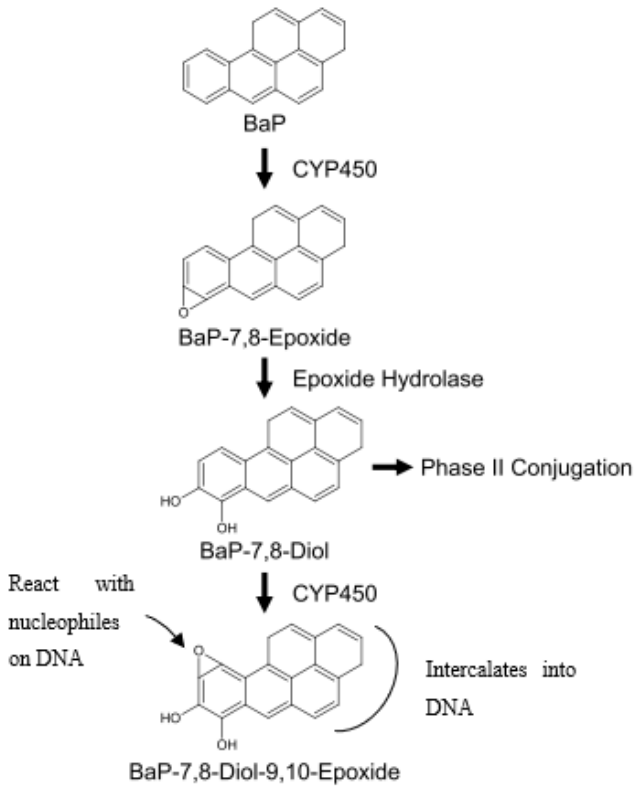

Figure 1.3 − Schematic pathway of benzo[a]pyrene metabolic activation. The figure is taken from Obach and Kalgutkar [64].

Therefore, the potential toxicity of PAHs in sediments can be assessed by considering the main carcinogenic PAH (i.e. benzo[a]pyrene). Indeed, in–situ PAH toxicity can be compared to that shown by the benzo[a]pyrene as the equivalent toxicity calculated through the following equation [63,65]:

$$TEQ = \Sigma Ci \times TEFi \qquad \text{(Eq. 1.3)}$$

where TEQ is the toxic equivalent quotient; Ci is the concentration of the individual PAH and $TEFi$ is the toxic equivalent factor related to the benzo[a]pyrene (Table 1.3). After defining the PAH toxicity, a site–specific risk analysis can be performed to assess the risk coupled with a contaminated site, by identifying actions and objectives to be achieved in order to protect human health and the environment [66].

1.2 PAH sources and environmental pathways

1.2.1 Pyrogenic and petrogenic sources

PAHs are mainly produced by pyrogenic and petrogenic processes [67]. Pyrogenic PAHs are formed by incomplete combustion or pyrolysis of the organic matter at temperatures ranging from 350 to 1,200 °C [53,65]. High temperatures lead to the break of carbon–carbon and carbon–hydrogen bonds and the formation of free radicals that can react with acetylene to form aromatic structures (Figure 1.4) [68]. These processes can occur during human or industrial activities (e.g. biomass heating systems, coal combustion, asphalt laying, vehicular emissions), and natural events (e.g. forest fires). Some pyrogenic PAHs are pyrene, benzo[a]pyrene, dibenzo[a, l]pyrene, tetraphene, dibenzo[a, h]anthracene and benzo[ghi]perylene [69,70]. Pyrogenic PAHs are generally found in areas surrounding industrial and coastal areas [71] since they have a tendency towards the accumulation in the sediment due to hydrophobic characteristics (see Section 1.1.1). Also, pyrogenic PAHs can remain in the sediment for a longer time being more recalcitrant rather than petrogenic PAHs [70].

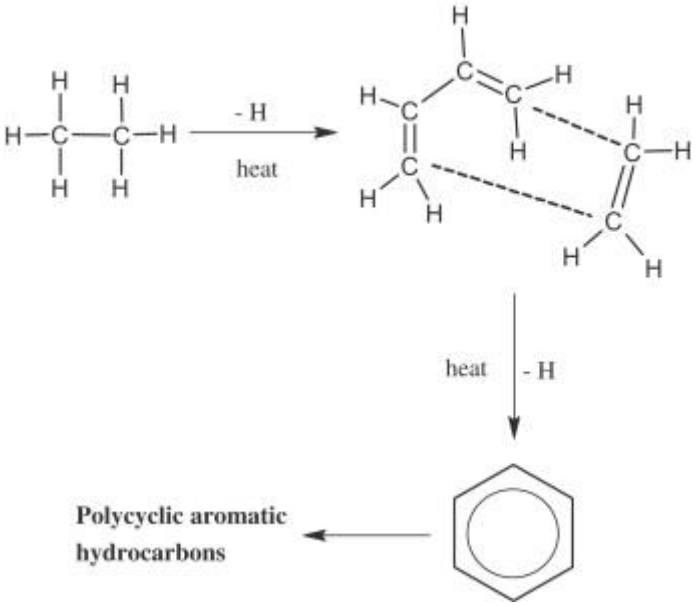

Figure 1.4 – Mechanism of formation of polycyclic aromatic hydrocarbons starting from ethane. The figure is taken from Ravindra et al. [68].

Petrogenic PAHs are generated by the decomposition of the organic matter at low temperatures (i.e. 100–150 °C) and geological formation times [53]. Some sources of petrogenic PAHs are the transport and storage activities of oil, lubricating oils, motor

oil, vehicle fuels, refinery products and oil spills. Petrogenic PAHs consist of 2–4 benzene rings including naphthalene, anthracene, phenanthrene and chrysene (Figure 1.1 and Table 1.1) [69].

A diagnostic method based on the ratio of contaminants found in the area of interest can be used to differentiate the origin of PAHs since it has been tested that the relationship between contaminants with similar molar mass is also characterized by comparable chemical–physical properties (Table 1.1 and 1.2) [72]. Several ratios such as phenanthrene/anthracene, fluoranthene/pyrene and benzo[a]anthracene/chrysene are used as markers to indicate the origin of petrogenic PAHs (Table 1.4) [73–75]. Since petroleum is composed of a higher phenanthrene concentration compared to anthracene, is also thermodynamically more stable than its isomer, thus a phenanthrene/anthracene ratio higher than 15 (Table 1.4) indicates a petrogenic pollution, whereas a ratio of lower than 10 (Table 1.4) indicates pyrogenic source.

Table 1.4 – Polycyclic aromatic hydrocarbon (PAH) ratios used to identify the PAH source [76].

PAH ratios	**Pyrogenic**	**Petrogenic**
PHE/ANT	<10	>15
FLU/PYR	>1	<1
BaA/CHR	<2	>2
ANT/(ANT+PHE)	>0.1	<0.1
FLU/(FLU+PYR)	>0.5	<0.4
BaA/(BaA+CHR)	>0.35	<0.2
BaP/(BaP+CHR)	>0.3	<0.3
Σ LMW/Σ HMW PAHs	<1	>1

PHE = Phenanthrene; ANT = anthracene; FLU = fluoranthene; PYR = pyrene; BaA = benzo[a]anthracene; CHR = chrysene; BaP = benzo[a]pyrene; LMW = Low molecular weight; HMW = High molecular weight.

In addition to the abovementioned sources, PAH can be generated from biological sources, i.e. from processes of biotransformation, biodegradation, synthesis and accumulation by bacteria, fungi, phytoplankton, algae and plants. Naphthalene and perylene are an example of PAHs that belong to this group [67].

1.2.2 PAHs in the environment

PAHs are ubiquitous in the environment since their presence in the atmosphere, freshwater and marine aquifer systems, soils and sediments. The interactions between the environment and flora or fauna can proceed through various natural transformations such as volatilization, photo–oxidation, bioaccumulation, adsorption and biodegradation (Figure 1.4) [69]. The chemical composition is not altered during PAH transfer processes such as the volatilization, which is regulated by Henry's law that show how substances with a higher Henry's coefficient (H) can better volatilize than compounds with a lower H (Table 1.2) [77]. On the contrary, the chemical and biological degradation (Figure 1.5) alter the PAH chemical structure by transforming PAHs to intermediates metabolites until their eventual total removal. Notwithstanding, PAH degradation rates due to natural attenuation is low and decrease with the increase of PAH molecular weight. For instance, LMW PAHs can be easily removed in the soil after atmospheric deposition through a biological process as a function of microorganisms involved in biodegradation aimed at using the contaminant as an energy source [48]. However, the biodegradation of the PAHs is also affected by several parameters such as soil characteristics (e.g. organic matter, presence of nutrients) and environmental factors (e.g. temperature, dissolved oxygen). Indeed, PAHs are less subject to photochemical or biological oxidation after their deposition onto sediments (Figure 1.5), especially when the environment is governed by anoxic conditions. Therefore, PAH adsorption onto sediment particles and subsequent PAH accumulation is one of the main route in the aquatic environment (Figure 1.5) [78].

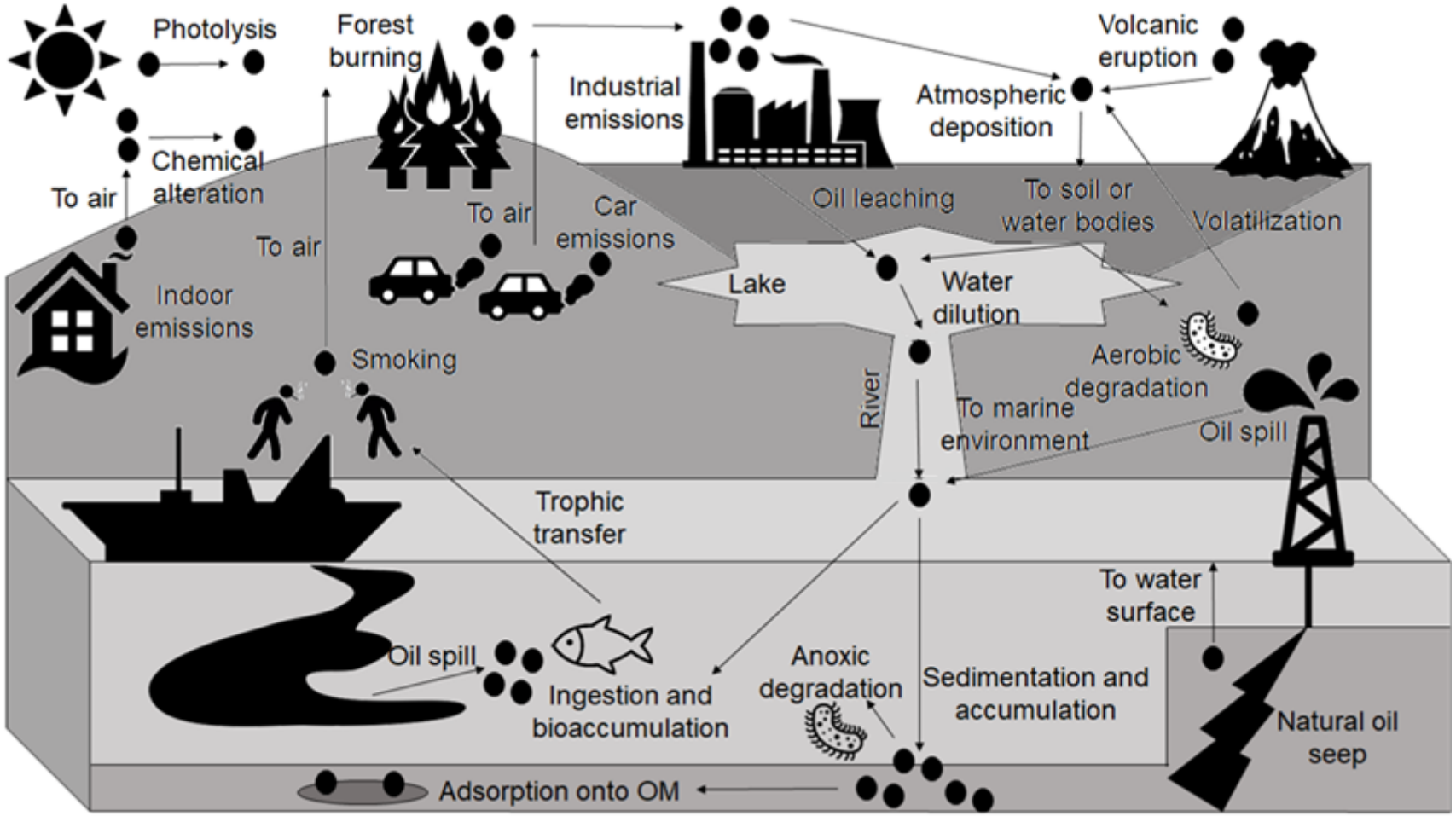

Figure 1.5 – The possible pathways of polycyclic aromatic hydrocarbons (●) in the environment. OM = organic matter.

1.2.3 PAHs in sediments and the harbor contamination issue

Road leaching, oil spills, atmospheric deposition, and untreated wastewater discharge can contribute to waterbody contamination (Figure 1.5) [79]. After an intricate PAH transport due to physical–chemical characteristics (e.g. log $K_{o/w}$, H) (Table 1.2) and environmental conditions (e.g. geomorphologic properties), naturally and artificially generated PAHs can be adsorbed onto the organic matter and subsequently combined with sediments (Figure 1.5) [80]. For instance, PAHs with low solubility (e.g. PHE, PYR, ANT) have a higher tendency to accumulate in sediments compared to those with a greater solubility such as naphthalene (Table 1) [81,82]. Afterwards, sediment–adsorbed PAHs can be driven by external factors such as water flow and bioaccumulation in fishes (Figure 1.5), thus posing a potential risk to human health [39]. According to Merhaby et al. [83], Mediterranean sediments exhibit a higher PAH concentration (i.e. up to approximately 1,700 mg kg^{-1}) in a calm zone such as a harbor compared to those shown in a dynamic environment such as a river body (i.e. up to approximately 600 mg kg^{-1}).

Since the dredging of harbour areas is highly required every year (i.e. up to 200 Mm^3 in Europe, SedNet) to allow navigation by maintaining a constant level of the seabed, there are subsequent issues for the sediment management (e.g. landfilling, coastal nourishment, reuse) due to the PAH pollution of dredged sediments. [11]. Therefore, the study of innovative and proper technologies for the remediation of PAH−contaminated marine sediments is of vital importance to the scientific community.

1.3 PAH bioavailability and bioaccessibility

Remediation techniques such as biological and physical treatments are widely used for the removal of PAHs from contaminated sediments (Table 1.5). However, these remediation treatments are strongly affected by the bioavailability level of the persistent organic pollutants (POPs) such as PAHs [84]. Ehlers and Luthy [85] explained the word “bioavailability” as the unique physical−chemical and biological interactions that define the exposition of living organisms to chemicals associated with soils and sediments. The expression ‘bioaccessibility’ instead includes the fraction of the compound that is bioavailable at present (i.e. real bioavailability) with the amount that is potentially bioavailable [86]. PAH bioaccessibility is generally assessed through the extraction with mild solvents (e.g. butanol) desorbing the pollutant fraction poorly sediment–associated [87] and demonstrated to be more practical for bioremediation

purposes also due to the limited time associated with the test [88]. On the contrary, PAH bioavailability can be determined through the employment passive samplers such as polyoxymethylene (POM) by measuring pore water PAHs with tests that can require approximately 30 days for reaching the equilibrium [89], and therefore, this measure is more suitable for determining bioavailable PAHs after using physical techniques (e.g. capping) [90].

In general, the bioavailability of an organic contaminant can be influenced by the adsorption of PAHs onto the sediment organic matter (SOM) and minerals, the transport mechanisms of PAHs in sediment (Figure 1.5) and the microbial adaptations to increase PAH bioavailability under conditions of limited bioavailability [91]. The adsorption of PAHs onto SOM can be affected by the presence of aromatic and aliphatic structures, the polarity, the spatial arrangement and the SOM physical conformation [92]. Both the aromatic and aliphatic structures are important for adsorption onto SOM, but neither prevails over the other. The presence of hydrophobic structures and porous particles can further improve the adsorption rate, whereas the presence of carbohydrates and/or peptides can decrease PAH adsorption [93]. Also, the adsorption of PAHs onto minerals can be associated with surface reactions and presence of micro–pores. Sediment minerals can show a high affinity with polar compounds due to the presence of silica by generating hydrophobic bridges [94]. However, the mineral content regulates PAH adsorption only when a low organic matter amount occurs in the sediment [91]. Indeed, Yang et al. [95] reported that SOM thickness can highly affect PAH bioavailability in the presence of a mineral complex. Finally, the transport of PAHs in the sediment can take place through combined diffusion processes as a function of octanol–water partition coefficients and Henry's law constant (Table 1.2) [96]. The mass transfer by the intra–particle diffusion and intra–organic matter are the major mechanisms contributing to the sequestration of PAHs in the sediment [97]. Therefore, when PAHs are not accessible to microorganisms, the diffusion mechanisms can increase their bioavailability [91]. The dissolved form of PAH into interstitial water is considered to be more bioavailable than the adsorbed fraction [88]. In addition to the dissolved phase alone, the adsorbed PAHs may also be bioavailable. PAHs adsorbed onto sediments can be released in the aqueous phase within the presence of a biosurfactant, otherwise, the adsorbed PAH can be directly degraded through an extracellular enzyme [98].

1.4 Remediation technologies for the removal of PAHs from contaminated sediments

The contamination by PAHs represents a potential risk to human health, and therefore several remediation techniques can be used to remediate contaminated sediments. The persistence of PAHs in sediments can be attributed to the failure of natural attenuation such as the degradation process, which depends on various parameters such as PAH physical–chemical properties (e.g. solubility, molecular weight), environmental conditions (e.g. pH, temperature) and sediment characteristics (e.g. organic substances, porosity) [3,53,79]. Therefore, the remediation of sediment is required by employing a range of physical–chemical, biological and thermal technologies (e.g. adsorption, aerobic bioremediation and thermal desorption) (Table 1.5) [35,99]. The thermal techniques (Table 1.5), in which the rise of temperature leads to volatilization or destruction of PAHs from the polluted sediment, are costly and harmful to the environment due to energy required for heating, and the destruction of the organic substance and living microflora initially existing in the sediment [100]. Bioremediation (Table 1.5) has proved to be an environmentally–friendly and inexpensive alternative approach by exploiting the metabolic capacity of the microorganisms to use the PAHs as growth substrate through aerobic or anaerobic processes [40]. However, the biodegradation process is strongly limited by the PAH bioavailability and other parameters such as pH, temperature and presence of nutrients [40]. Therefore, the physical–chemical (Table 1.5) processes can be applied by generally showing high PAH removal efficiencies [35]. Notwithstanding, these processes can be invasive for the environment and expensive to be implemented due to drawbacks such as the generation of spent effluents (e.g. sediment washing) and the addition of chemicals (e.g. chemical oxidation) [21,101], respectively.

Table 1.5 − The main conventional remediation techniques for contaminated sediments [12,35,76,102–105].

	Bioremediation	**Physical–chemical**	**Thermal**
Technologies	Composting, Landfarming, Bioreactor, Bioaugmentation, Biostimulation, Biosparging and Phytoremediation	Sediment washing, Immobilization, Stabilization, Chemical oxidation, Photocatalytic degradation, Elektrokinetic, Capping and Air sparging	Incineration, Thermal desorption, Vitrification
Advantages	Biotransformation of PAHs to a less toxic compound, Simple equipment, High safety, Low energy consumption, Cost saving, Can be applied both in–situ and ex–situ, Can be performed in both aerobic and anaerobic environments	Effective for dissolved and adsorbed contaminants, High removal efficiencies, Competitive costs, Short treatment time, Controlled production of VOCs, Possible combination with biological processes	Low treatment time, The remediated sediment can be reused, Reduced production of toxic substances, PAHs are destroyed, The polluted matrix can be used for energy production, High treatment efficiency, Applicable in emergency situations due to accidental discharge of PAHs

Disadvantages	Limited to biodegradable compounds, High remediation time, Slow microbial growth, Low PAH bioavailability, Superficial treatment, Highly dependent on environmental and operational factors, Can require an external energy source, Inoculated microorganisms can compete with the indigenous microbial structure	Risk of PAH mobilization, Large spent washing effluents, Preferential routes of the contaminant, Non–eco–friendly, Possible dispersion of chemicals, Reagent cost, Acidic pH values (Fenton process)	High cost due to energy consumption, Dredging required; Can be applied only ex–situ, Altered chemistry of sediment, Treatment of off–gas, Difficult to be implemented in industrialized and residential areas, A poor design of the intervention could create the migration of the pollutant, Could impact on groundwater
Costs €·m^{-3} of sediment	5–300	10–600	50–2,000
PAH removal	Up to 97%	>99%	>99%

PAH = Polycyclic aromatic hydrocarbon; VOCs = volatile organic compounds

Although some technologies can show great removal efficiencies (Table 1.5), high efforts for their implementation and management can be required. Indeed, it is necessary to identify the most technically, environmentally and economically sustainable remediation technique for a certain site. Indeed, the remediation process can be performed as in–situ or ex–situ when is carried out directly in/on the polluted site with considerable cost savings (e.g. capping) or after sediment dredging elsewhere (e.g. reactor) with improved efficiency, respectively. Although the operation of an ex–situ reactor may be an expensive treatment, remediation is not affected by external conditions by the setting and monitoring of the optimal parameters for speeding up the PAH removal from the contaminated matrix. Anyway, the research of proper remediation for contaminated sites should be rapidly developed by identifying techniques that allow to achieve the stringent goals imposed by national legislation [76].

1.5 Bioremediation

Bioremediation includes a pool of techniques in which microorganisms can be used for the removal of pollutants (e.g. PAHs) from an environmental matrix [106]. The microbial communities involved during the PAH biodegradation process can be composed of bacteria, fungi or algae, which can directly use PAHs as an energetic substrate or for cellular synthesis by enabling biomass growth [107]. Thus microorganisms can proceed through a PAH biomineralization into simpler compounds (e.g. catechol) by eventually transforming the pollutant into stable substances such as carbon dioxide and water, or methane under aerobic and anaerobic conditions, respectively [40]. Sometimes microorganisms can biodegrade a PAH by co–metabolism in which the simultaneous action of other similar compounds (e.g. pyrene and benzo[a]pyrene) or enzymes leads to the decrease of PAH concentrations [40]. During the mentioned mechanism, PAHs are indeed biotransformed to a lower molecular weight compound, thus the latter can be used as a source of carbon and energy by microorganisms [108]. However, the reaction intermediates can be toxic to the involved microbial community and even more reactive than the original pollutant.

The biodegradation process can occur under aerobic, anaerobic and anoxic conditions. The aerobic biodegradation of PAHs is well known in the literature and can present some limitations such as the difficulty to maintain the aerobic conditions due to high oxygen demand for the biological reactions [109]. On the other hand, the anaerobic degradation of PAHs does not require oxygen as an electron acceptor but can be difficult to be performed due to the complexity of the process [110]. Otherwise, anoxic conditions can be exploited by using nitrate or sulfate as electron acceptors since dominating PAH–contaminated marine sites [111]. However, the efficiency of the biodegradation process is influenced by the PAH bioavailability towards the microorganisms. Bioavailability mainly depends on the physical–chemical properties of involved PAH (Table 1.1 and 1.2) and sediment (e.g. organic substance), and therefore, the bioremediation can be enhanced by biostimulation, bioaugmentation or using surfactants [112].

1.5.1 Aerobic process

Aerobic bioremediation is a degradation process in which microorganisms can degrade pollutants in presence of oxygen. PAHs are oxygen–free compounds, and due to their low solubility in water (Table 1.1) inevitably require molecular oxygen as a terminal electron acceptor (TEA) (Table 1.8) to be metabolized by microorganisms [113]. Thus, aerobic bacteria strains through the oxygenase can degrade PAHs into

simpler molecules (Figure 1.6) using enzymes (i.e. monooxygenase and dioxygenase), which are formed by polypeptide chains and can catalyze the introduction of O_2 into PAHs.

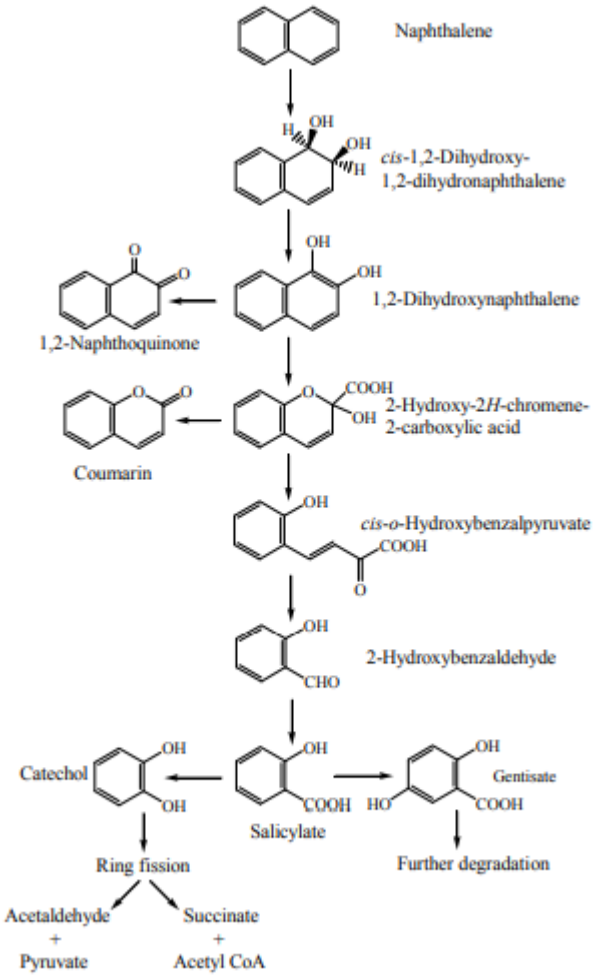

Figure 1.6 – Catabolic pathway of naphthalene by aerobic bacteria. The figure is taken from Seo et al. [114].

The catabolic degradation of naphthalene (Figure 1.6) here used as a model compound to understand the degradation pathway that generally occurs via aerobic bacteria is also a part of the degradation process of other PAHs such as PHE. Several bacteria strains (e.g. *Pseudomonas*, *Rhodococcus*, *Sphingomonas*, and *Streptomyces*) can use naphthalene as an energy source [114].

During the aerobic naphthalene degradation, the monooxygenase enzyme introduces only one oxygen atom into the organic pollutant, whereas the second oxygen atom is reduced to water via a reducing agent such as $NADH_2$ [115]. On the contrary, dioxygenase introduces two oxygen atoms in the hydroxyl form into the PAH

molecule [115]. Therefore, the first step of the aerobic bacterial degradation of PAHs is the hydroxylation of an aromatic ring through the activation of dioxygenase enzymes by producing a cis–dihydrodiol compound (Figure 1.6) [116]. Afterward, a PAH is re–aromatized with the dehydrogenase enzyme and subsequently the aromatic ring is cleavaged by adding a further O_2 with the dioxygenase [117,118]. A catechol is finally produced by the cleavage of salicylate, which is obtained by the meta–cleavage of 1,2–dihydroxynaphthalene [119] by leading to the pyruvate and acetyl CoA production (Figure 1.6) [120].

The main treatments and results referring to aerobic bioremediation are summarized in Table 1.6 as follows.

Table 1.6 – Summary of studies reporting the aerobic bioremediation of polycyclic aromatic hydrocarbon (PAH)–contaminated matrices.

Aerobic bioremediation	Investigated PAHs	Removal [%]	References
Composting	LMW and HMW PAHs	40.7–61.2 % for LMW PAHs and 18.7–33.1% for HMW PAHs	[121]
		20–60% for LMW PAHs and 30–80% for HMW PAHs	[35]
	Benzo[a]pyrene and fluoranthene	89–59 % during mesophilic phase and 71–59 % during thermophilic phase	[102]
	Naphthalene, acenaphthylene, acenaphthene, fluorene, anthracene and phenanthrene	89% at 38 °C and 45% at 55°C	[122]
Landfarming	Phenanthrene, anthracene and pyrene	22–67%	[123]
Combination of biostimulation and bioaugmentation during landfarming	HMW PAHs	76–87%	[124]

Landfarming treatment with the addition of sewage sludge	ΣPAHs, phenanthrene, pyrene, benzo[a]pyrene	36% for ΣPAHs; 100% for phenanthrene and benzo[a]pyrene, and 76% for pyrene	[102]
Bioaugmentation with a fungal–bacterial consortium and biostimulation of native microbiota	Phenanthrene, pyrene and benzo[a]pyrene	84%	[125]
Biostimulation and bioaugmentation with bacterial consortium	Fluorene, phenanthrene and pyrene	97 % with biostimulation, bioaugmentation was not significantly effective	[126]
Aerobic bioreactor	Naphthalene, acenaphthene, fluorene, phenanthrene, anthracene, fluoranthene, pyrene, benz[a]anthracene, chrysene, benzo[b]fluoranthene, benzo[k]fluoranthene, benzo[a]pyrene, dibenz[a,h]anthracene, benzo[g,h,i] and perylene	76% for ΣPAHs	[127]

LMW = Low molecular weight; HMW = High molecular weight.

The bioremediation techniques generally employed for PAH–contaminated sediments are landfarming and composting (Table 1.5 and 1.6), which are sustainable and economical technologies, which are performed under aerobic conditions [128]. Land farming is performed with periodic sediment turning over for the removal of LMW PAHs, and the microbial activity can be also stimulated with the addition of extra substances such as urea and phosphates, or allochthones bacteria [35]. For instance, Jacques et al. [123] reported a PAH degradation of 67, 48 and 22% for phenanthrene, anthracene and pyrene after 30 days of bioaugmented landfarming, respectively, to improve low removal efficiencies probably affected by limited bioavailability of pollutants [76]. Similarly, the composting is performed with the injection of air to allows the degradation of HMW PAHs with a reduction comprised between 20–60% and 37–80% after 54 and 100 days, respectively [35]. For example, Han et al. [121] achieved a PAH degradation comprised between approximately 19

and 60% for HMW and LMW PAHs, respectively. Also in this case, when composting lacks sufficient nutrient presence, a biostimulation method can be employed to improve and speed up the biodegradation processes [76].

Thus, the bioaugmentation and biostimulation (Table 1.7) processes can represent a booster for the well–established bioremediation treatments. The bioaugmentation (Table 1.7) is based on the addition of further microbial cultures with a high capability to biodegrade a specific compound, by previously enrichment in the laboratory [129]. This technique can be used when the indigenous microbial community is poor and cannot biodegrade PAHs. Although the biodegradation process can be improved, the inoculated microorganisms may compete with the existing microbial community and inevitably decrease the process efficiency [130]. Also, Wu et al. [131] showed that the introduction of an allochthonous species can lead to a decrease in microbial biodiversity since the surviving inoculum can increase in number and become predominant compared to other microorganisms. Indeed, better biodegradation results can be achieved with a heterogeneous microbial community [131]. Moreover, the expansion from lab–scale, to pilot and full–scale should be gradual to avoid drawbacks [132]. A further technique to be considered is biostimulation (Table 1.7), in which nutrients or amendments are added to the sediment to stimulate the activity of the existing microbial community [19]. In such a way, the carbon to nitrogen to phosphorous (C:N:P) molar ratio is balanced (e.g. 100:10:1) by adding fertilizers or organic amendments rich in nitrogen such as sewage sludge [133]. A drawback of this process can be that the organic substrate is competitive compared to PAHs [134], and at times, biostimulation can be combined with bioaugmentation to further enhance biodegradation efficiency [130]. Haleyur et al. [105] recently showed a high PAH removal (i.e. by approximately 94%) after 30 days of combined biostimulation and bioaugmentation in a soil initially contaminated by 1.5 g of PAHs·kg^{-1} of total solids. On the contrary, other studies reported that bioaugmentation cannot significantly contribute to the biodegradation process and therefore biostimulation is sufficient to achieve a satisfying bioremediation efficiency [105,135]. Further research focused on the introduction of external biosurfactants (e.g. lipopeptide) [136] to improve biostimulation (Table 1.7) by increasing PAH bioavailability [137]. In order to correctly use this methodology, it should be considered that the substances that are introduced can be toxic to microorganisms, become a preferential source of nutrition instead of PAHs, increase bacteriostatic properties and unintentionally mobilize the contaminants in the surrounding areas by enhancing their solubility [138].

Table 1.7 – Main advantages and disadvantages of biostimulation and bioaugmentation processes.

Treatment	Main feature	Advantages	Disadvantages
Bioaugmentation	Introduction of selected and engineered microbial species for the degradation of a specific PAH	High biodegradation efficiency after microbial inoculation; cost–saving; reduced time of biodegradation	Limited growth and reproduction of the microbial community; competition with indigenous species; hard to be implemented in–situ
Biostimulation	Introduction of nutrients, additives/surfactants that enhance the biological activity and characteristics of the site	Enhancement of biodegradation performances by the autochthonous microorganisms; improved degradation efficiencies than bioaugmentation	Natural amendments or synthetic additives can be degraded or show toxicity towards microorganisms; can increase bioavailability and mobility of PAHs

PAH = Polycyclic aromatic hydrocarbon.

1.5.2 Other terminal electron acceptors

Anoxic and anaerobic biodegradation of PAHs can occur when freely dissolved oxygen is limited or absent [139]. Indeed, microorganisms can use various TEAs different from O_2, i.e. SO_4^{2-}, NO_3^-, Fe^{3+}, Mn^{4+} and CO_2 [140] (Table 1.8) to enhance the conversion of PAHs into lower molecular weight compounds [141]. The breakdown of organic compounds releases electrons that can convert ADP to ATP and are accepted by the mentioned TEAs by obtaining water and other molecules (Table 1.8). Specifically, sulfate is biologically transformed to sulfide by sulfate–reducing bacteria, nitrate is converted to nitrogen gas by denitrifying bacteria, ferric iron and manganese oxides are reduced to Fe^{2+} and Mn^{+3} by metal–ion–reducing bacteria, respectively, and carbon dioxide can be reduced to biomethane by methanogens (Table 1.8) [4]. The ability to receive electrons is affected by TEA redox potential, which value is higher for nitrate (i.e. +433 mV) compared to metal ions, sulfate and carbon dioxide (i.e.+200, –200 and –380 mV, respectively) (Table 1.8) [140,142]. Therefore,

the anaerobic biodegradation through the reduction of CO_2 to CH_4 can occur when the other TEAs are limited or absent due to the lowest redox potential.

Table 1.8 – Redox potential and standard Gibbs free energy (ΔG^0) for terminal electron acceptors during polycyclic aromatic hydrocarbon degradation [4,140].

Electron acceptor	**Process**	**Redox potential [mV]**	**$\Delta G^{0'}$ [kJ·mol^{-1}]^a**	**Final products**
O_2	Aerobic metabolism	+818	–220	CO_2, H_2O
NO_3^-	Nitrate reduction	+433	–795[a]	N_2
Fe^{3+}	Metal ion reduction	+200	–228	Fe^{2+}
Mn^{4+}	Metal ion reduction	+200	NA	Mn^{3+}
SO_4^{2-}	Sulfate reduction	–200	–152	H_2S
CO_2	Methanogenesis	–380	–63	CH_4

a = calculated at pH 7 and 25 °C; b = nitrate reduction to nitrite is –163 kJ·mol^{-1} [143]; NA = not available.

The vast majority of PAHs cannot be solubilized in water and tends to accumulate in the sediment layers where anoxic and anaerobic conditions occur. Thus, the organic pollutants can be biodegraded through the ability of the abovementioned microorganisms, which swarm in these environments. This type of treatment is recommended in the presence of high PAH concentrations in order to limit aeration, and therefore remediation costs [35]. The studies conducted on bioremediation under anoxic and anaerobic conditions are summarized in Table 1.9.

PAH removal is enhanced under nitrate–reducing conditions (i.e. up to 96%, Table 1.9) than metal–ion– and sulfate–reducing, and methanogenic conditions (i.e. no effects, up to 88 and 91%, respectively). Therefore, nitrate is used as an electron acceptor in the presence of denitrifying bacteria [144] due to the redox potential close to that of oxygen (Table 1.8) [4]. When metal ions are involved, no significant effects on PAH biodegradation can be achieved [139] likely due to the fact that a high concentration of Fe^{3+} and Mn^{4+} as TEA can inhibit the anaerobic process by inducing toxic effects towards bacterial activity [145]. Likewise, the sulfate reduction process can exhibit toxicity toxic towards microorganisms due to hydrogen sulfide production [146]. Therefore, the scientific community is moving forward to the employment of anaerobic digestion (AD) processes aimed at producing an energetically valuable product (i.e. biomethane) by simultaneously remediating the contaminated site.

Table 1.9 – Summary of works reporting the anoxic and anaerobic degradation of polycyclic aromatic hydrocarbons (PAHs).

Conditions	Tested PAH	PAH degradation [%]	References
Nitrate–reducing	Naphthalene	up to 93% after 25 d	[147]
	Phenanthrene, naphthalene	17–96% after 30 d	[148]
	Benzo[a]pyrene	84% after 10 d	[149]
Metal–ion–reducing*	Phenanthrene, fluorene, fluoranthene and pyrene,	No significant effect	[139]
Sulfate–reducing	Fluorene and phenanthrene	65–88% after 21 d	[150]
	Naphthalene and benzo[a]pyrene	52–85% after 90 d	[151]
Methanogenesis	Fluorene, Phenanthrene, Anthracene, Fluoranthene and Pyrene	31–91% after 50 d	[135]
	Fluorene, phenanthrene and pyrene	>50% after 20 d in presence of glucose or acetate	[144]

* = includes iron(III).

1.5.3 Anaerobic digestion

AD is a biochemical process in which complex organic substances (e.g. carbohydrates and lipids) are converted into less complex biomolecules (e.g. monomers, fatty acids and acetate) and ultimately to biogas (i.e. CH_4 and CO_2) by involving various anaerobic microorganisms in absence of oxygen [152]. The biogas produced during AD is considered a form of green energy, which has several uses such as producing electricity and heat in the cogeneration plants [153]. The anaerobic degradation of PAHs occurs after the ring–opening through 4 main phases (Figure 1.7) called hydrolysis (Eq. 1.4.1), acidogenesis (Eq. 1.4.2), acetogenesis (Eq. 1.4.3) and methanogenesis (Eq. 1.4.4 and 1.4.5) [152], which are summarized as follows [154]:

$$n \cdot (C_6H_{10}O_5) + n \cdot H_2O \rightarrow n \cdot C_6H_{12}O_6 + n \cdot H_2 \quad (4.1)$$

$$C_6H_{12}O_6 \leftrightarrow 2 \cdot CH_3CH_2OH + 2 \cdot CO_2 \quad (4.2)$$

$$CH_3CH_2OH + 2 \cdot H_2O \leftrightarrow CH_3COO^- + 3 \cdot H_2 + H^+ \quad (4.3)$$

$$CO_2 + 4 \cdot H_2 \rightarrow CH_4 + 2 \cdot H_2O \quad (4.4)$$

$$CH_3COOH \rightarrow CH_4 + CO_2 \quad (4.5)$$

During the hydrolysis step (Figure 1.7), specialized extracellular enzymes secreted by microorganisms allow to biologically transform organic macromolecules (i.e. carbohydrates, proteins, and lipids) into simpler compounds such as monomeric sugars, amino acids, and long–chain fatty acids to favor their metabolization. Afterwards, the acidogenesis (Figure 1.7) consists of the biodegradation of the main hydrolysis products to obtain VFAs (e.g. propionic and butyric acid), ethanol, hydrogen, and carbon dioxide as intermediates of reaction. Subsequently, the acidogenesis products are further degraded to acetic acid during the third phase, i.e. acetogenesis (Figure 1.7). Finally, methanogenesis (Figure 1.7) takes place through the biogas production by hydrogenotrophic and acetoclastic microorganisms, which reduce carbon dioxide and acetate, respectively. The generated methane is mainly obtained via the degradation of acetate (i.e. approximately 60%, Eq. 1.4.5), whereas the remaining 30% is produced starting from H_2 and CO_2 (Eq. 1.4.4) [155].

Although the advantages from the energy point of view, the methanogenic phase is challenging to be sustained due to the limited ATP gain [155,156] and process drawbacks since several parameters are involved during AD (Table 1.10). The process is very sensitive and tends to inhibit itself easily since each phase occurs in series and also in parallel by microorganisms that synchronically work, thus the activity of one generates a substrate for the other [155]. Several factors can affect the activity of methanogens, such as temperature, pH, C/N ratio, moisture content and the presence of inhibiting substances (Table 1.10). Also, previous studies showed that the conversion of PAHs through methanogenesis can be less effective than the use of other TEAs such as nitrate (Table 1.9). This is most likely due to a lower Gibbs free energy ($\Delta G^{0'}$) for PAH degradation using carbon dioxide–reducing conditions (i.e. –63 $kJ \cdot mol^{-1}$) compared to nitrate–reducing conditions (i.e. –163 $kJ \cdot mol^{-1}$) under standard conditions and pH 7 (Table 1.8) [4].

Table 1.10 – Parameters affecting AD process [157–162].

Parameters	Units	Values
Temperature:		
Mesophilic	°C	25–45
Thermophilic		45–65
pH:		
Acidogenesis	–	5–6.5
Methanogenesis		6.5–8.0
Alkalinity	mg $CaCO_3 \cdot L^{-1}$	1,000–5,000
VFAs	$mg \cdot L^{-1}$ of acetic acid (HAc)	50–2,000
OLR:		
Mesophilic	kg $\cdot VSS \cdot m^{-3} \cdot d^{-1}$	0.8–6.4
Thermophilic		1.5–7.5
C:N ratio	mole/mole	10:1–35:1
C:N:P ratio	mole/mole	100:5:1–100:10:1
Moisture content	%	>60
SRT	d	15–30
HRT	d	7–30
Biogas composition:		
Biomethane	%	55–75
Carbon dioxide		30–45
Hydrogen sulfide		0–5
Nitrogen		0.5
Inhibiting substances	–	H_2S, NH_4, potential toxic elements

VFAs = volatile fatty acids; OLR = organic loading rate; VSS = suspended volatile solids; C:N = carbon to nitrogen; C:N:P = carbon to nitrogen to phosphorous; SRT = sludge retention time; HRT = hydraulic retention time.

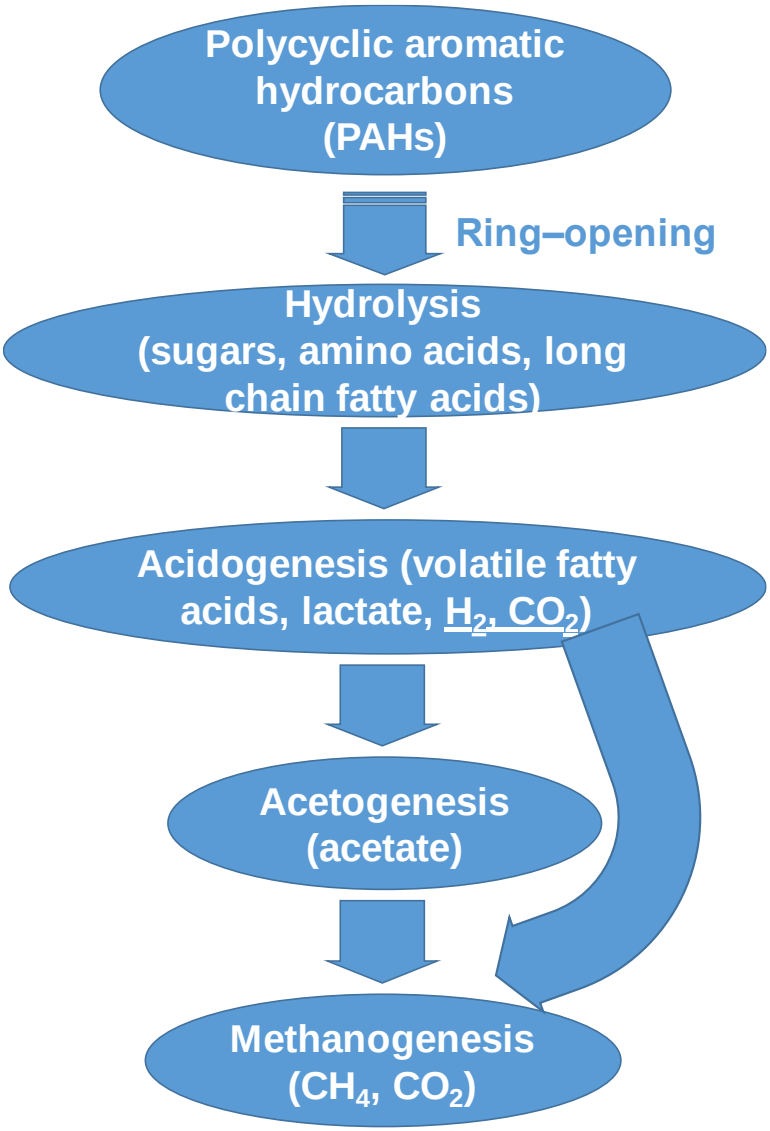

Figure 1.7 – Principal phases involved during the anaerobic digestion process.

Therefore, strategies to improve AD process can be the bioaugmentation and biostimulation, as also reported for aerobic processes (see Section 1.6.1). However, these techniques have been barely used for the remediation of PAH–contaminated sediments, and therefore, future studies should be aimed at enlightening the employment of organic wastes for simultaneous PAH degradation and biogas production.

1.6 Physical–chemical treatments

1.6.1 Sediment washing

Among the physical–chemical treatment, sediment washing (SW) can be used as an ex–situ method to remediate contaminated sediment after dredging operations [163].

Natural extracting agents such as organic solvent (e.g. methanol, humic acid, vegetable oil) and synthetic surfactants (e.g. cationic, non–ionic) can be employed during SW to remove the pollutant adhered to the solid matrix via desorption mechanism [35] (Table 1.11). It is commonly assumed that desorption biphasic rates (i.e. fast and slow) are involved during SW by following kinetic models such as an intra–particle diffusion kinetic. Indeed, the great part of PAH adsorbed within sediment pores can desorb at a slower rate than the fraction adsorbed onto the outer surface [164]. This remediation treatment can achieve a high removal efficiency of PAHs limiting the destruction of physical–chemical properties of sediment and microbial activity with a reduced operating cost [165,166]. However, the applicability and efficiency of SW can be affected by the organic fraction content in sediment [167] and pollutant properties (e.g. $K_{o/w}$, Table 1.2). Also, SW efficiency can be influenced by the quantity and type of the extracting agent, the solid to liquid (S/L) ratio and the remediation time [168]. Generally, removal efficiencies greater than 90% can be achieved by using an S/L ratio lower than 1:10, with a consequent increase of process cost (e.g. spent SW effluents) [35,76]. On the other hand, a low S/L ratio can lead to a decrease of time for reaching the equilibrium, which does not exceed 72 hours (Table 1.11) [169]. With regard to the type of extracting agents (Table 1.11), the use of surfactants generally enhances the SW efficiency by increasing PAH solubility due to the presence of the hydrophobic interior structures [166]. However, PAH removal efficiency can be lower than 90% when the dosage of extracting agent is below $2 g \cdot L^{-1}$, especially in the presence of cationic surfactants [104]. A non–toxic, biodegradable and economic alternative can be the use of vegetable oil (e.g. sunflower, peanut) (Table 1.11) as extracting solvent, which can also be combined with biological treatments [35,76]. Indeed, various studies obtained a PAH removal comprised between 52 and 100% (Table 1.11) by employing sunflower and peanut oils [170,171], the remaining vegetable oil in sediment can subsequently turn into a growth medium for the microbial community. Thus, in order to reach a complete PAH degradation, SW can be alternatively combined with advanced oxidation processes (AOPs) in which the complete mineralization of the extracting agent and pollutant can occur [172].

1.6.2 Treatment of spent sediment washing solution

The main disadvantage of SW process is the generation of a large amount of PAH–containing effluents, which require proper treatment to remove pollutants and allow to recover of the extracting agent for its reuse in a subsequent SW.

Table 1.11 – Summary of sediment washing treatments using organic solvents, surfactants and vegetable oil aimed at PAH desorption from contaminated sediments.

Extracting Agents	Compounds	S/L ratio (w/v)	Time [h]	Removal [%]	References
Mixture of water, acetone and ethyl acetate (10:40:50, v/v/v)	Naphthalene	1:8	1	87	[173]
Non–ionic surfactants, i.e. Brij 30, TRX100, Tergitol NP–10, Igepal CA–720 (0.1, 1, 4, 6 and 10%, v/v)	Phenanthrene	2:1	1	61	[174]
Cationic (Dodecylpyridinium bromide)				45	
Anionic surfactant (sodium dodecyl benzenesulfonate)	Phenanthrene and pyrene	1:13	24	71–95	[175]
Peanut oil	ΣPAHs	1:2	168	81–100	[170]
Sunflower oil	ΣPAHs	1:20–1:40	3	52–90	[171]

TRX= Triton X–100; ΣPAHs = total polycyclic aromatic hydrocarbons.

Several technologies can be applied for the treatment of spent SW solutions such as AOPs (Figure 1.8), physical adsorption (e.g. active carbons), biological treatments and integrated processes [27,176–178]. During the choice of mentioned alternatives, a major interest is focused on cost–saving, a low chemical used, energy input, sludge production, and effluent discharge after treatment [166]. The most effective processes for the removal of organic pollutants are AOPs such as electro–Fenton due to the generation of hydroxyl radicals ($OH^{\bullet}$) (Eq. 1.5.2) that enable the oxidation of PAHs without the addition of H_2O_2 (Eq. 1.5.1) [172,179].

$$O_2 + 2H^+ + 2e^- \rightarrow H_2O_2 \quad \text{(Eq. 1.5.1)}$$

$$Fe^{2+} + H_2O_2 \rightarrow Fe^{3+} + OH^- + OH^{\blacksquare} \quad \text{(Eq. 1.5.2)}$$

However, selective and complete mineralization of the target PAH cannot be achieved using AOPs in order to allow the recovery and reuse of the extracting agent

[180]. Also, the oxidation of PAHs can lead to the generation of oxygenated–PAHs, which are toxic for living organisms [181]. Finally, a further limitation of AOPs could be the requirement of a high amount of chemicals and consumption of energy [166].

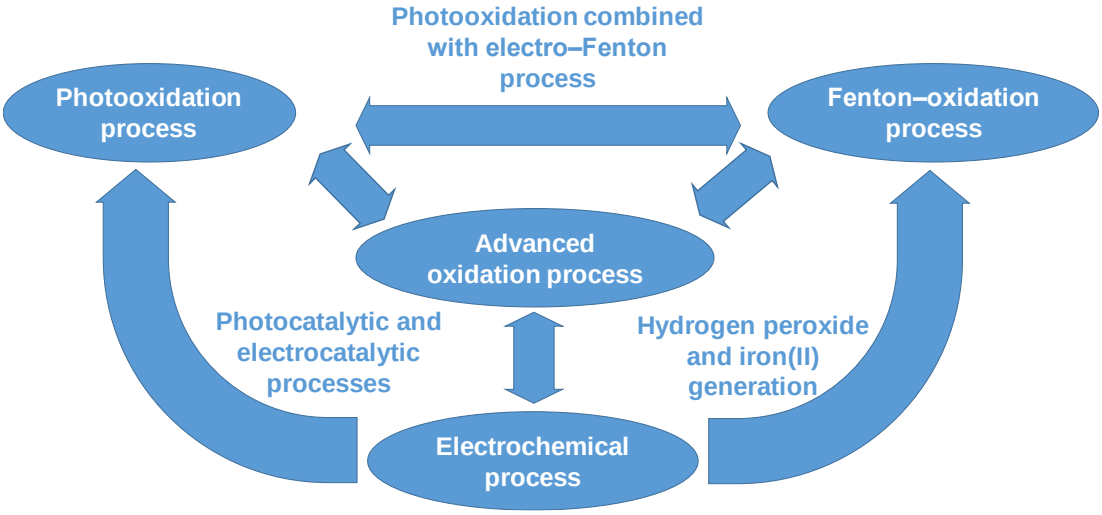

Figure 1.8 – The integration link among the typical advanced oxidation processes for the treatment of spent sediment washing effluents.

The biological treatment can be alternatively employed as an eco–friendly and cost–saving alternative to AOP. High PAH removal can be reached by optimizing the operating parameters such as pH, temperature and dissolved oxygen concentration in bioreactors where the available substrate is adsorbed onto biomass and subsequently biodegraded through engineered microorganisms (Table 1.12) [182].

Table 1.12 – Engineered microorganisms aimed at biodegrading polycyclic aromatic hydrocarbons (PAHs) in bioreactors [183].

PAH target	Microbial strains	Extracting agents
Naphthalene	*Corynebacterium* sp.	Decane, dodecane, hexadecane
Phenanthrene	*Pseudomonas* sp.	Silicone oil
	Pseudomonas aeruginosa	2,2,4,4,6,8,8–heptametilnonane
ΣPAHs	Mixed culture	Silicone oil

Previous studies reported high PAH biodegradation (i.e. about 80%) in sequential batch reactors after several weeks [184,185]. This is most likely due to the

recalcitrance of PAHs, PAH concentration, type of the extracting agent and the specific effects towards the microbial community. Further studies should be addressed in the future by focusing on the biodegradation mechanisms, PAH removal kinetics and the application of continuous–flow systems [166]. In order to decrease the use of chemicals, improve the selective PAH degradation and increase the amount of extracting agent employed for SW, an initial physical separation step can be performed prior to the degradation phase (i.e. integrated processes) through PAH adsorption onto carbonaceous materials such as activated carbon (AC) [186]. Notwithstanding, PAH adsorbed phase onto AC can occlude the adsorbent micropores by limiting the removal efficiency (i.e. up to 57%) [35]. On the contrary, AC can be subsequently regenerated via a thermal process for further PAH removal, but however, this solution is limited due to the high cost of required energy [187].

1.6.3 Use of carbonaceous adsorbents for PAH removal

Adsorption consists in the use of an adsorbent (e.g. AC) to entrap an adsorbate (e.g. POP) within an intricate porous structure in order to remediate a contaminated matrix (e.g. sediment) [188]. The main advantage is represented by the feasibility of this physical remediation treatment either in–situ or ex–situ (i.e. capping, Table 1.5). For instance, sediment capping is frequently employed in aquatic environments as an in–situ treatment for decreasing pollutant mobilization [189]. In this context, carbonaceous adsorbents (CAs) were extensively used for the adsorption of PAHs due to a high specific surface area (i.e. up to 1,300 $m^2 \cdot g^{-1}$, Table 1.13) and the presence of functional groups that lead to a great adsorption capacity [190]. Indeed, various studies investigated environmentally–friendly and economic CAs such as AC, which showed their effectiveness in order to decrease bioavailable PAHs (i.e. up to 74–99%, Table 1.13) in polluted sediments [48].

Table 1.13 – Summary of works reporting adsorption methods for the remediation of PAH–contaminated sediments.

CA	Specific surface area [$m^2 \cdot g^{-1}$]	Dosage [%, dry basis]	Contact time [d]	Decrease of pore water PAHs [%]	References
AC	900	3	30	74–84	[191]
AC	1,300	1–30	2	90–99	[192]
Graphene	7–391	0.1	1	17–75	[193]
Graphene	NA	0.1	1	68–99	[194]

CA = carbonaceous adsorbents; PAHs = polycyclic aromatic hydrocarbons.

The reduction of pore water PAHs (see Section 1.3) can occur through several interaction mechanisms between the adsorbate and adsorbent that are generally identified as weak interactions (e.g. hydrophobic interaction, Van der Waals forces) and strong interactions (e.g. π–π, electrostatic interaction) [195]. The involved adsorption interaction is affected by CA characteristics, and the occurrence of strong interactions can be generally preferred since these adsorbents can show a certain hysteresis index by leading to the desorption of PAHs [196]. An appropriate pore size allocation can supply mass transfer routes for PAHs and considerable surface areas can provide more active sites for PAH adsorption, thus enhancing the adsorption capacity and rate [197]. Cheng et al. [198] reported that CAs with micropores, mesopores, and macropores can show higher adsorption rates than CAs with only micropores at parity of adsorption equilibrium capacity. This can be attributed to the fact that small pore size is characterized by tight passage and long crossing channels by hindering effective mass transfer and diffusion of PAH molecules through CA [199]. Nevertheless, functional groups of CA surface can fulfill critical roles in the remediation of specific PAHs. The lack of heteroatoms mainly including O, N, H, S, P, and halogens can affect adsorbents' chemical properties by leading to low H/C and O/C ratios, which suggest high aromatization and carbonization [200]. Therefore, proper modifications of the adsorbent (e.g. acidic and alkaline activation) can be performed to either add or eliminate the surface functional groups (e.g. ―OH) to improve PAH adsorption onto CAs [201]. In addition to CA properties, the decrease of PAHs in pore water can be affected by CA dosage; PAH properties, initial PAH concentration, pH and ionic strength, natural organic matter, remediation time and mixing, whose effects are summarized in Table 1.14. The increase of CA dosage and ionic strength, the presence of LMW PAHs, a low amount of organic matter and pore water PAHs, a prolonged contact time and mechanical mixing (ex–situ) can enhance the adsorption efficiencies (Table 1.14). However, the employment of a high CA dosage can be costly and interfere with the habitat quality by reducing the dissolved organic carbon, thus affecting living organisms [202]. The sediment permeability, water retention capacity and nutrient content can be affected as well [203]. A further drawback can be associated with the recovery of CAs in order to avoid the release of PAHs after CA oxidation or CA swallowing by living organisms. Indeed, conventional separation methods such as sieving and centrifugation are not effective for CA recovery [204]. Therefore, CA modification via magnetite and lauric acid has been recently proposed to improve CA recovery [205,206].

Table 1.14 – Main parameters affecting the adsorption of polycyclic aromatic hydrocarbons (PAH) onto carbonaceous adsorbents (CAs) by excluding CA properties.

Parameters	Effects	References
CA dosage (%, dry basis)	Enhanced PAH adsorption with a dosage above 5%	[207]
PAH characteristics (i.e. molecular weight and ring arrangement)	LMW PAHs can be easily adsorbed within CA micropores; HMW PAHs cannot enter into CA micropores and remains adsorbed onto sediment OM due to the low diffusion coefficient	[208]
Initial PAH concentration in pore water	High removal efficiencies with low PAH concentrations; the adsorption efficiency can be increased with a higher CA dosage	[209]
pH value and ionic strength	High PAH adsorption when pH_{PZC} > pH (aqueous solution) > $pK_{a;}$ increased salting–out effect with great ionic strength	[210,211]
OM in sediment	Adsorption efficiency decrease with the raise of natural OM	[212]
Contact time	The increase of time enhances PAH adsorption	[213]
Mixing	Hard to be applied in–situ; mechanical mixing improves the removal of pore water PAHs	[214]

PZC = point of zero charges of Cas; pKa = ionization equilibrium constant of PAHs; OM = organic matter.

1.7 Thermal remediation

Thermal treatments can be reliable to carry out a rapid remediating intervention with high PAH removal efficiencies (i.e. >99%, Table 15) [215]. Indeed, thermal techniques are based on the use of heat to mobilize PAHs into gaseous flow (e.g. thermal desorption), break down the contaminants into simpler compounds (e.g. pyrolysis), destroy the pollutants (i.e. incineration), or immobilize them through stabilization or vitrification [100].

Thermal desorption (TD) is an invasive ex–situ technique aimed at releasing PAH concentrations by heating the contaminated sediment with temperatures typically above 100 °C [216]. TD can be classified into low–temperature (LTTD) and high–temperature (HTTD) when the heating is ranging between 100–300 and 300–600 °C, respectively. The involved temperature depends on the type of PAHs due to a different boiling point, which also affects the appropriate heating times. This remediation treatment should not be confused with incineration being PAH desorption and volatilization from the polluted matrix the main mechanism involved [217]. For instance, PAH combustion can lead to the production of carbon dioxide and water by employing higher temperatures than TD (i.e. up to 1,000 °C) [215]. On the contrary, desorption/volatilization mechanisms that occurs during TD are coupled with subsequent treatment of gaseous flow via destructive (e.g. thermal combustion, photocatalytic oxidation) or recovery techniques (e.g. membrane separator, solid adsorption) [218].

Although thermal techniques can achieve high PAH removal efficiencies (Table 15), TD is not generally recommended due to a high energy demand that is reflected in the total treatment costs (Table 1.5). Indeed, pollutant removal increases with the raise in temperature and heating time. Thus, a solid–liquid separation can be additionally performed prior to the TD to remove sediment moisture content by reducing the energy input [219]. A further drawback can be that TD can alter sediment physical–chemical and biological characteristics. Indeed, the desorption/volatilization of organic pollutant during TD is also coupled with the removal of SOM up to 85% after 1 hour [220]. Also, pH values can increase from about 6.9 up to 9.0 after TD (i.e. at 360 °C for 1 h) likely due to the removal of organic acids and release of cations from the SOM [221]. Therefore, TD–remediated sediments can affect plants and microbial population by decreasing biomass, and diversity and enzymatic activity, respectively, probably due to the changes in SOM and nutrient availability [222].

Table 1.15 – Summary of thermal remediation techniques aimed at polycyclic aromatic hydrocarbon (PAH) removal.

Thermal treatment	PAH concentration [mg kg^{-1}]	Investigated PAHs	PAH removal [%]	References
Incineration	1,000	Naphthalene, acenaphthene, acenaphthylene, fluorene, phenanthrene, fluoranthene, pyrene, benzo[a]pyrene, chrysene and benzo[b]fluoranthene	90	[223]
Thermal desorption	2,700	Naphthalene, acenaphthene, acenaphthylene, fluorene, phenanthrene, fluoranthene, pyrene, benzo[a]pyrene, chrysene, benzo[a]anthracene, benzo[b]fluoranthene, benzo[k]fluoranthene, indeno[1,2,3–cd]pyrene, benzo[g,h,i]perylene and dibenzo[a,h]anthracene	87–99.99	[224]
Venting thermal desorption	1,000	Naphthalene, phenanthrene, fluoranthene, pyrene, benzo[a]anthracene, benzo[b]fluoranthene, benzo[k]fluoranthene, benzo[a]pyrene, chrysene, benzo[g,h,i]perylene and indeno[1,2,3–cd]pyrene	90	[225]

CHAPTER 2. COMPARING PERFORMANCES, COSTS AND ENERGY BALANCE OF EX SITU REMEDIATION PROCESSES FOR PAH–CONTAMINATED MARINE SEDIMENTS

2.1 Introduction

Polycyclic aromatic hydrocarbons (PAHs) are a group of hazardous compounds that pose risks to human and ecological health [226]. Marine sediments are often contaminated by PAHs due to oil spillage and atmospheric deposition of particulate emissions produced by industrial activities [227,228]. Moreover, PAHs could be generated by early diagenetic reactions when a high abundance of perylene is detected in sediments [229–231]. A high quantity of contaminated marine sediments usually results in waste management problems after dredging [11], due to the limited natural attenuation of PAH pollution [17]. For this reason, PAH–contaminated sediments need to be remediated prior to sediment disposal or reuse, in accordance with the national regulation [232]. Bioremediation, sediment washing and thermal desorption are available ex–situ technologies that can be used for contaminated sediment remediation [21,217].

Bioremediation is an eco–friendly process involving microorganisms to remove PAHs from contaminated sites [233,234]. Bioremediation occurs through a biostimulation when nutrients or extra–organic sources are added to the soil to improve the metabolic activity of microorganisms [235–237]. An alternative to biostimulation is bioaugmentation, which consists in the supplementation of enriched indigenous or exogenous microorganisms in the polluted soil to speed up the remediation efficiency [105]. Bioremediation may be applied under anaerobic conditions employing methanogenic, sulfate–reducing and denitrifying conditions [238–240]. However, the

bioavailability of PAHs, meant as the available part of the contaminant for biological conversion [241], is often a limiting factor when maintaining a bioprocess in sediments or soils [233].

Physical–chemical remediation processes overcome the limiting factor of bioremediation, as they allow to also remove contaminants that are recalcitrant to microbial degradation. Among the physical–chemical techniques, sediment washing is an attractive technology due to its simplicity, low costs and high removal efficiency [165,242]. Sediment washing consists in the use of solvents or reagents to improve the mass transfer of hydrophobic pollutants from the soil matrix to the liquid phase [243,244]. Previous studies have proven the efficiency of different washing agents such as ethanol, 2–propanol, acetone and 1–pentanol for PAH removal [173].

Thermal desorption is a remediation technology with scientific and practical interest due to its high removal efficiency and low gas emissions in the presence of gas purification units [245]. Controlling the temperature of the thermal treatment enhances the desorption of organic pollutants from different matrices such as soils, sludge and sediments [15,224]. At higher temperatures, the removal efficiency of high–boiling point organic contaminants increases [246].

For bioremediation, sediment washing and thermal desorption, the water content plays a major role during the treatment. Wet conditions are widely applied during bioremediation to overcome the mass transfer limitations and provide a better environment for the microbial consortia involved [247,248]. However, a too high water content lowers the amount of soil or sediment to be treated in the unit of time. Regarding sediment washing, the use of a high solid–to–liquid ratio (e.g. 1:5 or 1:10) generally results in higher removal efficiencies but also a considerable amount of spent washing solution that must be treated prior to discharge [249,250]. During thermal desorption, an excessive presence of water increases the energy input to evaporate the contaminants as water sequesters part of the heat provided [218].

In this thesis, the use of dry conditions, a low solid–to–liquid ratio and low temperature was proposed for anaerobic bioremediation, sediment washing and thermal desorption, respectively. Nowadays, emerging concerns such as the saving of water resources, the production of energy in a sustainable way and the control of pollution are receiving more and more attention within a “water–energy nexus” perspective [251]. In this line, a techno–economic assessment of bioremediation, sediment washing and thermal desorption as ex–situ processes for the remediation of PAH–contaminated marine sediments as well as energy balance considerations were here provided. Phenanthrene (PHE), one of the most present PAHs in environment,

was selected as representative pollutant due to its intermediate toxicity, hydrophobicity and environmental persistence [17].

In particular, the specific objectives of this chapter were to 1) evaluate the efficiency of biostimulation/bioaugmentation, sediment washing and thermal desorption in removing PHE from marine sediments; 2) implement the experimental data on a commercial software in order to assess the remediation costs and 3) consider a balance of required and possibly recovered energy during each remediation approach to allow choosing the most appropriate and sustainable technology.

2.2 Materials and methods

2.2.1 Chemicals

Phenanthrene (grade ≥98%), potassium nitrate (grade ≥99%), sodium hydroxide (grade ≥97%) and sodium sulfate (grade ≥99%) were all purchased from Sigma–Aldrich (Germany). Acetone (grade 100%), acetonitrile (HPLC grade), butanol (grade ≥96%), sodium acetate (grade ≥99%) and sulfuric acid (grade ≥96%) were supplied by VWR (Italy). Ethanol (≥ 99.9%) was purchased from Merck (Germany). Deionized water with an electrical conductivity lower than 0.3 $\mu S \cdot cm^{-1}$ was used to prepare all solutions.

2.2.2 Sediment sampling and spiking

Marine sediments were collected from Formia seaside (Lazio Region, Italy) and the physical–chemical properties are reported in Table 2.1. No PAH was detected in the uncontaminated sediment. After characterization, the sediment was dried and passed through a 2–mm mesh to remove the coarse fraction. PHE was used as model PAH due to its intermediate aqueous solubility (i.e. 0.823 $mg \cdot L^{-1}$) and hydrophobicity (i.e. log K_{OW} 4.57) [239,252]. The uncontaminated sediment was spiked by dissolving PHE in acetone, according to literature procedure [253,254]. The selected value of initial PHE concentration was about 200 $mg \cdot kg^{-1}$ dry sediment, as reported by Arienzo et al. [255] for real PHE–contaminated marine sediments. Subsequently, the contaminated sediment was mixed, placed under a fume hood for 72 h to allow acetone evaporation and stored in glass containers in the dark [256]. Afterwards, an aging protocol was conducted for 37 days at room temperature [257] in order to simulate an actual PHE–contaminated sediment.

Table 2.1 – Physical–chemical characterization of the uncontaminated sediment, digestate and sewage sludge.

Parameter	Sediment		Digestate		Sewage sludge	
	Average	RSD	Average	RSD	Average	RSD
pH	7.85	0.05	8.59	0.10	7.88	0.7
TS [%]	79.82	0.09	6.55	0.44	12.06	0.25
VS [%]	1.35	0.06	4.40	0.35	9.87	0.11
TOC [g·kg TS^{-1}]	0.36	0.23	119.24	3.33	189.95	1.50
TKN [g·kg TS^{-1}]	0.01	0.01	21.07	0.47	1.99	0.18
A [g $CaCO_3 \cdot L^{-1}$]	0.23	0.01	12.90	0.05	3.05	0.03
NO_3^- [mg·L^{-1}]	19.24	3.15	34.55	1.30	72.16	0.89
SO_4^{2-} [mg·L^{-1}]	518.82	8.36	50.65	5.65	123.70	2.08
EC [mS·cm^{-1}]	1.91	0.11	2.68	0.06	0.87	0.07

TS = total solids; VS = volatile solids; TOC = total organic carbon; TKN = total Kjeldahl nitrogen; A = alkalinity; EC = electrical conductivity. Average and relative standard deviation (RSD) were calculated on n = 3 replicates.

2.2.3 Experimental design

2.2.3.1 Bioremediation

Bioremediation was conducted treating the contaminated sediment with combined biostimulation and bioaugmentation under denitrifying, methanogenic and sulfate–reducing conditions [135,258]. The selected sources of microorganisms were digestate and sewage sludge (Table 2.1), collected from a full–scale anaerobic digester located in Capaccio (Campania Region, Italy) and a wastewater treatment plant situated in Cassino (Lazio Region, Italy), respectively. Five operative conditions, i.e. contaminated sediment with *i)* sewage sludge (S), *ii)* digestate (D), *iii)* sewage sludge + 2,000 mg·L^{-1} of nitrate (SN, with NO_3^- supplied as potassium nitrate), *iv)* digestate + 2,000 mg·L^{-1} of sulfate (DS, with SO_4^{2-} supplied as sodium sulfate), *v)* digestate + 2,000 mg·L^{-1} of acetate (DA, with CH_3COO^- supplied as sodium acetate), were investigated. For each condition, 12 serum bottles (100 mL) were loaded with a dry portion of sediment (10 g) mixed with the inoculum at a ratio of 10:1 (dry w/dry w) and filled with water to reach a total moisture content of 60% [259,260]. Afterwards, all the bottles were flushed with argon to guarantee anaerobiosis, prior to being incubated in a water bath under mesophilic conditions (i.e. at 37±1 °C) [248] for 42 days and placed on a gyratory shaker at 160 rpm [261] to simulate a mechanical

agitation. The samples were collected after 7, 14, 21 and 42 days by sacrificing 3 bottles at a time for each condition. In SN, DS and DA, denitrifying, sulfate–reducing and methanogenic conditions were ensured by restoring the initial content of nitrate, sulfate and acetate, respectively, when the observed NO_3^-, SO_4^{2-} and CH_3COO^- concentrations were below 50 $mg \cdot L^{-1}$.

2.2.3.2 Sediment washing

Sediment washing tests were performed in glass bottles (80 mL) at room temperature [262], with a 1:3, 1:5 and 1:10 solid–to–liquid (S:L) ratio. A solution with 50% of ethanol (ETOH) and water (w/w) was used as washing agent [243]. Sediment samples (6 g) were shaken at 200 rpm in a horizontal shaker for 24 h [165], and PHE concentration was determined by sacrificing 3 bottles for each S:L ratio after 1, 2, 5, 15, 30, 60, 180, 360, 720 and 1,440 minutes.

2.2.3.3 Thermal desorption

Thermal desorption, testing low temperatures in 1 hour of experimentation [245], was carried out with ceramic crucibles containing 10 g of sediment each [224] and introduced in a muffle furnace at 100, 150 and 200°C. PHE concentrations were measured after 5, 15, 30 and 60 minutes sacrificing 3 crucibles per time for each temperature.

2.2.4 Analytical methods

Total solids (TS) (Astm 1998), volatile solids (VS) [264], pH [265], electrical conductivity (EC) [266], total organic carbon (TOC) [267], alkalinity (A) and Kjeldahl nitrogen (TKN) (APHA 2005), sulfate and nitrate concentrations [268] were measured according to the methods reported elsewhere. The samples were centrifuged at 4,000 rpm for 30 min to separate the liquid fraction from the solid phase [242]. PHE was extracted from samples by ultra–sonication [269] and was quantified using a LC–20AD HPLC (Shimadzu, Japan) equipped with a Kinetex® 3.5 µm PAH (150x4.6 mm) column (Phenomenex, USA) and an SPD–20A UV detector (Shimadzu, Japan) set at 254 nm. PHE bioavailability was predicted using a butanol extraction [85,270]. Biomethane, nitrogen gas (i.e. N_2) and N_2O production was measured with a water displacement method with an alkaline trap (12% of sodium hydroxide) to remove carbon dioxide and hydrogen sulfide [271,272]. The gas composition (i.e. $\%CH_4$, $\%N_2$, $\%N_2O$) was determined with a 3400 GC–TCD/ECD gas chromatograph (Varian–Agilent, USA) equipped with a Restek Packed column. Total VFAs, reported as

equivalent acetic acid concentration (mg HAc·L^{-1}), were analyzed according to Mancini et al. [272], using the previously described HPLC equipped with a Rezex ROA–Organic Acid H^+ column (Phenomenex, USA) and a SPD–20A UV detector set at 210 nm.

2.2.5 Economic analysis

The costs for sediment remediation (€·m^{-3}) were estimated considering the most performing operating conditions in terms of PHE removal used during bioremediation, sediment washing and thermal desorption. The retention time and temperature were implemented in the Remedial Action Cost Engineering and Requirements (RACER) software (11.5 version, AECOM, USA) as crucial operating parameters strongly affecting the remediation efficiencies and costs. Indeed, a higher temperature can enhance the microbial metabolism rate [273], PAH dissolution and vaporization [40,246] as well as increase the energy cost. In contrast, a lower retention time results in a reduced capital cost [274] as smaller reactors would be required. The contamination area, the safety level of machining operation and mobilization distance were assumed as 7,646 m^3 (i.e. 10,000 CY) [275], high (A) and 1.6 km (i.e. 1 mi), respectively. The assumption of a short mobilization distance was done to minimize the percentage of this cost in favor of the remediation cost. Moreover, the costs of dredging, water removal by leaking drums and disposal were not considered because common for all the processes considered in this study. Detailed information about input parameters in RACER are reported in Table 2.2 and in Appendix A. Note that the obtained costs were only indicative of real values, since costs were modeled without specific components of the site (e.g. treatment goals due to national legislation). The RACER software contains the latest assembly unit price information from the 2016 Government Cost Book (USACE TRACES, Huntsville).

2.2.6 Energy balance

A rough estimate of the energy balance was performed for the bioremediation, sediment washing and thermal desorption experimental conditions implemented in RACER. All energy requests were reported as kWh·m^{-3} of sediment.

The energy required for the maintenance of mesophilic conditions during the bioremediation process was estimated as a function of water heat exchanger, gas boiler and pump suggested by RACER. The energy necessary for the water heat exchanger was derived as follows [276]:

$$\dot{Q} = \dot{m} \cdot C_{p,w} \cdot \Delta T \qquad \text{(Eq. 2.1)}$$

where $\dot{Q}$ is the amount of heat per time unit (kW); $\dot{m}$ is the mass flow rate of the water ($kg \cdot s^{-1}$); $C_{p,w}$ represents the heat capacity of water ($kJ \cdot (kg \cdot K)^{-1}$) and ΔT is the temperature difference of water between the outlet and inlet of the heat exchanger (i.e. 17 K). Hence, the energy consumption E_c (kWh) was obtained by multiplying the sum of Eq. (2.1), boiler and pump power (kW) with the retention time of the biological process (h). Moreover, the specific energy recovery $\overline{E_r}$ ($kWh \cdot kg\ VS^{-1}$) during the bioremediation process was estimated from the obtained biomethane yield, as reported by Mancini et al. [272]:

$$\overline{E_r} = BMP \cdot \left(\frac{CHP}{100}\right) \cdot C_f \quad \text{(Eq. 2.2)}$$

where BMP is the final cumulative biomethane yield ($m^3\ CH_4 \cdot kg\ VS^{-1}$); CHP represents a combined heat and power unit (with a 50% conversion efficiency) and C_f is the conversion factor (i.e. $10\ kWh \cdot m^{-3}$). Hence, the energy recovered E_r (kWh) was obtained by multiplying Eq. (2.2) and the content of VS (kg). The energy balance for bioremediation process was calculated by subtraction of E_c with E_r.

The energy necessary for sediment washing (kWh) was obtained with RACER, whereas the energy needed for thermal desorption was estimated as follows:

$$E_{td} = \frac{(m_w \cdot C_{p,w} + m_{PHE} \cdot C_{p,PHE} + m_s \cdot C_{p,s}) \cdot \Delta T + m_w \cdot C_{l,w} + m_{PHE} \cdot C_{l,PHE}}{3600} \quad \text{(Eq. 2.3)}$$

where E_{td} is the amount of energy per time unit (kWh); m_w, m_{PHE} and m_s are the mass of water, PHE and sediment (kg), respectively; $C_{p,PHE}$ and $C_{p,s}$ are the heat capacity values of PHE [277] and sediment, respectively ($kJ \cdot (kg \cdot K)^{-1}$); $C_{l,w}$ and $C_{l,PHE}$ are the heat of vaporization of water and PHE [278] ($kJ \cdot kg^{-1}$), respectively; and ΔT is the temperature difference between the desorption chamber and inlet (i.e. 180 K).

2.2.7 Statistical analyses

Data were analyzed by one–way analysis of variance (ANOVA) followed by the post–hoc Tukey test to evaluate significant differences ($p < 0.05$) among the operating conditions investigated. All statistical analyses were performed with Minitab 19 Statistical Software (Minitab LLC, USA).

Table 2.2 – Parameters implemented in the RACER software for bioremediation, sediment washing and thermal desorption, as ex–situ remediation technologies used in this thesis.

Remediation parameters	Bioremediation	Sediment washing	Thermal desorption
Contamination ([a]VOCs. SVOCs. fuels)	SVOC	SVOC	SVOC
Distance off–site facilities (km)	1.6	1.6	1.6
Place of treatment (on–site. off–site)	Off–site	Off–site	Off–site
Retention time (h)	336	1	[c] –
Safety level ([b] A. B. C. D. E)	A	A	A
Soil type (Soil. sediment. sludge)	Hazardous sediment	Hazardous sediment	Hazardous sediment
Temperature (°C)	35	20	< 320
Volume of solid (m^3)	7,646	7,646	7,646
Main components	Bioreactor	Pump	[d] LTTD equipment
	Gas boiler	Sediment washing system	Process gas purification
	[e] Nitrate	Structural slab	Structural slab
	Pump	Surfactant	
	Structural slab	Wastewater holding tanks	
	Water Heat Exchanger	Wheel loader	

a = volatile and semi–volatile organic compounds; b= high to low; c = not required; d = Low Temperature Thermal Desorption; e = under SN

Bioremediation = SN and S; Sediment washing = S:L ratio of 1:3; Thermal desorption = 200°C.

2.3 Results and discussion

2.3.1 Bioremediation

2.3.1.1 PHE biodegradation

The remaining PHE (%) after 0, 7, 14, 21 and 42 days of bioremediation under all the operating conditions (i.e. SN, S, DS, DA and D) is shown in Figure 2.1a. PHE removal slowly proceeded during the initial 7 days as PHE (%) at "t_7" was not significantly different than PHE at "t_0" ($p > 0.05$), except for D where a 17% PHE removal was observed at "t_7" ($p < 0.05$). The low, common PHE removal was probably due to an initial acclimation period of the microbial consortia involved, whereas the difference between the D, DS and DA conditions was associated with the higher sulfate and acetate concentration, which likely resulted in a slight inhibition of the bacteria in digestate.

A significant PHE degradation ($p < 0.05$) of 59, 47, 41, 58 and 54% was observed after 14 days in SN, S, DS, DA and D (Figure 2.1a), respectively. Moreover, the observed pH values among the experimental conditions (i.e. 7.3÷8.1) were consistent with those shown as optimal for PAH degradation (i.e. 6÷8) [279]. Considering sulfate, dioxide carbon and nitrate as major electron acceptors in PAH biodegradation [280], and assuming that 1 μmol of CO_2 may be used to produce 1 μmol of CH_4, a reduction of 43 μmol of SO_4^{2-}, 81 μmol of CO_2 and 86 μmol of NO_3^- was obtained per μmol of PHE under sulfate–reducing, methanogenic and denitrifying conditions (data not shown), respectively. These results suggest that sulfate was a more efficient electron acceptor, as also reported by Chang et al. [258]. Nonetheless, after 14 days PHE removal in DS was lower ($p < 0.05$) than that achieved in SN and DA, probably due to the presence of other forms of electron donors instead of PHE. A continuous reduction of sulfate (i.e. about 200 μmol of SO_4^{2-} per week), a significant consumption of acetic acid ($p < 0.05$) after 21 days (Figure 2.1c) and no significant difference ($p > 0.05$) in biomethane yield after 7 days (Figure 2.1b) were observed in DS, suggesting that acetate was presumably coupled to sulfate reduction. Similarly, Zhang and Lo [146] observed that acetate may be preferentially used by bacteria to facilitate sulfate reduction in the absence of methane production.

During the conversion to methane by methanogens, acetate may donate electrons in favor to PAH degradation [144]. However, no statistically differences ($p > 0.05$) in PHE removal between S, DA and D were observed after 14 days, despite a higher

acetate reduction ($p < 0.05$) observed in S (Figure 2.1a and 2.1c). Ebihara and Bishop [281] reported that acetate supplementation for the biodegradation of recalcitrant organic contaminants may inhibit or have no effect. This suggests that in this study only a small fraction of acetate was likely coupled to PHE considering an initial concentration of 2,000 mg acetate·kg^{-1} TS (i.e. 199 μmol of acetate for each μmol of PHE), and a higher contamination would have instead been necessary to see a significant effect.

In the time lapse between 14 and 42 days, PHE degradation considerably slowed down and reached 68, 53, 45, 64 and 64% in SN, S, DS, DA and D, respectively, being only enhanced under denitrifying and methanogenic conditions ($p < 0.05$) probably because the predicted biodegradation (i.e. 58 %) was achieved (Figure 2.1a). The predicted biodegradation is representative of the bioavailable PAH amount [282], which is the bioaccessible fraction to microorganisms [283], and the observed value (Figure 2.1a) was comparable to those observed in other PHE–contaminated marine sediments (i.e. 44÷70%) [3,66]. It is well known that limitations in the bioremediation of PAH–contaminated soils exist due to the low bioaccessibility of PAHs, as shown in the final phase of the process. On the other hand, a reduced bioaccessibility may be a positive aspect because would lead to a reduced amount of highly accessible PAHs [284], consequently mitigating the environmental risk.

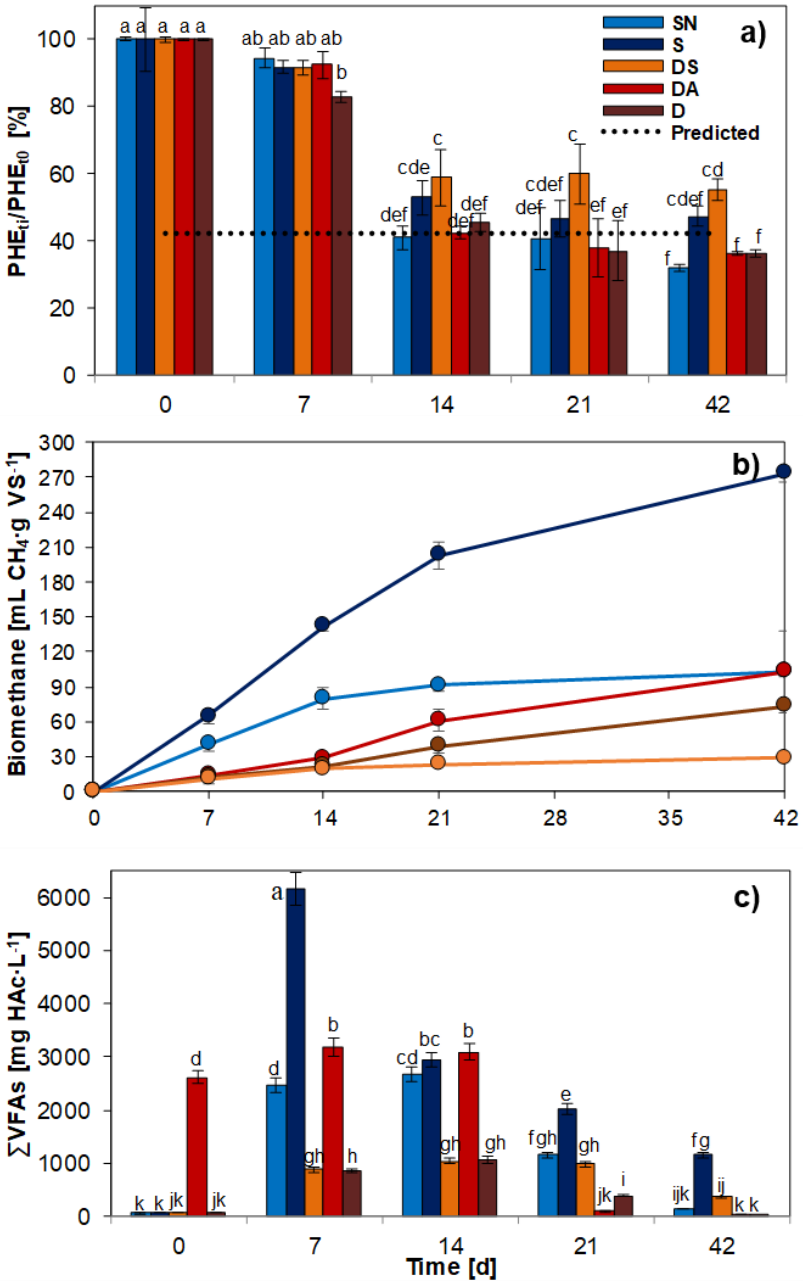

Figure 2.1 – Ratio [%] between the PHE concentration at time "t" and that at time "t_0" in the contaminated sediment (a); cumulative, specific biomethane yield [mL CH_4·g VS^{-1}] (b); and total VFA concentrations [mg HAc·L^{-1}] during 42 days of anaerobic biostimulation/bioaugmentation (c).

The same letter (Tukey test) represents no significant differences ($p > 0.05$) among different treatments. Error bars indicate deviation standard values of analyses in triplicate.

2.3.1.2 Biogas composition and VFA evolution during PHE biodegradation

The cumulative biomethane yield obtained during 42 days of bioremediation under all the operating conditions (i.e. SD, S, DS, DA and D) is shown in Figure 2.1b. After 7 days, a biomethane production of 40, 65, 11, 14 and 13 mL $CH_4 \cdot g\ VS^{-1}$ was observed in SN, S, DS, DA and D, respectively. The recorded pH values (data not shown) were optimal for methanogens growth [285] and, thus, did not represent a limiting factor for biomethane production.

Between 7 and 14 days, the biomethane yield significantly raised ($p < 0.05$) by about 50% in S reaching a cumulative production of 142 mL $CH_4 \cdot g\ VS^{-1}$ (Figure 2.1b), accompanied by a significant consumption of acetate (Figure 2.1c). In SN, a lower cumulative biomethane production (i.e. 80 mL $CH_4 \cdot g\ VS^{-1}$) than that obtained in S ($p < 0.05$) was achieved probably because of the occurrence of heterotrophic denitrification [286]. Indeed, the observed N_2 percentage in the gas phase raised from 15 to 69% in SN after 14 days (data not shown). N_2O was below the detection limit (i.e. 0.1%) during denitrification likely due the large availability of biodegradable organic carbon [287]. N_2O is a greenhouse gas with a stronger impact than carbon dioxide. The absence of N_2O formation confirms the sustainability of biological PHE removal under denitrifying conditions, not leading to the release of high–impact gas streams.

After 21 days (Figure 2.1b), the cumulative biomethane production was lower ($p < 0.05$) in DS (i.e. 23 mL $CH_4 \cdot g\ VS^{-1}$) than DA and D (i.e. 61 and 39 mL $CH_4 \cdot g\ VS^{-1}$, respectively). The observed sulfate reduction of approximately 1,000 mg $SO_4^{2-} \cdot L^{-1}$ in DS (data not shown) suggests that sulfate reducing bacteria likely outcompeted other anaerobic microorganisms, such as methanogenic archaea [288,289]. Therefore, the limited biomethane yield in DS coupled to the low PHE removal (Figure 2.1a and 2.1b) probably indicated that methanogenesis promoted the anaerobic PAH degradation, as also reported by Chang et al. [152].

After 42 days (Figure 2.1b), S resulted in a higher ($p < 0.05$) cumulative biomethane yield (i.e. 273 mL $CH_4 \cdot g\ VS^{-1}$, respectively) than SN, DS, DA and D (i.e. 103, 29, 103 and 73 mL $CH_4 \cdot g\ VS^{-1}$, respectively), indicating a higher biomethane potential of sewage sludge than the digestate most likely due to a lower organic stability.

The total VFA evolution during 42 days of bioremediation under all operating conditions (i.e. SN, S, DS, DA and D) is shown in Figure 2.1c, with the highest VFA concentrations being observed after 7 days. S showed a significantly higher ($p < 0.05$)

VFA accumulation (i.e. 6,173 mg HAc·L^{-1}) than SN, DS, DA and D (i.e. 2,467, 879, 3,181 and 1,064 mg HAc·L^{-1}, respectively). The sewage sludge resulted in a higher VFA yield (i.e. 113 mg HAc·g VS^{-1}) than digestate (i.e. 22 mg HAc·g VS^{-1}), again demonstrating a higher biodegradability.

VFA concentrations significantly decreased ($p < 0.05$) from day 14 onwards (Figure 2.1c) due to the activity of methanogens inoculated with both sewage sludge and digestate (Figure 2.1b). In SN and DS, acetate consumption was probably also coupled to nitrate or sulfate reduction, as discussed above. Further information about specific VFAs are reported in the supporting information accompanying the manuscript (data not shown).

2.3.2 Sediment washing

PHE removal after 1, 2, 5, 15, 30 and 60 min with ETOH washing at S:L ratios of 1:3, 1:5 and 1:10 is shown in Figure 2.2. The removal of PHE from the contaminated sediment was regulated by the partition coefficient in the solution phase, in agreement with the general behavior of hydrophobic compounds [290,291]. Hence, the partitioning process may be summarized in two phases (Figure 2.2): (a) a first phase (the initial 5 minutes), where the labile fraction of PHE (i.e. about 70%) was readily desorbed; (b) a second phase (between 5 and 60 minutes), where the residual PHE fraction (i.e. about 30%) was slowly extracted due to the equilibrium between solid and liquid phase.

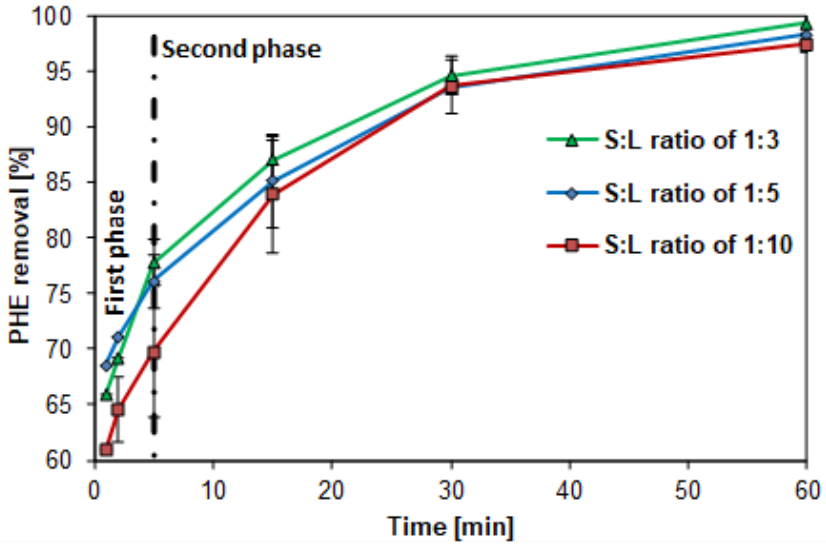

Figure 2.2 – PHE removed [%] from contaminated sediment at different time points by an ETOH/water washing agent (50/50%, w/w) using different solid–to–liquid (S:L) ratios (i.e. 1:3, 1:5 and 1:10).

Error bars indicate deviation standard values of analyses in triplicate.

After 60 minutes (Figure 2.2), no statistical differences ($p > 0.05$) were observed among the different S:L ratios and more than 97% of PHE was removed, suggesting that 1.5 g of ETOH was sufficient to treat efficiently 1 g of sediment, as observed for an S:L ratio of 1:3. These findings are highly important because the reduction of contact time and S:L ratio (i.e. 60 minutes and 1:3, respectively) during sediment washing may involve a less capacity of sediment washing plant. Moreover, one washing time was sufficient to extract more than 90% of PHE from the sediment, decreasing the operational costs [165] and allowing ethanol to be recovered by distillation with a loss of about 10% [173].

In this thesis, the obtained PHE extraction (Figure 2.2) was probably enhanced by a low organic matter content in the sediment (Table 2.1) being PAHs lipophilic compounds. Sun et al. [242], indeed, showed that PHE removal increased (i.e. 94, 71, 38 and 24%) with the decreasing of organic carbon in soil (i.e. 0.79, 1.36 1.88, and 2.33%, respectively). Similarly, Yap et al. [243] obtained a sediment washing efficiency of 80% with a co–solvent volumetric fraction and an S:L ratio of 0.8 and 1:2, respectively. In this work, the used co–solvent volumetric fraction (i.e. 0.6) enhanced PHE extraction because the micro–emulsion effect of alcohol molecules on the water structure was presumably improved, as also reported by Dougan et al. [292] in a methanol/water system.

2.3.3 Thermal desorption

The residual PHE (%) during 60 minutes of thermal desorption at 100, 150 and 200°C is illustrated in Figure 2.3. After 5 minutes, no significant PHE removal ($p > 0.05$) was observed as PHE presumably remained in the sediment as melted [245]. Thermal desorption started after 15 minutes (Figure 2.3) and PHE removal was higher ($p < 0.05$) at 200°C (i.e. 47%) than at 150°C (i.e. 12%). At 100°C, PHE was not desorbed ($p > 0.05$) probably because a higher temperature than the PHE melting point (i.e. 101°C) was necessary to promote desorption [246]. The desorption mechanism followed the thermodynamic principle, with the desorption of PHE increasing at higher temperatures, which allowed the breakdown of benzene rings [293]. After 60 minutes (Figure 2.3), PHE was desorbed by 32 and 88% ($p < 0.05$) at 150 and 200°C, respectively, following an exponential kinetics with a correlation coefficient of 0.97, as also reported by Smith et al. [245].

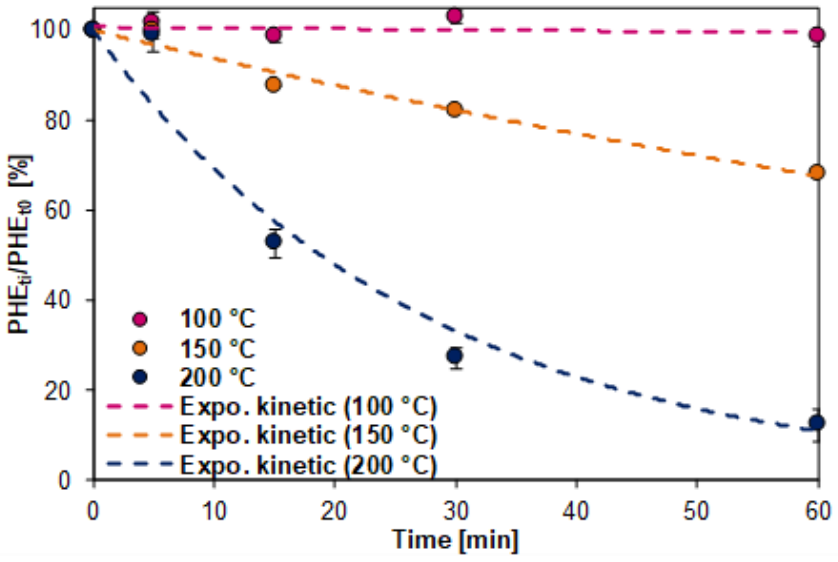

Figure 2.3 – Ratio [%] between the PHE concentration at time "t" and that at time "t_0" in the contaminated sediment during 1 hour of thermal desorption.

The lines are referred to an exponential kinetic model with a R^2 of 0.97. Error bars indicate deviation standard values of analyses in triplicate.

The results obtained showed that PHE removal was efficiently accomplished at 200°C, suggesting that the operating temperature and PHE vapor pressure (i.e. 10^{-2} Pa) positively influenced PHE desorption [294]. A higher PHE desorption to nearly 100% could be obtained increasing the temperature to 250°C, as reported by Renoldi

et al. [224]. However, too high temperatures can result in the PAH isomerization, i.e. the transformation of a specific PAH into more reactive PAHs [15]. PHE isomerization did not probably occur in this work since the chromatographic analysis did not show any other peak than PHE.

2.3.4 Techno–economic feasibility

The experimental conditions resulting in the highest PHE removal, which were SN (i.e. 68%), S:L ratio of 1:3 (i.e. 97%) and low temperature thermal desorption (i.e. LTTD) at 200°C (i.e. 88%) for bioremediation, sediment washing and thermal desorption, respectively, were selected for the economic analysis. The costs of remediation obtained by using in RACER the input data (Table 2.2) for each ex–situ treatment investigated are reported in Table 2.3. Bioremediation had the lowest total cost (i.e. 274 €·m^{-3}), followed by sediment washing and LTTD (i.e. 371 and 1,782 €·m^{-3}, respectively).

Using bioremediation, the main costs (data not shown) were associated with the structural slab and bioreactor (i.e. 33 and 28% of the total cost, respectively). The highest costs of sediment washing (data not shown) were related to the washing system and operation labor (i.e. 37 and 20% of the total cost, respectively), while the cost for LTTD (data not shown) was mostly due to the thermal desorption equipment and heating (i.e. 95%). The mobilization of the contaminated sediment accounted for less than 3% of total cost for all the remediation technologies due to the short selected distance (i.e. 1.6 km) between the treatment plants and the contaminated site. Moreover, the cost for liquid treatment prior to disposal/demobilization must not be neglected during sediment washing (i.e. 2%), although RACER does not consider the distillation process for ETOH recovery and cost saving, as discussed in subsection 2.3.2. Compared to sediment washing, bioremediation is more expensive in terms of materials consumed for bioreactor construction due to a longer retention time that requires the use of higher reaction volumes [295]. On the other hand, the labor cost is higher in sediment washing likely due to more significant manpower for a continuous load of sediments, admixture of chemicals and plant maintenance. Regarding LTTD, the energy used for the heating furnace may justify the highest cost of equipment, as reported in subsection 2.3.5.

These results (Table 2.3) suggest that the use of bioremediation provides an economic benefit [296]. Nevertheless, bioremediation is affected by PAH bioaccessibility (subsection 2.3.1.1) that does not allow a complete PHE removal (Figure 2.1a) and requires large bioreactor volumes due to a long PAH biodegradation

time (i.e. 14 days). Sediment washing leads to higher overall costs as a result of repeated charging and discharging of the washing system (Table 2.3), but also a higher PHE removal (Figure 2.2). In each case, the reuse of the remediated sediments (e.g. for coastal replenishment and road–under surfaces) should be also taken into consideration in order to provide a more in–depth techno–economic analysis of the most suitable remediation technology. In contrast, the use of thermal desorption is not recommended due to the lower efficiency (Figure 2.3) than sediment washing at the same retention time (i.e. 1 hour) and the higher cost of remediation (Table 2.3) that must be added to the costs of dredging (i.e. 1,290 €·m^{-3}) [249], always accounted for an ex–situ sediment treatment.

2.3.5 The water–energy–nexus

This thesis shows that decreasing the operating temperature (i.e. 200°C or lower) and the amount of liquid phase used (i.e. 60% water content and S:L ratio of 1:3 for bioremediation and sediment washing, respectively) is a more efficient approach to remediate PHE–contaminated sediments in terms of both removal percentages and costs. On top of this, the energy balance should also be considered during the selection of the most appropriate remediation technology. Indeed, the reduction of energy consumption and the rational use of water resources are two of the objectives of the water–energy nexus [251].

The energy required for each remediation condition here considered, i.e. SN, S:L ratio of 1:3 and LTTD at 200 °C, and obtained by Eq. (2.1), RACER software and Eq. (2.3), respectively, is reported in Table 2.3. LTTD resulted in the highest energy consumption (i.e. 417 kWh·m^{-3}), followed by bioremediation and sediment washing (i.e. 48 and 14 kWh·m^{-3}, respectively). Sediment washing required a lower energy since the process was conducted under milder conditions (i.e. ambient temperature). The use of higher temperatures during bioremediation and LTTD led to an increase of the energy consumption. However, the biomethane produced during bioremediation allowed the recovery of 21 kWh·m^{-3}, with an overall energy balance of –27 kWh·m^{-3}. For a further comparison, the condition resulting in the highest ($p < 0.05$) biomethane yield and similar ($p > 0.05$) PHE removal (i.e. S) was also considered. The energy recovered by using biomethane in a CHP unit raised to 32 kWh·m^{-3} (net energy balance of –16 kWh·m^{-3}, similar to that obtained with sediment washing), and the overall costs decreased to 228 €·m^{-3} as nitrate supplementation was not necessary.

These results (Table 2.3) show that the energy consumption was probably the main impact factor of total cost during thermal desorption, as discussed above. Sediment

washing suggests that the energy used for the process is not always a function of the total cost [295], and other parameters such as operation labor are also important. During anaerobic bioremediation of PHE–contaminated sediment, the biomethane production may be an opportunity to heat the anaerobic bioreactor leading to cost and energy savings and a lower environmental impact [276]. However, the cost of collecting biomethane and burning it safely should be also considered for the scale up of the technology.

2.4 Conclusions

PHE is particularly widespread in marine environment, and the costs of common disposal methods for contaminated sediments have induced to find more eco–friendly and sustainable solutions. In this chapter, anaerobic bioremediation, sediment washing and thermal desorption allowed to effectively remediate PHE–contaminated sediments with low organic content (i.e. 0.36 g TOC·kg TS^{-1}) decreasing the PHE amount by 68, 97 and 88%, respectively, using a low liquid phase (i.e. 60% and S:L ratio of 1:3) and low temperature (i.e. 200°C). A cost assessment, conducted by implementing the retention time and temperature of laboratory scale experiments in the RACER software and accompanied by an energy balance, revealed that anaerobic bioremediation was the least demanding technology in terms of costs (i.e. 228 €·m^{-3}) and required a similar energy consumption (i.e. –16 kWh·m^{-3}) to sediment washing. On the other hand, sediment washing was more effective in PHE removal and, therefore, the choice of the most sustainable technology would depend on the contamination threshold values imposed by the national legislation.

Table 2.3 – Total cost [€·m^{-3}], energy balance [kWh·m^{-3}] per unit of volume of sediment treated, and PHE removal efficiency [%] obtained with bioremediation, sediment washing and thermal desorption.

Ex–situ remediation	**Total cost [€·m^{-3}]**	**Required energy [kWh·m^{-3}]**	**Recovered energy [kWh·m^{-3}]**	**Energy balance [kWh·m^{-3}]**	**PHE removal efficiency [%]**
*Bioremediation**	274	48	21	–27	68
*Bioremediation***	228	48	32	–16	53
Sediment washing	371	14	0	–14	97
Thermal desorption	1782	417	0	–417	88

* = SN; ** = S

SN = contaminated sediment + sewage sludge + 2,000 mg·L^{-1} of nitrate; S = contaminated sediment + sewage sludge; Sediment washing = S:L ratio of 1:3; Thermal desorption = 200°C.

CHAPTER 3. REMOVAL OF POLYCYCLIC AROMATIC HYDROCARBONS DURING ANAEROBIC BIOSTIMULATION OF MARINE SEDIMENTS

3.1 Introduction

Polycyclic aromatic hydrocarbons (PAHs) are a group of total petroleum hydrocarbons known to be carcinogenic and mutagenic [144,297,298]. These organic pollutants are naturally released into the environment from petrogenic and pyrogenic sources [299]. However, most of them are produced by human activities such as gas emissions deriving from industrial processes, agricultural activities and household heating [300]. As a result of atmospheric deposition, PAHs migrate to soils and aqueous matrices [228] and highly accumulate in sediments due to their low water solubility and hydrophobic nature [301,302]. PAHs may even be released by accidental discharge during transport, use, or disposal of petroleum products [3]. Many studies have reported and quantified PAH accumulation in marine sediments worldwide [303–305]. When sediments are dredged to promote the navigation of deep hull boats, the high amount of pollutants sorbed onto the sediments results in waste management concerns [11]. Dredged sediments can be re–used or landfilled if the contamination levels are below the legislation limits [232], whereas a remediation is required when the threshold values are exceeded. Among the available remediation techniques, bioremediation represents an eco–friendly approach as microorganisms are used to remove contaminants from soils and sediments [234].

Biostimulation and bioaugmentation are commonly employed as bioremediation strategies. Biostimulation consists in the supplementation of nutrients (i.e. N, P and K) [236] or amendments such as fertilizers, municipal sewage sludge, compost, organic wastes and humic substances [235] to enhance the activities of autochthonous microbial populations. In bioaugmentation, indigenous or exogenous PAH degrading bacteria are

seeded in the polluted soil to increase the remediation efficiency [105]. In some cases, biostimulation and bioaugmentation are used simultaneously [135]. A lot of factors influence the degradation rates such as pH, water content, C/N ratio, oxygen content, temperature, site characteristics, and the concentration of contaminants [279,306,307]. In particular, the PAH bioaccessibility, meant as the available part of contaminant for biological conversion [241], plays an important role in PAH–contaminated soil bioremediation. A low PAH bioaccessibility usually reduces the bioremediation efficiency being these complex molecules highly recalcitrant to microbial degradation [308]. The use of surfactants has been proposed to improve the bioaccessibility and biodegradability of PAHs [250,309]. However, a higher bioaccessibility may result in an increase of the releasable PAH amount and, thus, the related environmental risk [283].

Biostimulation has more extensively been applied under aerobic conditions during composting of PAH–containing soils [135,310–313]. Anaerobic biostimulation has instead larger margins for interesting scientific evidences. Recent studies tested compost, pig dung, NPK fertilizer and biochar as biostimulating agents to enhance PAH degradation in soil and sediments under methanogenic, sulfate and nitrate–reducing conditions [238,239,248]. Up to date, literature lacks of studies investigating in detail the variation of the PAH bioavailable fraction during biostimulation and the composition of the anaerobic digestion metabolites. Moreover, no studies have so far given an emphasis on the correlation between PAH degradation and the steps of anaerobic digestion.

In this thesis, the use of digestate and fresh organic fraction of municipal solid waste (OFMSW) to improve PAH biodegradation in contaminated marine sediments under anaerobic conditions has been proposed for the first time. Digestate is a semi–stabilized by–product of anaerobic digestion, rich in carbon, nutrients (i.e. nitrogen and phosphorous) and microorganisms [314,315]. OFMSW is a heterogeneous material consisting of a mixture of food, garden wastes and paper [316], and characterized by high humidity and biodegradability [317]. The application of digestate and OFMSW as amendments for the biostimulation of PAH–contaminated sediments represents a promising reuse strategy in a perspective of circular economy.

The specific objectives of this chapter were to 1) investigate the effect of the amendments on PAH removal and bioaccessibility, 2) characterize the volatile fatty acids (VFAs) and biogas composition, 3) find a relationship between the evolution of PAH degradation and anaerobic digestion, 4) model the PAH degradation with biphasic first–order kinetic.

3.2 Materials and methods

3.2.1 Sediment

Fifteen kg of uncontaminated marine sediments were manually collected from the seaside of Formia (Lazio Region, Italy) at approximately 1 m depth from the sea level, prior to being placed in a hermetic glass vessel, transported to the laboratory and finally stored at room temperature. The physic–chemical characteristics of the sediment are reported in Table 3.1. After characterization, the sediment was dried at 50 °C in a laboratory oven for 48 hours and passed through a 2–mm mesh [318] to remove the coarse fraction.

3.2.2 Amendments

Digestate and OFMSW were used as inoculum and sources of extra organics in the biostimulation experiments. The digestate was obtained from a full–scale anaerobic digester located in Capaccio (Campania Region, Italy) treating buffalo manure and cheese whey. OFMSW consisted of a mixture of food waste taken from the canteen of University of Cassino and Southern Lazio, spent coffee and garden waste. The properties of the digestate and OFMSW used are reported in Table 3.1.

Table 3.1 – Physical–chemical characterization of the uncontaminated sediment, digestate and OFMSW.

Material	pH	%TS	%VS	TOC (g·kg TS^{-1})	TKN (g·kg TS^{-1})	EC ($mS \cdot cm^{-1}$)
Sediment	7.85±0.05	79.47±0.03	1.42±0.03	1.76±0.97	*	1.92±0.40
Digestate	8.57±0.02	6.99±0.46	3.99±0.34	66.14±1.66	29.08±2.66	1.86±0.13
OFMSW	4.53±0.04	30.86±0.49	29.68±0.58	81.37±1.00	2.96±0.29	0.72±0.01

***** = below the detection limit of 0.5 $mg \cdot kg^{-1}$; TS = total solids; VS = volatile solids; EC = electrical conductivity; TOC = total organic carbon; TKN = total Kjeldahl nitrogen. Mean and standard deviation values were calculated on n = 3 replicates.

3.2.3 Procedure for sediment spiking

The selected PAHs were phenanthrene (PHE, grade ≥98%), anthracene (ANT, grade ≥99%), fluoranthene (FLU, grade ≥98%) and pyrene (PYR, grade ≥98%), all purchased from Sigma–Aldrich (Germany). 1,000 mg of each PAH was dissolved in 3 L acetone (VWR, Italy grade 100%) and added to each portion of uncontaminated sediment (5 kg)

to obtain an initial PAH concentration of 200 $mg \cdot kg^{-1}$ dry sediment [253,254]. This initial PAH concentration was chosen to simulate the contamination values found in previous studies [255]. Subsequently, the contaminated sediment (CS) was manually mixed and placed under a fume hood for 72 h to evaporate the solvent [256]. Finally, with the aim to reproduce the "natural aging" of the sediments and promote the sorption of PAHs onto the sediment particles, the CS was stored for 6 months in darkness at room temperature based on the aging procedure described by Lukić et al. [257].

3.2.4 Experimental setup

Biostimulation experiments were conducted using 100 mL serum bottles (Figure S1), with each bottle containing 10 g of dry sediment mixed with amendment at a ratio of 10:1 (dry w/dry w) [260], and a moisture content of 60% to ensure microbiological activity. Five operative conditions, i.e. CS + digestate (D), CS + digestate and nutrients (DN), CS + OFMSW (O), CS + OFMSW and nutrients (ON), and CS + digestate and OFMSW (DO) were investigated. The nutrient solution consisted of (in $mg \cdot L^{-1}$ distilled water): 505.00 KNO_3, 295.00 $Ca(NO_3)_2 \cdot 4H_2O$, 493.00 $MgSO_4 \cdot 7H_2O$, 68.00 KH_2PO_4 (Sigma–Aldrich, Germany grade ≥98%), 22.50 EDTA iron (III) (VWR, Italy grade ≥ 12.5%) as macronutrients, and 2.86 H_3BO_3, 1.81 $MnCl_2 \cdot 4H_2O$, 0.22 $ZnSO_4 \cdot 7H_2O$, 0.05 $CuSO_4 \cdot 5H_2O$, 0.12 $Na_2MoO_4 \cdot 2H_2O$ (VWR, Italy grade ≥98%) as micronutrients [319]. The selected nutrients have been reported to be optimal for plant growth, but were added to CS to further stimulate the degradation of organic matter by microorganisms, as reported by Khaliq et al. [320]. Indeed, Leys et al. [321] observed a similar N/P of 14:1 as optimal ratio for PAH–contaminated soil biostimulation.

For each condition, 30 identical bottles were used. N_2 was used as inert gas to flush the bottles and ensure strictly anaerobic conditions. Subsequently, all the bottles were aseptically sealed with rubber septa and aluminum crimps, prior to being incubated in a water bath under mesophilic conditions (i.e. at 37±1 °C) [248] for 120 days and placed on a gyratory shaker at 130 rpm [322]. For each condition, samples were collected after 3, 10, 20, 30, 40, 50, 60, 70, 90 and 120 days by sacrificing 3 bottles at a time. In addition, a volatilization system using activated carbon as sorbent [323] was set up in a temperature–controlled chamber at 37±1 °C to discriminate PAH volatilization from biological treatment.

Control tests were run without amendments to monitor PAH removal in the presence of only CS and water. Other controls were operated in the absence of CS to evaluate the biogas production yield from digestate and OFMSW under the five different conditions, which was then used to calculate the net biogas production in the presence of CS.

Furthermore, a biocide experiment in presence of 2,000 mg·$HgCl_2$ kg^{-1} of CS (VWR, Italy grade ≥99.5) was also performed to exclude any abiotic PAH removal mechanism [324].

3.2.5 Analytical procedures

Total solids (TS) and volatile solids (VS) were measured according to APHA [325] and U.S. EPA [326]. The pH was measured in a 1:2 (sample:water) suspension [244] using a Sentix/940 pH–electrode (WTW, USA). The electrical conductivity (EC) was determined by measuring the electrical resistance of a 1:5 (sample:water) suspension [266] with a TetraCon/925 (WTW, USA) conductivity cell. Total organic carbon (TOC) was extracted by 0.1 mol·L^{-1} of pyrophosphate and sodium hydroxide [232] and quantified with a TOC–L Series (Shimadzu, Japan) equipment. The analyses of total Kjeldahl nitrogen (TKN) were performed to measure the concentration of ammonia–N and organic–N according to the method proposed by Kjeldahl [327] using a K–425 speed digester (Büchi, Switzerland). Sulfate concentrations were analyzed by ion chromatography (IC) using an 883 Basic IC Plus (Metrohm, Switzerland) as reported by Kiskira et al. [268].

PAHs were extracted from CS samples as described by Sun et al. [269]. A CS sample of 0.5 g was dried and then placed in a 25 mL flask with 10 mL acetone (VWR, Italy grade 100%) and 1 mL of 50 mg·L^{-1} benzo[a]pyrene (B[a]P) (Sigma–Aldrich, Germany grade ≥96%) solution as internal standard (recovery efficiency of 99±3%). Afterwards, the flask was ultra–sonicated at 40 °C for 30 minutes before filtering the sample on a 0.45 μm glass microfiber filter (Whatman, USA) prior to analysis. PAHs were analyzed using a LC–20AD HPLC (Shimadzu, Japan) equipped with a Kinetex® 3.5 μm PAH (150x4.6 mm) column (Phenomenex, USA) heated at 35 °C and an SPD–20A UV detector (Shimadzu, Japan) set at 254 nm. A water/acetonitrile (VWR, HPLC grade) solution (50:50) was used as eluent phase at a flowrate of 1.2 mL·min^{-1} [328].

For the determination of PAH bioaccessibility, a solution with 20 mL butanol (VWR, Italy grade ≥96%) and 1 mL of 50 mg·L^{-1} benzo[a]pyrene (B[a]P), was placed in a 25 mL flask. Afterwards, 2 g of sediment and 2 g of anhydrous Na_2SO_4 (Sigma–Aldrich, Germany grade ≥99%), were added. Then, the flask was shaken on rotary tables at 160 rpm for 16 hours [85,270]. The extracted sample was filtered on a Whatman glass microfiber filter (0.45 μm) before analysis.

Biogas production was measured after 3, 10, 20, 30, 40, 50, 60, 70, 90 and 120 days in the biostimulation experiments with a water displacement method [271]. The biogas produced in the control experiments without PAHs was subtracted from that achieved in

the bottles with CS. The biogas composition in terms of CH_4, CO_2 and H_2 was analyzed using a 3400 GC–TCD gas chromatograph (Varian–Agilent, USA) equipped with a Restek Packed column [329] and using argon as gas carrier.

Total VFAs, expressed in equivalent of acetic acid (mg HAc·L^{-1}), were monitored as anaerobic digestion metabolites. Formic, acetic (HAc), propionic, *iso*–butyric (HiB), *n*–butyric (HnB), *iso*–valeric, *n*–valeric, *iso*–caproic, hexanoic and heptanoic acids were determined as reported by Mancini et al. [272]. The samples were centrifuged at 10,000 rpm for 5 min, and the supernatant was properly diluted and analyzed with the HPLC above described. A Rezex ROA–Organic Acid H^+ column (Phenomenex, USA) heated at 40 °C and an SPD–20A UV detector (Shimadzu, Japan) set at 210 nm were used. A water solution with 0.67 g·L^{-1} of sulfuric acid (VWR, Italy grade ≥96%) was used as mobile phase at a flowrate of 0.8 mL·min^{-1}.

3.2.6 PAH degradation kinetics

PAH degradation kinetics were evaluated for each biostimulation test. K_1 and K_2, considering a biphasic first–order kinetic model [330,331], were calculated using the following equations:

$C(t) = C_0 \cdot e^{-K_1 \cdot t}$ when $t \leq t_b$ (Eq. 3.1)

$C(t) = C_0 \cdot e^{-K_1 \cdot t_b} \cdot e^{-K_2 \cdot (t - t_b)}$ when $t > t_b$ (Eq. 3.2)

where C_0 is the initial PAH concentration; K_1 and K_2 (d^{-1}) are the fast and slow PAH degradation rates, respectively, and t_b (d) is the time at which the degradation rate changes.

3.2.7 Statistical analyses

The obtained data were analyzed by one–way analysis of variance (ANOVA) followed by a Tukey test to evaluate statistically significant differences between the tested operating conditions. The correlation between different parameters was estimated by the standard Pearson sample correlation coefficient ($r_{variable1–variable2}$) with both–sided alternative. All statistical analyses were performed with XLStat statistical software for Microsoft Excel (2019.1.3 version, Addinsoft, USA). Statistical significance was assumed at $p < 0.05$.

3.3 Results and discussion

3.3.1 PAH removal with digestate, OFMSW and nutrients as amendments

PAH removal was observed under all the operating conditions after 120 days of anaerobic biostimulation (Figure 3.1). During the volatilization test, the presence of PAHs in the volatile phase was negligible (data not shown), as also reported by Loehr et al. [332]. Furthermore, the PAH concentration did not decrease in the biocide test (data not shown), indicating that the PAH removal in the biostimulation tests could be attributed to microbial activity.

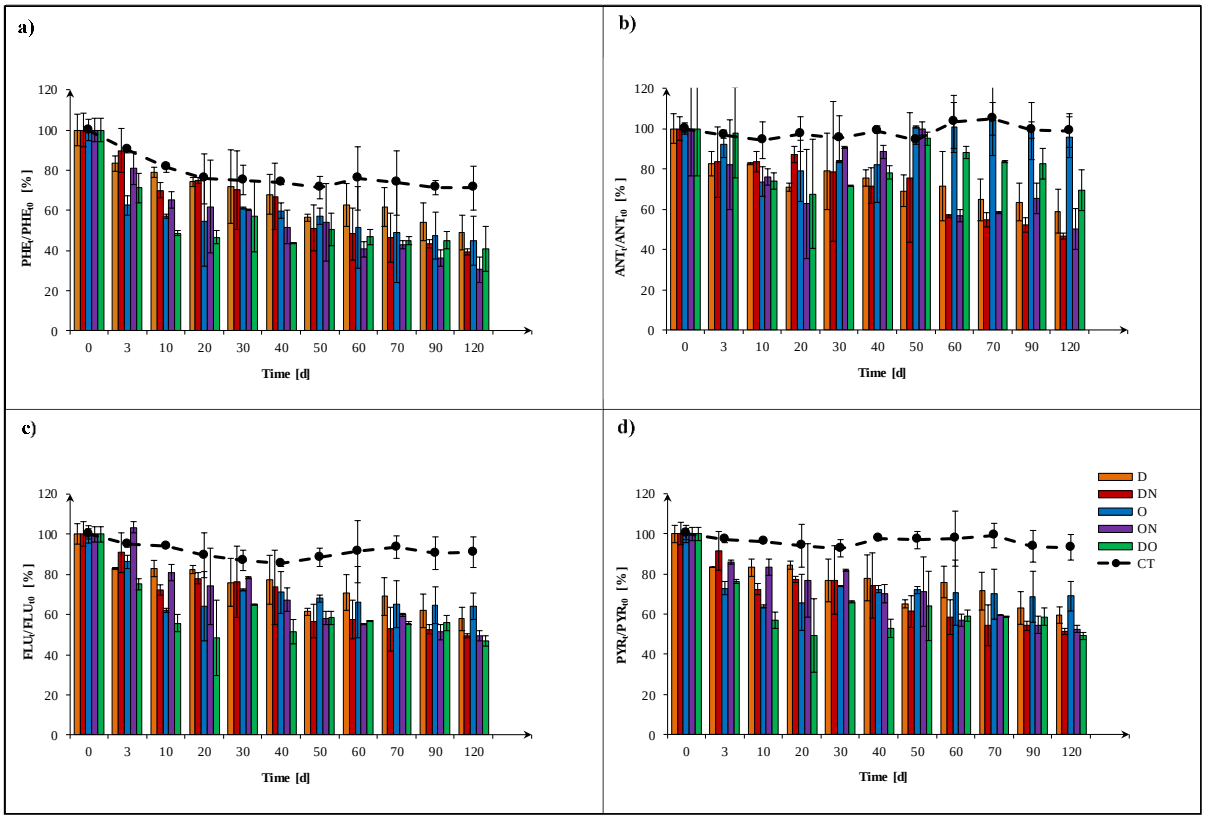

Figure 3.1 – Ratio [%] between the concentration at time "t" and that at time "t_0" [d] of PHE (a), ANT (b), FLU (c) and PYR (d) in the contaminated sediment during the 120 days of anaerobic biostimulation.

D = CS + digestate; DN = CS + digestate and nutrients; O = CS + OFMSW; ON = CS + OFMSW and nutrients; DO = CS + digestate and OFMSW; CT = control test. Error bars indicate the standard deviation values of analyses in triplicate.

The total PAH degradation ranged between 10 and 20% in the first 3 days. The use of mesophilic conditions over ambient temperature probably decreased the soil–water partition coefficient [333] enhancing the PAH dissolution in water and bioaccessibility [273]. Coover and Sims [334] showed that increasing the temperature from 10 to 30 °C enhanced PAH degradation in the first 60 days. Also, the increase of pH presumably played an important role in stimulating the PAH degradation. Kästner et al. [335] observed that a rise of pH led to an increase of the active microbial community and a consequent higher PAH removal. In this study, the total PAH degradation increased to 25÷45% under all experimental conditions from day 4 to day 40 (Figure 3.1), when pH raised from 6.0 to 6.4 in O, from 6.0 to 8.0 in ON, from 7.8 to 8.4 in D and DN, and from 7.5 to 8.1 in DO (data not shown). Subsequently, pH remained constant probably due to

the soil buffer, which released ions (H_3O^+ and HCO_3^-) in water during the production of carbon dioxide [321].

In the lapse of time between 3 and 20 days, sulfate decreased by 73÷92% (data not shown) from an initial concentration of approximately 300 mg $SO_4^{2-} \cdot L^{-1}$ in D, DN (i.e. after 3 days) and DO (i.e. after 10 days), most likely due to biological sulfate reduction. During the conversion to sulfide, sulfate can be used as terminal electron acceptors in favor of PAH degradation [140]. However, a low total PAH degradation (less than 9%, Figure 3.1) occurred in D, DN and DO during this period, indicating that sulfate reduction slightly contributed to PAH removal. This is corroborated by a similar PAH removal efficiency obtained in O and ON where sulfate reduction was not observed, probably due to the absence of sulfate–reducing bacteria in OFMSW. These results suggest that PAH degradation was coupled to the reduction of other electron acceptors, such as carbon dioxide, under methanogenic conditions (as discussed in section 3.3.4).

After 120 days, the PAH degradation in D (i.e. 43%) and DO (i.e.48%) was higher ($p < 0.05$) than in O (i.e. 31%) (Figure 3.1), indicating that the use of digestate as organic amendment was more effective than OFMSW because simultaneously induced a biostimulation and a bioaugmentation of the PAH–contaminated sediment. Furthermore, the combination of digestate and OFMSW positively affected the total PAH degradation probably because the addition of OFMSW balanced the C:N ratio to 5:1. Similarly, Frutos et al. [259] observed a higher PAH biodegradation at a C:N ratio of 5:1 with a moisture content of 60%. The addition of the nutrient solution enhanced PAH removal in DN and ON ($p < 0.05$), reaching similar degradation of 53 and 55% ($p > 0.05$), respectively, after 120 days. The lowest PAH degradation ($p < 0.05$) was observed in CT (i.e. 12%), confirming the efficacy of biostimulation in PAH–contaminated soil remediation.

Similarly, Zhang and Lo [146] observed a total petroleum hydrocarbons removal of approximately 53% in marine sediments after 30 weeks of biostimulation with 20 mmol of methanol. However, Sayara et al. [248] showed a total PAH removal of 84÷87% after 50 days of treatment, with an initial PAH concentration of about 1,000 mg·kg TS^{-1}. The discrepancy with this study can be explained by the fact that Sayara et al. [248] worked under wet conditions (i.e. TS of 10 %), which likely increased the hydrolysis rate and reduced the physical limitation related to mass transfer [247].

With regard to the specific PAHs, the removal of PHE was higher ($p < 0.05$) than that achieved for the high molecular weight PAHs (HMWs) since a lower molecular weight results in a higher PHE degradability [322]. After 20 days, PHE degradation was higher ($p < 0.05$) in O, ON and DO (i.e. 44, 38 and 53% respectively) than D and DN (i.e. 26%) before considerably slowing down. However, PHE removal resumed in ON from day 50

onwards and raised up to 69% after 120 days ($p < 0.05$). Moreover, after 120 days no statistically differences were observed between D and DN ($p > 0.05$), and PHE removal reached a final value of 51 and 61% (Figure 3.1 a), respectively. A PHE degradation of 29% ($p < 0.05$) was also observed in CT probably due to existing microbes, which were capable to use PHE as carbon source [336].

ANT degradation rate was lower ($p < 0.05$) than that achieved with PHE, and this was probably due to its low aqueous solubility [337]. When OFMSW was used as amendment, the biodegradation of ANT markedly fluctuated (Figure 3.1 b). In the first 20 days, ANT was degraded by about 25% but ANT concentration increased back to the initial value after 50 days ($p > 0.05$). Then, ANT removal started again and reached almost 30 and 50% in DO and ON ($p < 0.05$), respectively. An increase of PAH concentration in soil during biostimulation can occur under anaerobic conditions due to a reversed PAH biotransformation. This process involves the condensation of PAH–rings to other forms of PAHs under oxygen deficient conditions [338,339]. This trend was not observed in D and DN, where ANT degradation was statistically different ($p < 0.05$) reaching a final removal efficiency of 41 and 53%, respectively.

The presence of organic co–substrates enhanced HMW (i.e. FLU and PYR) biodegradation by about 30÷40% ($p < 0.05$) compared to CT. After 10 days, FLU was biodegraded by 12, 28, 38, 19 and 44% in D, DN, O, ON and DO ($p < 0.05$), respectively (Figure 3.1 c). FLU removal restarted after 30 days and reached 42 and 50% in D and DN ($p < 0.05$), respectively. In ON, FLU reduction followed a linear trend from day 40 onwards, with a final removal percentage of 51%. However, after 120 days the FLU removal was similar between DN, DO and ON ($p > 0.05$). PYR removal (Figure 3.1 d) was similar to that obtained for FLU ($r_{PYR–FLU} = 0.99$). Patel et al. [340] showed that FLU degradation increased from 31 to 67% after 9 days in the presence of a NPK fertilizer as amendment, confirming the positive impact of biostimulation on HMW biodegradation.

3.3.2 Evolution of PAH bioaccessibility during biostimulation

The bioavailable concentrations of all PAHs at "t_0" and "t_{120}" (d) are reported in Table 3.2. After the aging time (6 months), the bioavailable percentage of PAHs in the sediments (CT) was 50, 39, 46 and 56% of the total concentration for PHE, ANT, FLU and PYR, respectively. These percentages are comparable to those reported for other PAH–contaminated marine sediments in the literature [3,66,282,341,342].

Under all biostimulating conditions, the initial bioavailable concentration of PAHs was higher than that in CT, with a statistically significant difference ($p < 0.05$) observed in D, DN and DO. This was probably supported by the presence of humic acids in the digestate

[343] and probably explained the linear trend of ANT degradation occurred in D and DN in the first 120 days ($p < 0.05$) and the fast HMW degradation ($p < 0.05$) observed in DO after 10 days of anaerobic biostimulation (Figure 3.1 and Table 3.4). Humic acids presumably acted as surfactants with the aromatic components being capable to interface with PAHs [344], and thereby inducing a higher PAH mass transfer to microorganisms [252]. Similarly, Kobayashi and Sumida (2015) reported that humic acids with a high aromatic property are efficient for sorption of PYR. Liang et al. [346] observed an increase of PYR degradation by indigenous microbes with the addition of humic acids to soil.

After 120 days of biostimulation, the total PAH bioaccessibility significantly decreased ($p < 0.05$) compared to the initial value (Table 3.2). PHE bioaccessibility was reduced by 52, 56, 54, 66 and 45% in D, DN, O, ON and DO, respectively. ANT bioaccessibility was 49, 51, 31 and 50% lower in D, DN, ON and DO, respectively, than that at t_0, with the bioavailable concentration remaining unchanged when ANT was not degraded. The bioavailable concentrations of HMWs decreased by 47, 32, 42, 49 and 53% in D, O, DN, DO and ON, respectively. Interestingly, no significant differences ($p > 0.05$) were observed by comparing the amount of PAH removed in terms of total (Figure 3.1) and bioavailable (Table 3.2) concentration. Moreover, the concentration of not bioavailable PAHs was not statistically different after 120 days ($p > 0.05$) but was still lower than the bioavailable fraction ($p < 0.05$). This shows that the microorganisms could probably degrade only the bioavailable fraction of PAHs, while the not bioavailable PAHs were presumably sorbed onto the sediment particles hindering the microbial activity towards them [347].

The bioaccessibility reduction suggests that biostimulation was effectively capable to reduce the amount of highly accessible PAHs, consequently mitigating the environmental risk [283]. However, PAH bioaccessibility was still higher than 35% and, therefore, a further treatment may be necessary to completely remove the bioavailable PAH fraction. A possible solution could be the continuation of biostimulation for a longer time or the supplementation of amendments several times during the treatment.

- Biogas production and volatile fatty acids evolution

The net cumulative biogas production obtained with all the amendments is shown in Figure 3.2. In O, ON and DO, biogas was only composed by H_2 (i.e. 45, 30 and 12%, respectively) and CO_2 in the first 3 days (data not shown). After 10 days of biostimulation, biohydrogen production was higher ($p < 0.05$) in O and ON (i.e. 80 and 60 mL $H_2 \cdot g\ VS^{-1}$, respectively) than under the other conditions (Figure 3.2 d, e). H_2 percentage in the

biogas gradually decreased until being below the detection limit on day 30 under all the operating conditions.

Biomethane production was observed after only 3 days in D, DN and DO (Figure 3.2 a, b, c). This was probably ascribed to the more acclimated methanogenic microorganisms already existing in digestate that quickly promoted the onset of methanogenesis [348]. Under the ON condition, biomethane was only observed from day 50 on, with the CH_4 percentage increasing up to 70% (the remaining 30% was CO_2) on day 120. A final cumulative production of approximately 140 mL $CH_4 \cdot g\ VS^{-1}$ (Figure 3.2 d) was achieved in ON, i.e. significantly higher ($p < 0.05$) than the 82, 9 and 4 mL $CH_4 \cdot g\ VS^{-1}$ obtained in DO, DN and D, respectively. At the end of the experiment, CH_4 production in ON still showed an increasing trend, indicating that the biomethane yield could have been higher if biostimulation had been prolonged. Compared to what observed in ON, biomethane was not detected in O. As also reported by Ariunbaatar et al. [349], the supplementation of trace metals with the nutrient solution probably stimulated the biomethane production in ON. Moreover the pH in ON was in the optimal range (i.e. 6.5÷8.5) for the activity of methanogens after 40 days [285], whereas pH did not exceed 6.4 in O.

The production and speciation of VFAs was typical of anaerobic digestion (Figure 3.2) [350]. Indeed, VFAs increased when biohydrogen was produced and decreased when biomethane production started. The highest VFA production in O and ON (i.e. 25,000 and 20,000 mg $HAc \cdot L^{-1}$, respectively), was significantly higher ($p < 0.05$) than that obtained in DO, DN and D (i.e. 7,000, 1,700 and 900 mg $HAc \cdot L^{-1}$, respectively) (Figure 3.2), presumably due to the higher content of VS and transformability of OFMSW than digestate [351]. Among the VFAs produced, HAc was the main acid ($p < 0.05$) with a peak of 850, 16,000, 1,600, 4,100 and 14,200 mg $HAc \cdot L^{-1}$ in D, O, DN, DO and ON, respectively. A higher HnB concentration ($p < 0.05$) in O and ON (i.e. about 10,300 and 9,000 mg $HAc \cdot L^{-1}$, respectively) than D, DN and DO (i.e. about 120, 80 and 2,400 mg $HAc \cdot L^{-1}$) was probably associated with the high presence of carbohydrates in the OFMSW [352]. In addition, the presence of *iso*–valeric and *n*–valeric in O, ON and DO (i.e. about 550 and 100, 500 and 150, 150 and 100 mg $HAc \cdot L^{-1}$, respectively) was presumably related to protein fermentation [350]. A rise of pH from 6.0 to 8.0 probably enhanced propionic acid production in ON (i.e. 1,000 mg $HAc \cdot L^{-1}$), as reported by Horiuchi et al. [353].

Table 3.2 – Bioavailable concentration [mg·kg TS^{-1}] of each PAH (PHE, ANT, FLU and PYR) in the contaminated sediment before and after 120 days of anaerobic biostimulation.

Conditions	PHE [mg·kg TS^{-1}]		ANT [mg·kg TS^{-1}]		FLU [mg·kg TS^{-1}]		PYR [mg·kg TS^{-1}]	
	t_0	t_{120}	t_0	t_{120}	t_0	t_{120}	t_0	t_{120}
D	168.81 ± 4.07	81.12 ± 9.16	170.37 ±14.23	87.47 ± 8.48	194.63 ± 5.72	104.06 ± 9.66	180.33 ± 3.72	91.29 ± 6.36
DN	158.17 ± 0.49	69.41 ± 7.65	169.91 ±1.94	83.79 ± 10.82	178.07 ± 2.79	91.40 ± 6.44	142.87 ± 2.90	82.58 ± 5.33
O	106.77 ± 2.14	48.88 ± 1.11	97.97 ±1.66	99.83 ± 4.66	131.06 ± 14.73	90.45 ± 3.57	106.33 ± 4.53	72.62 ± 6.18
ON	113.55 ± 1.41	38.35 ± 13.30	89.45 ±2.48	61.86 ± 2.10	143.91 ± 1.75	66.04 ± 17.60	117.69 ± 3.38	55.04 ± 6.55
DO	129.70 ± 1.44	70.97 ± 7.58	122.88 ±1.44	62.04 ± 7.82	157.56 ± 1.74	81.59 ± 19.01	127.57 ± 1.36	65.13 ± 17.06
CT	100.49 ± 1.51	61.81 ± 5.32	78.65 ±7.55	79.14 ± 3.35	112.85 ± 6.18	95.28 ± 3.54	92.49 ± 0.78	78.05 ± 3.00

D = CS + digestate; DN = CS + digestate and nutrients; O = CS + OFMSW; ON = CS + OFMSW and nutrients; DO = CS + digestate and OFMSW; CT = control. Mean and standard deviation values were calculated on n = 3 replicates.

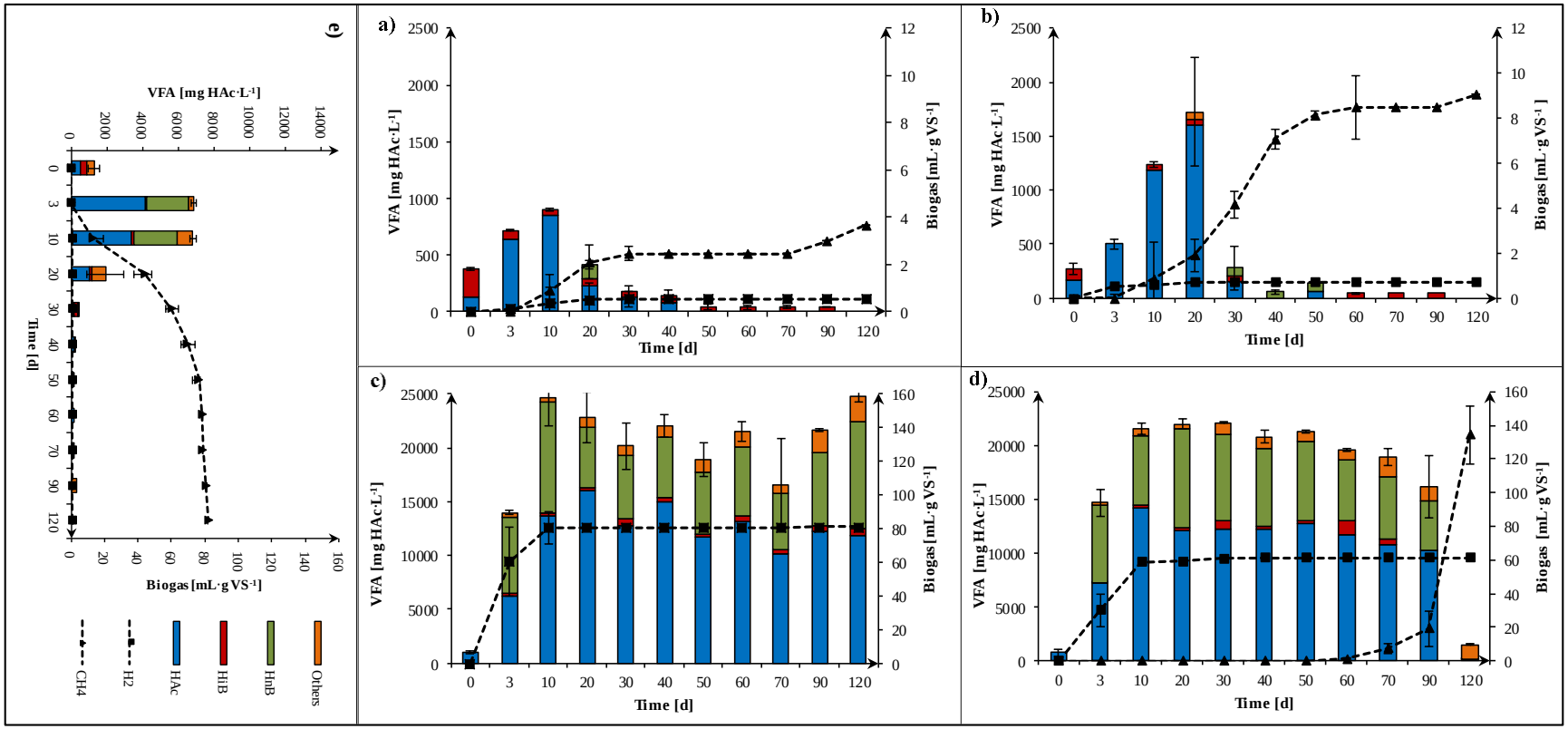

Figure 3.2 – Correlation between cumulative biogas production, in terms of biohydrogen (H_2) and biomethane (CH_4) [mL·g VS^{-1}], and VFA evolution [mg HAc·L^{-1}] during 120 days of anaerobic biostimulation.

a) D = CS + digestate; b) DN = CS + digestate and nutrients; c) O = CS + OFMSW; d) ON = CS + OFMSW and nutrients; e) DO = CS + digestate and OFMSW. HAc = acetic acid; HiB = iso–butyric acid; HnB = n–butyric acid; Others = formic, propionic, *iso*–valeric, *n*–valeric, *iso*–caproic, hexanoic and heptanoic acids. Error bars indicate deviation standard values of analyses in triplicate.

3.3.3 Relationship between PAH degradation and anaerobic digestion

This study shows that microorganisms were stimulated to degrade PAHs and produced biogas by using co–substrates during the biostimulation of a PAH–contaminated sediment. Indeed, PAH degradation was increased by changing the boundary conditions, i.e. the addition of extra carbon source and microorganisms. A lower biogas production ($p < 0.05$) was observed using only digestate as biostimulating amendment. On the contrary, the addition of OFMSW resulted in a higher H_2 and CH_4 production due to its higher biodegradation potential than digestate.

PAH degradation was analyzed by comparing the total PAH removal observed under both acidogenic and methanogenic conditions, i.e. during biohydrogen and methane production, respectively (Figure 3.3 a). When acidogenic conditions were maintained, the total PAH removal was higher in O ($p < 0.05$) than D, DN, ON and DO, where a similar removal was observed ($p > 0.05$). Whereas, under methanogenic conditions the total PAH removal was not significantly different between D and DO ($p > 0.05$) and was higher in ON and DN ($p < 0.05$). Methanogenesis was accompanied by a higher PAH removal than acidogenesis ($p < 0.05$) under all the conditions except for O, where methanogenesis did not occur being the pH constantly lower than 6.4.

Previous studies also analyzed the PAH degradation under methanogenic or acidogenic conditions, but a comparison between the PAH removal achieved during acidogenesis and methanogenesis has not been approached before. Genthner et al. [354] reported that methanogenic microorganisms serving as the terminal electron sink via interspecies hydrogen transfer made the PAH biodegradation more feasible than nitrate– or sulfate–reducing bacteria. In agreement, Chang et al. [152] showed that the addition of bromoethanesulfonic acid to PAH–containing sediments eliminated methanogens, resulting in a complete inhibition of methane production and PAH degradation. Feng et al. [355] observed an enhancement of PHE degradation by acidogenic bacteria during the fermentation of waste activate sludge.

Biomethane production yields are intimately correlated to the consumption of HAc by methanogens. HAc is a reaction intermediate of anaerobic digestion and a possible correlation between the accumulation of HAc and PHE degradation was considered. The correlation was described by plotting the difference between the remaining PHE_{ti} and PHE_{ti+1} and between HAc_{ti+1} and HAc_{ti} amount expressed as natural logarithm (Figure 3.3 b), where t_i is the i–th time (days), considering all biostimulating conditions and significant differences in PAH biodegradation ($p < 0.05$). A Pearson test showed

a high correlation between HAc production and PHE removal ($r_{HAc–PHE}$ = 0.98) with a linear trend (R^2 = 0.96). This result supports the observed PHE biodegradation occurred during the first 20 days. Similarly, Su et al. [356] observed an increase of PHE degradation from 9 to 22% in acetate–amended river sediments after 30 days of bioremediation. The presence of acetate has also been reported to promote the growth of a porous biofilm onto a sand grain surface and stimulate PHE degradation [281].

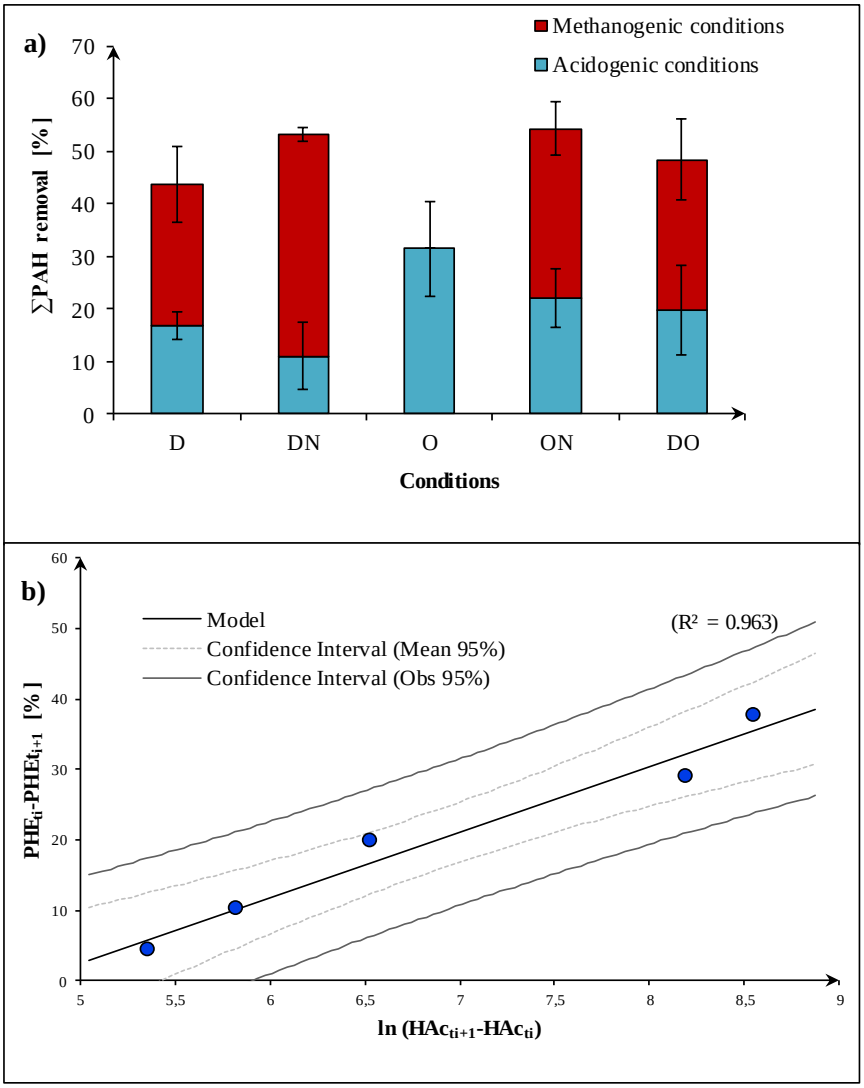

Figure 3.3 – a) Total PAH removal [%] under acidogenic and methanogenic conditions after 120 days of biostimulation. b) Pearson correlation between the remaining ($PHE_{ti} – PHE_{ti+1}$) [%] and ln ($HAc_{ti+1} – HAc_{ti}$) concentrations.

D = CS + digestate; DN = CS + digestate and nutrients; O = CS + OFMSW; ON = CS + OFMSW and nutrients; DO = CS + digestate and OFMSW. Error bars indicate deviation standard values relative to analyses in triplicate.

3.3.4 PAH degradation kinetics

The total PAH degradation kinetics and kinetic parameters in D, DN, O, ON and DO using a biphasic first–order kinetic model are shown in Figure 3.4 and reported in Table 3.3. The selected time (t_b), at which the degradation rate (K) changes, was 10 days. Fast and slow degradation rates (K_1 and K_2) were estimated from the slope of the plot of $\sum PAH_t/\sum PAH_{t0}$ ratio (%) versus time (t, days) for $t \leq t_b$ and $t > t_b$, respectively.

The correlation coefficient R^2 (Table 3.3), varying from 0.743 to 0.933, suggests that biphasic first–order kinetic model was suitable to simulate the biostimulation process. All calculated K_1 values were an order of magnitude higher than K_2 values (Table 3.3). Comparing the five conditions (Table 3.3), K_1 was higher in DO (i.e. 0.055 d^{-1}) than in D, DN, O and ON (i.e. 0.023, 0.030, 0.038 and 0.027 d^{-1}, respectively), whereas K_2 was higher in ON and DN (i.e. 0.005 d^{-1}) than in D, O and DO (i.e. 0.003, 0.001 and 0.001 d^{-1}, respectively). The observed K_1 and K_2 (Table 3.3) suggest that the combination of digestate and OFMSW had a short–term effect (< 10 days) and the nutrient solution had a long–term effect (> 10 days) on PAH removal.

Table 3.3 – Biphasic (fast and low) kinetic models of total remaining PAHs [%] in D, DN, O, ON and DO during 120 days of biostimulation. The degradation rates (K_1 and K_2, day^{-1}) and R^2 (correlation coefficients) are referred to $C = C_0 \cdot e^{-K1 \cdot t}$ and $C = C_0 \cdot e^{-K1 \cdot tb} \cdot e^{-K2 \cdot (t-tb)}$ first–order kinetic models.

Conditions	**∑PAHs**		
	K₁ [d⁻¹]	***K₂ [d⁻¹]***	***R²***
D	0.023	0.003	0.896
DN	0.030	0.005	0.933
O	0.038	0.001	0.743
ON	0.027	0.005	0.916
DO	0.055	0.001	0.880

D = CS + digestate; DN = CS + digestate and nutrients; O = CS + OFMSW; ON = CS + OFMSW and nutrients; DO = CS + digestate and OFMSW.

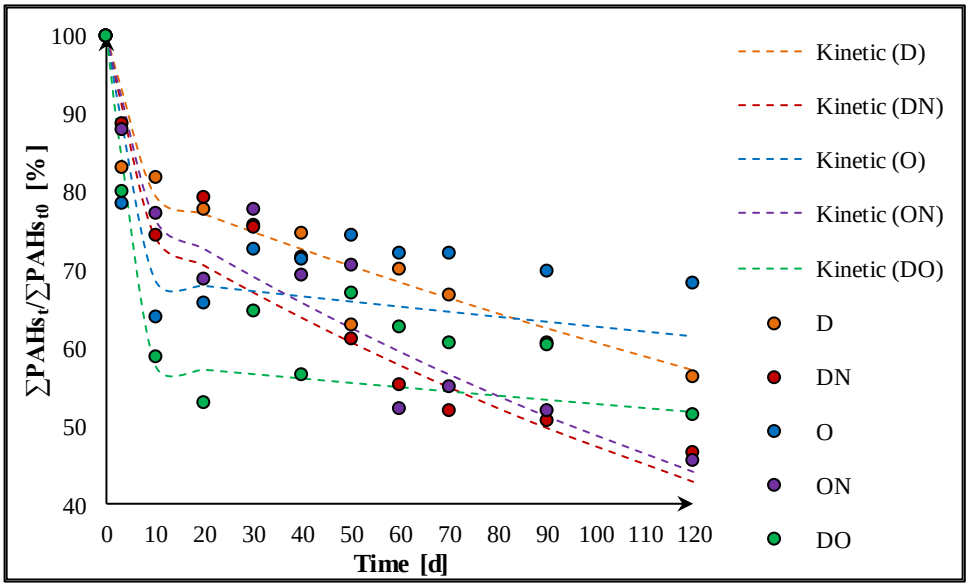

Figure 3.4 – Biphasic (fast and low) kinetic models of total remaining PAHs [%] in D, DN, O, ON and DO during 120 days of biostimulation. The lines are referred to $C = C_0 \cdot e^{-K1 \cdot t}$ *and* $C = C_0 \cdot e^{-K1 \cdot tb} \cdot e^{-K2 \cdot (t-tb)}$ *first–order kinetic models.*

D = CS + digestate; DN = CS + digestate and nutrients; O = CS + OFMSW; ON = CS + OFMSW and nutrients; DO = CS + digestate and OFMSW.

The degradation rates and the related correlation coefficients of biphasic first–order kinetics in D, DN, O, ON and DO are reported for each PAH in Table 3.4. The high–to–low order of degradation rates was observed to be PHE > HMWs > ANT in DO and ON for a fast and slow kinetic, respectively. The highest PHE degradation rates were observed in DO and ON (i.e. K_1 = 0.076 and K_2 = 0.007 d^{-1}, respectively). ANT degradation was faster in D and DN than under the other conditions (i.e. K_1 = 0.023 and K_2 = 0.006 d^{-1}, respectively). The correlation coefficient (i.e. $R^2 < 0.5$) did not fit the ANT degradation trend in O, ON and DO as the kinetics described a continuous reduction of contaminant while the ANT concentration increased after 20 days. Regarding to HMWs, the highest K_1 and K_2 were obtained in DO (i.e. almost 0.06 d^{-1}) and ON (i.e. 0.05 d^{-1}), respectively. The O condition resulted in a slower HMW degradation than DO and ON (i.e. almost 0.05 and 0.001 d^{-1} for a fast and slow kinetic, respectively).

A comparison between the PAH degradation kinetics obtained in this thesis and other studies on anaerobic biodegradation of PAHs is reported in Table 3.4. Chang et al. [322] showed that the inoculation of a PAH–adapted microbial consortium under methanogenic conditions allowed to reach K values of 0.196, 0.125 and 0.165 d^{-1} for PHE, ANT and PYR, respectively. Li et al. [331] observed a degradation rate of 0.012

and 0.011 d^{-1} for FLU and PYR, respectively, in mangrove sediments with enriched consortium bacteria. Agarry and Owabor [238] obtained an increasing K from 0.009 to 0.021 d^{-1} for ANT with the addition of pig dung as amendment.

As lower degradation rates were obtained in this study than in those present in the literature under methanogenic conditions, the microorganisms probably needed a longer acclimation time in the contaminated sediment to perform a higher and faster PAH removal. Indeed, given the complexity and toxicity of the molecules, PAHs are usually recalcitrant to biodegradation and not essential for microorganism growth, unless they are the sole carbon source. During slow kinetics, the degradation of PAHs (electron donors) was probably accompanied by the reduction of dioxide carbon (electron acceptor), as discussed above. However, the observed degradation rates during fast kinetics were higher than those reported by Agarry and Owabor [238] and Li et al. [331]. During this phase, microorganisms probably degraded the organic matter (electron donor) and during extracellular respiration the released electrons were indirectly transported by electron shuttles (i.e. riboflavin, flavin mononucleotide, phenazines) between the cell surface and PAHs (electron acceptor), allowing PAH degradation [91].

Table 3.4 – Degradation rates (K, day^{-1}) and R^2 (correlation coefficients) of a biphasic first–order kinetics describing the removal of PHE, ANT, FLU and PYR during fast and slow biostimulation. The results obtained in this study were compared to those reported in the literature under similar operating conditions.

Conditions	LMW[a] first kinetic model						HMW first kinetic model						Ref.
	PHE			ANT			FLU			PYR			
	K [d^{-1}]		R^2	K [d^{-1}]		R^2	K [d^{-1}]		R^2	K [d^{-1}]		R^2	
	Fast	Slow		Fast	Slow		Fast	Slow		Fast	Slow		
D	0.027	0.004	0.933	0.023	0.003	0.871	0.022	0.003	0.840	0.022	0.003	0.826	–
DN	0.036	0.006	0.942	0.021	0.006	0.870	0.032	0.005	0.913	0.032	0.004	0.920	–
O	0.065	0.003	0.804	0.03	0.001	0.006	0.048	0.001	0.925	0.05	0.001	0.663	–
ON	0.045	0.007	0.973	0.03	0.004	0.386	0.019	0.005	0.928	0.021	0.005	0.910	–
DO	0.076	0.002	0.940	0.028	0.001	0.427	0.062	0.001	0.881	0.059	0.001	0.849	–
EB[b] + *NaHCO$_3$*	0.023		0.957	*[c]		*	0.012		0.832	0.011		0.966	[331]
Methanogenic	0.196		**[d]	0.125		**	*		*	0.165		**	[322]
Pig dung	*		*	0.021		**	*		*	*		*	[238]

D = CS + digestate; DN = CS + digestate and nutrients; O = CS + OFMSW; ON = CS + OFMSW and nutrients; DO = CS + digestate and OFMSW; [a] = low molecular weight PAHs; [b] = enriched bacteria; [c] = not investigated; [d] = data not shown.

3.3.5 Conclusions

The increase of the amount of PAH–contaminated sediments requires the development of new strategies for an efficient and sustainable ex situ remediation. This chapter suggests that anaerobic biostimulation of PAH–contaminated sediments allowed to successfully decrease the concentration of total and bioavailable PAHs up to 55%. The supplementation of digestate, fresh OFMSW and nutrients led to the occurrence of methanogenic conditions in favor of the enhancement of PAH degradation. Among the experimental conditions, ON resulted in the highest PAH removal (similar to DN) and led to a significantly higher biomethane production (i.e. 140 mL $CH_4 \cdot g\ VS^{-1}$). The possibility of producing bioenergy from soil bioremediation is an important aspect, as all or part of the treatment costs may be covered. Further research should be focused on the process optimization, the study of the involved microbial communities as well as the PAH degradation pathways during the treatment.

CHAPTER 4. PHENANTHRENE BIODEGRADATION IN A FED–BATCH REACTOR TREATING A SPENT SEDIMENT WASHING SOLUTION: TECHNO–ECONOMIC IMPLICATIONS FOR THE RECOVERY OF ETHANOL AS EXTRACTING AGENT

4.1 Introduction

Sediment washing (SW) has extensively been studied for the remediation of dredged sediments contaminated by polycyclic aromatic hydrocarbons (PAHs), being an operationally simple, highly effective and relatively economic ex–situ technology [22,242]. SW is a physical–chemical process consisting of the deployment of solvents or surfactants as extracting agents, in order to remove PAHs from polluted sediments via solubilization [166] by reducing the high octanol–water partition coefficient (K_{ow}) of PAHs [357]. Despite low solid–to–liquid (S/L) ratios (e.g. 1:10) allow to enhance SW efficiency, a large amount of spent SW solution, which has to be subsequently treated prior to discharge into the environment, is generated [358–360].

Among the technologies used for the treatment of spent SW effluents, chemical oxidation has widely been applied, given its great efficiency towards highly recalcitrant organic contaminants [361,362]. However, chemical oxidation is costly and the degradation of PAHs can be followed by the generation of oxygenated–PAHs, which are by–products known to be more toxic and persistent than PAHs [48,99]. Therefore, a biological treatment can be alternatively applied as a more cost–effective

and eco–friendly approach, using engineered microorganisms capable to completely mineralize PAHs [27,363].

Aerobic conditions are commonly used to speed up PAH biodegradation compared to anaerobic conditions [40,364]. The bacterial metabolism is also affected by other parameters such as PAH concentration and bioaccessibility, the presence of nutrients (i.e. nitrogen and phosphorus), pH and temperature [16]. In addition, the type of extracting agent employed during SW is a further key parameter to be accounted for during the biodegradation process [180].

Synthetic surfactants (e.g. non–ionic) have largely been proposed above their critical micelle concentration during SW due to the hydrophobic interior and hydrophilic exterior structure that enhances PAH solubility [365]. Indeed, previous studies focused their attention on the biological treatment of spent phenanthrene (PHE)–contaminated SW solutions, also containing Tween® 80 or Triton™ X–100 as extracting agents (Table 4.1). However, high concentrations of non–ionic surfactants can be toxic to the microorganisms employed in the downstream treatment of SW solutions. At the same time, too low surfactant concentrations are often not effective for a complete PAH removal from the sediment [26,366]. Therefore, the use of biosolvents such as ethanol (EtOH) could represent a promising alternative to synthetic surfactants, being EtOH both effective for SW and tolerable by PAH–degrading bacteria.

EtOH is considered a green solvent that can be biologically synthesized on an industrial scale through the fermentation of biofeedstocks, such as lignocellulosic materials, and successfully used as a co–solvent during SW for the removal of hydrophobic contaminants [24,367]. Indeed, SW has been reported to achieve a PHE removal higher than 97% using a 1:1 (w/w) mixture of EtOH and water as extracting agent. In addition, the whole SW process can be optimized through an EtOH recovery back to the SW treatment unit by distillation, thus decreasing the costs for newly–added reagents and the amount of spent SW solution to be treated [173,368].

Up to date, scientific literature lacks studies investigating the biological treatment of a spent PHE–polluted SW solution containing EtOH as extracting agent. Moreover, no studies reported the biodegradation of PHE in a fed–batch reactor but only in batch flasks, thus implying good margins for interesting scientific evidences. Hence, the specific objectives of this chapter were to *i)* biologically treat a spent SW solution containing EtOH by testing different initial PHE concentrations within 6 operation cycles of a 1 L fed–batch reactor; *ii)* investigate the effects of operating parameters, i.e. dissolved organic carbon (DOC), nitrogen, phosphorous, volatile suspended solids

(VSS), dissolved oxygen (DO) and pH on PHE biodegradation through a Pearson correlation; *iii)* model PHE degradation via zero– and first–order kinetics; *iv)* perform a techno–economic assessment on the whole process chain, particularly taking into account the recovery of EtOH as a resource to be reused in SW treatment units.

Table 4.5 – Comparison between the results obtained in this thesis and those reported in the literature with bioreactors treating phenanthrene (PHE)–contaminated sediment washing solutions.

Washing effluent treatment	**Bioremediation condition**			**Washing agent**		**PHE [mg·L^{-1}]**	**Main microbial genera**	**PHE removal**		**Reference**
	pH	**Temperature [°C]**	**Agitation [rpm]**	**Type**	**Conc. [mg·L^{-1}]**			**Time [d]**	**Efficiency [%]**	
Aerobic bioreactor	8.0	37	150	Tween® 80	10,000	17.8	*Pseudomonas*	3	90	[369]
Aerobic bioreactor	6.5 – 7.5	23	300	Tween® 80	1,310	25	–[a]	2.4	≥99	[250]
Bioaugmentation biostimulation	n. a.[b]	30	180	Tween® 80	2,500	8.26	*Bacillus, Capnocytophaga, Acinetobacter and Staphylococcus*	7	44–≥99	[27]
Immobilized bacteria (PVA–SA)[c]	n. a.	25	150	Tween® 80	2500 – 5,000	20[d]	*Klebsiella*	30	42–89	[358]
Immobilized bacteria (hydrogel)	n. a.	28	200	Triton™ X–100	4,000	0.80	*Mycobacterium*	3	15–99	[370]

a = not characterized wastewater; b = not available; c = polyvinyl alcohol and sodium alginate; d = fluoranthene and pyrene (20 $mg \cdot L^{-1}$ each); e = not determined; f = considering an abundance of 18%.

4.2 Materials and methods

4.2.1 Chemicals

Calcium chloride dihydrate (grade ≥99%), magnesium chloride hexahydrate (grade ≥99%), mercury(II) chloride (grade ≥98%), PHE (grade ≥98%), sodium carbonate (grade ≥99%), sodium hydroxide (grade ≥98%), sodium chloride (grade ≥99%) and sodium sulfate (grade ≥99%) were supplied by Sigma–Aldrich (Germany). Acetone (grade 100%), acetonitrile (HPLC grade), ammonium chloride (grade 100%), chrysene (grade 100%), EtOH (≥ 99.9%), potassium dihydrogen phosphate (grade ≥99%), deconex® 31 antifoam and sulfuric acid (grade ≥95%) were all purchased from VWR (Italy). n–Hexane (grade 95%) was provided by ROMIL (UK). Ultrapure water (electrolytic conductivity ≤0.05 $\mu S \cdot cm^{-1}$) was used to prepare all solutions.

4.2.2 Enrichment of PHE–degrading bacteria

A portion of 10 g of PAH–contaminated sediment previously described elsewhere (chapter 2) was suspended with 95 mL of a saline solution (i.e. 0.85% NaCl) in a glass bottle (100 mL) [371]. A portion of supernatant of 5 mL was subsequently transferred into a 250 mL Erlenmeyer flask containing 45 mL of sterilized mineral salt medium (MSM) with a pH adjusted to 7.0 with 1 M of H_2SO_4 and a PHE concentration of 50 $mg \cdot L^{-1}$, here used as the sole carbon source [371] and representative of PAHs being intermediate in solubility and hydrophobicity. MSM consisted of (in $mg \cdot L^{-1}$ of deionized water): 500 KH_2PO_4, 400 NH_4Cl, 330 $MgCl_2 \cdot 6H_2O$, 50 $CaCl_2 \cdot 2H_2O$ and 400 NaCl [372]. PHE was added to the MSM with acetone (≤2%, v/v), which evaporated within 24 hours [373,374].

The enrichment of the PHE–degrading community was performed in triplicate under aerobic conditions, placing the flasks at room temperature and on a horizontal shaker at 200 rpm [375] until PHE was no longer detected. Afterwards, 5 mL of enrichment were withdrawn from each of the triplicates and sub–cultured with 45 mL of fresh MSM–PHE solution [371]. After 15 sub–culture operations, the obtained microbial consortium was used as an inoculum of PHE–degrading bacteria [376] for the biological treatment of a synthetic spent SW solution.

4.2.3 Treatment of spent SW solution in a fed–batch bioreactor

PHE biodegradation was performed in a 1,500 mL glass reactor with a working volume of 1,000 mL (Figure 4.1), which was constantly maintained at 30 ± 2 °C using a temperature control unit (JULABO GmbH, Germany). The treatment of the PHE–containing SW solution was studied in fed–batch mode, using six different cycles operated with an initial PHE concentration of 20 (cycle 1), 50 (cycle 2), 67 (cycle 3), 76 (cycle 4), 140 (cycle 5) and 120 (cycle 6) $mg \cdot L^{-1}$, for a total duration of 31 days. The investigated PHE concentrations were used imagining to simulate the PHE concentration deriving from different PAH–contaminated sediments [255].

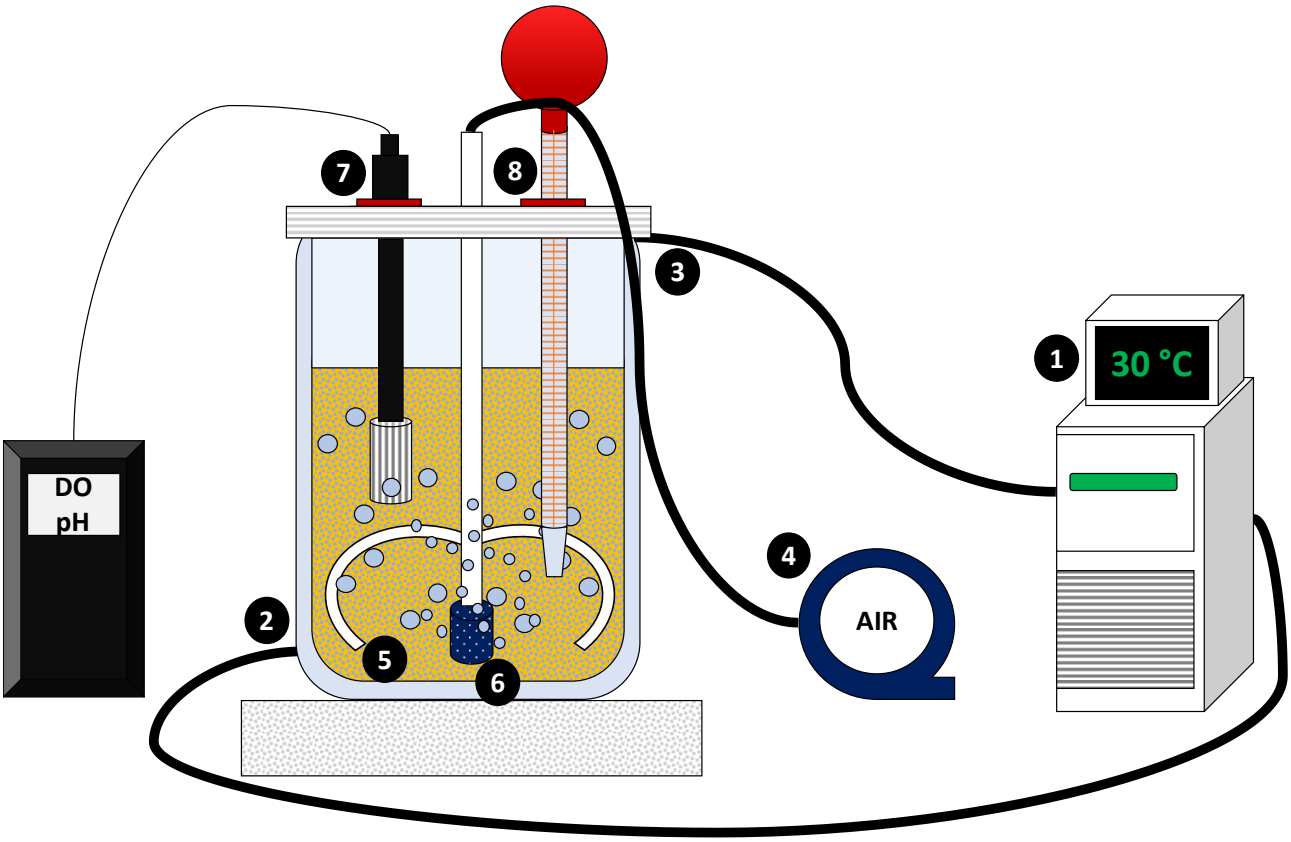

Figure 4.5 – Experimental set–up of the fed–batch bioreactor used in this study. 1) Temperature control unit connected to the reactor liner at 2) and 3) for the recirculation of 30 °C heated water; 4) aquarium pump used to ensure the mixing and aerobic conditions via large 5) and fine 6) bubbles, respectively; 7) port used for dissolved oxygen (DO) and pH measurements; 8) sampling port, also used for pH adjustments and supplementation of the fresh synthetic sediment washing solution.

At the beginning of the operation (cycle 1), the reactor contained 100 mL of the enriched PHE–degrading microbial culture (section 4.2.2) in order to obtain a volumetric ratio of 10% with the total working volume. A nutrient solution (i.e. 787 mL) composed of KH_2PO_4 and NH_4Cl, and buffered with 1,334 $mg \cdot L^{-1}$ of Na_2CO_3 [377], was added to the reactor (Figure 4.1) to biostimulate PHE removal by balancing the carbon–to–nitrogen–to–phosphorus (C/N/P) molar ratio to 100:1.3:0.05, which was suggested as optimal for PAH degradation by Wilson and Jones [378]. Finally, 113 mL of synthetic SW solution (with 0.59 and 0.01% of NaCl and Na_2SO_4, respectively) were introduced into the reactor reaching approximately 50,000 $mg \cdot L^{-1}$ of EtOH (except for cycle 1), and used as a source of PHE. The characteristics of the spent SW solution were deduced from that used in chapter 2, as summarized in Table 4.2.

Table 4.6 – Phenanthrene (PHE) removal (%) from contaminated sediment vs time (d) using a mixture of EtOH and water as washing agent (1:1, w/w) with several solid–to–liquid (S/L) ratios (i.e. 1:3, 1:5 and 1:10). Error bars refer to RSD values of analyses in triplicate. Data of sediment washing are taken from chapter 2.

Time [min]	**SW* conditions**					
	S/L ratio 1:3		***S/L ratio 1:5***		***S/L ratio 1:10***	
	PHE removal [%]	*RSD [%]*	*PHE removal [%]*	*RSD [%]*	*PHE removal [%]*	*RSD [%]*
0	0.00	0.00	0.00	0.00	0.00	0.00
1	65.91	0.34	68.56	0.03	60.91	0.38
2	69.27	0.12	71.20	0.02	64.58	2.98
5	77.83	2.10	76.16	2.38	69.78	5.98
15	87.10	1.78	85.17	4.17	83.99	5.23
30	94.68	1.70	93.61	2.40	93.72	0.72
60	99.40	1.62	98.38	0.10	97.55	0.81

*SW = sediment washing

Cycle 1 was operated at the lowest PHE concentration with the aim also to acclimatize the microorganisms to the new experimental conditions [250], and a lower EtOH concentration (i.e. approximately 11,000 $mg \cdot L^{-1}$) was subsequently introduced into the reactor. PHE concentration was reduced in cycle 6 to evaluate the possible inhibitory effects on the growth of the involved microbial species. Each cycle was interrupted when PHE degradation stopped or a 99% removal of dissolved organic carbon was reached. Afterwards, an aliquot of 113 mL was taken from the reactor maintaining active agitation (Figure 4.1) and replaced with a fresh SW solution also containing the required nutrients for microbial

growth and pH buffer. For the whole operation of the reactor, the liquid phase was continuously mixed and kept under aerobic conditions through an aquarium pump by supplying humidified air via a glass tube (large bubbles) and a porous diffuser (fine bubbles), respectively. When DO was detected below 1 $mg \cdot L^{-1}$, DO concentration was corrected up to 5 $mg \cdot L^{-1}$ by manually increasing the aeration flowrate (Figure 4.1). The pH value was daily adjusted to 7.4 with 1 M of H_2SO_4 or NaOH (Figure 4.1) in order to minimize any interference with PHE degradation [321]. Antifoam agent (i.e. 0.5 $mL \cdot L^{-1}$) was added in the early stage of each cycle to avoid foam production due to the air injection in the presence of a high concentration of EtOH. Aluminum folio was used to wrap the wall of the reactor and avoid the onset of competing phototrophic reactions.

In addition, an inoculum–free reactor was operated under the same abovementioned conditions as a control with 113 mL SW solution + 787 mL nutrients + 100 mL autoclaved water and the addition of 1,000 $mg \cdot L^{-1}$ of $HgCl_2$ as biocide test, in order to evaluate any abiotic loss (e.g. by volatilization) of PHE and EtOH [379].

4.2.4 Sampling, analytical procedures and revealing of microbial communities

The content of total suspended solids (TSS) and VSS was determined after each operative cycle using the filtration–based method through glass microfiber filters (Whatman, USA) [380]. DO and pH values were measured directly in the reactor (Figure 4.1) with an IDS FDO® 925 and SenTix® 950 pH electrode (WTW, USA), respectively. Samples for the quantification of DOC, ammonia nitrogen ($N–NH_4^+$), phosphorus ($P–PO_4^{3-}$) and PHE were daily taken from a sampling port located on the top of the reactor (Figure 4.1). The amount of DOC was analyzed using a TOC–L Series (Shimadzu, Japan) as reported by Matassa et al. [381]. $N–NH_4^+$ was quantified with a spectrophotometer PhotoLab® S6 (WTW, USA) using the indophenol blue method [382]. The $P–PO_4^{3-}$ concentration was determined by ion chromatography (IC) employing an 883 Basic IC Plus (Metrohm, Switzerland) [383]. PHE was extracted from samples and quantified via an LC–20AD HPLC (Shimadzu, Japan), as extensively described in chapter 2 and 3. Before the PHE extraction, 1 mL of 50 $mg \cdot L^{-1}$ chrysene solution was added as the surrogate standard [384].

The composition of the microbial community populating the reactor after the 31 days of fed–batch reactor operation was analyzed through a preliminary DNA extraction with a ZR Fecal/Soil Microbe DNA MiniPrep™ Kit (Zymo Research, USA). The yield of DNA extracted from the sample was assessed as described

by Claassen et al. [385]. Polymerase chain reaction (PCR) amplification, Illumina sequencing, sequence filtering and taxonomic classification were carried out as extensively reported by Haleyur et al. [105]. Library quantification was determined through a 2100 Bioanalyzer (Agilent Technologies, USA).

4.2.5 Kinetic study and calculations

PHE biodegradation kinetics were evaluated under each investigated condition by comparing zero– (Eq 4.1) and first– (Eq 4.2) order kinetic models since such kinetics were extensively used to ascertain the degradation kinetic parameters in bioreactors treating PHE. k and $t_{1/2}$ parameters were calculated as follows [386]:

$$C(t) = C(t_0) - kt \quad \text{(Eq 4.1)}$$

$$C(t) = C(t_0) \cdot e^{-k \cdot t} \quad \text{(Eq 4.2)}$$

$$t_{1/2} = \frac{C(t_0)}{2 \cdot k} \quad \text{(Eq 4.3)}$$

$$t_{1/2} = \frac{\ln(2)}{k} \quad \text{(Eq 4.4)}$$

where C_0 is the initial PHE concentration; k (d^{-1}) is the PHE degradation rate; $t_{1/2}$ (d) is the half–life time, used to evaluate the due time to obtain a 50% C degradation. Consequently, $t_{1/2}$ was calculated both for zero– (Eq 4.3) and first– (Eq 4.4) order kinetic models.

As an indicator of the biosurfactant production during the foam formation periods, the emulsification index was calculated by dividing the height of the emulsified layer by the total height of the liquid column, as previously described by Gupta et al. [387]. The cell surface hydrophobicity (CSH) was evaluated spectrophotometrically after n–hexane addition [20] using a diluted sample to an optical density (OD_{605}) of 1.0 [388].

The free energy liberated from the mineralization of PHE (ΔG_d) was calculated under aqueous conditions by subtracting the Gibbs free energy of reactants formation ($\Delta G_{f,r}$) from that of products formation ($\Delta G_{f,p}$) in reaction 1 [389]. Similarly, the free energy of the oxygen half–reaction (ΔG_a) was estimated following reaction 2. $\Delta G_{f,r}$ and $\Delta G_{f,p}$ were taken for each involved compound from Woo and Rittmann [390].

$$\left(\frac{1}{66}\right) C_{14}H_{10} + \left(\frac{28}{66}\right) H_2O \rightarrow \left(\frac{14}{66}\right) CO_2 + H^+ + e^- \quad \text{(Eq. 4.5)}$$

$$\left(\frac{1}{4}\right) O_2 + H^+ + e^- \rightarrow \left(\frac{1}{2}\right) H_2O \quad \text{(Eq. 4.6)}$$

Afterwards, ΔG_d and ΔG_a were combined in order to obtain the overall energy yield (ΔG_r) of the PHE degradation process, which was expressed as kcal·eeq^{-1}.

4.2.6 Statistical analysis

A one–way analysis of variance (ANOVA) coupled with a Tukey test was executed to evaluate the significant differences (p <0.05) between the experimental conditions. A standard Pearson test with both–sided alternative was carried out to examine the correlation coefficients ($r_{variable,1–variable,2}$) between the PHE and the other investigated parameters (i.e. DOC, nitrogen, phosphorous, VSS, DO and pH). The statistical evaluation was performed with the XLStat software (2020.5.1 version, Addinsoft, USA).

4.2.7 Economic estimation

A rough evaluation of the remediation costs associated with the entire process chain was performed by including SW operations, EtOH supply and recovery, and the treatment of the spent SW solution. The cost of SW operations considering workers, construction supplies, pumping and tubes, earthmoving, and storage vessels was assumed as 142 €·m^{-3} of sediment [180,391]. The price of EtOH used during SW was considered equal to 0.31 €·L^{-1} [392] and the expenditure for EtOH recovery through solar distillation was 0.12 €·L^{-1} of EtOH [393]. The biological treatment of the spent PHE–polluted SW solution under aerobic conditions at 30 °C was assumed to result in a cost of 12.5 €·m^{-3} of effluent [369,387]. All calculations were standardized on mass basis (ton) supposing a sediment density of 1.6 ton·m^{-3} and a maximum field capacity of 35% (v/v), which generally refers to marine sediments [394–396].

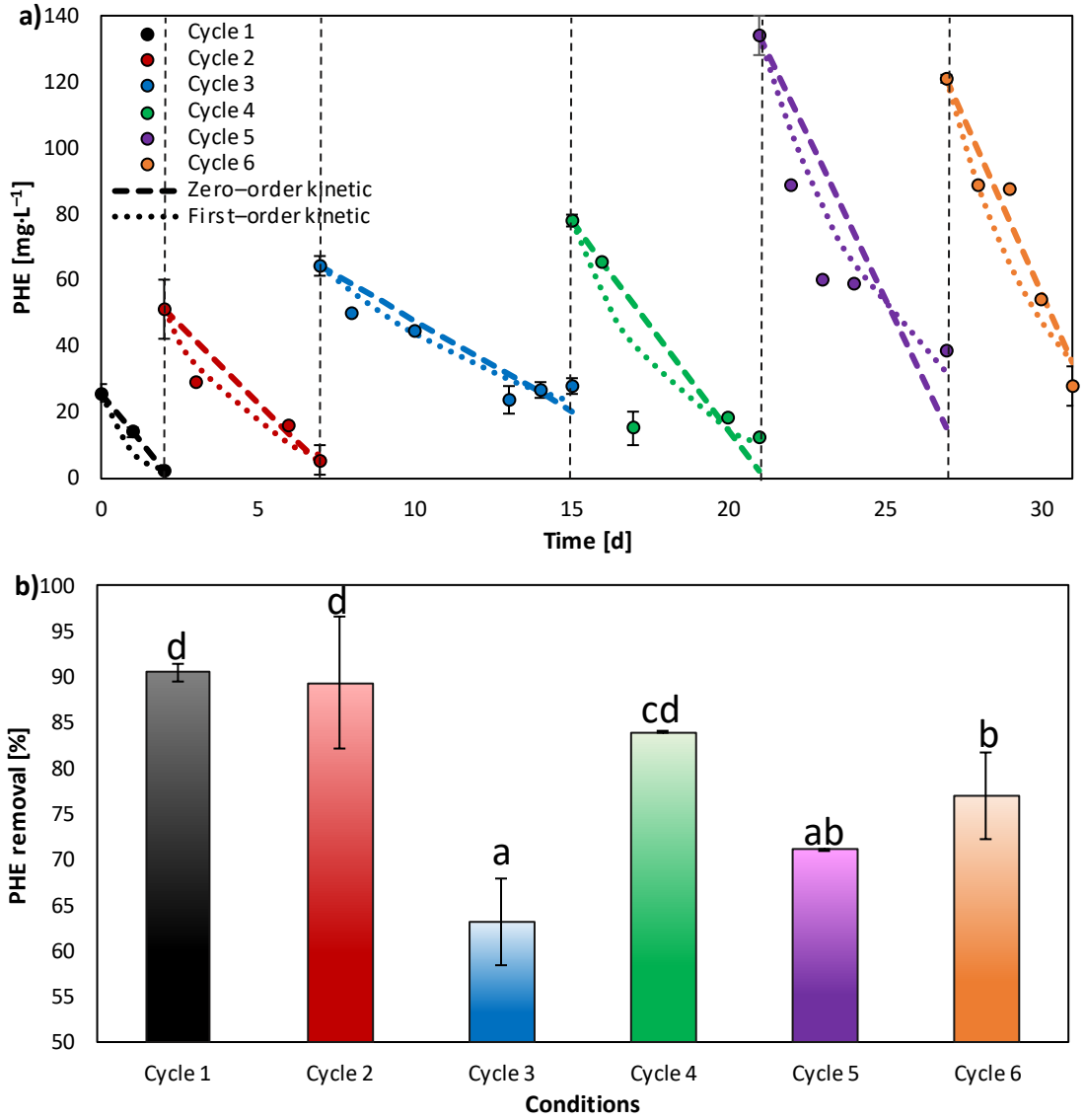

Figure 4.6 – a) Phenanthrene (PHE) concentrations (mg·L^{-1}) vs time (d) during the biological treatment of a spent sediment washing solution and b) results of the statistical comparison (Tukey test) of PHE removal (%) at the end of each cycle in the fed–batch bioreactor.

The dashed and dotted curves in panel **a)** refer to those used in the zero– (Eq 4.1) and first– (Eq 4.2) order kinetic models, respectively. The same letters (Tukey test) did not represent statistical differences ($p > 0.05$) between the experimental conditions. Values are the averages of triplicate analyses and error bars indicate the RSD.

4.3 Results and discussion

4.3.1 Influence of monitoring parameters on phenanthrene removal

A PHE removal between 63 and 91% (Figure 4.2a and b) was obtained at the end of each cycle during the aerobic biodegradation of the synthetic PHE–containing spent SW solution. The abiotic loss of PHE was negligible (data not shown), indicating that PHE was completely removed by the bacterial activity, in agreement with Chiavola et al. [397].

PHE biodegradation was significantly lower (p <0.05) in cycle 5 and 6 (i.e. 71 and 77%, respectively) (Figure 4.2b) than in cycle 1 and 2 (i.e. 91, 89%, Figure 4.2 b), which in turn was slightly higher (p >0.05) compared to cycle 4 (i.e. 84%, Figure 4.2b). The increase of PHE concentration from 20 to 140 mg·L^{-1} generally led to a decrease of the PHE removal efficiency probably due to the toxic effect of PHE or degradation intermediates to microorganisms (see section 4.3.2 and 4.3.5), as also reported by Waigi et al. [119]. Likewise, Pedetta et al. [398] showed a lower PHE degradation (i.e. by 75%) with a PHE concentration of 150 mg·L^{-1} compared to Sun et al. [399], who obtained a PHE removal of 85% with an initial concentration of 50 mg·L^{-1}.

The degradation of PHE in cycle 3 only reached 63% (Figure 4.2a and b) likely due to a buffer failure that led to an abrupt pH decrease from 7.4 to 4.4 (Figure 4.3e) on day 10 of reactor operation. Similarly, Janbandhu and Fulekar [400] reported acidification during the biodegradation of PHE, with pH decreasing from 7.0 to 5.2–5.6. Although the correlation between PHE and pH was weak (i.e. $r_{PHE–pH} = 0.433$) in this work due to the continuous pH adjustment, the decrease of pH can be attributed to the accumulation of hydrogen ions caused by PHE degradation [401]. Neutral pHs typically facilitate hydrocarbon degradation (e.g. PAHs), whereas acidic pHs negatively affect the microbial activity [40], as further supported by the decline of PHE removal after 10, 17 and 23 days in cycles 3, 4 and 5 (Figure 4.2a), respectively. However, PHE–degrading bacteria were only temporarily inhibited and resumed their activity after 1–3 days due to an increase of pH to 7.4 by NaOH addition (Figure 4.2a and 3e, respectively) [335].

The biodegradation of PHE in cycle 5 and 6 could be also negatively influenced by the anoxic conditions (i.e. DO <1 mg·L^{-1}) that occurred on days 23–24 and 28–29 (Figure 4.2d), which led to a slight reduction (p >0.05) of PHE concentrations, as also suggested by the negative Pearson coefficient between

DO and PHE (i.e. $r_{PHE–O2}$ = –0.704). During the operation of the reactor at an initial PHE concentration increasing from 80 to 140 mg·L^{-1}, a high biomass growth up to approximately 3,600 mg VSS·L^{-1} (Figure 4.4) was observed, thus increasing the oxygen demand (Figure 4.3d) [402] and leading to an excessive decrease of DO. Therefore, the optimization of the aeration in the aerobic treatment of PHE–containing solutions should be carefully evaluated in future studies. This would allow to maintain the minimum DO concentration, which has no detrimental effects on the metabolism of PHE–degrading microorganisms and concomitantly keeps the aeration costs as low as possible.

PHE degradation was also accompanied by a decrease of DOC, $N–NH_4^+$ and $P–PO_4^{3-}$ above 99% (Figure 4.3a, b and c, respectively). DOC was mainly made up of the EtOH used to solubilize PHE during SW. The biocide test revealed a DOC reduction of approximately 60%, which can be attributed to the EtOH volatilization, indicating an actual biological removal of EtOH of about 40%. In contrast, Da Silva and Alvarez [403] obtained an abiotic EtOH removal lower than 8% during the degradation of a mixture of benzene, toluene, ethylbenzene and xylene. The discrepancy with the study of Da Silva and Alvarez [403] can be explained by a considerably lower EtOH concentration (i.e. 1,000 mg·L^{-1}), compared to that used in the present work (i.e. 50,000 mg·L^{-1}), which resulted in a low EtOH volatilization. This is also confirmed by what observed in cycle 1, where a not significant (p >0.05) abiotic EtOH removal was obtained with an initial EtOH concentration of 11,000 mg·L^{-1}. Furthermore, EtOH volatilization was likely promoted here by the extensive aeration used to ensure aerobic conditions for the PHE–degrading community (Figure 4.3d) [404].

The inorganic macronutrients (i.e. nitrogen and phosphorous) supplemented were needed to stimulate the activity of bacteria and effectively resulted in new biomass production (Figure 4.4), in agreement with Zang et al. [20]. This is also indicated by the Pearson coefficient (i.e. $r_{PHE–N}$ = 0.702 and $r_{PHE–P}$ = 0.538) that demonstrates a good correlation between $N–NH_4^+$ and $P–PO_4^{3-}$ consumption (Figure 4.3b and c, respectively) and PHE biodegradation. Hence, up to approximately 90% of PHE removal was achieved using a C/N/P ratio of 100:1.3:0.05, which was higher compared to the widely accepted C/N/P ratio of 100:10:1 [405]. This confirms what observed by Leys et al. [321], who showed that PAH–degrading bacteria need a low nutrient amount, implying a lower operation cost in case N and P have to be externally provided.

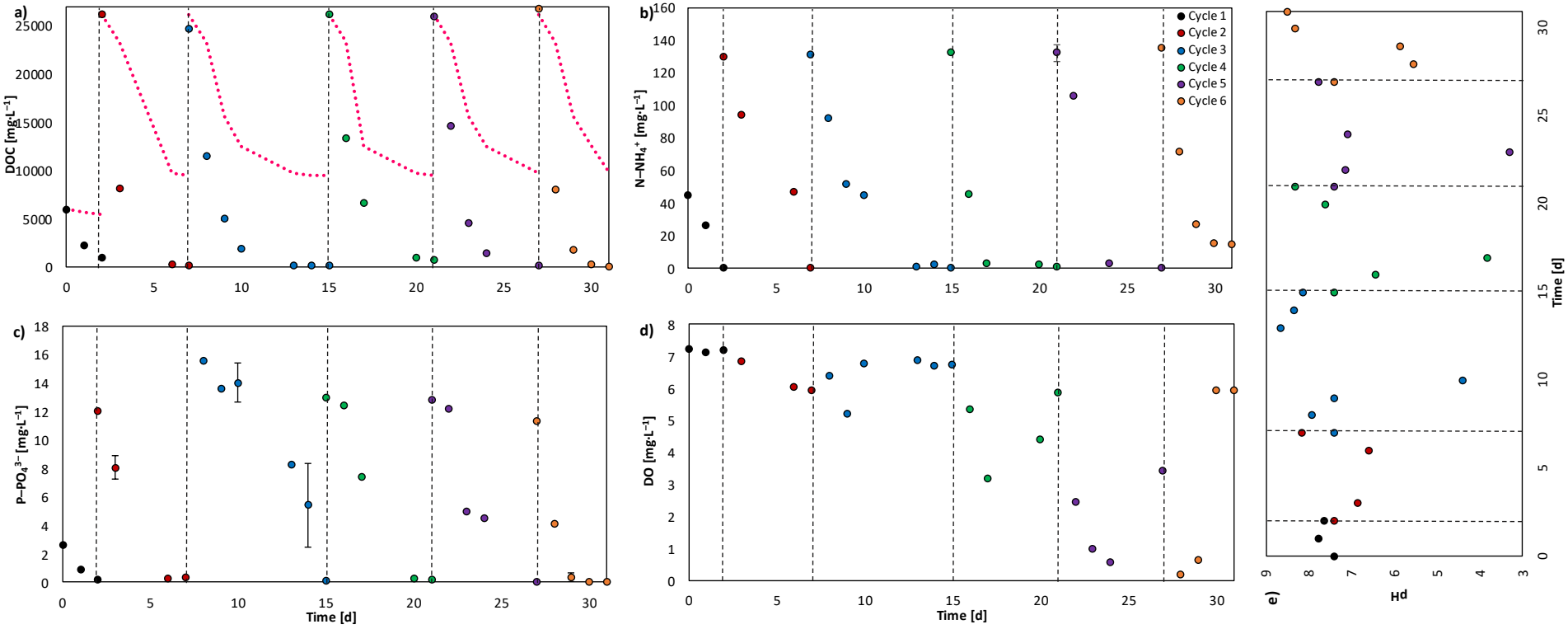

Figure 4.7 – Evolution of a) dissolved organic carbon (DOC), b) $N–NH_4^+$, c) $P–PO_4^{3-}$, d) dissolved oxygen (DO) ($mg·L^{-1}$) and e) pH values vs time (d) during the biological treatment of a phenanthrene–containing spent sediment washing solution in a fed–batch bioreactor.

The dashed curve in panel a) refers to the amount of DOC detected in the abiotic test. Values are the averages of triplicate analyses and error bars indicate the RSD.

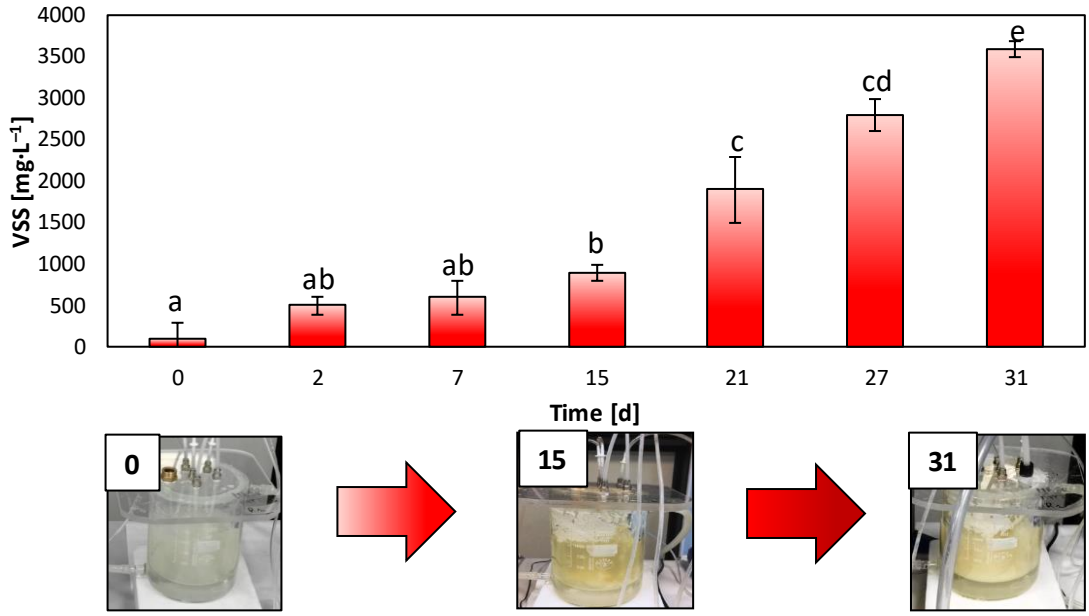

Figure 4.8 – Evolution of volatile suspended solids (VSS) (mg·L^{-1}) vs time (d) in the fed–batch bioreactor after each investigated cycle, i.e. at 20 (cycle 1), 50 (cycle 2), 67 (cycle 3), 76 (cycle 4), 140 (cycle 5) and 120 (cycle 6) mg PHE·L^{-1}. Photos of reactor are reported below the evolution of VSS after 0, 15 and 31 days.

The same letters (Tukey test) did not represent statistical differences (p >0.05) between the experimental conditions. Values are the averages of triplicate analyses and error bars indicate the RSD.

4.3.2 Mechanisms involved in the biodegradation of phenanthrene

The biodegradation mechanisms involved in the removal of PHE from the SW solution can be essentially summarized in 2 stages. In the early phase (i.e. first 3 days) of each cycle, part of PHE was dissolved due to the presence of EtOH. Therefore, the main involved bacteria degraded PHE, being it directly available as substrate [406].

Per each cycle, the soluble PHE concentration was probably lower from day 4 onwards due to a decreased presence of EtOH after EtOH degradation and volatilization (section 4.3.1). Hence, bacteria probably produced biosurfactants or biodemulsifiers to improve PHE biodegradation [20,407]. This is corroborated by the remarkable formation of foam in this stage despite the addition of the antifoam agent (data not shown). Indeed, the calculation of the emulsification index indicates values

of approximately 18–29%, which are similar to that reported by Gupta et al. [387] (i.e. 24%) when using a PAH (i.e. pyrene) as the sole carbon source. An emulsification index of about 20–30% can be related to a considerable amount of biosurfactants produced to emulsify PHE [387,408]. In addition, lower concentrations of nitrogen (Figure 4.3b) probably stimulated the emulsification phenomenon due to the combination of amino acids and fatty acids, which were not all used as cell components for bacterial growth, as recently shown by Zang et al. [20].

It is possible to state that the foam was involved in PHE degradation also due to a CSH comprised between 13 and 37% [20], which probably favored PHE uptake through biosorption and then transmembrane transport after PHE adhesion to cells [387,409]. Afterwards, PHE cleavage likely occurred via the hydroxylation of the K–region and the production of 1,2–dihydroxyphenanthrene (Figure 4.5), which was mediated by the aryl dehydrogenase enzyme in the presence of oxygen [410,411]. 1,2–dihydroxyphenanthrene can be further converted through either phthalate or salicylate routes [412]. However, the presence of *Achromobacter and Sphingobacterium* as major bacterial genera involved in PHE biodegradation in this study (see section 4.3.4) would suggest that 1,2–dihydroxyphenanthrene bioconversion followed the salicylate pathway to form 1,2–dihydroxynaphthalene (Figure 4.5) [400,413].

The biotransformation to 1,2–dihydroxynaphthalene probably occurred via 2–hydroxy–1–naphthoic acid (2H1NA) metabolization by the hydroxy–1–naphthoate dioxygenase (Figure 4.5), as also confirmed by the yellowish color of the microbial biomass (Figure 4.4) [414,415]. 2H1NA accumulation probably raised with the increase of initial PHE concentration, thus reducing the PHE removal performances (see section 4.3.1) due to 2H1NA inhibitory effects on bacteria and/or the toxicity induced by its decarboxylated metabolites (e.g. 2–naphtol) [416].

Eventually, 1,2–dihydroxynaphthalene was probably meta–cleavaged to salicylic acid, which could be subsequently catalyzed by salicylate oxygenase obtaining catechol [119], ultimately leading to the TCA (tricarboxylic acid) cycle and the complete mineralization to H_2O and CO_2 [120].

Phenanthrene

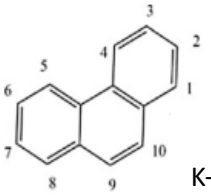

K–region

aryl dehydrogenase

1,2–dihydroxyphenanthrene

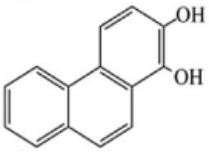

2–hydroxy–1–naphthoic acid

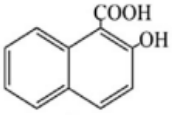

hydroxy–1–naphthoate dioxygenase

1,2–dihydroxynaphthalene

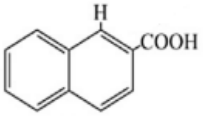

meta–cleavage pathway

Salicylic acid

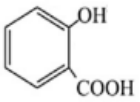

salicylate oxygenase

Catechol

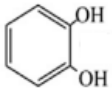

Figure 4.9 – Expected metabolic pathway for the degradation of phenanthrene in this study. TCA = tricarboxylic acid.

4.3.3 Phenanthrene biodegradation kinetics

PHE biodegradation kinetics and kinetic parameters in cycle 1–6 using both zero– (Eq 4.1) and first– (Eq 4.2) orders are shown in Figure 4.2b and reported in Table 4.3. The degradation rate (k) was assessed from the slope of the PHE ($mg \cdot L^{-1}$) *vs.* time (d) plot. The relatively high correlation coefficients (R^2) and low error sum of squares (SS_E) (i.e. 0.652–0.928 and 36.731–833.443, respectively) (Table 4.3), indicate that the first– was better than the zero–order kinetics in simulating the aerobic PHE biodegradation from the synthetic SW solution [193]. This is in agreement with other studies that modeled PHE biodegradation with the first–order kinetic [417]. However, R^2 in cycle 4 (i.e. 0.652, Table 4.3) did not fit well the PHE degradation trend, as the kinetics described a continuous reduction of the contaminant while the PHE concentration remained almost constant between days 17 and 21 due to a pH decrease to almost 4.0 (Figure 4.3e).

The k value was higher in cycle 1 (i.e. 1.177 d^{-1}) than in cycles 2, 3, 4, 5 and 6 (i.e. 0.391, 0.127, 0.329, 0.238 and 0.308 d^{-1}, respectively) (Table 4.3), further confirming that the increase of the initial PHE concentration decelerated PHE degradation [386]. The half–life time ($t_{1/2}$), calculated from the k in the first–order model (Table 4.3), accordingly varied from 0.589 to 2.912 d (Table 4.3) in cycle 1 and 5, respectively. Furthermore, the obtained $t_{1/2}$ values confirmed that 50% of PHE degradation can be reached in less than 6 days, as previously reported by Pourbabaee et al. [418]. Thus, results are consistent with the experimental trend observed during PHE biodegradation, confirming that initial PHE concentrations below 50 $mg \cdot L^{-1}$ led to a higher PHE removal efficiency (section 4.3.1).

Table 4.7 – Zero– and first–order kinetic models of phenanthrene (PHE) degradation (mg·L^{-1}) in cycle 1, 2, 3, 4, 5 and 6, during the treatment of a PHE–containing spent sediment washing solution in a fed–batch bioreactor.

Conditions	Zero–order kinetic $C(t) = C(t_0) - kt$				First–order kinetic $C(t) = C(t_0) \cdot e^{-kt}$			
	k [d^{-1}]	$t_{1/2}$ [d]	R^2	SS_E	k [d^{-1}]	$t_{1/2}$ [d]	R^2	SS_E
Cycle 1	11.584	1.104	0.999	0.004	1.177	0.589	0.928	36.731
Cycle 2	9.3075	2.743	0.852	170.813	0.391	1.773	0.902	59.676
Cycle 3	5.4984	5.855	0.845	87.167	0.127	5.458	0.875	42.173
Cycle 4	12.602	3.098	0.609	1,421.040	0.329	2.107	0.652	719.982
Cycle 5	19.805	3.386	0.516	1,846.501	0.238	2.912	0.788	833.443
Cycle 6	21.414	2.826	0.954	201.341	0.308	2.250	0.881	485.648

The degradation rates (k, d^{-1}) and half–life times ($t_{1/2}$, d) are referred to the investigated kinetic models (Eq 4.1 and 2). The error sum of squares (SS_E) is calculated as the sum of the squared deviation of predicted values with respect to observed values.

Previous researchers also evaluated the first–order PHE–degradation kinetics. Lin et al. [419] calculated a k value of 0.108 d^{-1} with an initial PHE concentration of 50 mg·L^{-1} using *Pseudomonas* BZ–3 under optimized conditions. Likewise, Chang et al. [322] showed a k of 0.196 d^{-1} for PHE using an acclimated PAH–degrading consortium under methanogenic conditions. The degradation rate obtained by Wang et al. [420] was only 0.023 d^{-1} in batch experiments with an initial PHE concentration of 100 mg·L^{-1}. The authors ascribed this to a longer acclimation time to PHE required by immobilized *Sphingomonas* and *Pseudomonas* species than cell suspensions.

Therefore, the present thesis achieved a higher PHE degradation rate in comparison with the existing studies, likely due to the presence of bacteria belonging to the *Stenotrophomonas* genus (section 4.3.4), which is reported to have a synergistic effect on PHE removal with other PHE–degrading bacteria [421]. Moreover, the aerobic conditions are more favorable for PHE degradation compared to methanogenic conditions, due to the higher potential of O_2 as terminal electron acceptor than CO_2 (i.e. +818 and –380 mV, respectively). Indeed, ΔG_r associated with the aerobic mineralization of PHE was here estimated to be –25.40 kcal·eeq^{-1}, which was more thermodynamically feasible compared to that reported under anaerobic conditions (i.e. –0.84 kcal·eeq^{-1}) [389].

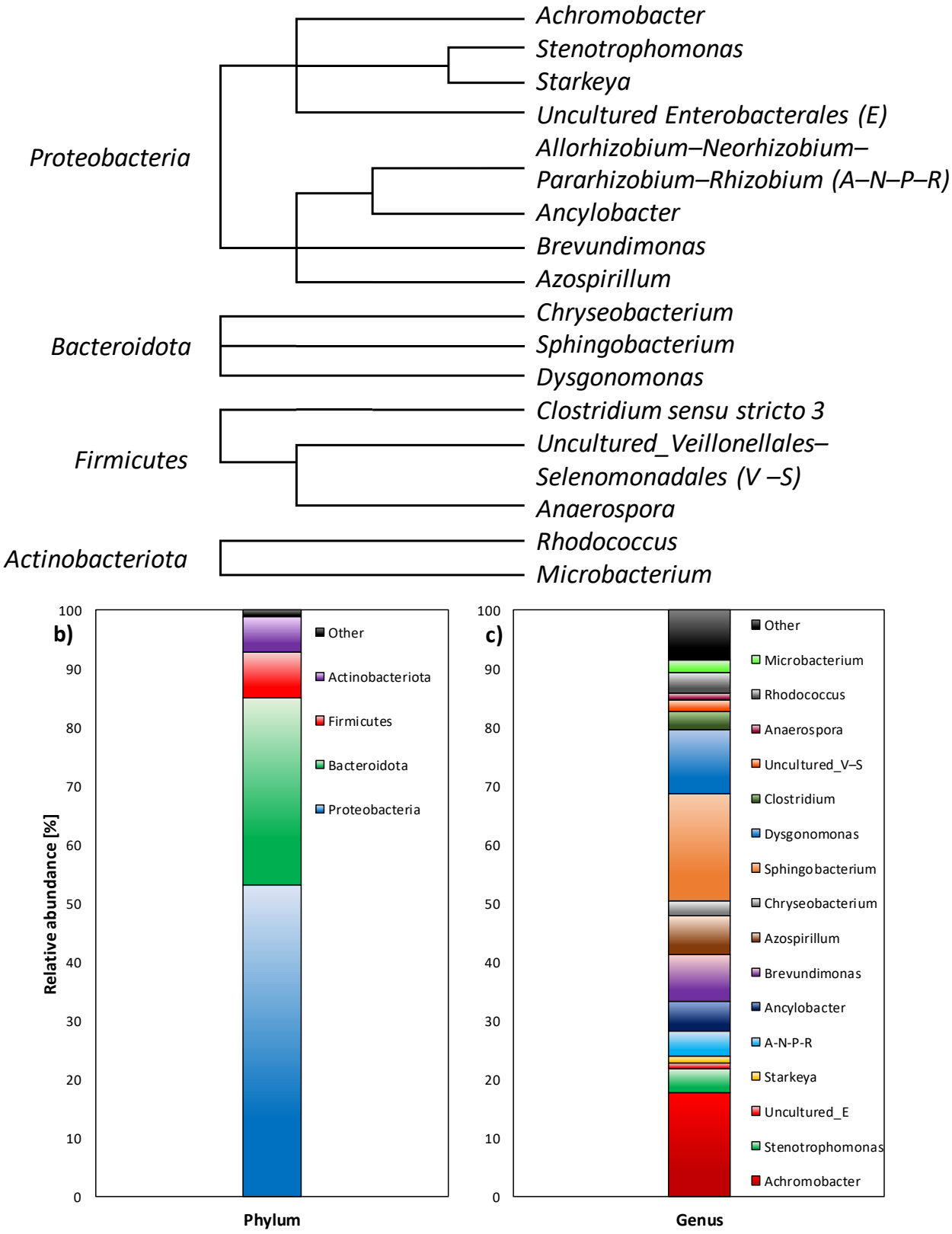
Achromobacter
Stenotrophomonas
Starkeya
Uncultured Enterobacterales (E)
Allorhizobium–Neorhizobium–
Pararhizobium–Rhizobium (A–N–P–R)
Ancylobacter
Brevundimonas
Azospirillum
Chryseobacterium
Sphingobacterium
Dysgonomonas
Clostridium sensu stricto 3
Uncultured_Veillonellales–
Selenomonadales (V –S)
Anaerospora
Rhodococcus
Microbacterium
Proteobacteria
Bacteroidota
Firmicutes
Actinobacteriota
b)
c)
Relative abundance [%]
100
90
80
70
60
50
40
30
20
10
0
Other
Actinobacteriota
Firmicutes
Bacteroidota
Proteobacteria
Phylum
Other
Microbacterium
Rhodococcus
Anaerospora
Uncultured_V–S
Clostridium
Dysgonomonas
Sphingobacterium
Chryseobacterium
Azospirillum
Brevundimonas
Ancylobacter
A-N-P-R
Starkeya
Uncultured_E
Stenotrophomonas
Achromobacter
Genus

Figure 4.10 – a) Phylogenetic tree showing the genetic relationships of phenanthrene–degrading bacteria, b) bacterial composition at the phylum level and c) genus level after the 31 days of fed–batch reactor operation.

4.3.4 Identification of PHE–degrading bacteria

The taxonomic classification revealed the abundance of *Proteobacteria* and *Bacteroidota* phyla accounting for more than 80% of the total reads in samples (Figure 4.6b) [422]. Most of PHE–degrading bacteria were phylogenetically assigned to *Proteobacteria* (i.e. 53%, Figure 4.6b), likely due to the capability of this microbial phylum to adapt to hydrocarbon–polluted environments [423,424]. The *Bacteroidota* phylum showed an abundance of 32% (Figure 4.6b) and was previously associated with PAH degradation in contaminated soils [425]. *Firmicutes* and *Actinobacteria* phyla were relatively abundant in the bioreactor (i.e. 8 and 6%, respectively) (Figure 4.6b), and the bacteria belonging to them can be considered as active PHE–degraders accompanying the *Proteobacteria* phylum [426,427].

The microbial community distribution at the genus level by considering a relative abundance higher than 1% [428] is shown in Figure 4.6c. *Achromobacter*, *Sphingobacterium* and *Dysgonomonas* genera showed a copiousness of 18, 18 and 11% (Figure 4.6c), respectively, which was significantly higher (p <0.05) than that shown by the remaining bacteria constituting the colony (Figure 4.6c). *Achromobacter* and *Sphingobacterium* genera can be involved in the degradation of high dissolved PHE concentrations (i.e. up to 200 $mg \cdot L^{-1}$) [429,430], as well as in the remaining part of DOC being also capable to use EtOH as substrate [400]. These bacteria are extremely relevant for the bioremediation of PAH–contaminated sites due to their capability to produce biosurfactants and rhamnolipids that enhance PAH bioavailability [400]. In addition, the *Achromobacter* genus can generate biodemulsifiers, which are reported to be more efficient compared to normal biosurfactants due to the higher surface activity and breaking emulsion efficiency [20].

The *Dysgonomonas* genus was previously found with a bacterial abundance comprised between 6 and 9% in untreated fuel and raw refinery wastewater [431,432], respectively, under anaerobic conditions. Species belonging to *Dysgonomonas* were reported as facultative anaerobic bacteria [433] and capable of being enriched on both EtOH and PAHs [434]. Therefore, they could have played a role in this thesis when DO concentrations decreased below 1 $mg \cdot L^{-1}$ in cycles 4 and 5 (section 4.3.1), while PHE biodegradation proceeded despite a slight decrease by about 1% (Figure 4.2a). Further studies should be conducted to explore the potential of PHE biodegradation

under anaerobic conditions, in order to reduce the high operating costs associated with the aeration of the mixed liquor.

A relative abundance below 10% (Figure 4.6c) was found for the other bacterial genera, of which many are reported to potentially degrade PHE or PAHs. *Brevundimonas* exhibited the highest copiousness (i.e. 8%, Figure 4.6c), and was pointed out to have a significant ability for PHE degradation [435]. Similarly, *Azospirillum* showed a relative abundance of 7% (Figure 4.6c) and could be implicated during the early stages of PHE biodegradation (section 4.3.2), mainly in the presence of the largest nutrient availability [436,437]. In addition, *Stenotrophomonas* (Figure 4.6b) was identified with a richness of 4% (Figure 4.6b), and could have supported the other bacteria to completely mineralize PHE being capable to degrade PHE metabolites into CO_2 and H_2O [438]. *Chryseobacterium* (Figure 4.6c) was recently isolated in a liquid medium containing a mixture of PAHs and surfactants (including hydroxypropyl–β–cyclodextrin) [439,440]. *Ancylobacter*, *Rhodococcus*, *Microbacterium* and *Starkeya* genera (Figure 4.6c) were also listed to have a broad response to PHE [441–443].

Future studies should be aimed at refining the enrichment of those microbial species highly specialized in PHE degradation, in order to decrease the duration of the treatment and the amount of the EtOH concomitantly degraded. In this way, EtOH can be recovered and successfully reused as extracting agent in further SW applications.

4.3.5 Comparing performances of bioreactors treating PHE–contaminated SW solution

This study indicates that a PHE– and EtOH–containing spent SW solution can be treated with an efficiency up to approximately 91%, after the enrichment of a PHE–degrading consortium and the proper supplementation of nutrients (i.e. N and P).

Comparing the results of this thesis with those obtained by similar studies, the highest PHE removal percentage here observed (Figure 4.2 and Table 4.1) was slightly lower than that achieved in the bioreactors operated by other authors (i.e. approximately 99%, Table 4.1). Several operating parameters can affect PHE degradation [444], but the effect of the initial PHE concentration and the washing agent used are the most significant in this study (Table 4.1). Indeed, temperature (i.e. 30 °C) and agitation were constantly maintained, and could not be a limiting factor for PHE–degrading bacteria (section 4.3.4) [445]. pH and DO played a major role in PHE biodegradation (section 4.3.1) but cannot be used as parameters for comparison due to lacking information about those in other studies (Table 4.1).

With regard to the initial PHE concentration, 20–140 mg·L^{-1} of PHE here used was averagely higher than the 0.80–25 mg·L^{-1} of the other works. Increasing PHE concentration led to a slower PHE degradation (sections 3.1 and 3.3), likely due to the inhibitory effect of the substrate or intermediate metabolites such as 2H1NA (see sections 3.2) that generated toxicity to microorganisms [446]. On the other hand, approximately 20–95 mg·L^{-1} of PHE per cycle were biodegraded in the current study (Figure 4.2 a), showing a certain flexibility of the fed–batch reactor that could cope with various PAH concentrations, as a result of heterogeneous contamination of sediments or different SW efficiencies [447]. A step forward would be the operation of a continuous–flow bioreactor to obtain a long–term high–rate PHE removal and select the most performing bacteria by properly regulating the hydraulic retention time [448].

About the presence of the extracting agent in the spent SW solution, EtOH was concomitantly degraded with PHE, as also corroborated by the correlation between PHE and DOC (i.e. $r_{PHE–DOC}$ = 0.700). Schaefer et al. [449] reported that EtOH was a preferred substrate over other organic pollutants (e.g. PHE) for the growth of an acclimated degrading consortium (see section 4.3.4), thus becoming a competing substrate [450]. Indeed, the achievement of a selective degradation of PAHs due to the presence of extracting agents in the SW solution is rather difficult [180]. This would be more probable if a less biodegradable and more persistent extracting agent, such as Tween® 80, is used [451]. However, non–ionic surfactants (e.g. Tween® 80) are reported to have toxic effects on PAH–degrading bacteria at concentrations higher than 5,000 mg·L^{-1} [27]. Therefore, if PAHs are not effectively removed from the SW solution due to the microbial inhibition by non–ionic surfactants, several washing cycles would be required to successfully remediate the sediment. Thus, in spite of a concomitant high EtOH degradation, the use of EtOH does not interfere with the biodegradation of high PAH concentrations and can allow an easier and safer recovery of the extracting solution.

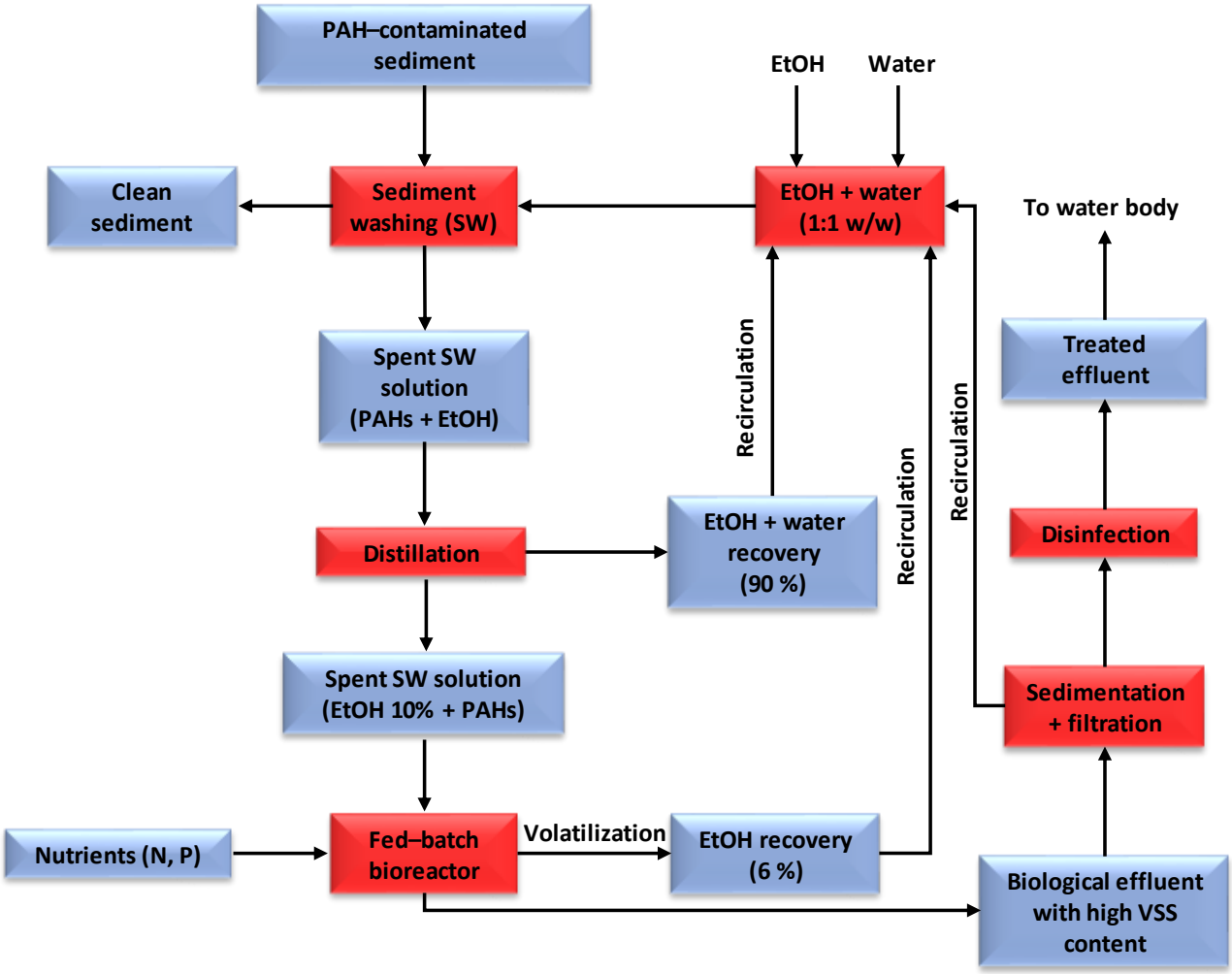

Figure 4.11 – Integrated cycle for i) the remediation of polycyclic aromatic hydrocarbon (PAH)–contaminated sediments via chemical sediment washing (SW), followed by ii) the treatment of spent SW solution through a fed–batch bioreactor and iii) the sequence of operations for ethanol recovery.

4.3.6 Sequence of operations for EtOH recovery and economic assessment

The high amount of spent SW effluents that can be generated downstream of the SW process can limit the use of SW in full–scale applications. Decreasing the consumption of washing agents with a high S/L ratio and promoting the recovery of the used reagents can allow to reduce the amount of spent SW solution to be treated. A possible sequence of operations for EtOH recovery is illustrated in Figure 4.7, and the economic assessment reported below was conducted using 1 ton of PHE–contaminated sediment as basis.

The sediment polluted by PHE can be firstly remediated in a SW plant with a S/L ratio of 1:3 (w/w) by using a mixture of EtOH and water (1:1) as extracting agent and reaching a removal efficiency of almost 100% (Table 4.2). After a solid–liquid separation [167], roughly 2.81 tons of spent SW solution per ton of sediment can be subsequently distilled achieving an EtOH recovery up to 1.26 tons. The remaining part of the spent SW solution can be treated in a fed–batch bioreactor (as that used in this thesis) reaching a PHE removal up to 91% (Table 4.1) and a further recovery of EtOH (i.e. up to 0.08 tons, Figure 4.7) by volatilization (section 4.3.1) and condensation. The recovered EtOH can be used for the preparation of a fresh SW solution, while the effluent from the bioreactor can be further treated and safely released into the environment (Figure 4.7) [452]. Otherwise, a dephlegmator fractional condenser can be used for the volatilized EtOH to improve its recovery over 90% [453], thus allowing the production of high–purity EtOH to be marketable.

The economic assessment on the entire process chain including the SW operation, EtOH supply, and the biological treatment of spent SW solution revealed a total cost of 722 €·ton^{-1}, as the sum of 89, 593 and 40 €·ton^{-1}, respectively. The purchase of EtOH evidently represents the main cost of the entire process and, therefore, EtOH recovery strategies (i.e. distillation and condensation) have been considered. The overall recovery of 1.35 tons of EtOH including the cost of distillation and spent SW solution treatment would result in a saving of 372 €·ton^{-1}, thus resulting in a net expenditure of 350 €·ton^{-1}, and a reduction of the whole treatment cost by approximately 50%. The cost of 350 €·ton^{-1} is comprised in the range 36–480 €·ton^{-1}, previously indicated for the remediation of polluted sediments using SW [454]. This encourages the application of such a resource recovery approach, having positive implications on both the environmental and techno–economic aspects of the SW technology.

4.4 Conclusions

This chapter indicates that a PHE–polluted SW solution can be biologically treated in a fed–batch bioreactor achieving a PHE removal up to 91%. PHE was biodegraded by a bacterial community mainly composed of *Achromobacter*, *Sphingobacterium* and *Dysgonomonas* genera, following a first–order kinetic with a k and R^2 of 0.127–1.177 d^{-1} and 0.652–0.928, respectively. A techno–economic assessment revealed a possible EtOH recovery up to 1.35 tons, thus allowing a net expenditure of 350 €·ton^{-1} covering SW operation, EtOH supply and recovery, and the biological treatment of the spent

SW solution. This contributes to the creation of a sustainable resource–recovery approach, having an elevated potential for application at a larger scale. Future studies should be aimed at the optimization of the bioreactor operation by maximizing the PHE loading rates in continuous–flow systems and fine–tuning the DO level in the liquid phase.

CHAPTER 5. COUPLING OF DESORPTION OF PHENANTHRENE FROM MARINE SEDIMENTS AND BIODEGRADATION OF THE SEDIMENT WASHING SOLUTION IN A NOVEL BIOCHAR IMMOBILIZED–CELL REACTOR

5.1 Introduction

Marine sediments are considered one of the principal sinks of persistent organic pollutants (POPs) reaching the aquatic ecosystems. Among the main POPs affecting sediment quality, polycyclic aromatic hydrocarbons (PAHs) are carcinogenic and mutagenic petroleum–derived substances mostly discharged by human activities [455,456]. The PAH contamination of sediments poses important concerns with regard to sediment dredging in harbors, since a high presence of PAHs considerably restricts the reuse or disposal of sediments. This implies the need for ex–situ technologies for the remediation of dredged sediments, among which sediment washing (SW) has widely been used due to its operational simplicity, high effectiveness and relative cheapness [27].

SW is classified as a physical–chemical technology, which consists in the use of extracting agents (e.g. surfactants) to allow PAH desorption from contaminated sediments [22]. In particular, non–ionic surfactants are generally employed for this purpose due to the higher solubilization potential and lower supply cost than anionic and cationic surfactants [457]. Non–ionic surfactants such as Tween® 80 (TW80) have largely been employed above their critical micelle concentration (CMC) for enhancing

PAH desorption from soils. TW80 micelles incorporate PAHs into the hydrophobic interior structure, leading to a decreased interfacial tension between the contaminant and water [25]. Nonetheless, only Iglesias et al. [458] previously investigated SW for the remediation of phenanthrene (PHE)–polluted sediments by employing a mixture of TW80 and saponin. Therefore, further studies are needed to give an emphasis on the evaluation of influencing parameters, such as the solid–to–liquid (S:L) ratio and washing time, on SW of PHE–polluted sediments in the presence of TW80.

Despite the abovementioned advantages of the SW technology, this process commonly entails the generation of considerable amounts of spent SW effluent due to the low solid–to–liquid (S:L) ratios (e.g. 1:10 or 1:20) used to improve SW effectiveness [358]. Such hazardous liquid stream requires an adequate treatment prior to being released into the environment [459]. Out of the different technologies available for treating spent SW solutions, biological processes can be applied as the most cost–saving and environmentally–friendly solutions, leveraging the ability of engineered microorganisms to effectively remove PAHs [460]. Aerobic conditions are generally used to accelerate PAH degradation in comparison to anaerobic conditions [461]. Indeed, aerobic bacterial genera (e.g. *Pseudomonas, Sphingomonas*) with specific functional genes, such as PAH ring–hydroxylating dioxygenase, have been reported to speed up PHE degradation into simpler molecules (e.g. 1,2–dihydroxynaphthalene) [462,463]. In addition, the adoption of immobilized–cell bioreactors can increase the retention of microorganisms forming a biofilm onto inert carriers, thus leading to shorter hydraulic retention times (HRTs) compared to suspended–cell bioreactors [28].

The selection of the most suitable supporting media for microbial immobilization plays a major role for the proper bioreactor functioning [464]. A valid biofilm carrier should be neither toxic to the involved microbial community nor contaminate the environment and easily promote biofilm attachment and growth [465]. Previous studies reported the employment of activated carbon, ceramsite and walnut shells as biocarriers for immobilizing cells in continuous–flow bioreactors treating hydrocarbons– and PAH–containing streams [29,461,464]. Therefore, biomaterials such as carbonaceous adsorbents, including biochar (BC), can represent a promising and sustainable solution for the immobilization of microorganisms due to a good surface area, providing an efficient support for microbial growth and, in certain cases, representing a source of nutrients [466]. BC is a porous material mostly manufactured through the pyrolysis of a carbon–based feedstock and can adsorb PAHs as a function of the carbon content, surface area and presence of different functional groups [467].

Up to date, BC has widely been used for the remediation of PAH–contaminated sediments, aiming to promote the direct PAH transfer from the sediment to BC. Only a few reports focused on the use of BC immobilized–microorganisms, but all these studies aimed at exclusively investigating the bioremediation of soils [468,469] and not explore the potential of BC attached–cells to treat spent SW solutions.

In this thesis, both the desorption of phenanthrene (PHE) from marine sediments using TW80 as extracting agent and, for the first time, the biodegradation of the obtained spent SW solution in a BC immobilized–cell reactor has been proposed. So far, the degradation of PHE, here used as the model PAH compound, from TW80 solutions has more extensively been studied in batch flasks [250,470,471], while a continuous–flow bioreactor operation has larger margins for interesting scientific evidences. The specific objectives of this chapter were to *i)* investigate the effect of TW80 concentration, S:L ratio and desorption time on the SW process of PHE–contaminated marine sediments in batch tests; *ii)* biologically treat the resulting spent SW solution in a BC immobilized–cell reactor operated in both batch and continuous–flow modes; *iii)* model PHE desorption from sediments and PHE adsorption onto BC using the most commonly used kinetics; *iv)* identify the dominant PHE–degrading bacterial families and genera throughout the bioreactor operation; *v)* conduct a techno–economic assessment on the whole process to evaluate its upscaling potential.

5.2 Materials and methods

5.2.1 Chemicals

Hexane (grade ≥95%), magnesium sulfate (grade ≥97%), PHE (grade ≥98%), potassium chloride (grade ≥ 99%), sodium azide (grade ≥99%), sodium carbonate (grade ≥99.5%), sodium chloride (grade ≥99%) and sodium hydroxide (grade ≥98%) were all purchased from Sigma–Aldrich (Germany). Ammonium nitrate (grade ≥99%), Deconex® 31 antifoam, potassium dihydrogen phosphate (grade 100%), sodium phosphate dibasic (grade ≥99%) and TW80 (reagent grade) were supplied by VWR (Italy). Acetonitrile and methanol (HPLC grade) were provided by Poch (Poland) and Biosolve (France), respectively. MilliQ water with an electrolytic conductivity equal to 0.05 μS cm^{-1} was used as the background for preparing all the solutions.

5.2.2 Sediment washing tests aimed at phenanthrene desorption

With the aim to evaluate the effect of the TW80 concentration on PHE desorption [27], one gram [472] of dry PHE–contaminated marine sediment, previously characterized elsewhere (see chapter 2), was added to each 50 mL Erlenmeyer flask with 20 mL of SW solution having different TW80 concentrations (i.e. 108, 270, 540, 1,080, 2,700, 5,400 and 10,800 $mg \cdot L^{-1}$), which were previously used for soil remediation [457]. Afterwards, the flasks were sealed with glass stoppers and placed on a gyratory shaker at 200 rpm for 24 hours at room temperature [472], and thereafter the quantity of desorbed PHE was evaluated. Another set of batch experiments was subsequently carried out to evaluate the desorption kinetics with a 1:4, 1:8, 1:12, 1:16 and 1:20 S:L ratio (w/v), while keeping a constant TW80 concentration (i.e. 10,800 $mg \cdot L^{-1}$) in the SW solution depending on the results achieved in the first desorption tests. The amount of desorbed PHE was determined by sacrificing a flask for each S:L ratio after 1, 2, 5, 15, 30, 60, 120, 240, 480, 960 and 1,440 minutes. All operating conditions in the described tests were reproduced in triplicate.

5.2.3 Treatment of the spent sediment washing solution using biochar immobilized–bacteria

5.2.3.1 Inoculum and biochar

The fresh inoculum was taken from the effluent of a lab–scale bioreactor treating a spent PHE–contaminated SW solution for over 2 months and consequently characterized for the identification of PHE–degrading bacteria (see chapter 4). BC was obtained through pyrolysis of willow twigs collected from an experimental station located in Bezek (Poland). Prior to pyrolysis, the feedstock was chopped and sieved to obtain a fraction below 2 mm. The pyrolysis was conducted in a PRS 168 × 380/90G furnace (Czylok, Poland) with a heating rate of 10 $°C \cdot min^{-1}$ reaching the ultimate temperature of 400 °C, which was kept for 3 h under an oxygen–free environment via a constant nitrogen flow of 3.0 $L \cdot min^{-1}$ ensured by a mass flow controller (Brooks, USA) [473].

5.2.3.2 Bacterial immobilization and initial batch reactor operation

The immobilization procedure was carried out in a 500–mL glass column containing 250 mL of the inoculum and 5 g of BC [239] at ambient temperature for 48 hours with continuous shaking [468] through aeration. At the end of this period, a slurry (i.e. BC + inoculum) sample of 1 mL was taken and centrifuged at 10,000 rpm for 15 minutes [474] prior to proceeding with the taxonomic classification [464].

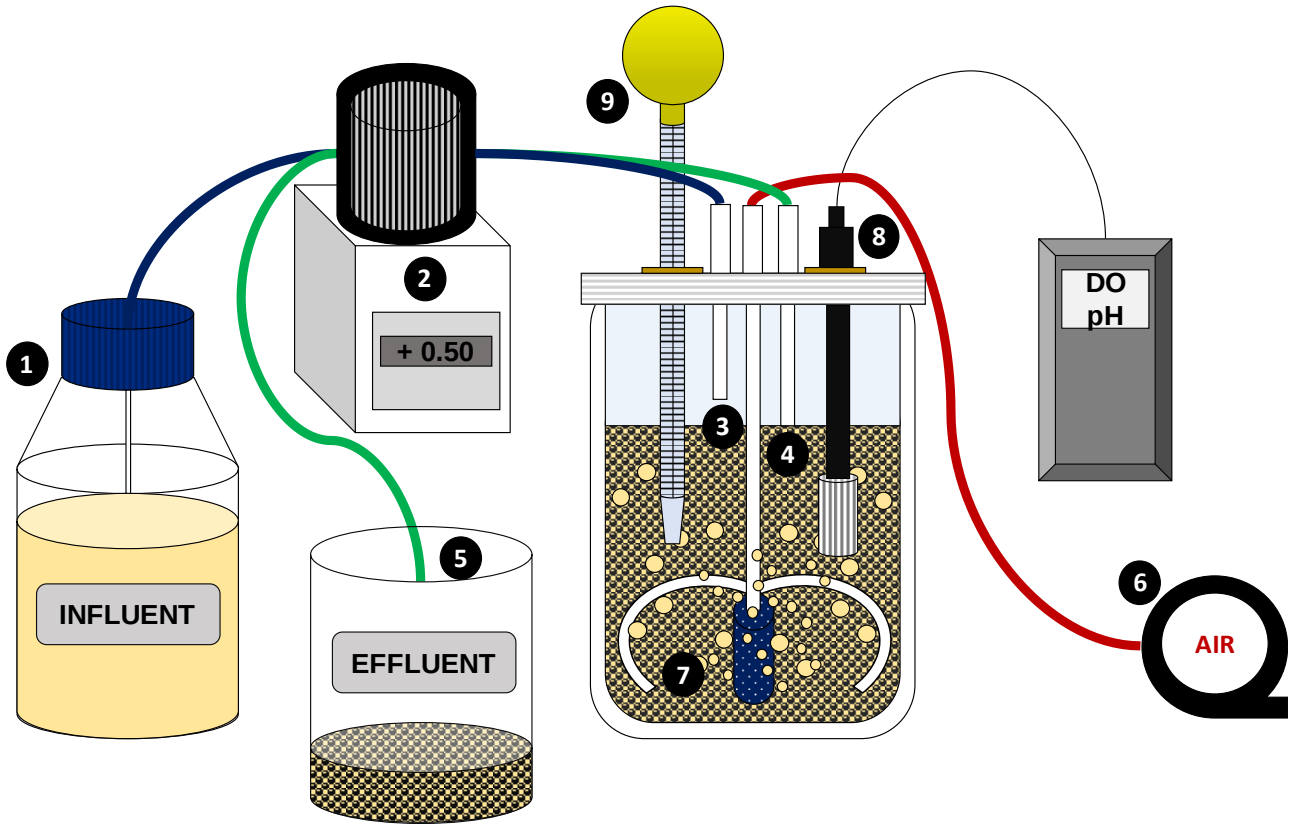

Figure 5.12 – Experimental set–up of the continuous–flow bioreactor (primary reactor – PR) employed in this thesis: 1) glass bottle containing the synthetic sediment washing solution; 2) peristaltic pump for 3) influent feeding and 4) effluent suction; 5) tank for the effluent storage; 6) aquarium pump used to guarantee 7) the mixing and aerobic conditions; 8) port used for the measurements of dissolved oxygen (DO) and pH; 9) sampling port, also used for pH adjustments.

Afterwards, the slurry was vacuum filtered and the obtained solid phase was transferred to a 1,550 mL glass reactor (Figure 5.1), and placed in contact with a 1,000 mL synthetic spent PHE–containing SW solution reaching a working volume of approximately 1,050 mL. At this stage, the synthetic spent SW solution was prepared to obtain PHE and TW80 concentrations of approximately 20 and 2,700 $mg \cdot L^{-1}$, respectively, in the reactor. Also, the initial pH of the synthetic SW solution was set at 7.5 with 1 M NaOH. Under these conditions, the bioreactor was aerobically operated in batch mode for 7 days at room temperature with the aim to promote the acclimatization of bacteria to PHE and TW80 [27] and the growth of biofilm onto BC. The air inflow and pH were not controlled during this phase.

Together with the described primary reactor (PR), two inoculum–free reactors (i.e. C1 and C2, respectively) were operated as controls under the abovementioned conditions (i.e. same PHE and TW80 concentrations and pH used in PR under aerobic

conditions) for evaluating any other possible PHE removal mechanisms. C1 was run to evaluate the abiotic loss of PHE [379] due to e.g. volatilization in the absence of BC. 5 $g \cdot L^{-1}$ of willow BC was dosed in C2, which was operated to assess the PHE adsorption onto BC. Both C1 and C2 reactors were operated with 1,000 mL of SW solution and 200 $mg \cdot L^{-1}$ of NaN_3 as biocide agent [475].

The PHE concentration was determined with three replicates (i.e. 1 mL each) in the supernatant of PR, C1 and C2 after 1, 2, 4, 8, 24, 48, 84, 120 and 168 hours. The content of total suspended (TSS) and volatile suspended solids (VSS) was estimated after 168 hours in three replicates of 40 mL each. Two samples of 1 and 4 mL were also taken after 168 hours in PR for the determination of the cell surface hydrophobicity (CSH) and microbial community structure, respectively.

5.2.3.3 Continuous–flow operation of the bioreactor treating the spent sediment washing solution

After the batch phase, the PHE degradation in PR was studied for 43 days in a continuous–flow mode (Figure 5.1) with an HRT of 3.5 days at room temperature. For the entire period, PR was fed (Figure 5.1) with a synthetic SW solution containing approximately 35 and 10,800 $mg \cdot L^{-1}$ of PHE and TW80, respectively, which were retrieved from the results of the SW batch tests by considering the highest concentration of solubilized PHE. 1 mL of an autoclaved mineral salt medium (MSM) consisting of NaCl, $MgSO_4$, NH_4NO_3, KH_2PO_4, Na_2HPO_4 and KCl (i.e. 19, 7, 1, 2, 3, and 0.7 ‰, respectively) [476] was also included in the synthetic solution. The pH of the synthetic SW solution was finally adjusted to 7.5 with 1 M NaOH.

The continuous flow was guaranteed with a Minipuls 3 peristaltic pump (Gilson, USA) for influent feeding and effluent suction (Figure 5.1), maintaining a constant level in PR (i.e. 1,050 mL). BC particles, acting as biofilm carriers, were mainly retained in PR with a metallic grid [29] and their amount was restored after each HRT with the addition of fresh BC (i.e. averagely 25 mg), which value was deduced by checking the TSS content in the effluent of a further blank reactor operated with only deionized water and BC. The slurry phase (i.e. BC + immobilized cells + spent SW solution) of PR was vigorously mixed and maintained under aerobic conditions via an aquarium pump (Figure 5.1) [29] by providing air through a glass tube (large bubbles) and a porous stone (fine bubbles). The dissolved oxygen (DO) concentration was maintained above 8.0 $mg \cdot L^{-1}$ [477] by manually adjusting the aeration flowrate. The pH value was kept in the optimal range of 6.5–8.5 [478] by supplying Na_2CO_3 (i.e.

1,000 mg·L^{-1}) in powder form (Figure 5.1). One mL·L^{-1} of antifoam agent was manually added to PR once a day to suppress foam generation due to the air inflow in the presence of high TW80 concentrations. Aluminum foil was used to cover the wall of PR (Figure 5.1) and prevent the onset of phototrophic reactions.

Three samples (i.e. 2 mL each) were daily collected from the PR effluent for the analysis of both PHE and dissolved organic carbon (DOC). The daily measurements of DO and pH were performed directly in PR (Figure 5.1). The TSS and VSS concentrations were determined after 43 days in three samples of 40 mL each. The composition of the microbial community populating the BC and the CSH were also analyzed at the end of PR operation by sampling 1 and 4 mL from the bioreactor, respectively.

5.2.4 Analytical methods

TSS and VSS contents were quantified using the centrifuge–based procedure [380]. The amount of ashes in BC was estimated according to the standard methods [479]. The elemental composition of BC was determined through a CHN 2400 series analyzer (Perkin–Elmer, USA), and the O content was subsequently calculated by subtracting the quantity of C, H, N and ash (%) from the 100% of dry substance [480]. The specific surface area (S_{BET}) of BC was evaluated with nitrogen adsorption–desorption isotherms obtained from an ASAP 2420 surface area and porosity analyzer (Micromeritics, USA), as extensively reported by Siatecka et al. [473]. Fourier–transform infrared photoacoustic spectroscopy (FT–IR/PAS) was used to determine the functional groups in the BC through an FT–IR Nicolet 8700A spectrometer (Thermo Scientific, USA) equipped with a photoacoustic detector MTEC300 (helium atmosphere) over the range of 4000–400 cm^{-1} [481]. The pH of BC was measured after 24 hours in a liquid phase composed of deionized water and BC with an S:L ratio (w/v) of 1:10 [482] using a SenTix® 950 pH electrode (WTW, USA). The measurement of DO was conducted with an IDS FDO® 925 (WTW, USA). DOC concentration was analyzed via a TOC–L Series (Shimadzu, Japan) according to the method reported elsewhere [483]. The cell suspension was determined with an optical density (OD) at 605 nm [484] using a PhotoLab® S6 spectrophotometer (WTW, USA). The procedures for DNA extraction and quantification, PCR amplification, library quantification, Illumina sequencing, sequence filtering and taxonomic classification were carried out as described in chapter 4. Functional genes associated with the biodegradation of PHE were analyzed through the PICRUSt2 platform (https://github.com/picrust/picrust2) [485].

Samples for PHE quantification were centrifuged at 3,000 rpm for 30 minutes [26] and filtered through a 0.45 μm glass microfiber filter (Whatman, USA) prior to the analyses. Liquid–phase PHE was analyzed using a 1260 Infinity II HPLC equipped with an InfinityLab Poroshell 120 EC–C18 (3.0 × 5 mm; 2.7 μm) column heated at 30 °C and a diode array detector (Agilent, Germany) set at 254 nm [361]. An acetonitrile/5% methanol in water (85:15, v/v) solution was used as the mobile phase [486] at a flowrate of 0.9 mL·min^{-1}. The injection volume for the samples was 10 μL.

5.2.5 Data elaboration

5.2.5.1 Calculations

The molar solubilization ratio (MSR) and the weight solubilization ratio (WSR), which express the moles and mass of PHE dissolved per mole or mass of TW80 above surfactant CMC, respectively, were deduced from the slope of the solubilization curve [386]. The micelle–water partition coefficient (K_m), indicating the solubilization capacity of TW80, was calculated as the ratio between the mole fraction of PHE in the micellar pseudophase (X_m) and in the micelle–free aqueous phase (X_a) [487].

The amount of desorbed PHE (q_t, mg·kg^{-1}) from the sediment to the SW solution for each investigated S:L ratio (Section 6.2.2) was calculated as follows (Eq. 5.1) [25]:

$$q_t = S_w^* \cdot (V_{TW80}/W_s) \quad \text{(Eq. 5.1)}$$

where S_w^* (mg·L^{-1}), V_{TW80} (L) and W_s (kg) are the solubilized PHE, the volume of surfactant solution and the mass of sediment, respectively.

The Gibbs free energy (ΔG_s, kcal·mol^{-1}) liberated from the incorporation of PHE particles into TW80 micelles was obtained from the following expression (Eq. 2) [488]:

$$\Delta G_s = -R \cdot T \cdot ln(K_m) \quad \text{(Eq. 5.2)}$$

where R and T are the universal gas constant (i.e. 8.314 J·mol^{-1}·K^{-1}) and the temperature (i.e. 298.15 K), respectively. A K_m of 5.98 [487] was used for comparing that obtained in the present study.

The adsorbed mass of PHE ($q_{e,t}$, mg·g^{-1}) onto BC was calculated by considering the decrease of the solute concentration in the aqueous phase over time (Eq. 5.3) [489]:

$$q_{e,t} = \frac{(C_{0,t} - C_{e,t}) \cdot V}{M} \quad \text{(Eq. 5.3)}$$

where $C_{o,t}$ and $C_{e,t}$ are the PHE concentrations in C1 and C2 (mg·L^{-1}) (see Section 6.2.3.2) after each time (h), respectively, and V and M are the volume of the solution (L) and the mass of adsorbent (g), respectively.

The colony–forming units (CFU) per mL were correlated to the VSS content through the OD at 600 nm [401,490] by subtracting the aliquot due to the presence of BC. CSH was calculated after the addition of 1 mL of hexane to 4 mL of a diluted cell suspension to an OD of 1, as reported by Zang et al. [20].

5.2.5.2 Kinetic study

PHE desorption kinetics were evaluated by comparing Elovich (Eq. 5.4), fractional power (Eq. 5.5) and intraparticle diffusion (Eq. 5.6) kinetic models via the OriginPro software (8.5 version, OriginLab Corporation, USA). The experimental q_t values were modeled by the following equations [491]:

$$q_t = a + k_1 \cdot \ln(t) \quad \text{(Eq. 5.4)}$$

$$q_t = k_2 \cdot t^v \quad \text{(Eq. 5.5)}$$

$$q_t = k_3 \cdot t^{\frac{1}{2}} + c \quad \text{(Eq. 5.6)}$$

where k_1 ($mg \cdot kg^{-1} \cdot \ln(min)^{-1}$), k_2 ($mg \cdot kg^{-1} \cdot min^{-v}$) and k_3 ($mg \cdot kg^{-1} \cdot min^{1/2}$) are the rate constants of desorption, and a ($mg \cdot kg^{-1}$), v and c ($mg \cdot kg^{-1}$) are the constants of the Elovich, fractional power and intraparticle diffusion models, respectively.

The Elovich and intraparticle diffusion models (Eq. 7 and 8, respectively) were also used for assessing the adsorption kinetics by considering the $q_{e,t}$ defined in Section 6.2.5 [489]. In addition, the pseudo–first– and –second–order kinetics (Eq. 9 and 10, respectively) were employed to model the experimental adsorption data as follows [196]:

$$q_{e,t} = \frac{1}{\beta} \cdot \ln(\alpha \cdot \beta) + \frac{1}{\beta} \cdot \ln(t) \quad \text{(Eq. 5.7)}$$

$$q_{e,t} = K_{ip} \cdot \sqrt{t} + C \quad \text{(Eq. 5.8)}$$

$$\ln(q_e - q_{e,t}) = \ln(q_e) - k_4 \cdot t \quad \text{(Eq. 5.9)}$$

$$\frac{t}{q_{e,t}} = \frac{1}{k_5 \cdot q_e^2} + \left(\frac{1}{q_e}\right) \cdot t \quad \text{(Eq. 5.10)}$$

where α ($mg \cdot g^{-1} \cdot h^{-1}$) and β ($g \cdot mg^{-1}$) are the initial adsorption rate and the ratio between the surface coverage and activation energy for the Elovich model, respectively. K_{id} ($mg \cdot g^{-1} \cdot h^{-1/2}$) and C ($mg \cdot g^{-1}$) are the diffusion rate constant and boundary layer thickness for the intraparticle diffusion, respectively. Also, q_e is the equilibrium solid phase concentration of PHE ($mg \cdot g^{-1}$), k_4 ($1 \cdot h^{-1}$) and k_5 ($g \cdot mg^{-1} \cdot h^{-1}$) are the adsorption rate constants of pseudo–first– and –second–order kinetics, respectively.

5.2.6 Statistical analysis

The analysis of variance (ANOVA) followed by a Tukey's HSD (honestly significant difference) test was performed to assess statistical differences ($p < 0.05$) among the processed data. The statistical analysis was executed with the OriginPro software (8.5 version, OriginLab Corporation, USA).

5.2.7 Economic evaluation

A rough assessment of the costs was conducted by considering the whole remediation process, i.e. SW and treatment of the spent SW solution. The costs associated with SW operations and biological treatment of the PHE–contaminated TW80 solution under aerobic conditions were assumed as 120.57 and 12.50 € per m^3 of sediment and effluent [369,391], respectively. In addition, the price of TW80 and BC was fixed to 4.00 and 2.22 €·kg^{-1} [180], respectively. A sediment density of 1.6 ton·m^{-3} was supposed for the calculation [394], and the final cost was standardized on a sediment mass basis (ton) by considering a unit sediment volume (m^3).

5.3 Results and discussion

5.3.1 Sediment washing

5.3.1.1 Investigation of the most effective Tween® 80 concentration

A PHE solubilization between approximately 2 and 9 $mg \cdot L^{-1}$ (Figure 5.2a) was obtained in the surfactant solution after 1,440 minutes of SW in the tests aimed at determining the effectiveness of TW80 and the most performing TW80 concentration.

The lowest TW80 concentration (i.e. 108 $mg \cdot L^{-1}$) used in this thesis can be considered as the effective CMC (CMC_{eff}), i.e. the concentration at which the first micelle is formed [27], since the PHE concentration was close to 2 $mg \cdot L^{-1}$ [487]. However, the mentioned CMC_{eff} was higher compared to that generally reported for TW80 in pure water (i.e. 13 $mg \cdot L^{-1}$) [457], likely due to the loss of a part of the surfactant that could be adsorbed onto the sediment particles [25,492]. The solubilization parameter values obtained for MSR, WSR and K_m (i.e. about 0.003, 0.001 and 4.223, respectively) further supported this theory [487,493], due to a lower solubilization capacity of the surfactant when PHE is adsorbed onto sediment particles rather than present in a crystal form in the liquid phase [494]. Notwithstanding, the mentioned CMC_{eff} corresponded to approximately 2 g $TW80 \cdot kg^{-1}$ of sediment, which was considerably lower compared to the values previously determined for PHE–contaminated soils (i.e. 10 g $TW80 \cdot kg^{-1}$) [27]. This could be ascribed to the different content of organic matter in the sediment that can play an important role in PAH retention, as reported by Grasso et al. [495]. Indeed, the organic matter can bind PHE via strong interactions such as π–π, subsequently affecting PHE desorption from the soil [491].

The amount of solubilized PHE significantly increased ($p < 0.05$) from approximately 20 to 91% (Figure 5.2a) by varying the TW80 concentration from CMC_{eff} to 10,800 $mg \cdot L^{-1}$, likely due to a higher number density of micelles [487]. The use of a TW80 concentration up to about 10,000 $mg \cdot L^{-1}$ is generally used for SW processes [457]. For instance, Tao et al. [472] recently showed that PHE desorption can be enhanced from approximately 10 to 68% in a co–contaminated soil with PHE and Cu, by increasing TW80 concentrations in the surfactant solution from 1,000 to 10,000 $mg \cdot L^{-1}$. However, the slight discrepancy in terms of desorption efficiency compared to this thesis (Figure 5.2a) could be explained by the presence of a high concentration of toxic metals [25] in the work of Tao et al. [472]. Saeedi et al. [496] showed that the polar part of soil organic substances can generate further hydrophobic

sites for PAH adsorption in the presence of metals, thus affecting PAH desorption from the soil. Hence, the TW80 concentration in the SW solution was kept at 10,800 mg L^{-1} for the subsequent SW tests performed at different S:L ratios.

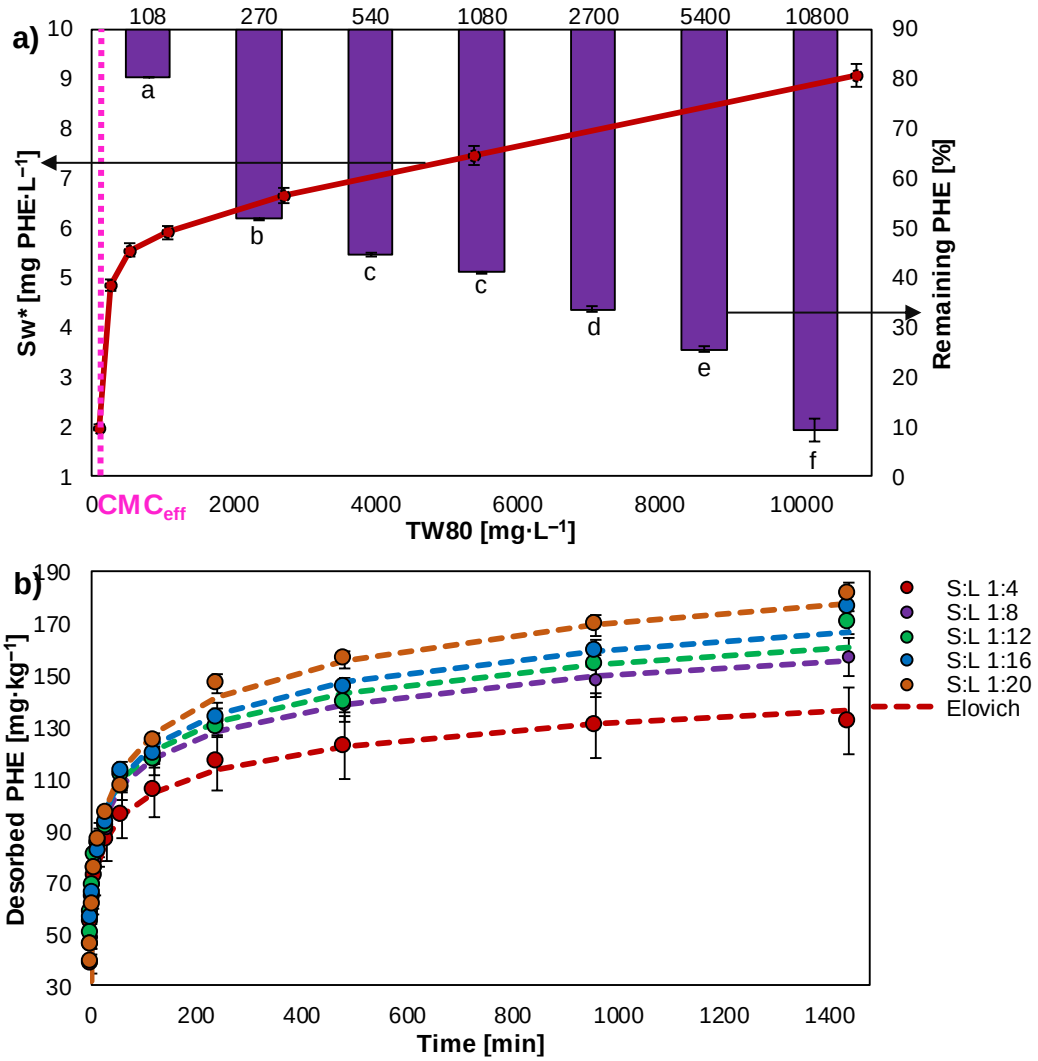

Figure 5.13 – Phenanthrene (PHE) solubilization (S_w, mg·L^{-1}) in the surfactant solution at different Tween® 80 (TW80) concentrations (solid line) and the remaining PHE (%) in the polluted sediment (histogram) (a). Desorbed PHE (mg·kg^{-1}) from contaminated sediments at different time points (min) using a TW80 concentration of 10,800 mg·L^{-1} with different solid–to–liquid (S:L) ratios (i.e. 1:4, 1:8, 1:12, 1:16 and 1:20, w/v) (b, c).*

The experimental curves (b) were fitted by the Elovich kinetic (dash line). The different letters (Tukey test) indicate statistical differences ($p < 0.05$). The averages and error bars were determined on triplicates.

5.3.1.2 Effect of the solid–to–liquid ratio on phenanthrene extraction

The amount of desorbed PHE was approximately 132, 157, 170, 176 and 181 $mg \cdot kg^{-1}$ (Figure 5.2b) after 1,440 minutes of SW with 10,800 mg L^{-1} of TW80 by using an S:L ratio of 1:4, 1:8, 1:12, 1:16 and 1:20, respectively. Although the S:L ratio of 1:20 showed the highest PHE removal (i.e. about 91%, Figure 5.2b) from the contaminated sediment, PHE desorption was not statistically affected ($p < 0.05$) by the increase of the S:L ratio from 1:4 upwards (i.e. 66−88%, Figure 5.2b), confirming what reported elsewhere [168,497]. Gharibzadeh et al. [27] reported that the increase of the surfactant dosage from 10 to 50 g $TW80 \cdot kg^{-1}$ of soil can significantly enhance PHE desorption, but a further supplementation of TW80 may result in a lower desorption improvement rate. This is what most likely occurred in the present study, since the TW80 amount employed at an S:L ratio of 1:4 was approximately 43 g $TW80 \cdot kg^{-1}$ of sediment.

Hence, an S:L ratio of 1:4 is enough for the optimization of SW [23] and would lead to similar efficiencies obtained with lower S:L ratios but also to considerable savings in terms of amount of surfactant [361], equipment and energy [359]. Moreover, a high S:L ratio allows to generate a lower volume of spent SW solution to be treated, with a subsequent decrease of the post–treatment costs and a further reduction of the entire process expenses [497]. If required, the remaining amount of PHE could be further extracted from the sediment with a subsequent SW cycle, since the extraction capacity of TW80 may not considerably vary in terms of desorption efficiency in different cycles [472].

5.3.1.3 Effect of time on sediment washing and phenanthrene desorption kinetics

The desorption curves of PHE at different S:L ratios are presented in Figure 5.2b. A fast PHE desorption, reaching an efficiency comprised between 48 and 56% (Figure 5.2b and c), was observed in the initial 60 minutes. This was then accompanied by a sub–horizontal profile, indicating a subsequent slower desorption phase entailing an extra 18−37% PHE removal efficiency (Figure 5.2b) till the end of the experiment. This result was similar to that reported by López–Vizcaíno et al. [498]. When the adsorption energy of the contaminant is high, the desorption from the solid particles is affected by the transport velocity from the sub–layer to the surfactant solution [499]. Indeed, the ΔG_s associated with PHE desorption from the sediment particles to the

TW80 solution was −5.77 kcal·mol^{-1}, which was less thermodynamically feasible compared to that predicted for PHE in crystal form (i.e. −8.16 kcal·mol^{-1}).

The PHE desorption kinetics parameters obtained for each S:L ratio (i.e. 1:4, 1:8, 1:12, 1:16 and 1:20) using the Elovich, fractional power and intraparticle diffusion models are reported in Table 5.1. The highest determination coefficient (R^2) (i.e. 0.984–0.992) and relatively lowest residual sum of squares (RSS) (i.e. 85.172–261.149) suggested that the Elovich kinetics better simulated the SW process (Figure 5.2b) compared to the fractional power model (i.e. R^2 = 0.950–0.990 and RSS = 150.989–521.416). Likewise, Amir et al. [491] reported that the Elovich model showed a higher R^2 (i.e. 0.933) than the fractional power function when modeling PHE desorption with a 10% (w/w) Triton™ X–100 and 0.01 M EDTA surfactant solution. The lowest R^2 showed by the intraparticle diffusion model (i.e. 0.747–0.874, Table 5.1) demonstrated that the final PHE desorption rate was not affected by the adsorbate diffusion into the adsorbent, likely due to the limited presence of pores [500]. Therefore, the Elovich kinetic model adequately explained the PHE chemidesorption previously discussed (Figure 5.2b), by implying that the active sites of the sediment were heterogeneous and manifested various activation energies for PHE desorption [501,502]. In addition, the a and k_1 values resulting from the plots of the Elovich kinetics of 31.612–45.502 mg·kg^{-1} and 12.701–20.023 mg·kg^{-1}·ln(min)$^{-1}$, respectively, further corroborated this theory by indicating that the PHE particles were not initially retained and could be easily desorbed [503]. These kinetic parameters were higher than those reported by Mohamadi et al. [504], who modeled PHE desorption from a contaminated soil with a TW80/EDTA solution through the Elovich model (i.e. 0.048 mg·kg^{-1} and 12.79 mg·kg^{-1}·h^{-1} for a and k_1, respectively). This is likely due to the co–presence of heavy toxic metals in the PHE–contaminated soil in the work of Mohamadi et al. [504] that limited PHE desorption, as described above (see Section 6.3.1.1).

Table 5.8 – Elovich, fractional power and intraparticle diffusion kinetic models of phenanthrene (PHE) desorption ($mg \cdot kg^{-1}$) during the sediment washing of PHE–contaminated marine sediments with a solid–to–liquid (S:L) ratio (w/v) of 1:4, 1:8, 1:12, 1:16 and 1:20.

Models	Parameters	S:L ratio				
		1:4	*1:8*	*1:12*	*1:16*	*1:20*
Elovich	$a\ [mg \cdot kg^{-1}]$	43.835	45.502	44.396	38.902	31.612
	$k_1\ [mg \cdot kg^{-1} \cdot ln(min)^{-1}]$	12.701	15.109	15.934	17.534	20.023
	R^2	0.989	0.994	0.984	0.985	0.992
	RSS	105.721	85.172	231.034	261.149	175.989
Empirical power	$k_2\ [mg \cdot kg^{-1} \cdot min^{-v}]$	52.914	55.891	54.957	51.766	48.954
	v	0.134	0.146	0.154	0.169	0.185
	R^2	0.950	0.981	0.990	0.989	0.978
	RSS	466.025	250.312	150.989	200.886	521.416
Intraparticle diffusion	$k_3\ [mg \cdot kg^{-1} \cdot min^{-(1/2)}]$	2.179	2.702	2.937	3.228	3.617
	$c\ [mg \cdot kg^{-1}]$	66.057	70.637	69.862	66.980	64.496
	R^2	0.747	0.825	0.874	0.872	0.842
	RSS	2376.563	2324.692	1867.668	2292.746	3673.605

The adsorption rate constants (i.e. k_1, k_2 and k_3) and the model constants (i.e. a, v and c) are referred to the investigated kinetics (Eq.s (5.4), (5.5) and (5.6)). R^2 = coefficient of determination; RSS = residual sum of squares.

5.3.2 Treatment of the synthetic phenanthrene–containing sediment washing solution

5.3.2.1 Phenanthrene removal under batch operating conditions

A PHE removal of 10 and 86% (Figure 5.3) was obtained after 168 hours of treatment of the synthetic spent PHE–containing SW solution in C2 and PR, respectively, operated in a batch mode. Since the PHE abiotic loss was negligible (i.e. 1% in reactor C1, Figure 5.3) [469], this suggests that PHE was mainly removed by both adsorption and biodegradation in the first week of PR operation. In particular, after 8 hours from the beginning of the operation, PHE removal in C2 and PR (i.e. approximately 5 and 4%, respectively) (Figure 5.3) was not statistically different ($p > 0.05$), thus indicating that PHE adsorption was the main PHE removal mechanism [164].

Table 5.9 – Elovich, intraparticle diffusion, pseudo–first– and –second–order kinetic models of phenanthrene adsorption onto biochar (mg·g^{-1}) under batch conditions.

Models	Parameters	Values
Elovich	α [mg·g^{-1}·h^{-1}]	0.240
	β [g·mg^{-1}]	22.984
	R^2	0.996
	RSS	0.001
Intraparticle diffusion	K_{id} [mg·g^{-1}·h$^{-1/2}$]	0.020
	C [mg·g^{-1}]	0.073
	R^2	0.863
	RSS	0.011
Pseudo–first–order	k_4 [1·h^{-1}]	0.170
	q_e [mg·g^{-1}]	0.260
	R^2	0.901
	RSS	0.008
Pseudo–second–order	k_5 [g·mg^{-1}·h^{-1}]	0.810
	q_e [mg·g^{-1}]	0.281
	R^2	0.958
	RSS	0.003

The adsorption rate constants (i.e. k_4, k_5, α and K_{ip}) and the model constants (i.e. q_e, β and C) are referred to the investigated kinetics (Eq.s (5.7), (5.8), (5.9) and (5.10)). R^2 = coefficient of determination; RSS = residual sum of squares.

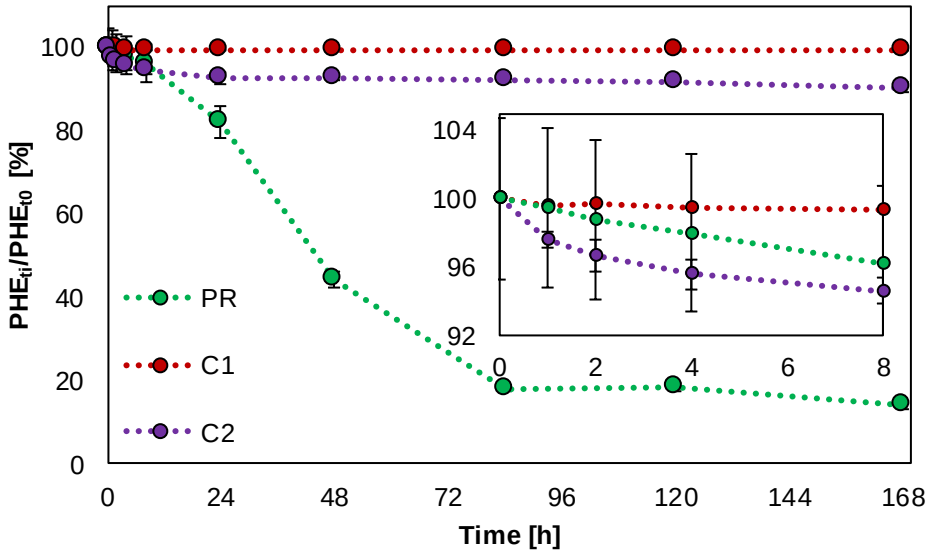

Figure 5.14 – Ratio (%) between the phenanthrene (PHE) concentration at time "t_i" and that at the time "t_0" (h) during the treatment of a spent sediment washing solution during the initial batch reactor operation.

The averages and error bars were determined on triplicates. PR = primary reactor; C1 = abiotic control; C2 = adsorption abiotic control.

The adsorption process can be generally described with three different phases, i.e. the external diffusion, the intraparticle diffusion and the fast stage in which the adsorbate is quickly adsorbed onto the active sites of the adsorbent [505]. For better predicting the occurrence of physisorption or chemisorption mechanisms during the transition of PHE from the TW80 solution to BC, the obtained experimental data within 168 hours were fitted with widely used kinetic models (see Section 6.2.6). The Elovich equation better described the adsorption due to the higher R^2 and lower RSS (i.e. 0.996 and 0.001, respectively) than the intraparticle diffusion, pseudo–first– and –second–order kinetic models (i.e. R^2 = 0.863–0.959 and RSS = 0.003–0.011, respectively) (Table 5.2). The Elovich kinetics was previously used for modeling PHE adsorption onto various adsorbents [502,506], and the obtained initial adsorption rate (i.e. α) of 0.240 $mg \cdot g^{-1} \cdot h^{-1}$ here obtained (Table 5.2) can be comparable to those of the mentioned studies (e.g. 0.216 $mg \cdot g^{-1} \cdot h^{-1}$ for sepiolite). The good fit of the Elovich model implies the occurrence of chemisorption mechanisms. The active sites of BC were likely heterogeneous and exhibited different activation energies for PHE adsorption [507].

The turning point occurred after 24 hours when PHE removal reached approximately 18% in PR (Figure 5.3), which was significantly higher ($p < 0.05$)

compared to that obtained in C2 (i.e. approximately 7%, Figure 5.3), indicating a higher occurrence of the biodegradation mechanism rather than adsorption for PHE removal. Moreover, PHE removal (i.e. 82%, Figure 5.3) statistically increased ($p < 0.05$) in PR after 84 hours and kept rising ($p > 0.05$) from 82 to 86% (Figure 5.3) by reaching a plateau until 168 hours. This is most likely due to a lower substrate availability after 84 hours compared to the initial stage (i.e. PHE of approximately 3 and 20 $mg \cdot L^{-1}$, respectively) (Figure 5.3), which could lead to a reduced PHE degradation rate by the involved bacteria [508]. The occurrence of a plateau could be also coupled with the accumulation of toxic secretions and the competition of intermediate metabolites at the expense of PHE biodegradation [509]. Similarly, Xu et al. [358] treated a PHE– and TW80–containing (i.e. 20 and 2,500 $mg \cdot L^{-1}$, respectively) soil washing solution with *Klebsiella* species immobilized onto polyvinyl alcohol–sodium alginate–nano alumina beds in batch mode. They reported a PHE removal of about 89%, which rapidly raised in the first 240 hours and subsequently reached a plateau. In the case of a continuous–flow reactor operation, these results would suggest an HRT of 3.5 days, which was indeed used in this thesis.

5.3.2.2 Phenanthrene degradation in a continuous–flow bioreactor

A PHE degradation of up to 96% (Figure 5.4a) was obtained after 43 days of continuous–flow PR operation under aerobic conditions and with an HRT of 3.5 days. The mentioned HRT was lower than those generally used (i.e. 5–16 days) for the removal of PAHs in a continuous–flow stirred–tank reactor (CSTR) [510–512], likely due to the good biomass retention offered by BC after bacteria immobilization [513].

During the first 15 days, the PHE removal efficiency significantly decreased ($p < 0.05$) from 93 to 30% (Figure 5.4a) with the effluent PHE concentration consequently increasing from approximately 3 to 25 $mg \cdot L^{-1}$. Similarly, Cassidy et al. [514] showed an increase of diesel concentration from 0.8 to 5.0 $g \cdot kg^{-1}$ of slurry diesel fuel in the effluent of a bioreactor, when moving from a sequencing batch reactor to a CSTR operation. This could be attributed to an acclimation time that bacteria require to adapt to the new conditions imposed by the continuous operation [515]. The increase of the inflow PHE concentration from approximately 20 to 35 $mg \cdot L^{-1}$ compared to the batch phase could also potentially lead to a toxicity shock for the bacterial community, directly associated with a higher PHE concentration or with metabolite accumulation [446,516].

From day 15 onwards, the effluent PHE concentration decreased ($p < 0.05$) by reaching a steady value ranging between approximately between 1 and 2 $mg \cdot L^{-1}$ (Figure 5.4a), which corresponded to a PHE removal efficiency of 94–96% (Figure 5.4a). The growth of biomass (i.e. almost 4,770 mg $VSS \cdot L^{-1}$ and $8 \cdot 10^9$ $CFU \cdot mL^{-1}$) at the end of the continuous–flow operation, as well as a more heterogeneous microbial community compared to the initial batch mode phase (Figure 5.5c), most likely affected the PHE removal efficiency positively (Figure 5.4a) [461,517]. Similarly, Moscoso et al. [460] showed an increase of PHE degradation up to almost 88% with the growth of biomass concentration from 0.02 to 0.77 $g \cdot L^{-1}$ by treating a PAH–contaminated TW80 solution in a CSTR.

Figure 5.4b shows the evolution of DOC along the continuous–flow PR operation. DOC was essentially made up of the TW80 used for PHE desorption during SW (see Section 6.3.1). The increasing TW80–inflow concentration (i.e. from 2,700 to 10,800 $mg \cdot L^{-1}$) during the shift from the batch to the continuous–flow phase led to a significant increase ($p < 0.05$) of the effluent DOC to almost 6,200 $mg \cdot L^{-1}$ in the first 15 days (Figure 5.4b). This can also explain the decrease of the PHE degradation efficiency described above (Figure 5.4a), as the raise of the TW80 amount might have induced toxicity towards some types of PHE–degrading bacteria [457]. In contrast, the

constancy of the TW80 concentration in the synthetic influent SW solution was likely one of the factors positively affecting the higher PHE removal from day 15 onwards (Figure 5.4a). Indeed, TW80 concentrations ranging between 250 and 10,000 $mg \cdot L^{-1}$ were reported to enhance PHE biodegradation by promoting bacterial growth [518,519], probably due to the modifications of the CSH or the promotion of the transmembrane transportation of PHE (see Section 6.3.2.3). Until day 43, DOC only slightly decreased ($p > 0.05$) from 6,200 to 5,435 $mg \cdot L^{-1}$ (Figure 5.4b), likely due to the low biodegradability generally shown by non–ionic surfactants such as TW80 [451]. Hence, the achievement of a selective PHE degradation can be an important aspect in view of the reuse of the regenerated SW solution for reducing the costs of the overall treatment process (i.e. SW + treatment of spent SW solution).

DO and pH values played a key role in PHE degradation (Figure 5.4). The continuous aeration (Figure 5.4c) was most probably beneficial for the metabolism of heterotrophic bacteria, for which oxygen acts as the terminal electron acceptor for PHE degradation [520]. Regarding the pH, the reduction of pH (Figure 5.4c) can be associated with the accumulation of hydrogen ions due to PHE biodegradation [401]. The BC probably acted as a buffering agent during the batch mode operation, since the pH at the beginning of the continuous–flow operation was almost 8.1 (Figure 5.4c), which was slightly higher than that of the synthetic SW solution (i.e. 7.5). Indeed, BC was characterized by an ash content of approximately 5% (Tables S1) that can be coupled with the presence of CO_3^{2-} [473], as also confirmed by the peak at around 870 cm^{-1} shown by the FT–IR/PAS spectrum (data not shown) [521]. However, the pH considerably dropped ($p < 0.05$) from almost 8.1 to 6.7 (Figure 5.4c) after 15 days of continuous–flow operation, thus requiring the addition of an external source of carbonate in order to avoid inhibition for the bacteria involved in PHE biodegradation at highly acidic conditions (e.g. at pH 5.0) [522]. Hence, the addition of Na_2CO_3 (i.e. 1,000 $mg \cdot L^{-1}$) after 16 and 32 days allowed to keep the pH between approximately 6.5 and 8.5 (Figure 5.4c) and prevented any interference for PHE–degrading bacteria [478].

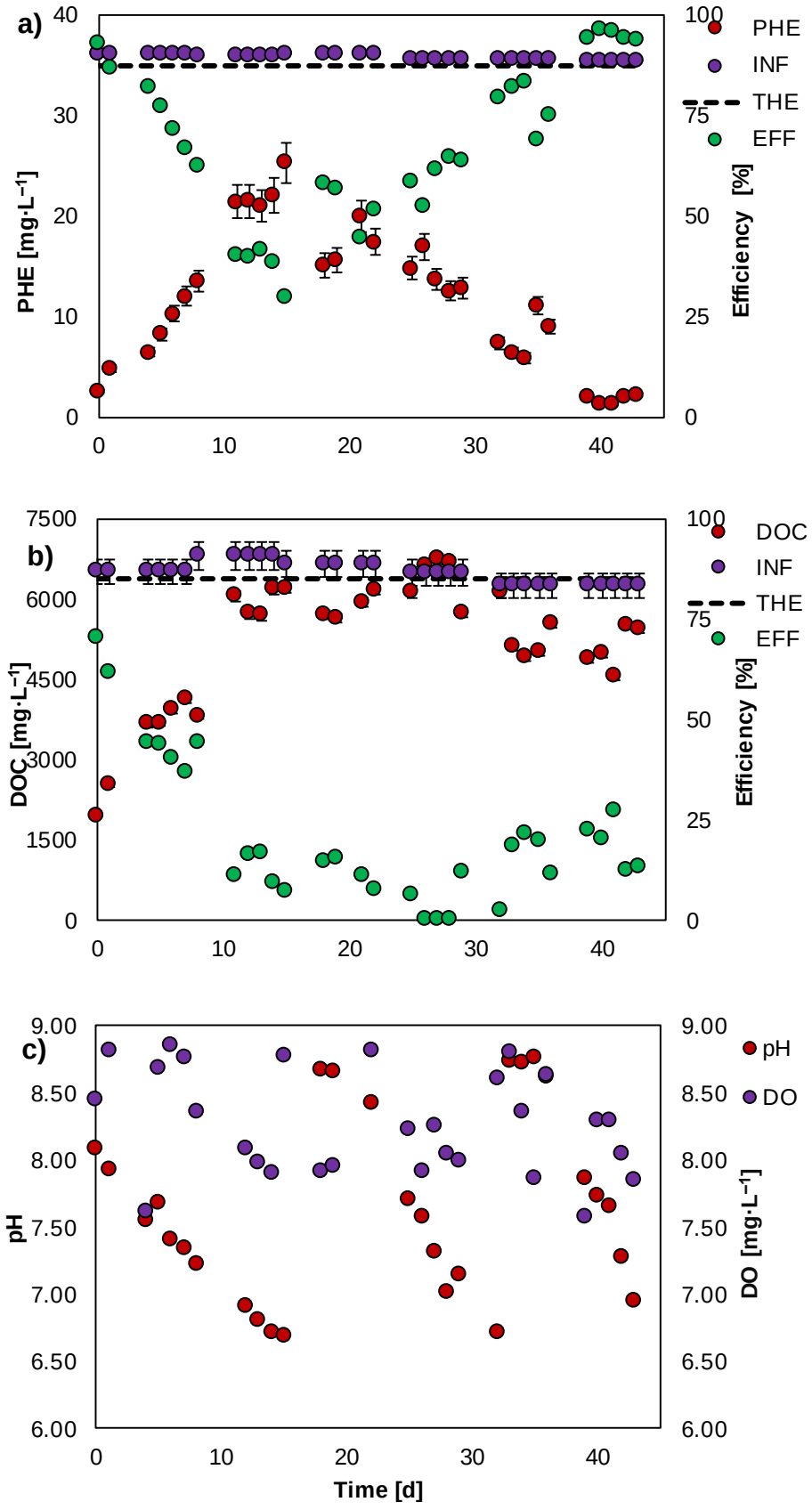
a)
PHE [mg·L⁻¹]
Efficiency [%]
PHE
INF
THE
EFF
b)
DOC [mg·L⁻¹]
Efficiency [%]
DOC
INF
THE
EFF
c)
pH
DO [mg·L⁻¹]
pH
DO
Time [d]

Figure 5.15 – Evolution of a) phenanthrene (PHE, mg·L^{-1}), b) dissolved organic carbon (DOC, mg·L^{-1}), c) dissolved oxygen (DO, mg·L^{-1}) and pH values vs time (d) in the continuous–flow bioreactor treating the spent sediment washing solution.

The averages and error bars were determined on triplicates. INF = actual PHE concentration in the influent; THE = theoretical PHE concentration in the influent; EFF = effluent PHE concentration.

5.3.2.3 Mechanisms occurring during phenanthrene degradation

PHE removal from the spent SW solution likely occurred through mechanisms taking place in two different phases. Firstly, freely dissolved PHE or attached PHE to micelles was adsorbed onto BC. Afterwards, PHE biodegradation by the BC immobilized–bacteria (see Section 6.3.2.1) occurred in both the aqueous and micellar phase, and was generally controlled by the diffusion of the particles towards the bacterial cell surface, enzyme or lipopolysaccharide [523]. The micelle–attached PHE could also be transferred to bacteria via uptake after hemi–micelle formation around the microbial cell [524].

The enhanced PHE degradation observed (i.e. 96%, Figure 5.4a) after the increase of TW80 concentration during the continuous–flow reactor operation was likely due to an increase of CSH from approximately 26 to 43% (data not shown), which improved the transmembrane transfer. Indeed, the addition of non–ionic surfactants (e.g. TW80) can either decrease or increase the CSH of bacteria due to the partition of TW80 onto the cell surface or the release of lipopolysaccharides [525,526], as a function of the initial cell surface characteristics (i.e. hydrophobic or hydrophilic cells) [409]. The increase of CSH likely confirmed the lipopolysaccharide mechanism [527] also due to the presence of Gram–negative bacteria in PR (Figure 5.5a) [455]. In addition, TW80 could govern the hydrogen ion shift in the cell layer to provide adenosine triphosphate (ATP) for the transmembrane transport of PHE, thus enhancing PHE intracellular biodegradation [528,529]. This improvement can be attributed to the presence of the *Alphaproteobacteria* class (i.e. 36%) (see Section 6.3.3), which was previously reported to be correlated with the H^+–ATP synthase subunit alpha [528], after the startup of the continuous–flow system.

Finally, PHE biodegradation likely proceeded via the hydroxylation of the aromatic rings due to the presence of oxygen and the biotransformation of PHE into simpler compounds by following either phthalate or salicylate routes, eventually leading to the production of carbon dioxide and water through the tricarboxylic acid cycle (TCA) (see chapter 4).

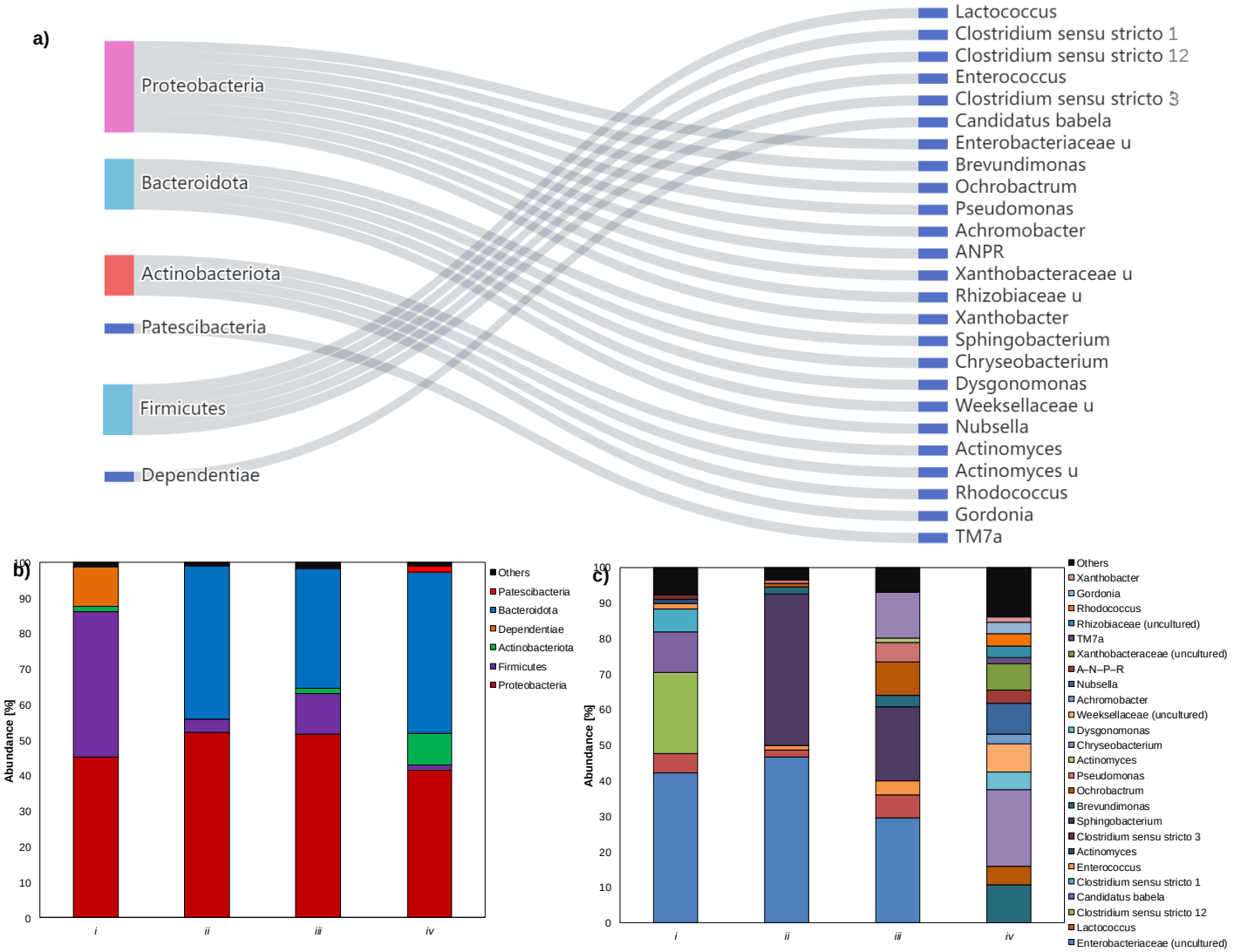
a)
Proteobacteria
Bacteroidota
Actinobacteriota
Patescibacteria
Firmicutes
Dependentiae
Lactococcus
Clostridium sensu stricto 1
Clostridium sensu stricto 12
Enterococcus
Clostridium sensu stricto 3
Candidatus babela
Enterobacteriaceae u
Brevundimonas
Ochrobactrum
Pseudomonas
Achromobacter
ANPR
Xanthobacteraceae u
Rhizobiaceae u
Xanthobacter
Sphingobacterium
Chryseobacterium
Dysgonomonas
Weeksellaceae u
Nubsella
Actinomyces
Actinomyces u
Rhodococcus
Gordonia
TM7a
b)
Abundance [%]
i
ii
iii
iv
Others
Patescibacteria
Bacteroidota
Dependentiae
Actinobacteriota
Firmicutes
Proteobacteria
c)
Abundance [%]
i
ii
iii
iv
Others
Xanthobacter
Gordonia
Rhodococcus
Rhizobiaceae (uncultured)
TM7a
Xanthobacteraceae (uncultured)
A–N–P–R
Nubsella
Achromobacter
Weeksellaceae (uncultured)
Dysgonomonas
Chryseobacterium
Actinomyces
Pseudomonas
Ochrobactrum
Brevundimonas
Sphingobacterium
Clostridium sensu stricto 3
Actinomyces
Enterococcus
Clostridium sensu stricto 1
Candidatus babela
Clostridium sensu stricto 12
Lactococcus
Enterobacteriaceae (uncultured)

Figure 5.16 – a) Phylogenetic tree showing the genetic relationships of phenanthrene–degrading bacteria, b) bacterial composition at the phylum level and c) genus level i) in the inoculum, ii) after the immobilization phase onto biochar, iii) at the end of the 7 days batch operation and iv) at the end of the 43 days the continuous–flow operation.

5.3.3 Phenanthrene–degrading bacteria and temporal evolution of the microbial community structure

The continuous–flow PR operation at an HRT of 3.5 days led to a high–efficiency PHE removal (see Section 6.3.2.2) and likely selected the best performing PHE–degrading strains immobilized onto BC [530].

In the original inoculum, the taxonomic classification (Figure 5.5) showed a copiousness of *Proteobacteria* and *Firmicutes* phyla accounting for more than 86% (Figure 5.5b). These phyla were previously classified as active PHE degraders in contaminated harbor and marine sediments [531,532]. Also, the *Dependentiae* phylum was revealed with an abundance of approximately 11% (Figure 5.5b) and was recently associated with the presence of PAHs in coastal samples [533].

The immobilization of bacteria onto BC led to a significant ($p < 0.05$) increase of the *Bacteroidota* phylum from less than 1 to about 43% (Figure 5.5b) at the expense of *Firmicutes* and *Dependentiae* phyla, which dramatically ($p < 0.05$) decreased their population below 4% (Figure 5.5b). The *Bacteroidota* phylum was previously shown to be the main phylum after *Proteobacteria* in the prickly ash seed oil meal–BC compost [534], and was reported to proliferate in highly PAH–contaminated marine sediments [18].

At the end of PR operation, the *Proteobacteria* and *Bacteroidota* phyla maintained ($p > 0.05$) their abundance relatively stable (i.e. approximately 42–51 and 34–45%, respectively) (Figure 5.5b) along with the stable performance of the reactor in terms of PHE removal. Interestingly, the *Actinobacteriota* abundance raised from approximately 1 to 9% after the batch and continuous–flow stages (Figure 5.5b), respectively, probably due to the increase of TW80 and PHE availability in PR (Figure 5.4a and b) and the ability of these bacteria to consume both TW80 and PHE under aerobic conditions [535,536].

The taxonomic classification at the genus level by taking into account a relative abundance above 1% [420] is presented in Figure 5.5c. A genus (uncultured) belonging to the *Enterobacteriaceae* family showed an abundance comprised between almost 30 and 47% (Figure 5.5c), and was probably the main genus involved in the PHE biodegradation during the batch phase [537]. The aeration and addition of BC was

likely coupled with the elimination of unwanted “companions”, such as the *Clostridium sensu stricto* genus (Figure 5.5c) from the inoculum [538], and could have enhanced the increase of the *Sphingobacterium* genus (i.e. up to 21%, Figure 5.5c) [539]. The latter was previously identified as a group of PHE degraders in soil samples collected from the petrochemical industry and oil refinery areas [540]. A relative copiousness below 30% (Figure 5.5c) was obtained at the end of the batch phase for other bacterial genera such as *Chryseobacterium*, *Ochrobactrum* and *Pseudomonas* (i.e. 13, 9 and 6%, respectively), all reported to degrade PHE [400,415,540].

Interestingly, the *Chryseobacterium* genus increased its richness up to about 22% (Figure 5.5c) at the end of the continuous–flow operation, likely due to the increase of TW80 and PHE concentrations (Figure 5.4). Species belonging to *Chryseobacterium* were reported to have a versatile metabolism by degrading simultaneously PHE and phenols and growing in liquid solutions with surfactants (e.g. hydroxypropyl–β–cyclodextrin) [439]. The microbial shift towards more metabolically versatile members in the latest stages of the biodegradation process was also described by Garrido–Sanz [541]. *Brevundimonas* co–occurred with an abundance of almost 11% (Figure 5.5c) and was previously reported to be capable for PHE degradation [435]. *Nubsella*, *Weeksellaceae* (uncultured), *Xanthobacteraceae* (uncultured) and *Dysgonomonas* genera, accounting for approximately 30% (Figure 5.5c) after 43 days of continuous–flow bioreactor operation, were also reported to exhibit a broad response to hydrocarbons and PAHs in previous studies [510,540,542,543].

Among the 16 annotated KEGG Orthology (KO) (Figure 5.6) belonging to the biodegradation and metabolism of xenobiotic compounds, KO00624 and KO00626 were involved in the PAH degradation pathway [544], thus confirming the role of the abovementioned bacteria in PHE removal. Some of the PAH–related degradation enzymes, such as 1,4–dihydroxy–2–naphthoyl–CoA hydrolase, 3–hydroxyanthranilate 3,4–dioxygenase, 4–hydroxyphenylpyruvate dioxygenase, 4–hydroxyacetophenone monooxygenase, 4,5–dihydroxyphthalate decarboxylase, protocatechuate 3,4–dioxygenase, protocatechuate 4,5–dioxygenase, dioxygenase, dehydrogenase, NADP–dependent aldehyde dehydrogenase and salicylate 5–hydroxylase, were previously reported in biochar–amended soils polluted by PAHs [545]. Also, the relative contents of functional genes associated to PHE degradation (Figure 5.6) increased after the continuous–flow bioreactor operation, further supporting the enhancement of the biodegradation process observed in the latest stage (Figure 5.4a) [546].

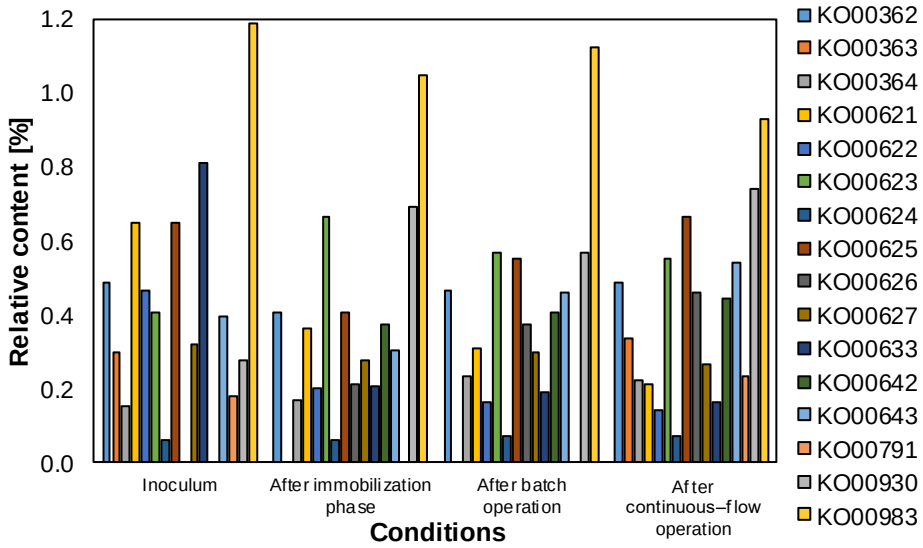

Figure 5.17 – Relative content (%) of functional genes related to the degradation of xenobiotic compounds i) in the inoculum, ii) after the immobilization of bacteria onto biochar, iii) after the 7 days of initial batch operation and iv) after the 43 days of continuous–flow reactor operation.

5.3.4 Preliminary economic assessment

This chapter shows that a PHE–contaminated sediment can be firstly remediated through a SW process using a surfactant solution containing TW80, allowing to reach a PHE removal efficiency of up to approximately 91% (Figure 5.2b). The generated amount of spent PHE–containing SW solution can be controlled by maintaining an S:L ratio up to 1:4 (Figure 5.2b). Subsequently, the SW solution can be treated in a continuous–flow bioreactor with BC immobilized–bacteria (Figure 5.1) achieving a PHE degradation up to 96% (Figure 5.4a) and a recovery of TW80 comprised between 75 and 100% (Figure 5.4b). Thus, a rough economic study was conducted on the whole process to evaluate its possible employment in full–scale applications.

The economic estimation by considering the SW operations, TW80 and BC purchase, and the biological treatment of the PHE–polluted TW80 solution showed a total cost of 342.60 €·ton^{-1} of sediment, as the sum of 75.36, 172.80, 44.44 and 50.00 €·ton^{-1}, respectively. Although the TW80 supply represents the major cost of the whole process, the TW80 recovery has not been considered since the calculation was based on the mass unit of sediment. Similarly, the BC utilization in the bioreactor operation is higher during the start–up phase, while is drastically diminished along further SW cycles generating extra spent SW solution. It should be also remarked that a part of the PHE adsorbed onto BC can be continuously degraded by bacteria, thus decreasing the regeneration cost and replacement of BC [29]. However, the total cost

of 342.60 €·ton^{-1} is included in the range of 36–480 €·ton^{-1}, previously reported for the SW of contaminated sediments [454], thus encouraging the employment of such approach for a real–scale project. A detailed energy evaluation and determination of the scale–up factor will be required for validating the studied process.

5.4 Conclusions

This chapter shows that BC can be an effective and sustainable biocarrier for immobilized–cell bioreactors treating PAH–polluted SW solutions. The continuous–flow PR operation allowed to achieve a PHE removal of up to 96% from a TW80–containing solution (i.e. 10,800 mg·L^{-1}) after 43 days. The SW solution was obtained from SW batch tests, in which PHE was desorbed from the contaminated sediment up to 91% after 1,440 minutes when an S:L ratio from 1:4 upwards was used. The Elovich kinetic model well simulated the desorption trend and was more suitable than the intraparticle diffusion, pseudo–first– and –second–order kinetic models (i.e. R^2 = 0.863–0.959 and RSS = 0.003–0.011, respectively) to simulate the PHE adsorption onto BC, which preceded PHE biodegradation as a mechanism during PHE removal in PR. The main PHE–degrading bacteria belonged to the *Proteobacteria*, *Bacteroidota* and *Actinobacteriota* phyla and accounted for approximately 96% of the total reads in the PR samples. Finally, a preliminary economic assessment conducted on the whole process revealed a total cost of 342.60 €·ton^{-1} of sediment, thus suggesting a possible creation of a sustainable remediation approach for the application of the entire process at a larger scale. Future studies should be addressed to the optimization of the continuous–flow operation, by for instance investigating the effects of the DO concentrations

CHAPTER 6. THE ADDITION OF BIOCHAR AS A SUSTAINABLE STRATEGY FOR THE REMEDIATION OF PAH–CONTAMINATED SEDIMENTS

6.1 Introduction

Sediments represent the main receptor of organic contaminants entering the aquatic ecosystem including polycyclic aromatic hydrocarbons (PAHs), which are hazardous petroleum–derived compounds principally released into the environment by anthropogenic activities [547,548]. When dredging the sediments mainly for harbor and waterway maintenance purposes [549], several concerns are posed to the disposal or reuse of dredged sediments due to their contamination [550]. Also, the re–suspension of particles contaminated by PAHs may be favored during dredging activities, thus increasing the environmental risk related to the dispersal of hazardous compounds [551]. Biological, physical–chemical and thermal remediation technologies have been applied to cope with the PAH–contaminated sediment concern (Figure 6.1), and are all associated with several drawbacks such as low efficiencies (mainly due to low PAH bioavailability), release of toxic by–products (e.g. oxygenated–PAHs) and high costs (e.g. due to the high temperatures involved), respectively [181].

The application of carbonaceous sorbents such as biochar is particularly effective, economic and environmental friendly for the remediation of sediments contaminated by PAHs [30] mainly via PAH immobilization. Biochar is a porous material mainly produced by pyrolysis or gasification of a carbon–based feedstock [552,553], and is capable to reduce the bioavailable PAH concentrations in sediments due to its high carbon content and specific surface area [554]. In addition, the use of biochar as sediment amendment gives birth to further virtuous, environmental implications. For instance, being manufactured starting from organic waste or other by–products (e.g.

sewage sludge) [555], biochar positively contributes to waste management practices and the accomplishment of a circular economy model [556]. The biochar is also applied as an agricultural amendment in carbon capture and storage (CCS) applications, refueling organic–poor soils with slow–release carbon and inorganic elements [557]. The other product obtained through pyrolysis or gasification of organic waste, namely "syngas", is a gas stream that can be used for energy and bioenergy recovery being composed by CO, H_2 and CH_4 [558], decreasing greenhouse gas emissions and potentially mitigating climate change [559].

The environmental applications of biochar in contaminated sediments has lately attracted the attention of the scientific community. Wang et al. [560] reviewed the use of biochar to remediate contaminated soils and sediments by toxic metals. Ni et al. [561] recently summarized the migration of persistent organic pollutants (e.g. PAHs) during the biochar utilization in soil–plant systems. Li et al. [203] mainly focused their review to the PAH adsorption by activated carbon (AC) and graphene in sediments. Nonetheless, previous reviews have dedicated less attention to shed light on the mechanisms and impacts associated with biochar addition to PAH–contaminated sediments. Hence, the current state of the knowledge on PAH removal due to biochar application in sediments is necessary to be investigated. This chapter is aimed at evaluating the mechanisms involved during adsorption, bioremediation and enhanced persulfate degradation of biochar–amended PAH–contaminated sediments, emphasizing the effect of various parameters on the efficiency of the different processes. The key factors controlling the biochar characteristics as well as its architecture and molecular composition have been carefully discussed. Moreover, the impact of biochar on PAH bioavailability and toxicity to living species has been discussed in detail to clarify the effective mitigation of the environmental risk. The lack of the existing literature has been identified suggesting future perspectives along which new research efforts should be addressed.

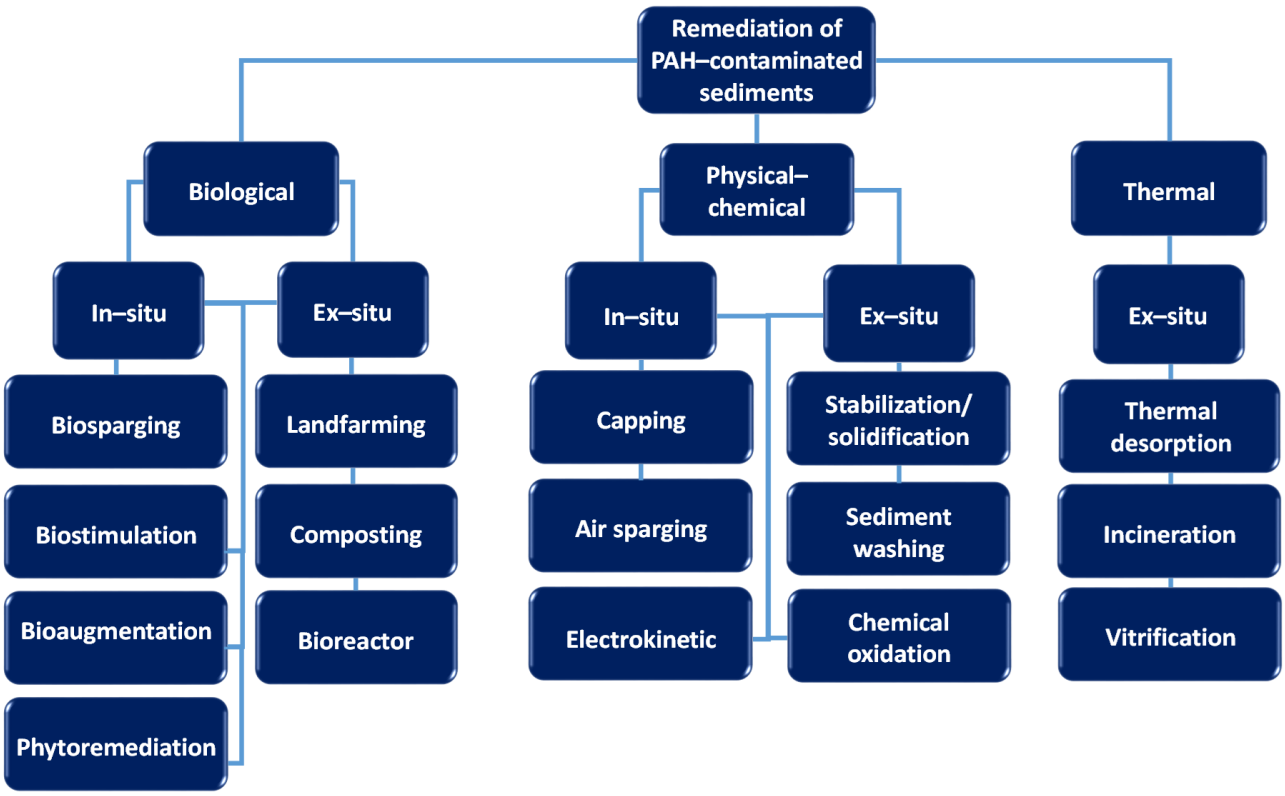

Figure 6.18 – Conventional biological, physical–chemical and thermal remediation technologies used for PAH–contaminated sediments.

6.2 The concern of PAH–contaminated sediments

6.2.1 Current state of PAH–contaminated marine, coastal, river, and lake sediments

PAHs are petroleum–derived compounds with at least 2 condensed benzene rings [210]. PAHs have a petrogenic or pyrogenic nature if derived from incomplete combustion or slow maturation of organic matter [562], respectively, and can be released into the environment by natural (e.g. volcanic eruptions, catagenesis) or anthropogenic (e.g. industrial processes, petroleum facilities) sources [563]. PAHs having a pyrogenic nature are adsorbed by suspended particles in the atmosphere and may end up into rivers, lakes and seaside via atmospheric deposition [564], whereas petrogenic PAHs are directly released into water bodies due to oil discharge or seepage [6]. Afterwards, PAHs accumulate in sediments as hydrophobic and persistent compounds [565] and can directly reach humans or be taken up by aquatic organisms and enter the food chain, posing risks to human health being carcinogenic and mutagenic contaminants [53]. Indeed, 28 PAHs were reported to be toxic contaminants in 2008 by the United States Environmental Protection Agency (US EPA) [35].

The distribution and concentration of PAHs is variable in sediments due to their origin source and transport processes. The PAH nature is commonly evaluated by comparing phenanthrene (PHE) and anthracene (ANT) concentrations, as pyrogenic and petrogenic sources generally release a PAH mixture being characterized by a PHE/ANT ratio lower or higher than 10, respectively [566]. The ratio between low (i.e. $\leq$ 3 rings) and high ($\geq$ 4 rings) molecular weight PAHs could alternately be assessed as smaller or higher than 1 in order to establish the pyrogenic or petrogenic PAH origin, respectively [567]. Wu et al. [39] recently reported that the total PAH concentration in river and coastal sediments can reach an average of 300 $mg \cdot kg^{-1}$, with such high contamination levels being mainly observed in areas with an extensive industrial activity. Moreover, Zeng et al. [568] and Meng et al. [569] related the occurrence of PAHs in lake sediments of China (i.e. up to 7.94 $mg \cdot kg^{-1}$) to urbanization (e.g. vehicle emission) and industrialization (e.g. biomass combustion).

The transport of PAHs is more complicated to determine because it strongly depends on physical–chemical properties of each PAH compound (e.g. octanol–water, vapor–particle partitioning) and environmental conditions (e.g. geomorphologic characteristics) [80]. Merhaby et al. [83] analyzed the current state of sediments in Mediterranean countries showing higher total PAH concentrations (i.e. up to 1,670

$mg \cdot kg^{-1}$) in harbors, bays and lagoons compared to those observed in rivers (i.e. up to 610 $mg \cdot kg^{-1}$), suggesting that PAHs are mainly transported from a dynamic environment (i.e. river streams) to a relatively calm zone (e.g. bays).

6.2.2 Dredging of contaminated sediments

Several millions of cubic meters of sediment are yearly dredged worldwide (e.g. 100–200·Mm^3 in Europe, SedNet) [570], with sediment dredging being a highly–spread practice especially in those countries with a high coast–to–inner land ratio [571]. Coastal, estuarine and fluvial sediments are generally dredged to preserve waterway depth in favor of navigation networks, thus promoting the reuse by coastal nourishment or disposal of dredged sediments [572].

However, when a high concentration of PAHs is found to be adsorbed onto the sediment particles, likely due to a scarce natural attenuation occurring over time, waste management issues [11,17] and potential risks for the environment and human health [573] arise. Moreover, PAH–contaminated sediment particles are re–suspended during dredging, and the toxicity towards the local ecosystem can be even increased [574]. Thus, sediments contaminated by PAHs have to be remediated according to national legislations [232], which implement guidelines and strategies provided by directives or government agencies in order to mitigate the sanitary and environmental risk [575]. For example, in Europe the attention about the dredged sediment issue has increased after the emanation of the Water Framework Directive [576], which established the environmental quality standards (EQSs) for sediments, which were subsequently adopted in the national regulations of many EU countries (e.g. Belgium, France, the Netherlands, Italy) [577].

6.2.3 Conventional technologies for the remediation of PAH–contaminated sediments

Biological, physical–chemical and thermal remediation technologies are available for PAH–contaminated sediments and can be employed in–situ or ex–situ (Figure 6.1) [13]. The treatment of PAHs without moving the sediment is referred as to in–situ treatment, whereas the ex–situ treatment is carried out after dredging and can be performed on–site or off–site if the sediment is remediated nearby or away from the original contaminated location, respectively [578]. In–situ remediation is undoubtedly less expensive [112] and more suitable for deep PAH contaminations compared to ex–situ methods as dredging and transportation of sediments are not required. On the other hand, dredging is commonly performed in harbors (section 5.2.2) and, therefore, in such cases ex–situ remediation is applied with the possibility to overcome the typical

shortcomings (e.g. the dispersion of the contaminants) of the in–situ treatment methods and to achieve higher PAH removal efficiencies. However, regardless where the treatment is performed, the level of contamination, remediation objectives and operating costs are the main factors determining the choice of the most suitable remediation technology to be applied [76].

Bioremediation involves microorganisms and plants to biologically decrease PAH concentrations in sediments [579]. The biological process is strongly influenced by the capability of the specific bacterial and plant species to degrade PAH, as well as by different parameters, such as pH, carbon to nitrogen ratio, moisture, temperature and PAH concentrations [307]. Bioremediation can be applied in sediments under aerobic or anaerobic conditions [580], and the most frequently used technologies are shown in Figure 6.1 [581]. Aerobic bioremediation requires a lower treatment time but higher costs due to aeration compared to anaerobic processes, in which the high–energy end products could be used to cover all or part of the energy demand. However, it is well known that bioremediation efficiency is limited by PAH bioavailability, which is the fraction of PAHs accessible and degradable by microorganisms or plants [234,582].

Physical–chemical treatments are commonly performed to go beyond the limitations of bioremediation, also intervening on the not bioavailable fraction of PAHs. A wide range of technologies, each characterized by a different basic principle (e.g. immobilization, solubilization, oxidation) is available (Figure 6.1) [583]. Physical–chemical technologies are affected by several operational parameters such as pH, reagent dosage, sediment permeability and the presence of organic matter [35]. Although the high efficiencies generally achieved in a relatively short time, some disadvantages are often associated with these technologies such as the cost of the chemicals employed and the high amount of exhausted effluents to be further treated after sediment washing (Figure 6.1) [250]. To face these limitations, electrokinetic remediation (Figure 6.1) can be alternatively used allowing to reach the removal of PAHs via the contaminant migration towards regions that are adjacent to electrodes [584,585]. The degradation of PAHs obtained via chemical oxidation (Figure 6.1) may be coupled with the formation of toxic by–products [99], i.e. oxygenated–PAHs, which contain ketones and quinones bound to the aromatic rings [586], making these products even more persistent and recalcitrant compared to PAHs [587].

Thermal remediation includes a group of processes in which the increase of temperature allows to remediate PAH–contaminated sediments by PAH volatilization and destruction, and is generally performed ex–situ (Figure 6.1) [588,589]. Nevertheless, heating requires higher costs compared to biological and physical–

chemical processes, and the high moisture content of contaminated sediment leads to a further energy demand [215]. A disadvantage of thermal technologies is also the destruction of the living microflora and organic matter originally present in the sediment [100].

6.2.4 Reuse of remediated sediments

Sediments are dredged for the maintenance of public waterways and are generally destined to disposal after a proper remediation treatment (section 5.2.3) or used for coastal nourishment [590]. In the last years, dredged sediments have been regarded as a waste to be valorized and different reuse strategies, such as in agriculture or in civil engineering applications, have been proposed in order to evaluate the possible benefits derived from remediated sediments.

Tozzi et al. [591] lately tested the use of bio–remediated harbor sediments for strawberry cultivation obtaining similar nutritional facts in terms of sugar, organic acids and minerals compared to the fruit conventionally cultivated. Moreover, strawberries mixed at 50% with peat substrate showed higher vitamin C content and antioxidant activity [592]. However, remediated sediments could still contain a minimum level of PAHs, which could migrate to the edible product. In this context, a better reuse for sediments could be the growth of plants for ornamental use, as reported by Mattei et al. [593].

The major application of remediated sediments is for civil engineering purposes, where the sediments are used after dewatering for the production of bricks and concrete, providing properties compatible with the technical regulations for construction [594,595]. Beddaa et al. [596] showed that 30% of sieved river sediments (i.e. the coarse fraction) could be used to obtain a stable concrete classified as C25/30, whereas the use of marine sediments can only respect the 1% chloride standards required for unreinforced concrete [597]. The main drawback is the presence of sulfate in sediments, which could lead to cracks in concrete due to formation of gypsum and ettringite [598]. Gebert et al. [599] recently showed that it is also possible to obtain biogas, with a potential of 2–12 $m^3 \cdot ton^{-1}$ of sediment, using sediments containing 3–11% of the organic matter. Hence, dredged sediments could contribute to biogas recovery after disposal if they find no space in any other application and contain a sufficient organic matter content.

With regard to the reuse of biochar–amended sediments, this practice is still in a raw phase. Wang et al. [600] recently showed the beneficial effect of biochar–sediment on cement hydration reaction. However, the geo–mechanical properties as well as the

EQSs of the sediments need to be evaluated after biochar addition [601] in order to perform an efficient and safe sediment reuse. Otherwise, the possibility to separate biochar from the sediments via sieving and centrifugation [204] can be considered at the end of the remediation treatment. Although the high separation efficiency reported (i.e. almost 90%), this method can be costly and invasive for the sediment characteristics [203] and, therefore, future studies should be focused on the use of more easily recoverable amendments (e.g. magnetic biochar).

Table 6.10 – Elemental composition, pH and surface area of biochars originated from various feedstocks at different pyrolysis temperatures. SA = surface area.

Feedstock	Temp. [°C]	pH	C [%]	H [%]	N [%]	O [%]	SA [$m^2 \cdot g^{-1}$]	References
Corn stalk	320	n. a.*	58.80	4.13	1.68	n. a.	2.81	[602]
Wood	340	n. a.	71.81	4.36	0.04	n. a.	23.83	[603]
Mangrove plant	400	6.3	43.26	0.54	1.34	n. a.	4.43	[604]
Wheat straw chips	400	8.2	77.38	3.99	3.74	14.89	93.84	[605]
Macadamia nut shell	250–500	n. a.	77.50	3.69	n. a.	n. a.	n. a.	[239]
Mangrove plant	600	6.7	52.44	0.41	0.97	n. a.	6.11	[604]
Acai pit	600	n. a.	77.20	n. a.	n. a.	n. a.	198.00	
Hardwood lump	600	n. a.	70.8	n. a.	n. a.	n. a.	224.00	[606]
Peanut hull	600	n. a.	31.9	n. a.	n. a.	n. a.	107.00	
Corn stalk	600	8.7	41.57	1.50	0.42	n. d.	6.30	[607]
Wheat straw	600	n. a.	60.2	1.60	0.50	37.20	n. a.	[608]
Pine dust	600	n. a.	22.10	n. a.	n. a.	n. a.	109.00	[606]
Barley straw	600	n. a.	49.2	n. a.	n. a.	n. a.	26.00	
Straw	700	9.9	53.85	2.00	0.92	6.14	8.60	[607]
Wheat straw chips	700	8.6	82.55	2.00	1.31	14.14	256.04	[605]
Pine biomass	600–900[a]	11.4	n. a.	n. a.	n. d.[b]	n. a.	n. a.	[609]
Pine wood	700–1,000	n. a.	n. a.	n. a.	n. a.	n. a.	358.00	[32]
Pine wood	n. a.[a]	n. a.	n. a.	n. a.	n. a.	n. a.	343.00	[208]

6.3 Biochar as a suitable amendment for PAH removal

6.3.1 Manufacture

Biochar is defined as a porous carbonaceous material produced by the thermochemical decomposition of biomass under absent or limited oxygen conditions [610]. The biomass is generally converted into biochar using pyrolysis and gasification as thermal processes [611]. The pyrolysis process is generally performed with no oxygen in a range of temperature between 200 and 1,000 °C (Table 6.1), and is classified into slow, intermediate and fast pyrolysis as a function of the residence time of the feedstock in the pyrolysis chamber [612,613]. The residence time is usually in the order of seconds and minutes for intermediate and slow pyrolysis, respectively, and lower than 10 s for fast pyrolysis [614], favoring the production of biochar (i.e. 25–35%) and bio–oil or syngas (i.e. 75%), respectively [615]. Gasification is a thermal process in which the feedstock is mainly converted to syngas under high temperatures (i.e. > 500 °C) and oxygen levels below the stoichiometric amount [616]. Generally, gasification has a lower biochar yield than pyrolysis [617].

Biochar can have different properties depending on the temperature used to maintain pyrolysis. For example, the increase of pyrolysis temperature (Table 6.1) leads to the decrease of particle size and hydrogen–to–carbon (H/C) and oxygen–to–carbon (O/C) ratios, in favor of a higher specific surface area and aromaticity of biochar [560], making biochar particularly suitable for the immobilization of PAHs in contaminated sediments through a strong adsorption mechanism. The biochar obtained via gasification is richer in alkaline salts and minerals, and can be used for the precipitation of potential toxic metals in contaminated sediments [618].

Biochar has also been recently produced via hydrothermal carbonization and microwave–assisted pyrolysis [619,620]. The hydrothermal carbonization is a suitable process for the conversion of biomass with a high moisture content into biochar, also called hydrochar [621]. The process is performed under 2–6 MPa of pressure at 180–250 °C, and the water already present in the biomass is used for the reaction [622]. The microwave–assisted pyrolysis is different to conventional pyrolysis as the process is controlled by the microwave power and irradiation time. Generally, the biochar yield increases by decreasing the microwave power [623]. The microwave–assisted pyrolysis offers many advantages, such as lower application time, higher electricity conversion efficiency and uniform heating at molecular level [624]. Despite

hydrothermal carbonization and microwave–assisted pyrolysis are promising processes, they have not been thus far applied for the production of biochar to be used for the remediation of PAH–contaminated sediments. This is likely due to the fact that the hydrothermal carbonization is suitable for feedstocks with a great moisture content, otherwise the addition of water is required. [625]. Moreover, microwave–assisted pyrolysis is more sensitive to the feedstock used than conventional pyrolysis [626]. Hence, more attention should be posed to hydrothermal carbonization and microwave–assisted pyrolysis in future for biochar manufacture intended for sediment remediation.

6.3.2 Types of feedstock originating biochar

The feedstock used for biochar manufacture can be classified as a primary product (e.g. wood biomass) or a by–product (e.g. a solid waste or a slurry) [627]. When possible, it is recommended to avoid using primary biomasses to limit deforestation and soil erosion, while the employment of residual feedstocks from the agri–food chain sector is an inexpensive and eco–friendly alternative [628], which could have a positive impact in countries with limited primary resources [629].

Many carbonaceous feedstocks have been applied to produce biochar for a PAH–contaminated sediment remediation, which can be mainly grouped in agricultural and wood–based wastes (Table 6.1), being composed by different types and quantities of organic and inorganic compounds [630] and differently affecting the final biochar yield and elemental composition [631]. Agricultural (e.g. straw) and wood–based wastes are lignocellulosic materials mainly composed by carbon (i.e. cellulose, hemicellulose and lignin) and oxygen elements [632]. The woody biomass has a higher lignin content compared to agricultural waste [633,634] and, therefore, is more suitable for a high–yield biochar manufacture [635]. On the other hand, agricultural and woody feedstocks are both made up of a low nitrogen and sulfur content [636], limiting the release of hazardous gases during biochar production [637]. These biomasses are often used in co–pyrolysis with coal to enhance coal cracking and obtain a high biochar quality due to presence of hydrogen in the feedstocks (Table 6.1) [638].

Other feedstocks can be used for biochar production, such as algae, animal manure, plastic, sewage sludge and tires. The biochar produced by algae (or microalgae), animal manure and sewage sludge is rich in nitrogen, inorganic compounds (e.g. P and K) and ash, respectively [639–641], making this biochar suitable for biostimulation of sediments. For example, Pariyar et al. [642] recently showed that manure−derived biochar has a higher cation exchange capacity than rice husk biochar (i.e. 670 and 410 $mmol \cdot kg^{-1}$ dry biochar, respectively), due to the presence of clay minerals. Moreover,

microalgal, manure and sewage sludge biochars have been already applied for PAH removal in water and soil [467,643,644]. The biochar derived from plastic and tires is surely a more innovative material and is mainly composed by carbon and hydrogen [645,646], suggesting that it could be particularly indicated for PAH adsorption due to its highly hydrophobic nature. None of these products (i.e. algae, animal manure, plastic, sewage sludge and tires) has been yet applied for the remediation of PAH–contaminated sediments, as a high volatile solid content results in a low amount of biochar produced as well as the content of metals in the original feedstocks (mainly manure) can negatively affect the final biochar characteristics. Therefore, a co–pyrolysis with agricultural or wood biomasses is recommended to increase the biochar yield and improve its quality [647].

6.3.3 Properties of biochar

The properties of biochar, including pH, elemental composition, specific surface area, metal and PAH content (Table 6.1), are mainly affected by pyrolysis temperature and feedstock characteristics [648]. The feedstock plays a role in determining the final carbon content and specific surface of biochar (Table 6.1). The total carbon content ranges between 22 and 83%, and is higher in crop residues (e.g. straw) than wood derived biochar [649]. On the contrary, the specific surface area is higher in wood (i.e. 24–358 $m^2 \cdot g^{-1}$) than crop residue (i.e. 3–256 $m^2 \cdot g^{-1}$) biochars as the pyrolysis of woody biomass generates pores of different sizes, including micropores [635].

The temperature of pyrolysis has a higher impact on pH, specific surface area and elemental composition of biochar [650]. The increase of temperature leads to an increase of specific surface area and pH (Table 6.1), probably due to the organic compound decomposition coupled with the generation of micropores [651], and the separation of alkali salts from the organic matter [482,652]. Moreover, the H, N and O content in biochar generally decreases with the increase of temperature (Table 6.1), likely due to volatilization that leads to dehydrogenation and deoxygenation reactions [653]. The amount of fly ashes increases at higher temperatures, while the content of functional groups (e.g. hydroxyl and carboxyl) is lower at increasing temperatures [654].

In addition, contaminants can be found in the biochar if originally present in the feedstock (e.g. heavy metals) or generated during the pyrolysis process (e.g. PAHs), [655,656]. Metal concentrations are generally higher in the final biochar compared to the raw material due to the high loss of organic matter during pyrolysis [657]. Different to metals, the increase of pyrolysis temperature from 500 to 700 °C can lead to a

reduction of the PAH concentration in the derived biochar (i.e. from almost 15 to <2 $mg \cdot kg^{-1}$) [658], also leading to a decrease of the ratio between low and high molecular weight PAHs due to volatilization and nuclear condensation phenomena [659]. This aspect deserves more attention in future studies when a contaminated matrix is converted into biochar to be used in environmental applications.

6.3.4 The interaction between biochar and PAHs

Biochar is a suitable material for the remediation of sites contaminated by organic contaminants (e.g. PAHs) due to its porous structures, high surface area and different functional groups [660]. Indeed, scanning electron microscopy (SEM) imaging has revealed the presence of PAHs adsorbed onto biochar surface (Figure 6.2), thus giving the possibility to reduce PAH bioavailability through strong adsorption and consequently their environmental toxicity.

Interactions between PAHs and biochar during adsorption can be classified as hydrophobic (i.e. partitioning, Van der Waals forces), donor–acceptor (e.g. π–π) and specific (i.e. hydrogen–π, cation–π) [31,661,662]. Generally, only one of the mentioned interactions dominates the process depending on the biochar properties, including pyrolysis temperature and the presence of particular functional groups [663]. The hydrophobic interaction is an entropic mechanism that can occur in two main phases: a) the first phase in which the PAH is partitioned in the hydrophobic domain of biochar due to the partitioning coefficient; b) the second phase where the PAH is weakly adsorbed onto the biochar surface via Van der Waals forces [664]. The interaction through PAH partitioning and Van der Waals forces mainly occurs with low–temperature pyrolyzed biochar as a function of biochar polarity [665].

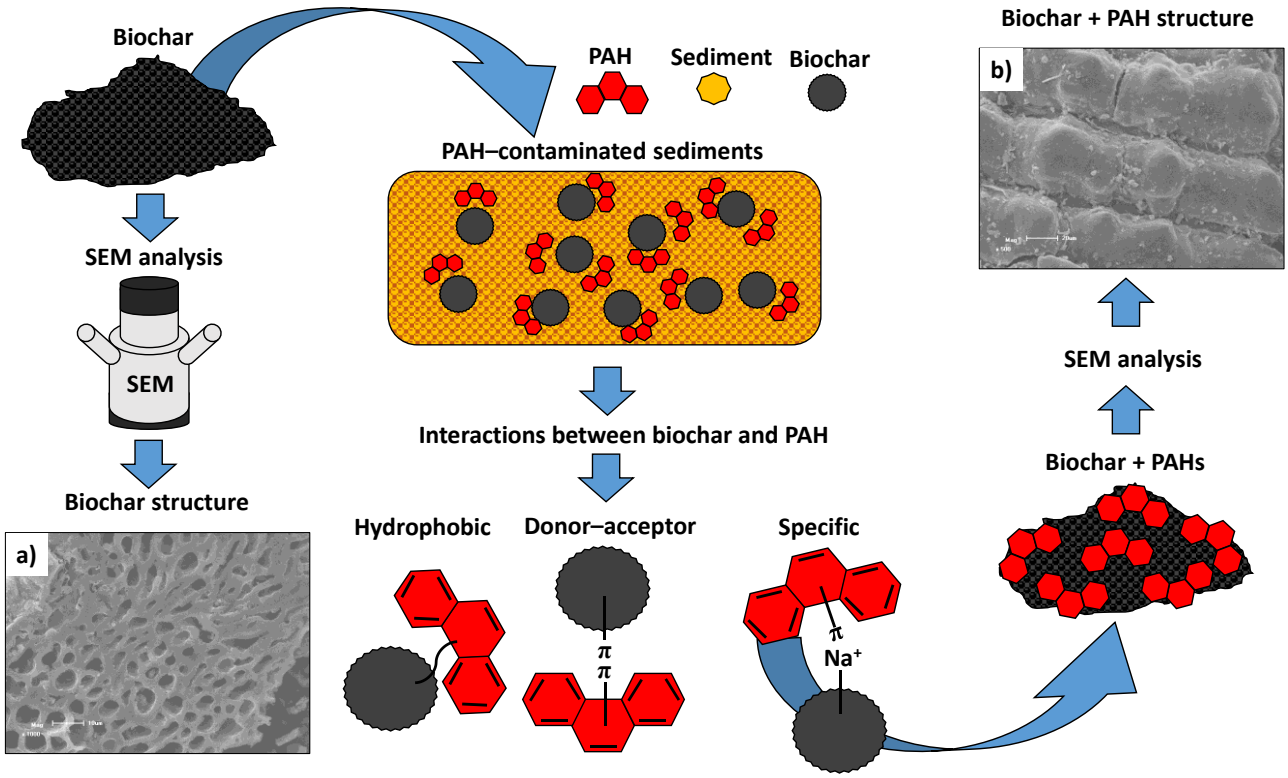

Figure 6.19 – Representation of hydrophobic, donor–acceptor and specific interactions occurring between biochar and PAHs. Scanning electron microscopy (SEM) images before a) and after b) PAH adsorption onto biochar surface are taken from Tang et al. [666].

A high–temperature pyrolyzed biochar leads to stronger electron donor–acceptor interactions due to a lower H/C ratio [667], resulting in a greater adsorption efficiency due to intermolecular (e.g. electrostatic, charge transfer, hydrophobic) forces [668]. Electron donor–acceptor is an enthalpy–based interaction in which two opposite regions (i.e. PAH donor and biochar acceptor) are attracted due to π electrons [669,670], with the π–π interactions showing a stronger bonding potential with the increase of biochar aromaticity [210]. Moreover, specific cation–π and hydrogen–π interactions may occur in the presence of cations (e.g. Na^+, K^+) and functional groups (i.e. –COOH, –OH, and $–NH_2$) in biochar, respectively [671,672]. Nonetheless, π–π interactions are more frequent being the interaction energy comprised in a larger range (i.e. 4–167 $kJ \cdot mol^{-1}$) compared to specific interactions [673].

It was widely accepted that PAH desorption from biochar is limited due to the strong adsorption mechanisms (e.g. π–π interactions), or the presence of micropores which can act as a physical trap for the adsorbed PAHs. However, changes in environmental conditions (e.g. pH), as well as the abiotic or biological degradation of

biochar, can promote the PAH desorption from biochar to the sediment, highlighting the importance of investigating this aspect in future research.

6.4 Mechanisms and impacts associated with biochar addition to PAH–contaminated sediments

6.4.1 Adsorption

6.4.1.1 One– vs. multi–PAH systems

Adsorption is the major mechanism induced by biochar addition to remove PAHs from sediment particles (Figure 6.3). Donor–acceptor, hydrophobic and specific interactions are mainly involved during PAH adsorption, as also explained in section 5.3.4, likely due to the planar and hydrophobic nature of PAHs. PAH adsorption onto biochar can be affected by different parameters, such as the specific PAH molecule, sorbent and sediment characteristics [48].

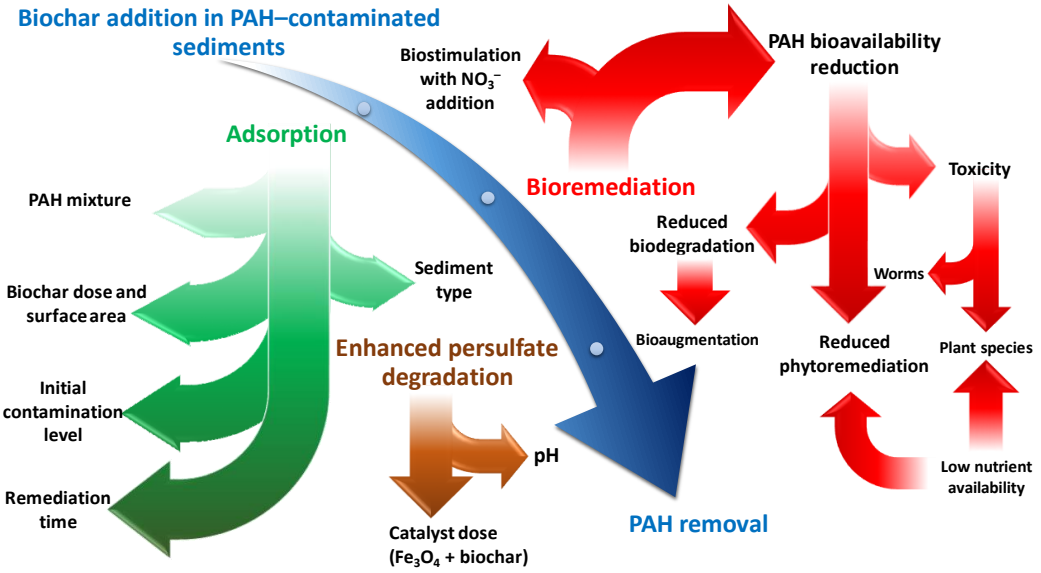

Figure 6.20 – Simplified schematic representation of the mechanisms and impacts associated with biochar addition to PAH–contaminated sediments. PAH adsorption onto biochar is influenced by the presence of a PAH mixture, the sediment origin, the initial PAH contamination level, the remediation time, the biochar dosage and surface area (green color). Bioremediation through biostimulation is stimulated by the presence of nitrate, while it is negatively affected when performed through bioaugmentation and phytoremediation by the decreased PAH bioavailability after biochar addition, which leads to toxic effects to living species due to a reduced nutrient availability (red color). The catalyst dose (Fe_3O_4 + biochar) and pH are parameters playing a key–role in persulfate degradation of PAHs (brown color).

Table 6.11 – Summary of the main results in terms of PAH removal efficiency obtained at different biochar dosages after biochar addition to PAH–contaminated sediments having different origins and initial PAH concentrations.

PAH	**Sediment**		**Experimental conditions**		**PAH removal**	
	Origin	*$\sum PAH_{t0}$ [mg·kg^{-1}]*	*Biochar dosage [w/w%]*	*Remediation time [d]*	**[%]**	**Ref.**
PYR[c]	River	< 0.1	1.3	100	29	[674]
PHE[c]	Lake and bay	0.5	0.1–0.5	4	11–60	[675]
ACE, PHE and FLU[c]	Canal	n. a.*	5.0	28	80	[606]
∑16 PAH[b]s	Estuary	8.0–15.4	5.0	28	98	[32]
FLR, PHE, ANT, FLU, PYR, B[a]ANT, and CHR[b]	Seaside	1,458.0	15.0	1	> 99	[676]
PHE and PYR[b, c]	Estuary	n. a.	1	56	52–69[a]	[604]
PHE[c]	Sand	5.0	1	24	57–65	[677]
PHE, ANT and PYR[b, c]	Seaside	10.0	4.0	30	> 95	[208]
PHE, PYR and CHR[c]	River	2.6–3.1	0.1–1.5	90	40–80	[602]
PHE[c]	River	15.0	1.3	100	34	[239]

* = not available; a = data referred to PYR; b = field–polluted sediments; c = lab–spiked sediments; ACE = acenaphthylene; ANT = anthracene; B[a]ANT = benzo[a]anthracene; CHR = chrysene; FLR = fluorene; FLU = fluoranthene; PHE = phenanthrene; PYR = pyrene.

PHE was the main investigated PAH in the scientific literature (Table 6.2), being the PAH that has average solubility and hydrophobicity properties [239,252]. PHE adsorption onto biochar was studied alone or with other PAHs (Table 6.2). Other studies showed the effect of biochar addition in sediments contaminated by naphthalene (NAPH) and pyrene (PYR) alone (Table 6.2) due to their higher abundance in the sediment investigated.

Yang et al. [239] observed a PHE adsorption of 34%, higher than that in the biochar–free control (i.e. 22%), after 100 d using pyrolyzed macadamia nut shells (obtained at 500 °C for 1 h) with a dose of 1.25% (w/w) in river sediments (Table 6.2). Cui et al. [675] showed an increasing PHE adsorption capacity (i.e. up to 60%) when using 0.5% (w/w) pyrolyzed rice straw in lake sediments for 4 d. A higher PHE adsorption (i.e. 57–65%) was obtained by Marchal et al. [677], who tested 1% (w/w) biochar in sand for 24 d (Table 6.2). PHE adsorption onto biochar particles was improved by doubling the PAH partition coefficient between suspension and water and increasing by 52% the carbon content of the system [675,677].

The use of biochar in the presence of multiple PAHs allows an enhancement of adsorption likely due to a decrease of the PAH solubility [678] (Figure 6.3). It is, however, important to notice that other factors, including sediment type, level of contamination, remediation time, biochar dose in sediment (w/w) and particle size also play a role during PAH adsorption (Figure 6.3). Wang et al. [602] showed after 90 d a PAH reduction up to 80% in pore water with the increase of the biochar dose from 0.1 to 1.5% by using pyrolyzed corn stalk and wood (obtained at 320 and 340 °C for 4 h, respectively) in river sediments (Table 6.2). Similarly, a PAH adsorption of almost 80% was obtained after 28 d with the addition of 5% peanut hull biochar (obtained at 600 °C for 2 h) to canal sediments [606]. Moreover, Gomez–Eyles and Ghosh [32] obtained a PAH reduction of approximately 98% in pore water after 28 d, with 5% pine wood biochar (obtained at 700–1,000 °C for 10 min) in marine sediments (Table 6.2). PAH adsorption was improved by 99% in the overlying and interstitial water adding 15% powdered coconut biochar to marine sediments (Table 6.2) [676].

The above–reported findings are further supported by the results obtained by other researchers [208,604,674], who investigated the effect of biochar on the adsorption of the sole PYR, PYR + PHE and PYR + ANT + PHE mixtures, respectively. The authors

used 1.25% of macadamia nut shell (produced at 500 °C), 1% of mangrove plant (produced at 600 °C) and 4% of pine wood (produced by gasification) biochar, respectively. PYR adsorption onto biochar reached 29% after 100 d when PYR was used as single PAH [674], while it increased to 52% after 56 d [604] and 95% after 30 d [208] when PYR was present in a mixture with PHE and ANT + PHE (Table 6.2), respectively. This demonstrates that PYR adsorption is less efficient when PYR is the sole PAH in the system. Moreover, Silvani et al. [208] reported that the adsorption mechanism was also enhanced by the high salinity of the marine sediments used, the high specific surface area and dosage of biochar (i.e. 343 $m^2 \cdot g^{-1}$ and 4%, respectively), and the initial PAH concentration (i.e. 10 $mg \cdot kg^{-1}$).

6.4.1.2 Adsorption–desorption kinetics and isotherms

Besides adsorption efficiencies, the PAH adsorption rate is another fundamental parameter to understand the performance of the biochar used as sorbent. In general, the adsorption rate is obtained by applying a kinetic model [679], which shows the required time to reach the equilibrium during the adsorption of PAHs onto the biochar surface [680]. The equilibrium is quickly or slowly reached depending on different parameters, including sediment and biochar properties [681].

A first–order kinetics is generally used, but further kinetic models (e.g. pseudo–first or second–order kinetics) can also be considered [682,683]. However, the mentioned kinetics could not fit well the whole adsorption process, but may be only valid for a limited time [684], implying the use of a kinetics describing both the fast and slow adsorption rates [685]. For example, Marchal et al. [677] reported a adsorption rate of 4.92 and 0.04 d^{-1} for a fast and slow kinetics, respectively, using biochar on sand. Johnson et al. [685] observed lower adsorption rates (i.e. 0.32 and <0.01 d^{-1} for a fast and slow kinetics, respectively) probably due to the lower organic content in the sand used. Moreover, the Elovich model can alternately be applied to fit the PAH adsorption process with a great correlation coefficient R^2 (i.e. 0.97–0.99), as recently shown by Cheng et al. [643].

The adsorption isotherms (i.e. Langmuir, Freundlich and linear) can be applied in aquatic environment to comprehend the PAH distribution onto biochar surface [181]. Freundlich isotherms are generally used due to higher correlation coefficient R^2 (i.e. up to 0.99) [604] compared to Langmuir and linear isotherms (i.e. up to 0.97 and 0.98, respectively) [608], suggesting that PAH adsorption is heterogeneous and occurs firstly in stronger sites of biochar surface [686]. Considering the intra–particle diffusion model, a higher adsorption rate can be achieved with a finer sorbent due to

the faster diffusion of PAH molecules. This would reduce the time required to reach the equilibrium [89]. Kang et al. [687] observed a decrease of the time needed to achieve 95% of the equilibrium from 17 to 1 d by decreasing the biochar particle size to below 125 μm.

A PAH adsorption–desorption mechanism from the amended biochar to the sediments can occur due to changes in pH and salinity. For example, the gastrointestinal fluids of living organisms have been reported to solubilize PHE from biochar particles, thus reversing the PAH adsorption process [688]. The possible presence of high salt concentrations in gut fluids can improve the "salting–out" effect by increasing the ionic strength in favor to the adsorption mechanism [689]. If a single–step desorption is considered, the mechanism would fit a logarithmic kinetic (R^2=0.99) and the Freundlich isotherm ($R^2 \geq 0.97$) [187,690]. On the other hand, by comparing the desorption and adsorption mechanism, the whole mechanism would be consistently hysteretic probably due to the irreversible binding of PAHs onto biochar and trapping of PAHs into microporous biochar [690,691].

6.4.2 Bioremediation

6.4.2.1 Effect of biochar addition on PAH bioavailability

PAH bioavailability is considered the accessible fraction of PAHs to living organisms [283], and is an important parameter allowing to determine the environmental fate of PAHs in sediments and the connected risk [85]. Passive samplers (e.g. polyethylene, silicone), mild solvents (e.g. butanol, Tenax®) and terrestrial invertebrates (e.g. *Chironomus plumosus)* (Table 6.3) are commonly employed during biochar–supplemented experiments to assess the PAH bioavailability in contaminated sediments as dissolved, biodegraded and bioaccumulated fraction of PAHs [692–694], respectively.

A lower PAH bioavailability is generally achieved in sediments after biochar addition (Figure 6.3), thus mitigating the environmental risk associated with the presence of PAHs [695]. Ho et al. [676] showed that the use of powdered coconut biochar is an effective method to significantly reduce the bioavailability of PAHs with a logarithmic octanol–water partitioning coefficient of 4–8. The supplementation of only 1.0% of corn stalk biochar could significantly decrease by 72% the bioavailable PHE fraction in river sediments [602]. A percentage up to 5% of wood biochar resulted in an efficient reduction of PAH bioavailability in sediments, being the biota sediment accumulation factor (i.e. < 0.10) lower than in control biochar–free tests (i.e. 0.21–

0.88, Table 6.3) [603]. However, Gomez–Eyles et al. [32,606] reported that a higher biochar percentage (i.e. > 5%) was required to achieve a similar PAH bioavailability by adding AC to sediments. The discrepancy with the results of Wang et al. [602] and Shen et al. [603] can be explained with a higher availability of the biochar pores [208] that induced a better PAH adsorption [696], while the higher biochar percentage used by Gomez–Eyles et al. [606] physically restrained the PAH transfer to biochar [697].

One study compared the use of conventionally–pyrolyzed biochar and magnetized biochar in river sediments [698]. After 30 d, the PAH bioavailability decreased by almost 50% with conventional biochar (Table 6.3), while magnetized biochar did not lead to a significant reduction of PAH bioavailability likely due to the pore occlusion by magnetite and the limited intraparticle diffusion [698]. The use of magnetized biochar was more effective when shaking the biochar–sediment mixture at 100 rpm [205] as the contact between biochar and PAHs was enhanced. The bioavailable PAH concentrations decreased by 68% (Table 6.3) in comparison to what observed in the control tests.

Chi and Liu [605] evaluated the addition of 3% wheat straw biochar, obtained at different pyrolysis temperatures (i.e. 400 and 700 °C for 4 h), and its effect on the PAH bioavailability in river sediments. After 54 d, the biochar obtained at 700 °C allowed a PHE and PYR bioavailability reduction by 69 and 55%, respectively, while a decrease by 29 and 23% of PHE and PYR bioavailability (Table 6.3), respectively, was obtained with the biochar produced at 400 °C [605]. Similarly, the PHE and PYR bioavailability was reduced by 46 and 17% (Table 6.3), respectively, after the application of nut shell biochar (obtained at 500 °C) to river sediments [239,674]. These results suggest that a lower PAH bioavailability is coupled with a higher pyrolysis temperature likely due to a greater aromaticity of the obtained biochar.

Table 6.12 – Effect of biochar addition on bioavailability and biodegradation of PAHs in contaminated sediments. The analytical method used to determine PAH bioavailability is also reported.

Bioavailability analytical method	PAH bioavailability reduction [%]	Effect on PAH biodegradation	References
Mild solvent extraction	17	Stimulation by 49%	[674]
Mild solvent extraction	23–69	Reduction by 37[a] and 61[b]%	[605]
Polydimethylsiloxane fibers	n. a.	Reduction up to 20%	[675]
Polyethylene sampler	50	n. a.	[698]
Polyethylene sampler	68	n. a.	[205]
Silicone sampler	n. a.	Reduction of 64%	[677]
n. a.	n. a.	Inhibition	[609]
Terrestrial invertebrates	> 50	n. a.	[603]
Terrestrial invertebrates	40–72	n. a.	[602]
Mild solvent extraction	46	Stimulation by 57%	[239]

* = not available; a = phytoremediation; b = biodegradation

6.4.2.2 Reduced biodegradation efficiencies in the presence of biochar

Bioaugmentation, biostimulation and phytoremediation are the most widely applied technologies for the bioremediation of PAH–contaminated sediments [699], Biostimulation and bioaugmentation consist on the supplementation of organic matter or nutrients, and enriched microorganisms to the sediment, respectively, to improve the PAH biodegradation under aerobic or anaerobic conditions (Figure 6.1) [700]. Bioremediation occurs with phytoremediation when plants are employed to remove PAHs from the contaminated sediment (Figure 6.1) mainly via rhizodegradation (i.e. PAH biodegradation in the root–zone compartment) or phytoextraction (i.e. PAH extraction in plant) [701]. However, bioremediation technologies are strongly affected by the amount of bioavailable PAHs in the sediment [702] and, thus, can be influenced by the addition of biochar.

A lower PAH biodegradation in biochar–amended experiments has been associated with a strong PAH adsorption by biochar and a consequently reduced PAH bioavailability [703,704], (Figure 6.3). Biochar addition has been reported to negatively affect bioaugmentation and phytoremediation likely due to an increase of pH [705], a decrease of PAH concentration in the sediment and the nutrient retention in biochar [706,707] (Figure 6.3). Thus, the use of biochar effectively decreases PAH bioavailability and allows to mitigate the associated environmental risk, but it may lead to a lower efficiency of bioremediation due to a lower bioavailable PAH concentration.

In regard to bioaugmentation, Cui et al. [675] investigated the use of coconut shell biochar coupled with *Mycobacterium vanbaalenii* in PHE–contaminated sediments (Table 6.3). PHE degradation in lake and estuary sediments was reduced by almost 20% and showed no significant variations compared to biochar–free controls [675]. Marchal et al. [677] also conducted bioaugmentation experiments using a *Sphingomonas sp.* inoculum (Table 6.3). The addition of biochar resulted in a lower microbial activity, with PHE biodegradation being lower in biochar + sediment (i.e. 12%) than in control tests (i.e. 27%). Similarly, Chi and Liu [605] reported a PAH degradation of 8–12 and 25–31% (Table 6.3) in the presence and absence of wheat straw biochar (400 °C for 4 h), respectively. Moreover, the suppression of indigenous PAH–degrading bacteria was observed by Ojeda et al. [609] after the addition of pine biomass biochar (obtained by gasification at 600–900 °C for 10 s) in river sediments (Table 6.3). Hence, the biochar addition clearly decreases the microbial activity in the sediment due to a lower PAH bioavailability, and this is more evident increasing the pyrolysis temperature probably because PAHs are more strongly adsorbed onto biochar. Thus, the use of biochar obtained at lower pyrolysis temperatures is recommended for a more efficient bioremediation of sediments, as biochar is richer in nutrients (mainly N and P) and can better stimulate PAH biodegradation ([561].

The PAH–degrading activity can be stimulated by the addition of electron acceptors in sediments under anaerobic conditions (e.g. sulfate, nitrate, carbon dioxide) [288,331,708]. In a combined biostimulation and bioaugmentation study (Figure 6.3), Yang et al. [239] obtained a higher PHE removal (i.e. 51–54%) in sediments with biochar, nitrate and immobilized bacteria than in biochar–free controls (i.e. 22%), (Table 6.3). Similarly, Chen et al. [674] reported an improvement of PYR biodegradation (i.e. 49%, Table 6.3) and the abundance of nitrate–reducing PAH degraders (e.g. *Stenotrophomonas, Gallionella*) in the concomitant presence of biochar and nitrate. PAHs were first adsorbed onto biochar enhancing the PAH

exposition to microorganisms, and then acted as electron donors during denitrification [709].

A stronger electron acceptor than nitrate, namely oxygen, is involved during PAH phytoremediation [710]. PAHs have a higher terminal electron acceptor potential in the presence of O_2 (i.e. +818 mV) compared to nitrate, sulfate and carbon dioxide (i.e. +433, –200 and –380 mV, respectively) [711]. Many studies report the release of oxygen from plant roots to rhizosphere–living microorganisms during phytoremediation, improving the PAH removal [712,713]. However, a lower PAH removal (i.e. 12–37%) in river sediments using *Vallisneria spiralis* (also known as tape grass) was observed in the presence of biochar than that achieved without biochar (i.e. 44–59%) (Table 6.3) due to the increase of nutrient retention in biochar that had a negative effect on plant growth (Chi and Liu, 2016) (Figure 6.3). Moreover, the PAH sequestration by biochar can hinder the symbiosis between rhizosphere microorganisms and *V. spiralis*, negatively impacting the PAH removal [714].

6.4.2.3 Effect on PAH toxicity to living species

By decreasing PAH bioavailability in sediments (section 5.4.2.1), biochar supplementation is also responsible of a decrease of the PAH toxicity, alleviating the vital functions of living organisms [715]. The toxicity in sediments is influenced by the biochar application time, dosage and specific surface area [716], as the increase of these parameters enhances the PAH removal in sediments. However, contrasting studies are still present in the scientific literature about the effect of biochar addition on the toxicity to living species [717].

The increase of corn stover biochar dosage from 1 to 10% caused a reduction of inhibition of *Lepidium sativum* (i.e. cress) in harbor sediments from 60 to almost 40% [607]. The application of 15% powdered coconut biochar improved the mysid and amphipod survival up to 100% in harbor sediments [676], due to a 99% PAH decrease. In contrast, Chi and Liu [605] observed a decreased *V. spiralis* growth after a 3% biochar addition in river sediments. The high nutrient retention in biochar negatively impacted the plant growth [707]. Similarly, Zheng et al. [718] showed the decrease of clam growth by 36% using 5% wood chip biochar in marine sediments, due to the reduction of the bioavailable organic matter for clams.

Regarding the specific surface area, a biochar with a particle size lower than 300 μm did not significantly reduce the toxic effects on *L. sativum* [607]. Similarly, the addition of biochar showed no significant changes in *Lytechinus variegatus* (i.e. green sea urchin) reproduction [205], *Chironomus plumosus* (i.e. buzzer midge) larvae

survival rate [603] and worm lipid content [32]. Although the PAH bioavailability decreases, a reduced particle size of biochar likely decreases the water availability also affecting the metabolism of living species (e.g. plants, worms), [213,719]. Moreover, a lower particle size may be more easily ingested by earthworms [720]. Zhang et al. [721] observed a significant ingestion by *Limnodrilus hoffmeisteri* (i.e. red worm) of bamboo biochar with a particle diameter comprised between 20 and 63 μm. Conversely, a higher biochar particle size (i.e. 300–500 μm) allowed a total elimination of the toxic effects [607]. This is more visible with those plants mainly capable to remove PAHs from sediments via phytoextraction. Jia et al. [604] recently reported the increase of *Kandelia obovata* biomass up to 47% due to a decrease of the PAH concentration in the plant from 2.26–2.52 to 0.72–0.95 $mg \cdot kg^{-1}$ after biochar addition in estuary sediments, suggesting that *K. obovata* was not a strongly tolerant plant to PAH exposure. The effect of the contact time on toxicity showed a greater seed germination for *L. sativum* up to 100% in harbor sediments by increasing the remediation time from 30 to 60 d with straw biochar [607]. In this case, the toxicity reduction is consistent with the maximum decrease of PAH bioavailability, which is commonly reached after 60 d.

In summary, the authors observed different effects during toxicity tests and, therefore, the biochar addition cannot be directly associated with decreased PAH bioavailability and toxicity. Other factors, such as water, organic matter and nutrient availability or the ingestion of small biochar particles, may affect the growth and metabolism of living species (Figure 6.3). The migration of PAHs from the ingested biochar particles to the living organism gut should be limited when PAHs are strongly adsorbed by biochar (e.g. through electron donor–acceptor interactions) [722]. The gut fluid subsequently released by the involved organisms can, however, solubilize PAHs from biochar [723], thus potentially leading to a higher toxicity in the sediments. Further studies should be performed to shed light on the PAH toxicity reduction associated with biochar addition.

6.4.3 Enhanced persulfate degradation

The co–application of persulfate, Fe^{2+} and biochar has been recently investigated to enhance chemical oxidation processes aimed at PAH removal in sediments [724–726], (Table 6.4). PAH can be degraded by a strong oxidizing species (i.e. $SO4^{-\bullet}$) obtained by persulfate activation in the presence of transition metal or organic matter, resulting in a reaction similar to the Fenton process [727,728].

Persulfate degradation of PAHs has been investigated using biochars obtained by pyrolysis of bamboo (at 800 °C and subsequently magnetized) [724], wood (at 300 °C) [726] and coal–tar pitch (at 300 °C for 1 h and subsequently magnetized) [725]. The experimental activity was performed by adding the biochar, persulfate and Fe_3O_4 (as catalyst) to harbor sediments using different catalyst doses and pHs at 25 °C for 24 h. Dong et al. [724] obtained a PAH degradation of 14, 21 and 78% (Table 6.4) using persulfate alone, Fe_3O_4 + bamboo biochar, and Fe_3O_4 + bamboo biochar + persulfate, respectively, with a catalyst dose of 3.33 $g \cdot L^{-1}$. A similar PAH removal of 76% (Table 6.4) was achieved with a higher dose of catalyst (i.e. 6.67 $g \cdot L^{-1}$) with Fe_3O_4 + wood biochar + persulfate, with PAH oxidation significantly increasing at catalyst doses from 1.67 to 6.67 $g \cdot L^{-1}$ likely due to a faster $SO4^{-\bullet}$ production [726]. A higher PAH oxidation (i.e. 87%, Table 6.4) was reached increasing the catalyst dose of Fe_3O_4 + coal–tar pitch biochar + persulfate to 10 $g \cdot L^{-1}$ [725] (Figure 6.3), likely due to the increase of iron species and active sites in biochar, which enhanced the donor–acceptor interactions and the $SO4^{-\bullet}$ generation [729].

PAH oxidation was improved from 80% (Table 6.4) upwards by decreasing the pH from 6 to 3 and combining persulfate and Fe_3O_4 with bamboo and wood biochar (Figure 6.3) [724]. This allowed higher $SO4^{-\bullet}$ activity and Fe_3O_4 solubilization in the acidic solution [241,730]. However, Dong et al. [725] obtained the highest PAH removal (i.e. 87%, Table 6.4) with a pH of 6 probably due a higher $OH^{\bullet}$ generation [731]. The discrepancy between the mentioned studies can be explained by the fact that hydroxyl radicals have a similar oxidation potential (i.e. 270 mV) compared to sulfate radicals (i.e. 260 mV) [732], but the catalyst dose was significantly different (Table 6.4). On the other hand, the most appropriate pH needs a careful assessment when aiming at reusing the sediment due to the effect of low pHs on the microbial community [733,734]. Despite the pH drop improves metal solubility during chemical oxidation, acidic pHs disturb the ecosystem, being incompatible in most cases with the vital functions of the living organisms [735].

Table 6.13 – Summary of PAH removal efficiencies obtained varying the catalyst dose (i.e. Fe_3O_4 + biochar) and pH during the enhanced persulfate activation for the remediation of PAH–contaminated sediments, amended with biochars obtained from different feedstocks and at 300 or 800 °C as pyrolysis temperatures.

Biochar		**Effect of catalyst dose**		**Effect of pH**		**References**
Feedstock	*Pyrolysis temperature [°C]*	*Fe_3O_4 + biochar[a] [g·L^{-1}]*	*∑PAH removal [%]*	*pH[b]*	*PAH removal [%]*	
Bamboo	800	1.67	70	3	86	[724]
		3.33	78	6	78	
		6.67	54	9	82	
Wood	300	1.67	68	3	84	[726]
		3.33	74	6	76	
		6.67	76	9	72	
Coal tar pitch	300	5.00	86	3	84	[725]
		10.00	87	6	87	
		20.00	85	9	72	

a = results are referred to pH 6; b = results are referred to the optimal catalyst dose

6.5 The effect of various parameters on the remediation of biochar–amended sediments

6.5.1 Sediment origin

The origin of sediments (e.g. river, estuary, seaside) has been reported to affect PAH adsorption (Figure 6.3) and biodegradation associated with biochar addition, mainly due to a different concentration of inorganic ions (e.g. Na^+, Cl^-) [736]. Generally, a higher PAH adsorption (i.e. up to 99%) on biochar has been observed in estuarine and marine sediments than that (i.e. up to 80%) reported for river sediments (Table 6.2). Gomez–Eyles et al. [606] showed that the adsorption of hydrophobic contaminants, including PAHs, on pine dust biochar can be enhanced in saline solutions (i.e. 10‰) compared to fresh water. The higher efficiency of PAH adsorption at increasing salinity has been ascribed to a decreasing PAH solubility in water, which may force PAH molecules onto the biochar surface [737]. Indeed, Sun et al. [738] observed the reduction of PHE solubility from 1.12 to 0.97 $mg \cdot L^{-1}$ by simulating a real seaside salinity (i.e. 32‰).

The increment of salt concentrations also results in a higher ionic strength and could increase the organic matter aromaticity [739], improve PAH adsorption onto biochar particles due to bridging interactions [203] and decrease the biochar mobility in capping applications [608]. Qian et al. [740] reported the enhancement of the "salting–out" effect on PAH adsorption by increasing the ionic strength from 0 to 10 mM. However, Yang et al. [608] reported no significant differences in NAPH adsorption onto biochar with a higher ionic strength (i.e. 25 mM) probably due to screening effect of the surface charge [741]. Therefore, the addition of metal ions leads to a positive effect on the adsorption of PAHs by enhancing the bridging interaction with biochar [742]. On the other hand, the co–presence of different organic and inorganic contaminants (e.g. metal ions) can induce a competition for the available adsorption sites of biochar [743].

Regarding bioremediation, the increase of salinity generally leads to a decreased PAH biodegradation due a reduction of PAH solubility [744]. However, Ojeda et al. [609] reported no differences in PAH degradation using biochar with different salinities (i.e. 15, 25 and 35‰) when reproducing estuarine conditions. This result can be explained with a microbial mechanism recently proposed by Cao et al. [702], who described hydrocarbon biodegradation under different salinity conditions. A salinity lower than 35‰ may enhance the hydrocarbon degradation due to a high cell surface

hydrophobicity, justifying the results obtained by Ojeda et al. [609]. On the other hand, the cell surface hydrophobicity is reduced with a higher salinity (i.e. 50–70‰), shifting the microorganism growth from oil to aqueous phase, and decreasing the hydrocarbon degradation [702]. Additional research on the effect of salinity on marine sediments after biochar addition is strongly encouraged in order to elucidate this aspect.

6.5.2 Initial PAH contamination level

The initial PAH concentration in sediments is another key parameter affecting the remediation efficiency when supplementing biochar (Figure 6.3). Considering the adsorption as major mechanism associated with biochar addition in the sediment, PAH adsorption can be enhanced at higher PAH contamination levels depending on the physical–chemical PAH characteristics [745]. The increment of PAH concentrations can also decrease the biochar mobility during capping applications likely due to the decrease of the primary energy barrier between biochar and the sediment surface [608].

Among the considered studies, an increase of the initial PAH concentration from <0.1 up to 10 $mg \cdot kg^{-1}$ resulted in a higher PAH removal from sediments by 95% (Figure 6.4). Hence, the beneficial effect due to the initial contamination level of the sediment could be related to a greater tendency of PAHs to interact with the biochar active sites [181]. In the presence of low PAH concentrations, the organic contaminant can be more strongly adsorbed onto sediment particles, being more persistent and harder to remove [746].

However, Han et al. [698] reported a decreased PAH removal (i.e. approximately by 50%) compared to that (i.e. up to 80%) achieved in a sediment with a 8–fold lower initial PAH concentration (Table 6.2) [602]. Many factors can be involved (e.g. type and dose of biochar), but an additional explanation could be the use of a naturally PAH–contaminated sediment, instead of an artificial one. Indeed, an artificially PAH–spiked sediment has generally higher bioavailable PAH concentrations [254], with PAHs being easier to be adsorbed onto biochar.

The adsorption mechanism could also be affected by the PAH involved in the process that is characterized by a distribution coefficient (K_d), which can in turn be affected by the added sorbent and the PAH itself. For example, Cui et al. [675] obtained a higher log K_d of PHE with coconut shell and rice straw biochar (i.e. 2.73–3.46 and 2.99–3.38, respectively) than with unamended experiments (i.e. 2.66–3.36), thus enhancing PHE adsorption onto biochar (section 5.4.1.1). Light molecular weight PAHs (i.e. 2–3 benzene rings) could be easily adsorbed onto biochar than high molecular weight PAHs (i.e. 4–5 benzene rings), which are more easily adsorbed on

natural organic matter [209]. Indeed, Han et al. [698] showed a higher log K_d for ANT (i.e. 6.0–6.4) compared to PYR (i.e. 5.8–6.2).

6.5.3 Remediation time

Regardless the remediation technology used, longer remediation times generally prompt to higher PAH removal efficiencies [747]. After the biochar addition in sediments, the contact time between biochar and PAHs results in a fast PAH biodegradation during the first days of treatment [187]. Afterwards, a slower PAH degradation may occur [677] likely due to a reduced PAH bioavailability in favor to adsorption onto biochar, as discussed in section 5.4.2.1. In fact, the amount of extractable PAHs from sediments by biochar is affected by the treatment time (Figure 6.3). A PAH fraction can be quickly desorbed from the sediment and transferred to the biochar surface (i.e. by 95%) in a relatively short time (i.e. 30 d, Figure 6.4) as a function of the specific PAH molecule, sediment properties and biochar characteristics [748]. The remaining fraction of PAHs is more slowly adsorbed onto biochar along the treatment duration till reaching the thermodynamic equilibrium, typically obtained within 60 d [749].

Further extending the treatment durations up to 100 d can even be a limiting factor for PAH adsorption onto biochar. A prolonged treatment can lead to a less performing adsorption mechanism [750,751] probably due to the biochar oxidation [752], which induces a more hydrophilic surface of biochar [753]. The biochar oxidation can occur after months or years through biotic and/or abiotic degradation [754], and PAHs can be desorbed up to 70% from the oxidized biochar [187], again increasing the bioavailable PAH fraction in the sediment. However, a low PAH adsorption (i.e. 40–50%) was also reported after only one month with wood biochar [677,698], indicating that the type of sorbent is a crucial parameter.

6.5.4 Biochar dosage and manufacture

The adsorption of organic contaminants (e.g. PAHs) on carbon sorbents (including biochar) is affected by the sorbent dosage and manufacture (Figure 6.3). The biochar dosage is normally expressed as biochar to sediment ratio (w/w) and controls the biochar repartition in pore water at the expense of the natural organic content of sediment [755]. The temperature and feedstock used for biochar manufacture strongly influence the final specific surface area of the biochar particles and the morphology of biochar. High pyrolysis temperatures and wood materials generally lead to a higher specific surface area of biochar [756], improving the interactions with PAHs due to a

better pore size distribution and a higher carbonization degree of biochar [714], as mentioned in section 5.3.3.

The studies about the application of biochar to remediate PAH–contaminated sediments (Figure 6.4) showed a rise of PAH removal from 10 to 98% by increasing biochar dose from 0.1 to 5.0%, and a further rise of biochar dosage up to 15% allowed a complete removal of PAHs from sediments [676]. Likewise, an increase of pyrolysis temperature (i.e. from 400 to 1,000 °C) enhanced the adsorption of PAHs onto biochar due to the higher specific surface area up to 358 $m^2 \cdot g^{-1}$ (Figure 6.4), as mentioned in sections 3.3.and 4.1.1.

However, the increase of pyrolysis temperature may also lead to the development of micropore deformation in biochar and to a reduced PAH adsorption [757] and, therefore, a reduced pyrolysis temperature could be applied. Wang et al. [602] reported a PHE adsorption of 72% similar to that achieved with wood biochar (obtained at 340 °C) using a low temperature pyrolyzed corn stalk (i.e. 320 °C), which is characterized by lower specific surface (section 5.3.3), but is more available and economic compared to wood derived biochar [758]. These data suggest that the specific surface area alone might not govern the PAH adsorption mechanism [759]. On the other hand, a smaller particle size of biochar could significantly decrease the time to achieve the equilibrium [760], as mentioned in section 5.4.1.2. Therefore, the methods or materials used should be evaluated case by case.

Thus, the rise of biochar dosage and pyrolysis temperature can enhance the repartition of PAHs on the biochar surface rather than on the sediment [759]. Ghosh et al. [761] reported a similar behavior of AC during PAH adsorption. Since biochar is cheaper than AC, this aspect could represent a benefit if a higher adsorbent dose is necessary [606]. On the other hand, the price of biochar is different in each country and averages $ 2,580 per ton [762], depending on different parameters such as processing requirements, pyrolysis conditions and reactor availability [763]. Thus, the use of an effective biochar dose (i.e. 5%) can be expensive when remediating a large amount of sediments, implying the need of a cost–benefit assessment.

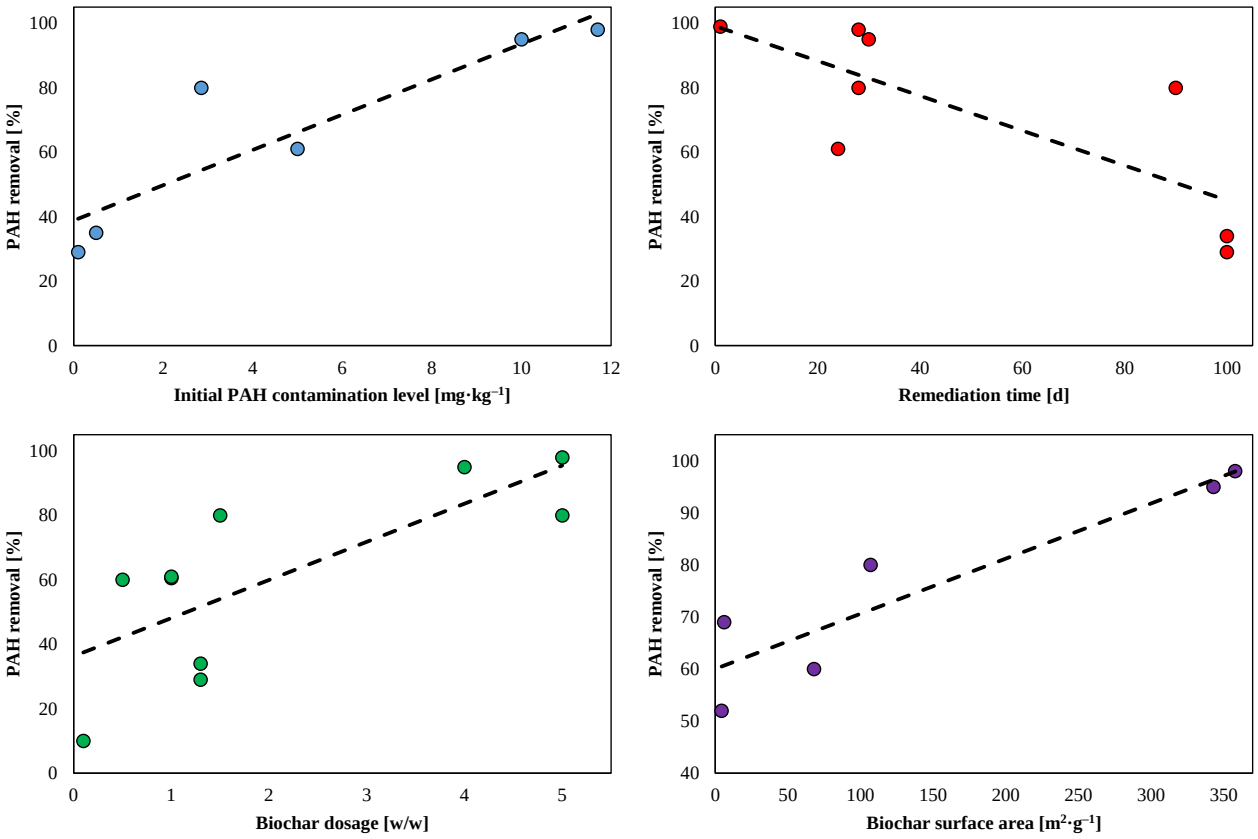

Figure 6.21 – The effect of initial PAH contamination level [mg·kg^{-1}], remediation time [d], biochar dosage [w/w] and biochar surface area [m^2·g^{-1}] on PAH removal in biochar–amended sediments. The data were taken from Tables 1 and 2 and used to describe the four trends.

6.5.5 pH

The sediment pH is influenced by the presence of organic, rock and mineral matter [764] and rules the main adsorption mechanisms (e.g. donor–acceptor, hydrophobic interaction) of PAHs onto biochar by changing biochar surface and electronic characteristics [765,766]. pH has an impact on PAH biodegradation when not comprised in the optimal range from 6.0 to 8.0 [258,322]. In addition, pH affects biochar mobility after capping [767] and the improvement of persulfate activation for PAH oxidation, as already reported in section 5.4.3.

All the investigated sediments reported in Table 6.2 have a basic pH (i.e. 7.5–8.5) that is further increased after the addition of biochar due to alkaline properties of biochar [768], as mentioned in section 5.3.3. In general, the increase of pH improves the π–π interactions [211], enhancing a strong planar and nonpolar molecule (i.e. PAHs) adsorption onto biochar (section 5.3.4). However, Yang et al. [608] reported no significant effect on NAPH adsorption onto biochar by increasing the pH from 5 to

10. Similarly, Chen et al. [741] showed a negligible NAPH adsorption variation by increasing pH from 2 to 11. These results suggest that the mechanism involved during PAH adsorption is slightly affected to the background solution pH, and mainly depends on the biochar manufacturing (i.e. pyrolysis temperature), as also reported in section 5.3.4. In addition, Yang et al. [608] used a relatively high temperature biochar (i.e. 600 °C) in which PAH adsorption is already coupled with π–π interactions, and therefore any rise of pH would slightly improve the adsorption mechanism. On the other hand, pH dependency can be enhanced with the presence of functional groups (e.g. –COOH, –OH) [666,769], which can be more often present in low temperature biochars (section 5.3.3).

So far, no study investigated the connection between pH and bioremediation after the addition of biochar to PAH–contaminated sediments. Previous research [239,674] showed an increasing PAH removal by combining biostimulation and bioaugmentation in biochar–amended sediments, providing no evidences about the pH effect on PAH–degrading bacteria (section 5.4.2.2). Since an increase of pH can significantly reduce the bioremediation efficiency [770], more studies should be conducted in this context in order to shed a further light on this aspect.

6.6 Conclusions and future recommendations

The use of biochar has proven to be a successful and sustainable solution for the remediation of sediments contaminated by PAHs. This chapter has highlighted that PAHs can completely migrate from the contaminated sediments onto the biochar surface via adsorption through hydrophobic, donor–acceptor or specific interactions, significantly reducing the PAH bioavailability. The adsorption efficiency mainly depends on remediation conditions (i.e. treatment time, biochar dosage), biochar (i.e. specific surface area) and sediment (i.e. origin, involved PAHs, initial PAH concentration) characteristics. To promote a chemical PAH oxidation, biochar enhances the activation of persulfate by applying Fe_3O_4 as a catalyst in sediments. PAH biodegradation is a minor mechanism for PAH removal from sediments after biochar addition, but it can be stimulated by almost 50% by using low temperature–produced biochar and simultaneously supplementing nitrate as electron acceptor. In contrast, biochars obtained at high pyrolysis temperatures are generally not suitable for bioaugmentation and phytoremediation due to a decrease of PAH bioavailability and an increase of pH, which can hamper the microbial activity until a complete inhibition. Some additional drawbacks, such as water and nutrient retention or the

ingestion of biochar particles, are associated with biochar–amended sediments enabling potential toxicity to plants or aquatic species. Likewise, the biochar oxidation after months of years from its application might promote the release of PAHs back to the sediments, thus increasing the PAH bioavailability and environmental.

Future studies should be addressed to evaluate the remediation potential of biochars produced from innovative feedstocks, such as plastic and tires, but also algae, animal manure and sewage sludge. For the latter, hydrothermal carbonization and microwave–assisted pyrolysis can represent interesting alternatives for biochar manufacture, being these substrates characterized by a high–water content. The role of electron acceptors (e.g. sulfate, nitrate) and pH during the biostimulation of biochar–amended PAH–polluted sediments definitely requires further investigation as well as the role of a high salinity (i.e. by 50‰). Inhibiting and toxic effects on the living species related to the reduction of water and nutrient availability shall be also clarified. It is also relevant to evaluate the impacts of biochar in full–scale applications, trying to minimize the biochar dosage (e.g. lower than 1%) and promoting the use of easily recoverable materials such as magnetized biochar in order to keep the application and recovery costs of the biochar low. This would also prevent the PAH desorption after a possible biochar oxidation and avoid changes in the biochar geo–mechanical properties in view of a sediment reuse for civil engineering purposes.

CONCLUSIONS

PAHs are largely spread in the aquatic environment, and drawbacks of conventional remediation techniques as well as the expenditures for alternative disposal of polluted sediments lead to seek more effective, environmentally–friendly and sustainable approaches. In this context, the present doctoral thesis firstly showed that it is possible to achieve higher efficiencies in terms of PAH removal (i.e. PHE), time and energy consumption by employing SW with EtOH (i.e. 97%, 1 hour and −14 kWh m^{-3}, respectively) compared to both LTTD (i.e. 88%, 1 hour and −417 kWh m^{-3}, respectively) and anaerobic bioremediation under either nitrate−reducing and methanogenic conditions (i.e. up to 68%, 14 days and −16 kWh m^{-3}, respectively). The latter, however, proved to be the cheapest technology with a final cost of 228 € m^{-3}, which can be affected by the power savings associated with the reuse of the biomethane produced to heat up anaerobic digestion.

Therefore, this thesis subsequently evaluated the anaerobic biostimulation of PAH−contaminated sediments by using digestate and OFMSW as amendments for enhancing both PAH removal efficiency and biogas generation. The simultaneous supplementation of OFMSW and nutrients improved the removal of PAHs (i.e. PHE, anthracene, fluoranthene and pyrene) by reaching a higher total PAH biodegradation and biogas yield (i.e. 55%, and 60 mL $H_2 \cdot g\ VS^{-1}$ and 140 mL $CH_4 \cdot g\ VS^{-1}$, respectively) compared to the use of digestate (i.e. 43% and 4 mL $CH_4 \cdot g\ VS^{-1}$, respectively). The employment of OFMSW as a sediment amendment can also represent a promising reuse strategy in the perspective of circular economy. Also, the addition of the selected nutrients was reported to be optimal for plant growth, and therefore, a further opportunity for favoring the in−situ restoration after the reuse of sediments for coastal nourishment. On the other hand, PAH bioaccessibility was still above 35% after 120 days, thus indicating the need of a further treatment to ultimately remove this fraction and consequently mitigate the environmental risk.

A biological process can be instead performed for treating a PHE–contaminated SW solution in a fed–batch bioreactor through the use of highly efficient–engineered bacteria (i.e. *Achromobacter*, *Sphingobacterium* and *Dysgonomonas* genera) by achieving a successful PHE removal up to 91%. The biological process was mainly

affected by the proper supplementation of nutrients (i.e. C/N/P ratio of 100:1.3:0.05), the initial PHE concentration value (i.e. above 50 mg L^{-1}), and the excessive decrease of dissolved oxygen and pH (i.e. below 1 mg L^{-1} and 7, respectively). Also, the adoption of a reduced amount of extracting agents by a high S/L ratio (e.g. 1:3, w/w) and the promotion of reagent recovery through distillation or condensation (i.e. up to 1.35 tons) can further encourage this approach by decreasing the volume of spent SW solution to be treated in the bioreactor (i.e. 2.81 tons per ton of sediment) and favoring the reuse or sale of washing agents. Therefore, the deployment of a biological treatment after the SW process can contribute to the development of an attractive sustainable resource–recovery approach, having favorable implications on both the environmental and techno–economic aspects due to a safe release of treated SW effluent and the decrease of the overall costs by 50%, respectively.

This thesis work moved forward on this research line in order to find unexplored extracting agents for SW and novel solutions for further enhancing the biological treatment of spent SW effluents. For this purpose, the biological treatment of a PHE– and TW80–containing SW solution in a BC immobilized–cell reactor was subsequently investigated. The SW process was firstly conducted in batch tests by achieving the highest PHE desorption of 91%. Afterwards, the resulting spent SW solution was aerobically treated in a continuous–flow bioreactor by reaching a PHE degradation up to 96% after 43 days, mainly due to the activity of bacteria belonging to the *Proteobacteria, Bacteroidota* and *Actinobacteriota* phyla attached on the surface of BC. A preliminary economic evaluation of the overall process (i.e. SW + PHE biodegradation in the BC immobilized–cell reactor) revealed that the process entails a total cost of 342.60 €·ton^{-1}, which respects the range of costs previously reported for the SW of contaminated sediments. Nonetheless, this cost can be further reduced due to the low TW80 biodegradability, which allows the reuse of the surfactant for SW, and the continuous biodegradation of PHE adsorbed onto BC that favors BC regeneration avoiding PHE adsorption.

Future studies should be addressed to evaluate the remediation potential derived by the reuse of the washing agent, the biological process optimization by maximizing the PAH loading rates, reducing the hydraulic retention time, and fine–tuning the DO level in the liquid phase to avoid foam production due to the air injection. The employment of an anaerobic digester for treating the spent SW solutions can be studied as well, by eventually assessing the biomethane production aimed at bioenergy generation. Also, PAH removal from sediment can be studied by employing phytoremediation in the presence of amendments, such as non–ionic surfactants (e.g. TW80), low temperature–

produced biochar (e.g. 400 °C) and acclimated bacterial mixtures (i.e. bioaugmentation). Finally, ecotoxicological tests can be carried out on plants (e.g. watercress) or benthic organisms (e.g. worms) to investigate the possible toxicity of treated SW effluent towards living organisms in order to prevent an improper discharge due to the presence of harmful reaction intermediates.

APPENDIX A

Parameter implementation in RACER

The Remedial Action Cost Engineering and Requirements (RACER) software was used for the economic analysis. A list of assumptions for each analyzed ex–situ remediation technology (i.e. bioremediation, sediment washing and thermal desorption) is reported in Table 2.2.

After selecting hazardous sediment and semi–volatile compounds (i.e. SVOCs) as site parameters, remedial action preferences were set. Bioremediation, sediment washing and thermal desorption were implemented on RACER by considering "ex–situ bioreactor, soil washing and off–site thermal treatment" as remediation technologies. Common preliminary parameters were the contamination area, the safety level of machining operation and mobilization distance (Table 2.2). For the ex–situ bioreactor, the distinguishing parameters were the flow rate, chemical oxygen demand (COD), pH, nutrients and water temperature. The characterizing features of soil washing were the size of soil washing plant, additives, water temperature, operation duration. The required off–site thermal treatment features were temperature, drums, fees and carbon adsorption gas.

Despite the differences in the examined technologies, the two most important considered parameters were retention time and temperature (Table 2.2) as crucial factors of treatment efficiency (i.e. microbial kinetics, PAH dissolution and vaporization). This kind of criteria were derived from the lab–scale conditions with the highest PHE removal, which were SN (i.e. 336 h and 37 °C), S:L ratio of 1:3 (i.e. 1 h and 20 °C) and thermal desorption (i.e. 1 h and 200 °C) for ex–situ bioreactor, soil washing and off–site thermal treatment, respectively.

After selecting the flow rate (i.e. 5.6 $L \cdot s^{-1}$) and the size of washing plant (i.e. 50 $tons \cdot h^{-1}$), the bioreactor volume (i.e. 70 m^3) and operation duration (i.e. 324 h) were calculated from the retention time and sediment volume to be treated for bioremediation and sediment washing, respectively. Moreover, by setting the temperature of bioremediation, gas water boiler and heat exchangers were automatically generated. For thermal desorption, low temperature thermal desorption

(i.e. <320 °C) was set to simulate the experiment at 200 °C, but nevertheless the retention time was unable to be selected. Regarding to the other reported parameters, the available information was established (i.e. COD, pH, nutrients and additives), and the unavailable features were set as default (i.e. drums, fees and carbon adsorption gas).

REFERENCES

[1] D. Thepnuan, N. Yabueng, S. Chantara, T. Prapamontol, Y.I. Tsai, Simultaneous determination of carcinogenic PAHs and levoglucosan bound to PM2.5 for assessment of health risk and pollution sources during a smoke haze period, Chemosphere. (2020) 127154. https://doi.org/10.1016/j.chemosphere.2020.127154.

[2] Y. Zheng, Y. Li, Z. Yue, Samreen, Z. Li, X. Li, J. Wang, Teratogenic effects of environmentally relevant concentrations of phenanthrene on the early development of marine medaka (Oryzia melastigma), Chemosphere. 254 (2020) 126900. https://doi.org/10.1016/j.chemosphere.2020.126900.

[3] D. Ghosal, S. Ghosh, T.K. Dutta, Y. Ahn, Current state of knowledge in microbial degradation of polycyclic aromatic hydrocarbons (PAHs): A review, Front. Microbiol. (2016). https://doi.org/10.3389/fmicb.2016.01369.

[4] K. Dhar, S.R. Subashchandrabose, K. Venkateswarlu, K. Krishnan, M. Megharaj, Anaerobic Microbial Degradation of Polycyclic Aromatic Hydrocarbons: A Comprehensive Review, in: Rev. Environ. Contam. Toxicol., Springer New York LLC, 2019: pp. 25–108. https://doi.org/10.1007/398_2019_29.

[5] D. Cossa, S.W. Fowler, C. Migon, L. Heimbürger-Boavida, A. Dufour, A Biogeochemical Approach to Contamination of the Ligurian Sea, in: Mediterr. Sea Era Glob. Chang. 2, Wiley, 2020: pp. 175–205. https://doi.org/10.1002/9781119704782.ch6.

[6] A. Ranjbar Jafarabadi, A. Riyahi Bakhtiari, L. Hedouin, A. Shadmehri Toosi, T. Cappello, Spatio-temporal variability, distribution and sources of n-alkanes and polycyclic aromatic hydrocarbons in reef surface sediments of Kharg and Lark coral reefs, Persian Gulf, Iran, Ecotoxicol. Environ. Saf. (2018). https://doi.org/10.1016/j.ecoenv.2018.07.056.

[7] A. Ukalska-Jaruga, B. Smreczak, The Impact of Organic Matter on Polycyclic Aromatic Hydrocarbon (PAH) Availability and Persistence in Soils, Molecules. 25 (2020) 2470. https://doi.org/10.3390/molecules25112470.

[8] C. Ribeiro, A.R. Ribeiro, M.E. Tiritan, Occurrence of persistent organic pollutants in sediments and biota from Portugal versus European incidence: A critical overview, J. Environ. Sci. Heal. Part B. 51 (2016) 143–153. https://doi.org/10.1080/03601234.2015.1108793.

[9] M. Zhang, S. Tao, X. Wang, Interactions between organic pollutants and carbon nanomaterials and the associated impact on microbial availability and degradation in soil: a review, Environ. Sci. Nano. 7 (2020) 2486–2508. https://doi.org/10.1039/D0EN00515K.

[10] S.W. Chiu, K.M. Ho, S.S. Chan, O.M. So, K.H. Lai, Characterization of

contamination in and toxicities of a shipyard area in Hong Kong, Environ. Pollut. 142 (2006) 512–520. https://doi.org/10.1016/j.envpol.2005.10.038.
[11] M. Sprovieri, M.L. Feo, L. Prevedello, D.S. Manta, S. Sammartino, S. Tamburrino, E. Marsella, Heavy metals, polycyclic aromatic hydrocarbons and polychlorinated biphenyls in surface sediments of the Naples harbour (southern Italy), Chemosphere. (2007). https://doi.org/10.1016/j.chemosphere.2006.10.055.
[12] T. Sayara, A. Sánchez, Bioremediation of PAH-Contaminated Soils: Process Enhancement through Composting/Compost, Appl. Sci. 10 (2020) 3684. https://doi.org/10.3390/app10113684.
[13] H.I. Gomes, C. Dias-Ferreira, A.B. Ribeiro, Overview of in situ and ex situ remediation technologies for PCB-contaminated soils and sediments and obstacles for full-scale application, Sci. Total Environ. (2013). https://doi.org/10.1016/j.scitotenv.2012.11.098.
[14] A. Cébron, J. Cortet, S. Criquet, A. Biaz, V. Calvert, C. Caupert, C. Pernin, C. Leyval, Biological functioning of PAH-polluted and thermal desorption-treated soils assessed by fauna and microbial bioindicators, Res. Microbiol. 162 (2011) 896–907. https://doi.org/10.1016/j.resmic.2011.02.011.
[15] C.J. Pope, W.A. Peters, J.B. Howard, Thermodynamic driving forces for PAH isomerization and growth during thermal treatment of polluted soils, J. Hazard. Mater. (2000). https://doi.org/10.1016/S0304-3894(00)00267-3.
[16] K.J. Hidalgo, I.N. Sierra-Garcia, B.M. Dellagnezze, V.M. de Oliveira, Metagenomic Insights Into the Mechanisms for Biodegradation of Polycyclic Aromatic Hydrocarbons in the Oil Supply Chain, Front. Microbiol. (2020). https://doi.org/10.3389/fmicb.2020.561506.
[17] H. Louati, O. Ben Said, A. Soltani, P. Got, C. Cravo-Laureau, R. Duran, P. Aissa, O. Pringault, E. Mahmoudi, Biostimulation as an attractive technique to reduce phenanthrene toxicity for meiofauna and bacteria in lagoon sediment, Environ. Sci. Pollut. Res. (2014). https://doi.org/10.1007/s11356-013-2330-5.
[18] F. Dell'Anno, E. Rastelli, M. Tangherlini, C. Corinaldesi, C. Sansone, C. Brunet, S. Balzano, A. Ianora, L. Musco, M.R. Montereali, A. Dell'Anno, Highly Contaminated Marine Sediments Can Host Rare Bacterial Taxa Potentially Useful for Bioremediation, Front. Microbiol. 12 (2021) 326. https://doi.org/10.3389/fmicb.2021.584850.
[19] H.Z. Hamdan, D.A. Salam, Microbial community evolution during the aerobic biodegradation of petroleum hydrocarbons in marine sediment microcosms: Effect of biostimulation and seasonal variations, Environ. Pollut. 265 (2020) 114858. https://doi.org/10.1016/j.envpol.2020.114858.
[20] H. Zang, Y. Dai, Y. Sun, T. Jia, Q. Song, X. Li, X. Jiang, D. Sui, Z. Han, D. Li, N. Hou, Mechanism of the biodemulsifier-enhanced biodegradation of phenanthrene by Achromobacter sp. LH-1, Colloids Surfaces B Biointerfaces. (2020). https://doi.org/10.1016/j.colsurfb.2020.111253.
[21] A. Agarwal, Y. Liu, Remediation technologies for oil-contaminated sediments, Mar. Pollut. Bull. 101 (2015) 483–490. https://doi.org/10.1016/j.marpolbul.2015.09.010.
[22] Y.J. Shih, P.C. Wu, C.W. Chen, C.F. Chen, C. Di Dong, Nonionic and anionic

surfactant-washing of polycyclic aromatic hydrocarbons in estuarine sediments around an industrial harbor in southern Taiwan, Chemosphere. (2020). https://doi.org/10.1016/j.chemosphere.2020.127044.
[23] A.P. Khodadoust, R. Bagchi, M.T. Suidan, R.C. Brenner, N.G. Sellers, Removal of PAHs from highly contaminated soils found at prior manufactured gas operations, J. Hazard. Mater. 80 (2000) 159–174. https://doi.org/10.1016/S0304-3894(00)00286-7.
[24] B.A. Palvasha, M.S. Nazir, Z. Tahir, H.A. Hussein, A.A.A. Bahamid, M.A. Abdullah, Green solvents for soil and sediment remediation, in: Green Sustain. Process Chem. Environ. Eng. Sci., Elsevier, 2021: pp. 37–65. https://doi.org/https://doi.org/10.1016/B978-0-12-821884-6.00013-9.
[25] F. Gharibzadeh, R.R. Kalantary, A. Esrafili, M. Ravanipour, A. Azari, Desorption kinetics and isotherms of phenanthrene from contaminated soil, J. Environ. Heal. Sci. Eng. 17 (2019) 171–181. https://doi.org/10.1007/s40201-019-00338-1.
[26] W. Zhou, X. Wang, C. Chen, L. Zhu, Enhanced soil washing of phenanthrene by a plant-derived natural biosurfactant, Sapindus saponin, Colloids Surfaces A Physicochem. Eng. Asp. 425 (2013) 122–128. https://doi.org/10.1016/j.colsurfa.2013.02.055.
[27] F. Gharibzadeh, R. Rezaei Kalantary, S. Nasseri, A. Esrafili, A. Azari, Reuse of polycyclic aromatic hydrocarbons (PAHs) contaminated soil washing effluent by bioaugmentation/biostimulation process, Sep. Purif. Technol. 168 (2016) 248–256. https://doi.org/10.1016/j.seppur.2016.05.022.
[28] A. Kostrytsia, S. Papirio, M. Khodzhaev, L. Morrison, G. Collins, P.N.L. Lens, U.Z. Ijaz, G. Esposito, Biofilm carrier type affects biogenic sulfur-driven denitrification performance and microbial community dynamics in moving-bed biofilm reactors, Chemosphere. 287 (2022) 131975. https://doi.org/10.1016/j.chemosphere.2021.131975.
[29] A.H. Sayyahzadeh, H. Ganjidoust, B. Ayati, MBBR system performance improvement for petroleum hydrocarbon removal using modified media with activated carbon, Water Sci. Technol. 73 (2016) 2275–2283. https://doi.org/10.2166/wst.2016.013.
[30] S. Wu, H. He, X. Inthapanya, C. Yang, L. Lu, G. Zeng, Z. Han, Role of biochar on composting of organic wastes and remediation of contaminated soils—a review, Environ. Sci. Pollut. Res. (2017). https://doi.org/10.1007/s11356-017-9168-1.
[31] C. Anyika, Z. Abdul Majid, Z. Ibrahim, M.P. Zakaria, A. Yahya, The impact of biochars on sorption and biodegradation of polycyclic aromatic hydrocarbons in soils—a review, Environ. Sci. Pollut. Res. (2015). https://doi.org/10.1007/s11356-014-3719-5.
[32] J.L. Gomez-Eyles, U. Ghosh, Enhanced biochars can match activated carbon performance in sediments with high native bioavailability and low final porewater PCB concentrations, Chemosphere. (2018). https://doi.org/10.1016/j.chemosphere.2018.03.132.
[33] A.A. Akinpelu, M.E. Ali, M.R. Johan, R. Saidur, M.A. Qurban, T.A. Saleh, Polycyclic aromatic hydrocarbons extraction and removal from wastewater by

carbon nanotubes: A review of the current technologies, challenges and prospects, Process Saf. Environ. Prot. 122 (2019) 68–82. https://doi.org/10.1016/j.psep.2018.11.006.
[34] D. Caniani, M. Caivano, G. Mazzone, S. Masi, I.M. Mancini, Effect of site-specific conditions and operating parameters on the removal efficiency of petroleum-originating pollutants by using ozonation, Sci. Total Environ. 800 (2021) 149393. https://doi.org/10.1016/j.scitotenv.2021.149393.
[35] S. Gan, E. V. Lau, H.K. Ng, Remediation of soils contaminated with polycyclic aromatic hydrocarbons (PAHs), J. Hazard. Mater. (2009). https://doi.org/10.1016/j.jhazmat.2009.07.118.
[36] S. Srivastava, M. Kumar, Biodegradation of polycyclic aromatic hydrocarbons (PAHs): A sustainable approach, in: Sustain. Green Technol. Environ. Manag., Springer Singapore, 2019: pp. 111–139. https://doi.org/10.1007/978-981-13-2772-8_6.
[37] W. Wang, G. Liu, J. Shen, H. Chang, R. Li, J. Du, Z. Yang, Q. Xu, Reducing polycyclic aromatic hydrocarbons content in coal tar pitch by potassium permanganate oxidation and solvent extraction, J. Environ. Chem. Eng. 3 (2015) 1513–1521. https://doi.org/10.1016/j.jece.2015.05.024.
[38] J.F. Ontiveros-Cuadras, A.C. Ruiz-Fernández, J.A. Sanchez-Cabeza, J. Sericano, L.H. Pérez-Bernal, F. Páez-Osuna, R.B. Dunbar, D.A. Mucciarone, Recent history of persistent organic pollutants (PAHs, PCBs, PBDEs) in sediments from a large tropical lake, J. Hazard. Mater. 368 (2019) 264–273. https://doi.org/10.1016/j.jhazmat.2018.11.010.
[39] L. Wu, R. Sun, Y. Li, C. Sun, Sample preparation and analytical methods for polycyclic aromatic hydrocarbons in sediment, Trends Environ. Anal. Chem. (2019). https://doi.org/10.1016/j.teac.2019.e00074.
[40] A.K. Haritash, C.P. Kaushik, Biodegradation aspects of Polycyclic Aromatic Hydrocarbons (PAHs): A review, J. Hazard. Mater. (2009). https://doi.org/10.1016/j.jhazmat.2009.03.137.
[41] S. McCready, D.J. Slee, G.F. Birch, S.E. Taylor, The distribution of polycyclic aromatic hydrocarbons in surficial sediments of Sydney Harbour, Australia, Mar. Pollut. Bull. (2000). https://doi.org/10.1016/S0025-326X(00)00044-8.
[42] B.G. Whitehouse, The effects of temperature and salinity on the aqueous solubility of polynuclear aromatic hydrocarbons, Mar. Chem. 14 (1984) 319–332. https://doi.org/10.1016/0304-4203(84)90028-8.
[43] S. Amézqueta, X. Subirats, E. Fuguet, M. Roses, C. Rafols, Octanol-water partition constant, in: Liq. Extr., Elsevier, 2019: pp. 183–208. https://doi.org/10.1016/B978-0-12-816911-7.00006-2.
[44] G.N. Lu, X.Q. Tao, Z. Dang, X.Y. Yi, C. Yang, Estimation of n-octanol/water partition coefficients of polycyclic aromatic hydrocarbons by quantum chemical descriptors, Cent. Eur. J. Chem. 6 (2008) 310–318. https://doi.org/10.2478/s11532-008-0010-y.
[45] D. Mackay, D. Callcott, Partitioning and Physical Chemical Properties of PAHs, in: Handb. Environ. Chem., Springer, Berlin, Heidelberg, 1998: pp. 325–345. https://doi.org/10.1007/978-3-540-49697-7_8.
[46] S.K. Sahu, G.G. Pandit, Estimation of octanol-water partition coefficients for

polycylic aromatic hydrocarbons using reverse-phase HPLC, J. Liq. Chromatogr. Relat. Technol. 26 (2003) 135–146. https://doi.org/10.1081/JLC-120017158.
[47] S. Zhang, H. Yao, Y. Lu, X. Yu, J. Wang, S. Sun, M. Liu, D. Li, Y.F. Li, D. Zhang, Uptake and translocation of polycyclic aromatic hydrocarbons (PAHs) and heavy metals by maize from soil irrigated with wastewater, Sci. Rep. 7 (2017) 1–11. https://doi.org/10.1038/s41598-017-12437-w.
[48] S.P. Maletić, J.M. Beljin, S.D. Rončević, M.G. Grgić, B.D. Dalmacija, State of the art and future challenges for polycyclic aromatic hydrocarbons is sediments: sources, fate, bioavailability and remediation techniques, J. Hazard. Mater. (2019). https://doi.org/10.1016/j.jhazmat.2018.11.020.
[49] E. Frapiccini, M. Panfili, S. Guicciardi, A. Santojanni, M. Marini, C. Truzzi, A. Annibaldi, Effects of biological factors and seasonality on the level of polycyclic aromatic hydrocarbons in red mullet (Mullus barbatus), Environ. Pollut. 258 (2020) 113742. https://doi.org/10.1016/j.envpol.2019.113742.
[50] A. Bartonitz, I.N. Anyanwu, J. Geist, H.K. Imhof, J. Reichel, J. Graßmann, J.E. Drewes, S. Beggel, Modulation of PAH toxicity on the freshwater organism G. roeseli by microparticles, Environ. Pollut. 260 (2020) 113999. https://doi.org/10.1016/j.envpol.2020.113999.
[51] Z.M. Karaczun, G. Obidoska, B. Żarska, Phytotoxicity and phytogenotoxicity of soil and air in the vicinity of a petrochemical plant in Płock (Poland), (n.d.). https://doi.org/10.1007/s11356-020-08788-z.
[52] H. Habe, T. Omori, Genetics of polycyclic aromatic hydrocarbon metabolism in diverse aerobic bacteria, Biosci. Biotechnol. Biochem. 67 (2003) 225–243. https://doi.org/10.1271/bbb.67.225.
[53] H.I. Abdel-Shafy, M.S.M. Mansour, A review on polycyclic aromatic hydrocarbons: Source, environmental impact, effect on human health and remediation, Egypt. J. Pet. (2016). https://doi.org/10.1016/j.ejpe.2015.03.011.
[54] T. Mihankhah, M. Saeedi, A. Karbassi, Contamination and cancer risk assessment of polycyclic aromatic hydrocarbons (PAHs) in urban dust from different land-uses in the most populated city of Iran, Ecotoxicol. Environ. Saf. 187 (2020) 109838. https://doi.org/10.1016/j.ecoenv.2019.109838.
[55] F.P. Serpe, M. Esposito, P. Gallo, L. Serpe, Optimisation and validation of an HPLC method for determination of polycyclic aromatic hydrocarbons (PAHs) in mussels, Food Chem. 122 (2010) 920–925. https://doi.org/10.1016/j.foodchem.2010.03.062.
[56] C.J. Smith, T.A. Perfetti, M.A. Rumple, A. Rodgman, D.J. Doolittle, “IARC Group 2A Carcinogens” reported in cigarette mainstream smoke, Food Chem. Toxicol. 38 (2000) 371–383. https://doi.org/10.1016/S0278-6915(99)00156-8.
[57] C.. Smith, T.. Perfetti, M.. Rumple, A. Rodgman, D.. Doolittle, “IARC Group 2B carcinogens” reported in cigarette mainstream smoke, Food Chem. Toxicol. 39 (2001) 183–205. https://doi.org/10.1016/S0278-6915(00)00164-2.
[58] R.M. Dickhut, E.A. Canuel, K.E. Gustafson, K. Liu, K.M. Arzayus, S.E. Walker, G. Edgecombe, M.O. Gaylor, E.H. MacDonald, Automotive Sources of Carcinogenic Polycyclic Aromatic Hydrocarbons Associated with Particulate Matter in the Chesapeake Bay Region, Environ. Sci. Technol. 34 (2000) 4635–

4640. https://doi.org/10.1021/es000971e.
[59] K. Straif, R. Baan, Y. Grosse, B. Secretan, F. El Ghissassi, V. Cogliano, D. Drewski, T. Partanen, K. Vähäkangas, I. Stücker, J. Borlak, V.J. Feron, M.M. Marques, P. Gustavsson, T. Fletcher, J. Arey, F.A. Beland, S. Burchiel, L. Flowers, R.A. Herbert, H. Mukhtar, S. Nesnow, T.M. Penning, R. Sinha, T. Shimada, Carcinogenicity of polycyclic aromatic hydrocarbons, Lancet Oncol. 6 (2005) 931–932. https://doi.org/10.1016/S1470-2045(05)70458-7.
[60] R.L. Santarelli, F. Pierre, D.E. Corpet, Processed meat and colorectal cancer: A review of epidemiologic and experimental evidence, Nutr. Cancer. 60 (2008) 131–144. https://doi.org/10.1080/01635580701684872.
[61] R. Goldman, L. Enewold, E. Pellizzari, J.B. Beach, E.D. Bowman, S.S. Krishnan, P.G. Shields, Smoking increases carcinogenic polycyclic aromatic hydrocarbons in human lung tissue, Cancer Res. 61 (2001) 6367–6371.
[62] L.Y. Li, J.R. Grace, Effect of Co-existing Heavy Metals and Natural Organic Matter on Sorption/Desorption of Polycyclic Aromatic Hydrocarbons in Soil: A Review, Pollution. 6 (2020) 1–24. https://doi.org/10.22059/poll.2019.284335.638.
[63] J. Edokpayi, J. Odiyo, O. Popoola, T. Msagati, Determination and Distribution of Polycyclic Aromatic Hydrocarbons in Rivers, Sediments and Wastewater Effluents in Vhembe District, South Africa, Int. J. Environ. Res. Public Health. 13 (2016) 387. https://doi.org/10.3390/ijerph13040387.
[64] R. Scott Obach, A.S. Kalgutkar, Reactive Electrophiles and Metabolic Activation, in: Compr. Toxicol. Second Ed., Elsevier Inc., 2010: pp. 309–347. https://doi.org/10.1016/B978-0-08-046884-6.00115-9.
[65] K. Hussain, R.R. Hoque, S. Balachandran, S. Medhi, M.G. Idris, M. Rahman, F.L. Hussain, Monitoring and Risk Analysis of PAHs in the Environment, in: Handb. Environ. Mater. Manag., Springer International Publishing, 2018: pp. 1–35. https://doi.org/10.1007/978-3-319-58538-3_29-2.
[66] J. Du, W.T. Mehler, M.J. Lydy, J. You, Toxicity of sediment-associated unresolved complex mixture and its impact on bioavailability of polycyclic aromatic hydrocarbons, J. Hazard. Mater. (2012). https://doi.org/10.1016/j.jhazmat.2011.11.099.
[67] L. Ferrara, M. Trifuoggi, M. Toscanesi, C. Donadio, D. Barra, G. Aiello, M. Arienzo, Source identification and eco-risk assessment of polycyclic aromatic hydrocarbons in the sediments of seawaters facing the former steel plant ILVA, Naples, Italy, Reg. Stud. Mar. Sci. 35 (2020) 101097. https://doi.org/10.1016/j.rsma.2020.101097.
[68] K. Ravindra, R. Sokhi, R. Van Grieken, Atmospheric polycyclic aromatic hydrocarbons: Source attribution, emission factors and regulation, Atmos. Environ. 42 (2008) 2895–2921. https://doi.org/10.1016/j.atmosenv.2007.12.010.
[69] S. Manzetti, Polycyclic Aromatic Hydrocarbons in the Environment: Environmental Fate and Transformation, Polycycl. Aromat. Compd. 33 (2013) 311–330. https://doi.org/10.1080/10406638.2013.781042.
[70] M. Sakizadeh, Spatial distribution and source identification together with environmental health risk assessment of PAHs along the coastal zones of the

USA, Environ. Geochem. Health. (2020). https://doi.org/10.1007/s10653-020-00578-3.
[71] M.B. Yunker, R.W. Macdonald, R. Vingarzan, R.H. Mitchell, D. Goyette, S. Sylvestre, PAHs in the Fraser River basin: A critical appraisal of PAH ratios as indicators of PAH source and composition, Org. Geochem. 33 (2002) 489–515. https://doi.org/10.1016/S0146-6380(02)00002-5.
[72] M. Tobiszewski, J. Namieśnik, PAH diagnostic ratios for the identification of pollution emission sources, Environ. Pollut. 162 (2012) 110–119. https://doi.org/10.1016/j.envpol.2011.10.025.
[73] M. Saha, A. Togo, K. Mizukawa, M. Murakami, H. Takada, M.P. Zakaria, N.H. Chiem, B.C. Tuyen, M. Prudente, R. Boonyatumanond, S.K. Sarkar, B. Bhattacharya, P. Mishra, T.S. Tana, Sources of sedimentary PAHs in tropical Asian waters: Differentiation between pyrogenic and petrogenic sources by alkyl homolog abundance, Mar. Pollut. Bull. 58 (2009) 189–200. https://doi.org/10.1016/j.marpolbul.2008.04.049.
[74] M. Der Fang, C.L. Lee, C.S. Yu, Distribution and source recognition of polycyclic aromatic hydrocarbons in the sediments of Hsin-ta Harbour and adjacent coastal areas, Taiwan, Mar. Pollut. Bull. 46 (2003) 941–953. https://doi.org/10.1016/S0025-326X(03)00099-7.
[75] E. Magi, R. Bianco, C. Ianni, M. Di Carro, Distribution of polycyclic aromatic hydrocarbons in the sediments of the Adriatic Sea, Environ. Pollut. 119 (2002) 91–98. https://doi.org/10.1016/S0269-7491(01)00321-9.
[76] S. Kuppusamy, P. Thavamani, K. Venkateswarlu, Y.B. Lee, R. Naidu, M. Megharaj, Remediation approaches for polycyclic aromatic hydrocarbons (PAHs) contaminated soils: Technological constraints, emerging trends and future directions, Chemosphere. (2017). https://doi.org/10.1016/j.chemosphere.2016.10.115.
[77] A. Schwardt, A. Dahmke, R. Köber, Henry's law constants of volatile organic compounds between 0 and 95 °C – Data compilation and complementation in context of urban temperature increases of the subsurface, Chemosphere. 272 (2021) 129858. https://doi.org/10.1016/j.chemosphere.2021.129858.
[78] O.O. Alegbeleye, B.O. Opeolu, V.A. Jackson, Polycyclic Aromatic Hydrocarbons: A Critical Review of Environmental Occurrence and Bioremediation, Environ. Manage. 60 (2017) 758–783. https://doi.org/10.1007/s00267-017-0896-2.
[79] W.L. Daniels, Remediation of PAH-Contaminated Soils and Sediments : A Literature Review Remediation of PAH-Contaminated Soils and Sediments : A Literature Review, (2020) 1–102.
[80] M.S. El-Shahawi, A. Hamza, A.S. Bashammakh, W.T. Al-Saggaf, An overview on the accumulation, distribution, transformations, toxicity and analytical methods for the monitoring of persistent organic pollutants, Talanta. (2010). https://doi.org/10.1016/j.talanta.2009.09.055.
[81] B. Chen, X. Xuan, L. Zhu, J. Wang, Y. Gao, K. Yang, X. Shen, B. Lou, Distributions of polycyclic aromatic hydrocarbons in surface waters, sediments and soils of Hangzhou City, China, Water Res. 38 (2004) 3558–3568. https://doi.org/10.1016/j.watres.2004.05.013.

[82] Y. Zeng, P.K.A. Hong, Slurry-phase ozonation for remediation of sediments contaminated by polycyclic aromatic hydrocarbons, J. Air Waste Manag. Assoc. 52 (2002) 58–68. https://doi.org/10.1080/10473289.2002.10470751.
[83] D. Merhaby, S. Rabodonirina, S. Net, B. Ouddane, J. Halwani, Overview of sediments pollution by PAHs and PCBs in mediterranean basin: Transport, fate, occurrence, and distribution, Mar. Pollut. Bull. (2019). https://doi.org/10.1016/j.marpolbul.2019.110646.
[84] B. Chen, J. Ding, Biosorption and biodegradation of phenanthrene and pyrene in sterilized and unsterilized soil slurry systems stimulated by Phanerochaete chrysosporium, J. Hazard. Mater. (2012). https://doi.org/10.1016/j.jhazmat.2012.05.090.
[85] L.J. Ehlers, R.G. Luthy, Peer Reviewed: Contaminant Bioavailability in Soil and Sediment, Environ. Sci. Technol. (2003). https://doi.org/10.1021/es032524f.
[86] M.J. Riding, K.J. Doick, F.L. Martin, K.C. Jones, K.T. Semple, Chemical measures of bioavailability/bioaccessibility of PAHs in soil: Fundamentals to application, J. Hazard. Mater. 261 (2013) 687–700. https://doi.org/10.1016/j.jhazmat.2013.03.033.
[87] K.T. Semple, A.W.J. Morriss, G.I. Paton, Bioavailability of hydrophobic organic contaminants in soils: Fundamental concepts and techniques for analysis, Eur. J. Soil Sci. 54 (2003) 809–818. https://doi.org/10.1046/j.1351-0754.2003.0564.x.
[88] M. Megharaj, B. Ramakrishnan, K. Venkateswarlu, N. Sethunathan, R. Naidu, Bioremediation approaches for organic pollutants: A critical perspective, Environ. Int. (2011). https://doi.org/10.1016/j.envint.2011.06.003.
[89] S. Ahn, D. Werner, H.K. Karapanagioti, D.R. McGlothlin, R.N. Zare, R.G. Luthy, Phenanthrene and pyrene sorption and intraparticle diffusion in polyoxymethylene, coke, and activated carbon, Environ. Sci. Technol. (2005). https://doi.org/10.1021/es050113o.
[90] J.M. Neff, S.A. Stout, D.G. Gunster, Ecological risk assessment of polycyclic aromatic hydrocarbons in sediments: identifying sources and ecological hazard., Integr. Environ. Assess. Manag. (2005). https://doi.org/10.1897/IEAM_2004a-016.1.
[91] X. Ren, G. Zeng, L. Tang, J. Wang, J. Wan, Y. Liu, J. Yu, H. Yi, S. Ye, R. Deng, Sorption, transport and biodegradation – An insight into bioavailability of persistent organic pollutants in soil, Sci. Total Environ. (2018). https://doi.org/10.1016/j.scitotenv.2017.08.089.
[92] G.A.C. Ehlers, A.P. Loibner, Linking organic pollutant (bio)availability with geosorbent properties and biomimetic methodology: A review of geosorbent characterisation and (bio)availability prediction, Environ. Pollut. 141 (2006) 494–512. https://doi.org/10.1016/j.envpol.2005.08.063.
[93] S.F. Hosseini, L. Ramezanzade, D.J. McClements, Recent advances in nanoencapsulation of hydrophobic marine bioactives: Bioavailability, safety, and sensory attributes of nano-fortified functional foods, Trends Food Sci. Technol. 109 (2021) 322–339. https://doi.org/10.1016/j.tifs.2021.01.045.
[94] A. Delle Site, Factors Affecting Sorption of Organic Compounds in Natural

Sorbent/Water Systems and Sorption Coefficients for Selected Pollutants. A Review, J. Phys. Chem. Ref. Data. 30 (2001) 187–439. https://doi.org/10.1063/1.1347984.
[95] Y. Yang, L. Shu, X. Wang, B. Xing, S. Tao, Mechanisms regulating bioavailability of phenanthrene sorbed on a peat soil-origin humic substance, Environ. Toxicol. Chem. (2012). https://doi.org/10.1002/etc.1844.
[96] A.R. Johnsen, L.Y. Wick, H. Harms, Principles of microbial PAH-degradation in soil, Environ. Pollut. (2005). https://doi.org/10.1016/j.envpol.2004.04.015.
[97] G.L. Northcott, K.C. Jones, Experimental approaches and analytical techniques for determining organic compound bound residues in soil and sediment., Environ. Pollut. (2000). https://doi.org/10.1016/S0269-7491(99)00199-2.
[98] V. Vasudevan, K.V. Gayathri, M.E.G. Krishnan, Bioremediation of a pentacyclic PAH, Dibenz(a,h)Anthracene- A long road to trip with bacteria, fungi, autotrophic eukaryotes and surprises, Chemosphere. 202 (2018) 387–399. https://doi.org/10.1016/j.chemosphere.2018.03.074.
[99] E. Ferrarese, G. Andreottola, I.A. Oprea, Remediation of PAH-contaminated sediments by chemical oxidation, J. Hazard. Mater. (2008). https://doi.org/10.1016/j.jhazmat.2007.06.080.
[100] J.E. Vidonish, K. Zygourakis, C.A. Masiello, G. Sabadell, P.J.J. Alvarez, Thermal Treatment of Hydrocarbon-Impacted Soils: A Review of Technology Innovation for Sustainable Remediation, Engineering. (2016). https://doi.org/10.1016/J.ENG.2016.04.005.
[101] Y. Sun, W.K. Niu, X.J. Hu, X.H. Ma, Y.J. Sun, Y. Wen, Oxidative degradation of polycyclic aromatic hydrocarbons in contaminated industrial soil using chlorine dioxide, Chem. Eng. J. 394 (2020) 124857. https://doi.org/10.1016/j.cej.2020.124857.
[102] B. Lukić, A. Panico, D. Huguenot, M. Fabbricino, E.D. van Hullebusch, G. Esposito, A review on the efficiency of landfarming integrated with composting as a soil remediation treatment, Environ. Technol. Rev. 6 (2017) 94–116. https://doi.org/10.1080/21622515.2017.1310310.
[103] A.T. Lawal, Polycyclic aromatic hydrocarbons. A review, 3 (2017) 1339841. https://doi.org/10.1080/23311843.2017.1339841.
[104] E. Von Lau, S. Gan, H.K. Ng, P.E. Poh, Extraction agents for the removal of polycyclic aromatic hydrocarbons (PAHs) from soil in soil washing technologies, Environ. Pollut. 184 (2014) 640–649. https://doi.org/10.1016/j.envpol.2013.09.010.
[105] N. Haleyur, E. Shahsavari, S.S. Jain, E. Koshlaf, V.B. Ravindran, P.D. Morrison, A.M. Osborn, A.S. Ball, Influence of bioaugmentation and biostimulation on PAH degradation in aged contaminated soils: Response and dynamics of the bacterial community, J. Environ. Manage. (2019). https://doi.org/10.1016/j.jenvman.2019.02.115.
[106] A.K. Pal, J. Singh, R. Soni, P. Tripathi, M. Kamle, V. Tripathi, P. Kumar, The role of microorganism in bioremediation for sustainable environment management, in: Bioremediation Pollut., Elsevier, 2020: pp. 227–249. https://doi.org/10.1016/B978-0-12-819025-8.00010-7.
[107] T.J. McGenity, B.D. Folwell, B.A. McKew, G.O. Sanni, Marine crude-oil

biodegradation: a central role for interspecies interactions, Aquat. Biosyst. 8 (2012) 10. https://doi.org/10.1186/2046-9063-8-10.
[108] R. Simarro, N. Gonzá Lez, L. Fernando Bautista, M.C. Molina, Biodegradation of high-molecular-weight polycyclic aromatic hydrocarbons by a wood-degrading consortium at low temperatures, (n.d.). https://doi.org/10.1111/1574-6941.12006.
[109] L. Lei, A.P. Khodadoust, M.T. Suidan, H.H. Tabak, Biodegradation of sediment-bound PAHs in field-contaminated sediment, Water Res. 39 (2005) 349–361. https://doi.org/10.1016/j.watres.2004.09.021.
[110] B. Wartell, M. Boufadel, L. Rodriguez-Freire, An effort to understand and improve the anaerobic biodegradation of petroleum hydrocarbons: A literature review, Int. Biodeterior. Biodegradation. 157 (2021) 105156. https://doi.org/10.1016/j.ibiod.2020.105156.
[111] T. Zhang, S.M. Gannon, K.P. Nevin, A.E. Franks, D.R. Lovley, Stimulating the anaerobic degradation of aromatic hydrocarbons in contaminated sediments by providing an electrode as the electron acceptor, Environ. Microbiol. 12 (2010) 1011–1020. https://doi.org/10.1111/j.1462-2920.2009.02145.x.
[112] L.W. Perelo, Review: In situ and bioremediation of organic pollutants in aquatic sediments, J. Hazard. Mater. (2010). https://doi.org/10.1016/j.jhazmat.2009.12.090.
[113] N. Parmar, A. Singh, H. Khan, Bioremediation of Contaminated Sites and Aquifers, in: Geomicrobiol. Biogeochem., Springer, Berlin, Heidelberg, 2014: pp. 261–296. https://doi.org/10.1007/978-3-642-41837-2_14.
[114] J.S. Seo, Y.S. Keum, Q.X. Li, Bacterial degradation of aromatic compounds, Int. J. Environ. Res. Public Health. 6 (2009) 278–309. https://doi.org/10.3390/ijerph6010278.
[115] J. Pérez-García, J. Bacame-Valenzuela, D.M. Sánchez López, J. de Jesús Gómez-Guzmán, M.L. Jiménez González, L. Ortiz-Frade, Y. Reyes-Vidal, Membrane proteins mediated microbial-electrochemical remediation technology, in: Dev. Wastewater Treat. Res. Process., Elsevier, 2022: pp. 265–285. https://doi.org/10.1016/B978-0-323-85657-7.00014-6.
[116] R. Ullrich, M. Hofrichter, Enzymatic hydroxylation of aromatic compounds, Cell. Mol. Life Sci. 64 (2007) 271–293. https://doi.org/10.1007/s00018-007-6362-1.
[117] C.E. Cerniglia, Biodegradation of polycyclic aromatic hydrocarbons, Biodegradation. 3 (1992) 351–368. https://doi.org/10.1007/BF00129093.
[118] S. Mallick, J. Chakraborty, T.K. Dutta, Role of oxygenases in guiding diverse metabolic pathways in the bacterial degradation of low-molecular-weight polycyclic aromatic hydrocarbons: A review, Crit. Rev. Microbiol. 37 (2011) 64–90. https://doi.org/10.3109/1040841X.2010.512268.
[119] M.G. Waigi, F. Kang, C. Goikavi, W. Ling, Y. Gao, Phenanthrene biodegradation by sphingomonads and its application in the contaminated soils and sediments: A review, Int. Biodeterior. Biodegrad. (2015). https://doi.org/10.1016/j.ibiod.2015.06.008.
[120] J.C. Shon, Y.J. Noh, Y.S. Kwon, J.H. Kim, Z. Wu, J.S. Seo, The impact of phenanthrene on membrane phospholipids and its biodegradation by

Sphingopyxis soli, Ecotoxicol. Environ. Saf. (2020). https://doi.org/10.1016/j.ecoenv.2020.110254.
[121] X. Han, H. Hu, X. Shi, L. Zhang, J. He, Effects of different agricultural wastes on the dissipation of PAHs and the PAH-degrading genes in a PAH-contaminated soil, Chemosphere. 172 (2017) 286–293. https://doi.org/10.1016/j.chemosphere.2017.01.012.
[122] B. Antizar-Ladislao, J. Lopez-Real, A.J. Beck, In-vessel composting-bioremediation of aged coal tar soil: Effect of temperature and soil/green waste amendment ratio, in: Environ. Int., Elsevier Ltd, 2005: pp. 173–178. https://doi.org/10.1016/j.envint.2004.09.012.
[123] R.J.S. Jacques, B.C. Okeke, F.M. Bento, M.C.R. Peralba, F.A.O. Camargo, Characterization of a polycyclic aromatic hydrocarbon-degrading microbial consortium from a petrochemical sludge landfarming site, Bioremediat. J. 11 (2007) 1–11. https://doi.org/10.1080/10889860601185822.
[124] H.I. Atagana, Bioremediation of creosote-contaminated soil in South Africa by landfarming, J. Appl. Microbiol. 96 (2004) 510–520. https://doi.org/10.1111/j.1365-2672.2003.02168.x.
[125] B. Lukić, D. Huguenot, A. Panico, E.D. van Hullebusch, G. Esposito, Influence of activated sewage sludge amendment on PAH removal efficiency from a naturally contaminated soil: application of the landfarming treatment, Environ. Technol. (United Kingdom). 38 (2017) 2988–2998. https://doi.org/10.1080/09593330.2017.1284903.
[126] K.S.H. Yu, A.H.Y. Wong, K.W.Y. Yau, Y.S. Wong, N.F.Y. Tam, Natural attenuation, biostimulation and bioaugmentation on biodegradation of polycyclic aromatic hydrocarbons (PAHs) in mangrove sediments, in: Mar. Pollut. Bull., 2005. https://doi.org/10.1016/j.marpolbul.2005.06.006.
[127] D.R. Singleton, S.D. Richardson, M.D. Aitken, Pyrosequence analysis of bacterial communities in aerobic bioreactors treating polycyclic aromatic hydrocarbon-contaminated soil, Biodegradation. 22 (2011) 1061–1073. https://doi.org/10.1007/s10532-011-9463-3.
[128] V. Kumar, S.K. Shahi, S. Singh, Bioremediation: An Eco-sustainable Approach for Restoration of Contaminated Sites, in: Microb. Bioprospecting Sustain. Dev., Springer Singapore, Singapore, 2018: pp. 115–136. https://doi.org/10.1007/978-981-13-0053-0_6.
[129] M. Herrero, D.C. Stuckey, Bioaugmentation and its application in wastewater treatment: A review, Chemosphere. 140 (2015) 119–128. https://doi.org/10.1016/j.chemosphere.2014.10.033.
[130] Ł. Ławniczak, M. Woźniak-Karczewska, A.P. Loibner, H.J. Heipieper, Ł. Chrzanowski, Microbial Degradation of Hydrocarbons—Basic Principles for Bioremediation: A Review, Molecules. 25 (2020) 856. https://doi.org/10.3390/molecules25040856.
[131] M. Wu, J. Wu, X. Zhang, X. Ye, Effect of bioaugmentation and biostimulation on hydrocarbon degradation and microbial community composition in petroleum-contaminated loessal soil, Chemosphere. 237 (2019) 124456. https://doi.org/10.1016/j.chemosphere.2019.124456.
[132] H. Ma, Y. Zhao, K. Yang, Y. Wang, C. Zhang, M. Ji, Application oriented

bioaugmentation processes: Mechanism, performance improvement and scale-up, Bioresour. Technol. 344 (2022) 126192. https://doi.org/10.1016/j.biortech.2021.126192.
[133] M.F. Ortega, D.E. Guerrero, M.J. García-Martínez, D. Bolonio, J.F. Llamas, L. Canoira, J.L.R. Gallego, Optimization of Landfarming Amendments Based on Soil Texture and Crude Oil Concentration, Water. Air. Soil Pollut. 229 (2018) 234. https://doi.org/10.1007/s11270-018-3891-1.
[134] M. Tyagi, M.M.R. da Fonseca, C.C.C.R. de Carvalho, Bioaugmentation and biostimulation strategies to improve the effectiveness of bioremediation processes, Biodegradation. 22 (2011) 231–241. https://doi.org/10.1007/s10532-010-9394-4.
[135] T. Sayara, E. Borràs, G. Caminal, M. Sarrà, A. Sánchez, Bioremediation of PAHs-contaminated soil through composting: Influence of bioaugmentation and biostimulation on contaminant biodegradation, Int. Biodeterior. Biodegrad. (2011). https://doi.org/10.1016/j.ibiod.2011.05.006.
[136] F.A. Bezza, E.M. Nkhalambayausi Chirwa, Biosurfactant-enhanced bioremediation of aged polycyclic aromatic hydrocarbons (PAHs) in creosote contaminated soil, Chemosphere. 144 (2016) 635–644. https://doi.org/10.1016/j.chemosphere.2015.08.027.
[137] D.W. Lee, H. Lee, B.O. Kwon, J.S. Khim, U.H. Yim, B.S. Kim, J.J. Kim, Biosurfactant-assisted bioremediation of crude oil by indigenous bacteria isolated from Taean beach sediment, Environ. Pollut. 241 (2018) 254–264. https://doi.org/10.1016/j.envpol.2018.05.070.
[138] V.K. Gaur, S. Gupta, A. Pandey, Evolution in mitigation approaches for petroleum oil-polluted environment: recent advances and future directions, Environ. Sci. Pollut. Res. (2021) 1–17. https://doi.org/10.1007/s11356-021-16047-y.
[139] C.-H.H. Li, Y.-S.S. Wong, N.F.-Y.Y. Tam, Anaerobic biodegradation of polycyclic aromatic hydrocarbons with amendment of iron(III) in mangrove sediment slurry, Bioresour. Technol. 101 (2010) 8083–8092. https://doi.org/10.1016/j.biortech.2010.06.005.
[140] A. Nzila, Biodegradation of high-molecular-weight polycyclic aromatic hydrocarbons under anaerobic conditions: Overview of studies, proposed pathways and future perspectives, Environ. Pollut. 239 (2018) 788–802. https://doi.org/10.1016/j.envpol.2018.04.074.
[141] X. Zhang, T. Yu, X. Li, J. Yao, W. Liu, S. Chang, Y. Chen, The fate and enhanced removal of polycyclic aromatic hydrocarbons in wastewater and sludge treatment system: A review, Crit. Rev. Environ. Sci. Technol. 49 (2019) 1425–1475. https://doi.org/10.1080/10643389.2019.1579619.
[142] A. Sikora, A. Detman, A. Chojnacka, M.K. Blaszczyk, Anaerobic Digestion: I. A Common Process Ensuring Energy Flow and the Circulation of Matter in Ecosystems. II. A Tool for the Production of Gaseous Biofuels, in: Ferment. Process., InTech, 2017. https://doi.org/10.5772/64645.
[143] R.K. Thauer, K. Jungermann, K. Decker, Energy conservation in chemotrophic anaerobic bacteria, Bacteriol. Rev. 41 (1977) 100–180. https://doi.org/10.1128/br.41.1.100-180.1977.

[144] R. Ambrosoli, L. Petruzzelli, J.L. Minati, F.A. Marsan, Anaerobic PAH degradation in soil by a mixed bacterial consortium under denitrifying conditions, Chemosphere. (2005). https://doi.org/10.1016/j.chemosphere.2005.02.030.
[145] C.H. Li, C. Ye, Y.S. Wong, N.F.Y. Tam, Effect of Mn(IV) on the biodegradation of polycyclic aromatic hydrocarbons under low-oxygen condition in mangrove sediment slurry, J. Hazard. Mater. 190 (2011) 786–793. https://doi.org/10.1016/j.jhazmat.2011.03.121.
[146] Z. Zhang, I.M.C. Lo, Biostimulation of petroleum-hydrocarbon-contaminated marine sediment with co-substrate: involved metabolic process and microbial community, Appl. Microbiol. Biotechnol. (2015). https://doi.org/10.1007/s00253-015-6420-9.
[147] J. Dou, X. Liu, A. Ding, Anaerobic degradation of naphthalene by the mixed bacteria under nitrate reducing conditions, J. Hazard. Mater. 165 (2009) 325–331. https://doi.org/10.1016/j.jhazmat.2008.10.002.
[148] K.J. Rockne, S.E. Strand, Anaerobic biodegradation of naphthalene, phenanthrene, and biphenyl by a denitrifying enrichment culture, Water Res. (2001). https://doi.org/10.1016/S0043-1354(00)00246-3.
[149] W. Qin, Y. Zhu, F. Fan, Y. Wang, X. Liu, A. Ding, J. Dou, Biodegradation of benzo(a)pyrene by Microbacterium sp. strain under denitrification: Degradation pathway and effects of limiting electron acceptors or carbon source, Biochem. Eng. J. 121 (2017) 131–138. https://doi.org/10.1016/j.bej.2017.02.001.
[150] J.-C. Tsai, M. Kumar, J.-G. Lin, Anaerobic biotransformation of fluorene and phenanthrene by sulfate-reducing bacteria and identification of biotransformation pathway, J. Hazard. Mater. 164 (2009) 847–855. https://doi.org/10.1016/j.jhazmat.2008.08.101.
[151] A. Ferraro, G. Massini, V.M. Miritana, A. Panico, L. Pontoni, M. Race, S. Rosa, A. Signorini, M. Fabbricino, F. Pirozzi, Bioaugmentation strategy to enhance polycyclic aromatic hydrocarbons anaerobic biodegradation in contaminated soils, Chemosphere. 275 (2021) 130091. https://doi.org/10.1016/j.chemosphere.2021.130091.
[152] W. Chang, Y. Um, T.R.P. Holoman, Polycyclic aromatic hydrocarbon (PAH) degradation coupled to methanogenesis, Biotechnol. Lett. (2006). https://doi.org/10.1007/s10529-005-6073-3.
[153] J.C. Solarte-Toro, Y. Chacón-Pérez, C.A. Cardona-Alzate, Evaluation of biogas and syngas as energy vectors for heat and power generation using lignocellulosic biomass as raw material, Electron. J. Biotechnol. 33 (2018) 52–62. https://doi.org/10.1016/j.ejbt.2018.03.005.
[154] A. Anukam, A. Mohammadi, M. Naqvi, K. Granström, A Review of the Chemistry of Anaerobic Digestion: Methods of Accelerating and Optimizing Process Efficiency, Processes. (2019). https://doi.org/10.3390/pr7080504.
[155] A. Nzila, Mini review: Update on bioaugmentation in anaerobic processes for biogas production, Anaerobe. 46 (2017) 3–12. https://doi.org/10.1016/j.anaerobe.2016.11.007.
[156] J. Dolfing, A. Xu, N.D. Gray, S.R. Larter, I.M. Head, The thermodynamic landscape of methanogenic PAH degradation, Microb. Biotechnol. 2 (2009)

566–574. https://doi.org/10.1111/j.1751-7915.2009.00096.x.
[157] X. Liu, B. Dong, X. Dai, Hydrolysis and acidification of dewatered sludge under mesophilic, thermophilic and extreme thermophilic conditions: Effect of pH, Bioresour. Technol. 148 (2013) 461–466. https://doi.org/10.1016/j.biortech.2013.08.118.
[158] N.M.G. Coelho, R.L. Droste, K.J. Kennedy, Evaluation of continuous mesophilic, thermophilic and temperature phased anaerobic digestion of microwaved activated sludge, Water Res. 45 (2011) 2822–2834. https://doi.org/10.1016/j.watres.2011.02.032.
[159] H. Zou, Q. Jiang, R. Zhu, Y. Chen, T. Sun, M. Li, J. Zhai, D. Shi, H. Ai, L. Gu, Q. He, Enhanced hydrolysis of lignocellulose in corn cob by using food waste pretreatment to improve anaerobic digestion performance, J. Environ. Manage. 254 (2020) 109830. https://doi.org/10.1016/j.jenvman.2019.109830.
[160] J. Zhang, W. Li, J. Lee, K.C. Loh, Y. Dai, Y.W. Tong, Enhancement of biogas production in anaerobic co-digestion of food waste and waste activated sludge by biological co-pretreatment, Energy. 137 (2017) 479–486. https://doi.org/10.1016/j.energy.2017.02.163.
[161] T. Amani, M. Nosrati, T.R. Sreekrishnan, Anaerobic digestion from the viewpoint of microbiological, chemical, and operational aspects - A review, Environ. Rev. 18 (2010) 255–278. https://doi.org/10.1139/A10-011.
[162] G. Lourinho, L.F.T.G. Rodrigues, P.S.D. Brito, Recent advances on anaerobic digestion of swine wastewater, Int. J. Environ. Sci. Technol. (2020). https://doi.org/10.1007/s13762-020-02793-y.
[163] J. Peng, Y. Song, P. Yuan, X. Cui, G. Qiu, The remediation of heavy metals contaminated sediment, J. Hazard. Mater. 161 (2009) 633–640. https://doi.org/10.1016/j.jhazmat.2008.04.061.
[164] S. Kang, G. Kim, J.K. Choe, Y. Choi, Effect of using powdered biochar and surfactant on desorption and biodegradability of phenanthrene sorbed to biochar, J. Hazard. Mater. 371 (2019) 253–260. https://doi.org/10.1016/j.jhazmat.2019.02.104.
[165] B.-D. Lee, M. Hosomi, Ethanol washing of PAH-contaminated soil and Fenton oxidation of washing solution, J. Mater. (2000). https://doi.org/10.1007/s10163-999-0012-7.
[166] C. Trellu, E. Mousset, Y. Pechaud, D. Huguenot, E.D. van Hullebusch, G. Esposito, M.A. Oturan, Removal of hydrophobic organic pollutants from soil washing/flushing solutions: A critical review, J. Hazard. Mater. (2016). https://doi.org/10.1016/j.jhazmat.2015.12.008.
[167] C.N. Mulligan, R.N. Yong, B.F. Gibbs, An evaluation of technologies for the heavy metal remediation of dredged sediments, J. Hazard. Mater. (2001). https://doi.org/10.1016/S0304-3894(01)00226-6.
[168] M. Harati, F. Gharibzadeh, M. Moradi, R.R. Kalantary, Remediation of phenanthrene & cadmium co-contaminated soil by using a combined process including soil washing and electrocoagulation, Int. J. Environ. Anal. Chem. (2021) 1–19. https://doi.org/10.1080/03067319.2021.1976168.
[169] Z. Zou, R. Qiu, W. Zhang, H. Dong, Z. Zhao, T. Zhang, X. Wei, X. Cai, The study of operating variables in soil washing with EDTA, Environ. Pollut. 157

(2009) 229–236. https://doi.org/10.1016/j.envpol.2008.07.009.
[170] J.K. Pannu, A. Singh, O.P. Ward, Vegetable oil as a contaminated soil remediation amendment: application of peanut oil for extraction of polycyclic aromatic hydrocarbons from soil, Process Biochem. 39 (2004) 1211–1216. https://doi.org/10.1016/S0032-9592(03)00254-1.
[171] Z. Gong, K. Alef, B.-M. Wilke, P. Li, Dissolution and removal of PAHs from a contaminated soil using sunflower oil, Chemosphere. 58 (2005) 291–298. https://doi.org/10.1016/j.chemosphere.2004.07.035.
[172] D. Huguenot, E. Mousset, E.D. van Hullebusch, M.A. Oturan, Combination of surfactant enhanced soil washing and electro-Fenton process for the treatment of soils contaminated by petroleum hydrocarbons, J. Environ. Manage. 153 (2015) 40–47. https://doi.org/10.1016/j.jenvman.2015.01.037.
[173] A. Silva, C. Deleruematos, A. Fiuza, Use of solvent extraction to remediate soils contaminated with hydrocarbons, J. Hazard. Mater. 124 (2005) 224–229. https://doi.org/10.1016/j.jhazmat.2005.05.022.
[174] M.-C. Chang, C.-R. Huang, H.-Y. Shu, Effects of surfactants on extraction of phenanthrene in spiked sand, Chemosphere. 41 (2000) 1295–1300. https://doi.org/10.1016/S0045-6535(99)00527-5.
[175] Q. Zhao, L. Weise, P. Li, K. Yang, Y. Zhang, D. Dong, P. Li, X. Li, Ageing behavior of phenanthrene and pyrene in soils: A study using sodium dodecylbenzenesulfonate extraction, J. Hazard. Mater. 183 (2010) 881–887. https://doi.org/10.1016/j.jhazmat.2010.07.111.
[176] J. Qu, M. Fan, The Current State of Water Quality and Technology Development for Water Pollution Control in China, Crit. Rev. Environ. Sci. Technol. 40 (2010) 519–560. https://doi.org/10.1080/10643380802451953.
[177] C.K. Ahn, Y.M. Kim, S.H. Woo, J.M. Park, Soil washing using various nonionic surfactants and their recovery by selective adsorption with activated carbon, J. Hazard. Mater. 154 (2008) 153–160. https://doi.org/10.1016/j.jhazmat.2007.10.006.
[178] E. Mousset, N. Oturan, E.D. van Hullebusch, G. Guibaud, G. Esposito, M.A. Oturan, Influence of solubilizing agents (cyclodextrin or surfactant) on phenanthrene degradation by electro-Fenton process - Study of soil washing recycling possibilities and environmental impact, Water Res. 48 (2014) 306–316. https://doi.org/10.1016/j.watres.2013.09.044.
[179] S. Satyro, M. Race, R. Marotta, M. Dezotti, D. Spasiano, G. Mancini, M. Fabbricino, Simulated solar photocatalytic processes for the simultaneous removal of EDDS, Cu(II), Fe(III) and Zn(II) in synthetic and real contaminated soil washing solutions, J. Environ. Chem. Eng. 2 (2014) 1969–1979. https://doi.org/10.1016/j.jece.2014.08.017.
[180] C. Trellu, Y. Pechaud, N. Oturan, E. Mousset, E.D. van Hullebusch, D. Huguenot, M.A. Oturan, Remediation of soils contaminated by hydrophobic organic compounds: How to recover extracting agents from soil washing solutions?, J. Hazard. Mater. (2021). https://doi.org/10.1016/j.jhazmat.2020.124137.
[181] S. Lamichhane, K.C. Bal Krishna, R. Sarukkalige, Polycyclic aromatic hydrocarbons (PAHs) removal by sorption: A review, Chemosphere. (2016).

https://doi.org/10.1016/j.chemosphere.2016.01.036.
[182] I. V. Robles-González, F. Fava, H.M. Poggi-Varaldo, A review on slurry bioreactors for bioremediation of soils and sediments, Microb. Cell Fact. 7 (2008) 5. https://doi.org/10.1186/1475-2859-7-5.
[183] A.J. Daugulis, Two-phase partitioning bioreactors: a new technology platform for destroying xenobiotics, Trends Biotechnol. 19 (2001) 457–462. https://doi.org/10.1016/S0167-7799(01)01789-9.
[184] S. Sundaramurthy, R. kant Tripathi, S. Suresh, R. kant Tripathi, M.N. Gernal Rana, REVIEW ON TREATMENT OF INDUSTRIAL WASTEWATER USING SEQUENTIAL BATCH REACTOR, IJSTM. 2 (2011).
[185] G. Hu, J. Li, G. Zeng, Recent development in the treatment of oily sludge from petroleum industry: A review, J. Hazard. Mater. 261 (2013) 470–490. https://doi.org/10.1016/j.jhazmat.2013.07.069.
[186] S. Deshpande, B.J. Shiau, D. Wade, D.A. Sabatini, J.H. Harwell, Surfactant selection for enhancing ex situ soil washing, Water Res. 33 (1999) 351–360. https://doi.org/10.1016/S0043-1354(98)00234-6.
[187] G. Marchal, K.E.C. Smith, A. Rein, A. Winding, S. Trapp, U.G. Karlson, Comparing the desorption and biodegradation of low concentrations of phenanthrene sorbed to activated carbon, biochar and compost, Chemosphere. (2013). https://doi.org/10.1016/j.chemosphere.2012.07.048.
[188] H. Han, M.K. Rafiq, T. Zhou, R. Xu, O. Mašek, X. Li, A critical review of clay-based composites with enhanced adsorption performance for metal and organic pollutants, J. Hazard. Mater. 369 (2019) 780–796. https://doi.org/10.1016/j.jhazmat.2019.02.003.
[189] I. Bortone, C. Labianca, F. Todaro, S. De Gisi, F. Coulon, M. Notarnicola, Experimental investigations and numerical modelling of in-situ reactive caps for PAH contaminated marine sediments, J. Hazard. Mater. (2020). https://doi.org/10.1016/j.jhazmat.2019.121724.
[190] X.-F. Tan, S.-S. Zhu, R.-P. Wang, Y.-D. Chen, P.-L. Show, F.-F. Zhang, S.-H. Ho, Role of biochar surface characteristics in the adsorption of aromatic compounds: Pore structure and functional groups, Chinese Chem. Lett. 32 (2021) 2939–2946. https://doi.org/10.1016/j.cclet.2021.04.059.
[191] J.R. Zimmerman, D. Werner, U. Ghosh, R.N. Millward, T.S. Bridges, R.G. Luthy, Effects of dose and particle size on activated carbon treatment to sequester polychlorinated biphenyls and polycyclic aromatic hydrocarbons in marine sediments, Environ. Toxicol. Chem. (2005). https://doi.org/10.1897/04-368R.1.
[192] D. Kupryianchyk, E.P. Reichman, M.I. Rakowska, E.T.H.M. Peeters, J.T.C. Grotenhuis, A.A. Koelmans, Ecotoxicological Effects of Activated Carbon Amendments on Macroinvertebrates in Nonpolluted and Polluted Sediments, Environ. Sci. Technol. 45 (2011) 8567–8574. https://doi.org/10.1021/es2014538.
[193] A.O. Adeola, P.B.C. Forbes, Influence of natural organic matter fractions on PAH sorption by stream sediments and a synthetic graphene wool adsorbent, Environ. Technol. Innov. 21 (2021) 101202. https://doi.org/10.1016/j.eti.2020.101202.

[194] A.O. Adeola, P.B.C. Forbes, Optimization of the sorption of selected polycyclic aromatic hydrocarbons by regenerable graphene wool, Water Sci. Technol. 80 (2019) 1931–1943. https://doi.org/10.2166/wst.2020.011.
[195] R. Gusain, N. Kumar, S.S. Ray, Recent advances in carbon nanomaterial-based adsorbents for water purification, Coord. Chem. Rev. 405 (2020) 213111. https://doi.org/10.1016/j.ccr.2019.213111.
[196] A.A. Akinpelu, M.K. Nazal, N. Abuzaid, Adsorptive removal of polycyclic aromatic hydrocarbons from contaminated water by biomass from dead leaves of Halodule uninervis: kinetic and thermodynamic studies, Biomass Convers. Biorefinery. 1 (2021) 1–13. https://doi.org/10.1007/s13399-021-01718-0.
[197] Z. Li, Y. Liu, X. Yang, Y. Xing, C.-J. Tsai, M. Meng, R.T. Yang, Performance of mesoporous silicas and carbon in adsorptive removal of phenanthrene as a typical gaseous polycyclic aromatic hydrocarbon, Microporous Mesoporous Mater. 239 (2017) 9–18. https://doi.org/10.1016/j.micromeso.2016.09.027.
[198] H. Cheng, Y. Bian, F. Wang, X. Jiang, R. Ji, C. Gu, X. Yang, Y. Song, Green conversion of crop residues into porous carbons and their application to efficiently remove polycyclic aromatic hydrocarbons from water: Sorption kinetics, isotherms and mechanism, Bioresour. Technol. 284 (2019) 1–8. https://doi.org/10.1016/j.biortech.2019.03.104.
[199] C.H. Sharp, B.C. Bukowski, H. Li, E.M. Johnson, S. Ilic, A.J. Morris, D. Gersappe, R.Q. Snurr, J.R. Morris, Nanoconfinement and mass transport in metal–organic frameworks, Chem. Soc. Rev. 50 (2021) 11530–11558. https://doi.org/10.1039/D1CS00558H.
[200] M. Stefaniuk, P. Oleszczuk, Characterization of biochars produced from residues from biogas production, J. Anal. Appl. Pyrolysis. 115 (2015) 157–165. https://doi.org/10.1016/j.jaap.2015.07.011.
[201] V.B. Cashin, D.S. Eldridge, A. Yu, D. Zhao, Surface functionalization and manipulation of mesoporous silica adsorbents for improved removal of pollutants: a review, Environ. Sci. Water Res. Technol. 4 (2018) 110–128. https://doi.org/10.1039/C7EW00322F.
[202] M.T.O. Jonker, S.A. Van Der Heijden, J.P. Kreitinger, S.B. Hawthorne, Predicting PAH bioaccumulation and toxicity in earthworms exposed to manufactured gas plant soils with solid-phase microextraction, Environ. Sci. Technol. (2007). https://doi.org/10.1021/es070404s.
[203] F. Li, J. Chen, X. Hu, F. He, E. Bean, D.C.W. Tsang, Y.S. Ok, B. Gao, Applications of carbonaceous adsorbents in the remediation of polycyclic aromatic hydrocarbon-contaminated sediments: A review, J. Clean. Prod. (2020). https://doi.org/10.1016/j.jclepro.2020.120263.
[204] M.I. Rakowska, D. Kupryianchyk, M.P.J. Smit, A.A. Koelmans, J.T.C. Grotenhuis, H.H.M. Rijnaarts, Kinetics of hydrophobic organic contaminant extraction from sediment by granular activated carbon, Water Res. (2014). https://doi.org/10.1016/j.watres.2013.12.025.
[205] Z. Han, S. Abel, J. Akkanen, D. Werner, Evaluation of strategies to minimize ecotoxic side-effects of sorbent-based sediment remediation, J. Chem. Technol. Biotechnol. (2017). https://doi.org/10.1002/jctb.5224.
[206] C.M. Navarathna, N. Bombuwala Dewage, C. Keeton, J. Pennisson, R.

Henderson, B. Lashley, X. Zhang, E.B. Hassan, F. Perez, D. Mohan, C.U. Pittman, T. Mlsna, Biochar Adsorbents with Enhanced Hydrophobicity for Oil Spill Removal, ACS Appl. Mater. Interfaces. 12 (2020) 9248–9260. https://doi.org/10.1021/acsami.9b20924.

[207] L. Bielská, L. Škulcová, N. Neuwirthová, G. Cornelissen, S.E. Hale, Sorption, bioavailability and ecotoxic effects of hydrophobic organic compounds in biochar amended soils, Sci. Total Environ. 624 (2018) 78–86. https://doi.org/10.1016/j.scitotenv.2017.12.098.

[208] L. Silvani, P.R. Di Palma, C. Riccardi, E. Eek, S.E. Hale, P. Viotti, M. Petrangeli Papini, Use of biochar as alternative sorbent for the active capping of oil contaminated sediments, J. Environ. Chem. Eng. (2017). https://doi.org/10.1016/j.jece.2017.10.004.

[209] Y. Choi, Y.M. Cho, W.R. Gala, R.G. Luthy, Measurement and modeling of activated carbon performance for the sequestration of parent-and alkylated-polycyclic aromatic hydrocarbons in petroleum-impacted sediments, Environ. Sci. Technol. (2013). https://doi.org/10.1021/es303770c.

[210] K. Yang, Y. Jiang, J. Yang, D. Lin, Correlations and adsorption mechanisms of aromatic compounds on biochars produced from various biomass at 700 °C, Environ. Pollut. (2018). https://doi.org/10.1016/j.envpol.2017.10.035.

[211] B. Pan, B. Xing, Adsorption mechanisms of organic chemicals on carbon nanotubes, Environ. Sci. Technol. (2008). https://doi.org/10.1021/es801777n.

[212] G. Cornelissen, Ö. Gustafsson, T.D. Bucheli, M.T.O. Jonker, A.A. Koelmans, P.C.M. Van Noort, Extensive sorption of organic compounds to black carbon, coal, and kerogen in sediments and soils: Mechanisms and consequences for distribution, bioaccumulation, and biodegradation, Environ. Sci. Technol. (2005). https://doi.org/10.1021/es050191b.

[213] L. Jakob, T. Hartnik, T. Henriksen, M. Elmquist, R.C. Brändli, S.E. Hale, G. Cornelissen, PAH-sequestration capacity of granular and powder activated carbon amendments in soil, and their effects on earthworms and plants, Chemosphere. (2012). https://doi.org/10.1016/j.chemosphere.2012.03.080.

[214] P. Oleszczuk, M. Kołtowski, Changes of total and freely dissolved polycyclic aromatic hydrocarbons and toxicity of biochars treated with various aging processes, Environ. Pollut. 237 (2018) 65–73. https://doi.org/10.1016/j.envpol.2018.01.073.

[215] P.L. O'Brien, T.M. DeSutter, F.X.M. Casey, E. Khan, A.F. Wick, Thermal remediation alters soil properties – a review, J. Environ. Manage. (2018). https://doi.org/10.1016/j.jenvman.2017.11.052.

[216] F.I. Khan, T. Husain, R. Hejazi, An overview and analysis of site remediation technologies, J. Environ. Manage. 71 (2004) 95–122. https://doi.org/10.1016/j.jenvman.2004.02.003.

[217] S. Kuppusamy, T. Palanisami, M. Megharaj, K. Venkateswarlu, R. Naidu, Ex-situ remediation technologies for environmental pollutants: A critical perspective, in: Rev. Environ. Contam. Toxicol., 2016. https://doi.org/10.1007/978-3-319-20013-2_2.

[218] C. Zhao, Y. Dong, Y. Feng, Y. Li, Y. Dong, Thermal desorption for remediation of contaminated soil: A review, Chemosphere. (2019).

https://doi.org/10.1016/j.chemosphere.2019.01.079.
[219] P.L. O'Brien, T.M. DeSutter, F.X.M. Casey, A.F. Wick, E. Khan, Evaluation of Soil Function Following Remediation of Petroleum Hydrocarbons—a Review of Current Remediation Techniques, Curr. Pollut. Reports. 3 (2017) 192–205. https://doi.org/10.1007/s40726-017-0063-7.
[220] P.L. O'Brien, T.M. DeSutter, F.X.M. Casey, N.E. Derby, A.F. Wick, Implications of Using Thermal Desorption to Remediate Contaminated Agricultural Soil: Physical Characteristics and Hydraulic Processes, J. Environ. Qual. 45 (2016) 1430–1436. https://doi.org/10.2134/jeq2015.12.0607.
[221] A. Pape, C. Switzer, N. McCosh, C.W. Knapp, Impacts of thermal and smouldering remediation on plant growth and soil ecology, Geoderma. 243–244 (2015) 1–9. https://doi.org/10.1016/j.geoderma.2014.12.004.
[222] Y.M. Yi, S. Park, C. Munster, G. Kim, K. Sung, Changes in Ecological Properties of Petroleum Oil-Contaminated Soil After Low-Temperature Thermal Desorption Treatment, Water, Air, Soil Pollut. 227 (2016) 108. https://doi.org/10.1007/s11270-016-2804-4.
[223] P. Acharya, P. Ives, Incineration at Bayou Bounfouca remediation project, Waste Manag. 14 (1994) 13–26. https://doi.org/10.1016/0956-053X(94)90017-5.
[224] F. Renoldi, L. Lietti, S. Saponaro, L. Bonomo, P. Forzatti, Thermal desorption of a PAH-contaminated soil: a case study, Trans. Ecol. Environ. (2003).
[225] M.S. Hosseini, In situ thermal desorption of polycyclic aromatic hydrocarbons from lampblack impacted soils using natural gas combustion, University of California, Los Angeles, 2006.
[226] C. Muangchinda, A. Yamazoe, D. Polrit, H. Thoetkiattikul, W. Mhuantong, V. Champreda, O. Pinyakong, Biodegradation of high concentrations of mixed polycyclic aromatic hydrocarbons by indigenous bacteria from a river sediment: a microcosm study and bacterial community analysis, Environ. Sci. Pollut. Res. (2017). https://doi.org/10.1007/s11356-016-8185-9.
[227] M.S. Mat-Shayuti, T.M.Y.S. Tuan Ya, M.Z. Abdullah, P.N.F. Megat Khamaruddin, N.H. Othman, Progress in ultrasonic oil-contaminated sand cleaning: a fundamental review, Environ. Sci. Pollut. Res. (2019). https://doi.org/10.1007/s11356-019-05954-w.
[228] J.J. Nam, G.O. Thomas, F.M. Jaward, E. Steinnes, O. Gustafsson, K.C. Jones, PAHs in background soils from Western Europe: Influence of atmospheric deposition and soil organic matter, Chemosphere. (2008). https://doi.org/10.1016/j.chemosphere.2007.08.010.
[229] S.G. Wakeham, C. Schaffner, W. Giger, Poly cyclic aromatic hydrocarbons in Recent lake sediments-II. Compounds derived from biogenic precursors during early diagenesis, Geochim. Cosmochim. Acta. (1980). https://doi.org/10.1016/0016-7037(80)90041-1.
[230] J.W. Readman, G. Fillmann, I. Tolosa, J. Bartocci, J.P. Villeneuve, C. Catinni, L.D. Mee, Petroleum and PAH contamination of the Black Sea, Mar. Pollut. Bull. (2002). https://doi.org/10.1016/S0025-326X(01)00189-8.
[231] S.G. Wakeham, E.A. Canuel, Biogenic polycyclic aromatic hydrocarbons in sediments of the San Joaquin River in California (USA), and current paradigms

on their formation, Environ. Sci. Pollut. Res. (2016). https://doi.org/10.1007/s11356-015-5402-x.
[232] P. Mattei, A. Cincinelli, T. Martellini, R. Natalini, E. Pascale, G. Renella, Reclamation of river dredged sediments polluted by PAHs by co-composting with green waste, Sci. Total Environ. (2016). https://doi.org/10.1016/j.scitotenv.2016.05.140.
[233] H. Yu, G.H. Huang, H. Xiao, L. Wang, W. Chen, Combined effects of DOM and biosurfactant enhanced biodegradation of polycylic armotic hydrocarbons (PAHs) in soil-water systems, Environ. Sci. Pollut. Res. (2014). https://doi.org/10.1007/s11356-014-2958-9.
[234] M. Cecotti, B.M. Coppotelli, V.C. Mora, M. Viera, I.S. Morelli, Efficiency of surfactant-enhanced bioremediation of aged polycyclic aromatic hydrocarbon-contaminated soil: Link with bioavailability and the dynamics of the bacterial community, Sci. Total Environ. (2018). https://doi.org/10.1016/j.scitotenv.2018.03.303.
[235] J. Qiao, C. Zhang, S. Luo, W. Chen, Bioremediation of highly contaminated oilfield soil: Bioaugmentation for enhancing aromatic compounds removal, Front. Environ. Sci. Eng. (2014). https://doi.org/10.1007/s11783-013-0561-9.
[236] T. Masy, S. Demanèche, O. Tromme, P. Thonart, P. Jacques, S. Hiligsmann, T.M. Vogel, Hydrocarbon biostimulation and bioaugmentation in organic carbon and clay-rich soils, Soil Biol. Biochem. (2016). https://doi.org/10.1016/j.soilbio.2016.04.016.
[237] P. Oleszczuk, S. Baran, Kinetics of PAHs losses and relationships between PAHs properties and properties of soil in sewage sludge-amended soil, Polycycl. Aromat. Compd. (2005). https://doi.org/10.1080/10406630591007170.
[238] S.E. Agarry, C.N. Owabor, Anaerobic bioremediation of marine sediment artificially contaminated with anthracene and naphthalene, Environ. Technol. (2011). https://doi.org/10.1080/09593330.2010.536788.
[239] X. Yang, Z. Chen, Q. Wu, M. Xu, Enhanced phenanthrene degradation in river sediments using a combination of biochar and nitrate, Sci. Total Environ. (2018). https://doi.org/10.1016/j.scitotenv.2017.11.130.
[240] L. Delgadillo-Mirquez, L. Lardon, J.P. Steyer, D. Patureau, A new dynamic model for bioavailability and cometabolism of micropollutants during anaerobic digestion, Water Res. (2011). https://doi.org/10.1016/j.watres.2011.05.047.
[241] M. Guo, Z. Gong, G. Allinson, P. Tai, R. Miao, X. Li, C. Jia, J. Zhuang, Variations in the bioavailability of polycyclic aromatic hydrocarbons in industrial and agricultural soils after bioremediation, Chemosphere. (2016). https://doi.org/10.1016/j.chemosphere.2015.10.027.
[242] Y. Sun, L. Ji, W. Wang, X. Wang, J. Wu, H. Li, H. Guo, Simultaneous Removal of Polycyclic Aromatic Hydrocarbons and Copper from Soils using Ethyl Lactate-Amended EDDS Solution, J. Environ. Qual. 38 (2009) 1591–1597. https://doi.org/10.2134/jeq2008.0374.
[243] C.L. Yap, S. Gan, H.K. Ng, Evaluation of solubility of polycyclic aromatic hydrocarbons in ethyl lactate/water versus ethanol/water mixtures for

contaminated soil remediation applications, J. Environ. Sci. (China). (2012). https://doi.org/10.1016/S1001-0742(11)60873-5.
[244] A. Ferraro, M. Fabbricino, E.D. van Hullebusch, G. Esposito, Investigation of different ethylenediamine-N,N′-disuccinic acid-enhanced washing configurations for remediation of a Cu-contaminated soil: process kinetics and efficiency comparison between single-stage and multi-stage configurations, Environ. Sci. Pollut. Res. 24 (2017) 21960–21972. https://doi.org/10.1007/s11356-017-9844-1.
[245] M.T. Smith, F. Berruti, A.K. Mehrotra, Thermal desorption treatment of contaminated soils in a novel batch thermal reactor, in: Ind. Eng. Chem. Res., 2001. https://doi.org/10.1021/ie0100333.
[246] C. Bulmău, C. Mărculescu, S. Lu, Z. Qi, Analysis of thermal processing applied to contaminated soil for organic pollutants removal, J. Geochemical Explor. (2014). https://doi.org/10.1016/j.gexplo.2014.08.005.
[247] A. Abbassi-Guendouz, D. Brockmann, E. Trably, C. Dumas, J.P. Delgenès, J.P. Steyer, R. Escudié, Total solids content drives high solid anaerobic digestion via mass transfer limitation, Bioresour. Technol. (2012). https://doi.org/10.1016/j.biortech.2012.01.174.
[248] T. Sayara, M. Pognani, M. Sarrà, A. Sánchez, Anaerobic degradation of PAHs in soil: Impacts of concentration and amendment stability on the PAHs degradation and biogas production, Int. Biodeterior. Biodegrad. (2010). https://doi.org/10.1016/j.ibiod.2010.02.005.
[249] S. Chattopadhyay, D. Chattopadhyay, Remediation of DDT and Its Metabolites in Contaminated Sediment, Curr. Pollut. Reports. (2015). https://doi.org/10.1007/s40726-015-0023-z.
[250] C. Trellu, O. Ganzenko, S. Papirio, Y. Pechaud, N. Oturan, D. Huguenot, E.D. van Hullebusch, G. Esposito, M.A. Oturan, Combination of anodic oxidation and biological treatment for the removal of phenanthrene and Tween 80 from soil washing solution, Chem. Eng. J. (2016). https://doi.org/10.1016/j.cej.2016.07.108.
[251] I. Meireles, V. Sousa, Assessing water, energy and emissions reduction from water conservation measures in buildings: a methodological approach, Environ. Sci. Pollut. Res. (2019). https://doi.org/10.1007/s11356-019-06377-3.
[252] K.E.C. Smith, M. Thullner, L.Y. Wick, H. Harms, Sorption to humic acids enhances polycyclic aromatic hydrocarbon biodegradation, Environ. Sci. Technol. (2009). https://doi.org/10.1021/es803661s.
[253] K.T. Steffen, S. Schubert, M. Tuomela, A. Hatakka, M. Hofrichter, Enhancement of bioconversion of high-molecular mass polycyclic aromatic hydrocarbons in contaminated non-sterile soil by litter-decomposing fungi, Biodegradation. (2007). https://doi.org/10.1007/s10532-006-9070-x.
[254] K.E. Mueller, J.R. Shann, PAH dissipation in spiked soil: Impacts of bioavailability, microbial activity, and trees, Chemosphere. (2006). https://doi.org/10.1016/j.chemosphere.2005.12.051.
[255] M. Arienzo, C. Donadio, O. Mangoni, F. Bolinesi, C. Stanislao, M. Trifuoggi, M. Toscanesi, G. Di Natale, L. Ferrara, Characterization and source apportionment of polycyclic aromatic hydrocarbons (pahs) in the sediments of

gulf of Pozzuoli (Campania, Italy), Mar. Pollut. Bull. 124 (2017) 480–487. https://doi.org/10.1016/j.marpolbul.2017.07.006.
[256] U.C. Brinch, F. Ekelund, C.S. Jacobsen, Method for spiking soil samples with organic compounds, Appl. Environ. Microbiol. (2002). https://doi.org/10.1128/AEM.68.4.1808-1816.2002.
[257] B. Lukić, D. Huguenot, A. Panico, M. Fabbricino, E.D. van Hullebusch, G. Esposito, Importance of organic amendment characteristics on bioremediation of PAH-contaminated soil, Environ. Sci. Pollut. Res. (2016). https://doi.org/10.1007/s11356-016-6635-z.
[258] B.V. Chang, S.W. Chang, S.Y. Yuan, Anaerobic degradation of polycyclic aromatic hydrocarbons in sludge, Adv. Environ. Res. 7 (2003) 623–628. https://doi.org/10.1016/S1093-0191(02)00047-3.
[259] F.J.G. Frutos, O. Escolano, S. García, M. Babín, M.D. Fernández, Bioventing remediation and ecotoxicity evaluation of phenanthrene-contaminated soil, J. Hazard. Mater. (2010). https://doi.org/10.1016/j.jhazmat.2010.07.098.
[260] W. Namkoong, E.Y. Hwang, J.S. Park, J.Y. Choi, Bioremediation of diesel-contaminated soil with composting, Environ. Pollut. (2002). https://doi.org/10.1016/S0269-7491(01)00328-1.
[261] A. Gielnik, Y. Pechaud, D. Huguenot, A. Cébron, G. Esposito, E.D. van Hullebusch, Bacterial seeding potential of digestate in bioremediation of diesel contaminated soil, Int. Biodeterior. Biodegradation. 143 (2019) 104715.
[262] M. Fabbricino, A. Ferraro, V. Luongo, L. Pontoni, M. Race, Soil washing optimization, recycling of the solution, and ecotoxicity assessment for the remediation of Pb-contaminated sites using EDDS, Sustain. (2018). https://doi.org/10.3390/su10030636.
[263] Astm-D-2216-98, Standard Test Method for Laboratory Determination of Water (Moisture) Content of Soil and Rock by Mass, ASTM Int. (1998). https://doi.org/10.1520/D4944-11.1.5.
[264] APHA, AWWA, WEF., Fixed and volatile solids ignited at 550°C 2540 E., Stand. Methods Exam. Water Wastewater. (2012). https://doi.org/ISBN 9780875532356.
[265] B. Gurung, M. Race, M. Fabbricino, D. Komínková, G. Libralato, A. Siciliano, M. Guida, Assessment of metal pollution in the Lambro Creek (Italy), Ecotoxicol. Environ. Saf. (2018). https://doi.org/10.1016/j.ecoenv.2017.11.041.
[266] S.C. Gupta, R.J. Hanks, Influence of Water Content on Electrical Conductivity of the Soil1, Soil Sci. Soc. Am. J. (2010). https://doi.org/10.2136/sssaj1972.03615995003600060011x.
[267] S. Chen, J. Zhang, X. Wang, Effects of alkalinity sources on the stability of anaerobic digestion from food waste, Waste Manag. Res. (2015). https://doi.org/10.1177/0734242X15602965.
[268] K. Kiskira, S. Papirio, E.D. van Hullebusch, G. Esposito, Influence of pH, EDTA/Fe(II) ratio, and microbial culture on Fe(II)-mediated autotrophic denitrification, Environ. Sci. Pollut. Res. (2017). https://doi.org/10.1007/s11356-017-9736-4.
[269] F. Sun, D. Littlejohn, M. David Gibson, Ultrasonication extraction and solid

phase extraction clean-up for determination of US EPA 16 priority pollutant polycyclic aromatic hydrocarbons in soils by reversed-phase liquid chromatography with ultraviolet absorption detection, Anal. Chim. Acta. (1998). https://doi.org/10.1016/S0003-2670(98)00186-X.
[270] Y. Yang, N. Zhang, M. Xue, S. Tao, Impact of soil organic matter on the distribution of polycyclic aromatic hydrocarbons (PAHs) in soils, Environ. Pollut. 158 (2010) 2170–2174. https://doi.org/10.1016/j.envpol.2010.02.019.
[271] Budiyono, I.N. Widiasa, S. Johari, Sunarso, The Kinetic of Biogas Production Rate from Cattle Manure in Batch Mode, Int. J. Chem. Biomol. Eng. (2010).
[272] G. Mancini, S. Papirio, P.N.L. Lens, G. Esposito, Effect of N -methylmorpholine- N -oxide Pretreatment on Biogas Production from Rice Straw, Cocoa Shell, and Hazelnut Skin, Environ. Eng. Sci. 33 (2016) 843–850. https://doi.org/10.1089/ees.2016.0138.
[273] S.V. Mohan, T. Kisa, T. Ohkuma, R.A. Kanaly, Y. Shimizu, Bioremediation technologies for treatment of PAH-contaminated soil and strategies to enhance process efficiency, Rev. Environ. Sci. Biotechnol. (2006). https://doi.org/10.1007/s11157-006-0004-1.
[274] C.F. Bustillo-Lecompte, M. Mehrvar, E. Quiñones-Bolaños, Cost-effectiveness analysis of TOC removal from slaughterhouse wastewater using combined anaerobic-aerobic and UV/H2O2 processes, J. Environ. Manage. (2014). https://doi.org/10.1016/j.jenvman.2013.12.035.
[275] Federal Remediation Technologies Roundtable, No Title, (n.d.). https://frtr.gov/.
[276] M. Esen, T. Yuksel, Experimental evaluation of using various renewable energy sources for heating a greenhouse, Energy Build. (2013). https://doi.org/10.1016/j.enbuild.2013.06.018.
[277] W. V. Steele, R.D. Chirico, A. Nguyen, I.A. Hossenlopp, N.K. Smith, Determination of ideal-gas enthalpies of formation for key compounds, in: AIChE Symp. Ser., 1990.
[278] M.V. Roux, M. Temprado, J.S. Chickos, Y. Nagano, Critically evaluated thermochemical properties of polycyclic aromatic hydrocarbons, J. Phys. Chem. Ref. Data. (2008). https://doi.org/10.1063/1.2955570.
[279] P. Tawari-Fufeyin, G.O. Adams, P.T. Fufeyin, S.E. Okoro, I. Ehinomen, Bioremediation, Biostimulation and Bioaugmention: A Review, Int. J. Environ. Bioremediation Biodegrad. (2015). https://doi.org/10.12691/ijebb-3-1-5.
[280] S. Maletić, S. Murenji, J. Agbaba, S. Rončević, M. Kragulj Isakovski, J. Molnar Jazić, B. Dalmacija, Potential for anaerobic treatment of polluted sediment, J. Environ. Manage. (2018). https://doi.org/10.1016/j.jenvman.2018.02.029.
[281] T. Ebihara, P.L. Bishop, Effect of Acetate on Biofilms Utilized in PAH Bioremediation, Environ. Eng. Sci. (2003). https://doi.org/10.1089/10928750260418944.
[282] C. Cuypers, T. Pancras, T. Grotenhuis, W. Rulkens, The estimation of PAH bioavailability in contaminated sediments using hydroxypropyl-β-cyclodextrin and Triton X-100 extraction techniques, Chemosphere. (2002). https://doi.org/10.1016/S0045-6535(01)00199-0.
[283] J.J. Ortega-Calvo, M.C. Tejeda-Agredano, C. Jimenez-Sanchez, E. Congiu, R.

Sungthong, J.L. Niqui-Arroyo, M. Cantos, Is it possible to increase bioavailability but not environmental risk of PAHs in bioremediation?, J. Hazard. Mater. (2013). https://doi.org/10.1016/j.jhazmat.2013.03.042.
[284] E. Andersson, A. Rotander, T. von Kronhelm, A. Berggren, P. Ivarsson, H. Hollert, M. Engwall, AhR agonist and genotoxicant bioavailability in a PAH-contaminated soil undergoing biological treatment, Environ. Sci. Pollut. Res. (2009). https://doi.org/10.1007/s11356-009-0121-9.
[285] J.A. Ogejo, L. Li, Enhancing biomethane production from flush dairy manure with turkey processing wastewater, Appl. Energy. (2010). https://doi.org/10.1016/j.apenergy.2010.04.020.
[286] G. Zou, S. Papirio, A. Ylinen, F. Di Capua, A.M. Lakaniemi, J.A. Puhakka, Fluidized-bed denitrification for mine waters. Part II: Effects of Ni and Co, Biodegradation. 25 (2013) 417–423. https://doi.org/10.1007/s10532-013-9670-1.
[287] M.J. Kampschreur, H. Temmink, R. Kleerebezem, M.S.M. Jetten, M.C.M. van Loosdrecht, Nitrous oxide emission during wastewater treatment, Water Res. (2009). https://doi.org/10.1016/j.watres.2009.03.001.
[288] S. Papirio, G. Esposito, F. Pirozzi, Biological inverse fluidized-bed reactors for the treatment of low pH- and sulphate-containing wastewaters under different COD/SO2-4 conditions, Environ. Technol. (United Kingdom). (2013). https://doi.org/10.1080/09593330.2012.737864.
[289] Y. Chen, J.J. Cheng, K.S. Creamer, Inhibition of anaerobic digestion process: A review, Bioresour. Technol. (2008). https://doi.org/10.1016/j.biortech.2007.01.057.
[290] A.T. Kan, G. Fu, M. Hunter, W. Chen, C.H. Ward, M.B. Tomson, Irreversible sorption of neutral hydrocarbons to sediments: Experimental observations and model predictions, Environ. Sci. Technol. (1998). https://doi.org/10.1021/es9705809.
[291] S. Thiele-Bruhn, G.W. Brümmer, Fractionated extraction of polycyclic aromatic hydrocarbons (PAHs) from polluted soils: Estimation of the PAH fraction degradable through bioremediation, Eur. J. Soil Sci. (2004). https://doi.org/10.1111/j.1365-2389.2004.00621.x.
[292] L. Dougan, S.P. Bates, R. Hargreaves, J.P. Fox, J. Crain, J.L. Finney, V. Réat, A.K. Soper, Methanol-water solutions: A bi-percolating liquid mixture, J. Chem. Phys. (2004). https://doi.org/10.1063/1.1789951.
[293] E.N. Pakpahan, M.H. Isa, S.R.M. Kutty, A. Malakahmad, Effect of temperature on the formation and degradation of polycyclic aromatic hydrocarbons, (2009).
[294] P. Kim, J. Lloyd, J.W. Kim, N. Abdoulmoumine, N. Labbé, Recovery of creosote from used railroad ties by thermal desorption, Energy. (2016). https://doi.org/10.1016/j.energy.2016.05.117.
[295] Y. Inoue, A. Katayama, Two-scale evaluation of remediation technologies for a contaminated site by applying economic input-output life cycle assessment: Risk-cost, risk-energy consumption and risk-CO 2 emission, J. Hazard. Mater. (2011). https://doi.org/10.1016/j.jhazmat.2011.06.029.
[296] V.P. Beškoski, G. Gojgić-Cvijović, J. Milić, M. Ilić, S. Miletić, T. Šolević, M.M. Vrvić, Ex situ bioremediation of a soil contaminated by mazut (heavy

residual fuel oil) - A field experiment, Chemosphere. (2011). https://doi.org/10.1016/j.chemosphere.2011.01.020.
[297] F. Madrid, M. Rubio-Bellido, J. Villaverde, A. Peña, E. Morillo, Natural and assisted dissipation of polycyclic aromatic hydrocarbons in a long-term co-contaminated soil with creosote and potentially toxic elements, Sci. Total Environ. (2019). https://doi.org/10.1016/j.scitotenv.2018.12.376.
[298] L. Corredera, S. Bayarri, C. Perez-Arquillue, R. Lazaro, F. Molino, A. Herrera, Multiresidue determination of carcinogenic polycyclic aromatic hydrocarbons in honey by solid-phase extraction and high-performance liquid chromatography, J. Food Prot. 74 (2011) 1692–1699.
[299] H.H. Soclo, P. Garrigues, M. Ewald, Origin of polycyclic aromatic hydrocarbons (PAHs) in coastal marine sediments: Case studies in Cotonou (Benin) and Aquitaine (France) Areas, Mar. Pollut. Bull. (2000). https://doi.org/10.1016/S0025-326X(99)00200-3.
[300] Y. Guo, K. Wu, X. Huo, X. Xu, Sources, distribution, and toxicity of polycyclic aromatic hydrocarbons., J. Environ. Health. (2011). https://doi.org/10.5772/10045.
[301] R. Duran, C. Cravo-Laureau, Role of environmental factors and microorganisms in determining the fate of polycyclic aromatic hydrocarbons in the marine environment, FEMS Microbiol. Rev. (2016). https://doi.org/10.1093/femsre/fuw031.
[302] R. Posada-Baquero, M. Grifoll, J.J. Ortega-Calvo, Rhamnolipid-enhanced solubilization and biodegradation of PAHs in soils after conventional bioremediation, Sci. Total Environ. (2019). https://doi.org/10.1016/j.scitotenv.2019.03.056.
[303] S. Albanese, B. De Vivo, A. Lima, D. Cicchella, D. Civitillo, A. Cosenza, Geochemical baselines and risk assessment of the Bagnoli brownfield site coastal sea sediments (Naples, Italy), J. Geochemical Explor. (2010). https://doi.org/10.1016/j.gexplo.2010.01.007.
[304] C.W. Chen, C.F. Chen, Distribution, origin, and potential toxicological significance of polycyclic aromatic hydrocarbons (PAHs) in sediments of Kaohsiung Harbor, Taiwan, Mar. Pollut. Bull. (2011). https://doi.org/10.1016/j.marpolbul.2011.04.047.
[305] P. Muniz, E. Danulat, B. Yannicelli, J. García-Alonso, G. Medina, M.C. Bícego, Assessment of contamination by heavy metals and petroleum hydrocarbons in sediments of Montevideo Harbour (Uruguay), Environ. Int. (2004). https://doi.org/10.1016/S0160-4120(03)00096-5.
[306] R.D. Delaune, W.H. Patrick, M.E. Casselman, Effect of sediment pH and redox conditions on degradation of benzo(a)pyrene, Mar. Pollut. Bull. (1981). https://doi.org/10.1016/0025-326X(81)90366-0.
[307] Y. Teng, Y. Luo, L. Ping, D. Zou, Z. Li, P. Christie, Effects of soil amendment with different carbon sources and other factors on the bioremediation of an aged PAH-contaminated soil, Biodegradation. (2010). https://doi.org/10.1007/s10532-009-9291-x.
[308] S. Lladó, S. Covino, A.M. Solanas, M. Viñas, M. Petruccioli, A. D'annibale, Comparative assessment of bioremediation approaches to highly recalcitrant

PAH degradation in a real industrial polluted soil, J. Hazard. Mater. (2013). https://doi.org/10.1016/j.jhazmat.2013.01.020.
[309] M. Bueno-Montes, D. Springael, J.J. Ortega-Calvo, Effect of a nonionic surfactant on biodegradation of slowly desorbing PAHs in contaminated soils, Environ. Sci. Technol. (2011). https://doi.org/10.1021/es1035706.
[310] K.L. Lau, Y.Y. Tsang, S.W. Chiu, Use of spent mushroom compost to bioremediate PAH-contaminated samples, Chemosphere. (2003). https://doi.org/10.1016/S0045-6535(03)00493-4.
[311] B. Antizar-Ladislao, J. Lopez-Real, A.J. Beck, Laboratory studies of the remediation of polycyclic aromatic hydrocarbon contaminated soil by in-vessel composting, Waste Manag. (2005). https://doi.org/10.1016/j.wasman.2005.01.009.
[312] T. Cajthaml, M. Bhatt, V. Šašek, V. Matějů, Bioremediation of PAH-contaminated soil by composting: A case study, Folia Microbiol. (Praha). (2002). https://doi.org/10.1007/BF02818674.
[313] Y. Zhang, Y.G. Zhu, S. Houot, M. Qiao, N. Nunan, P. Garnier, Remediation of polycyclic aromatic hydrocarbon (PAH) contaminated soil through composting with fresh organic wastes, Environ. Sci. Pollut. Res. (2011). https://doi.org/10.1007/s11356-011-0521-5.
[314] M. Sapp, M. Harrison, U. Hany, A. Charlton, R. Thwaites, Comparing the effect of digestate and chemical fertiliser on soil bacteria, Appl. Soil Ecol. (2015). https://doi.org/10.1016/j.apsoil.2014.10.004.
[315] I.H. Franke-Whittle, A. Confalonieri, H. Insam, M. Schlegelmilch, I. Körner, Changes in the microbial communities during co-composting of digestates, Waste Manag. (2014). https://doi.org/10.1016/j.wasman.2013.12.009.
[316] R. Campuzano, S. González-Martínez, Characteristics of the organic fraction of municipal solid waste and methane production: A review, Waste Manag. (2016). https://doi.org/10.1016/j.wasman.2016.05.016.
[317] W. Peng, A. Pivato, Sustainable Management of Digestate from the Organic Fraction of Municipal Solid Waste and Food Waste Under the Concepts of Back to Earth Alternatives and Circular Economy, Waste and Biomass Valorization. (2017). https://doi.org/10.1007/s12649-017-0071-2.
[318] R. Cesaro, G. Esposito, Optimal operational conditions for the electrochemical regeneration of a soil washing EDTA solution, J. Environ. Monit. (2009). https://doi.org/10.1039/b816295f.
[319] D.R. Hoagland, D.I. Arnon, The water-culture method for growing plants without soil, 1950. https://doi.org/citeulike-article-id:9455435.
[320] A. Khaliq, M.K. Abbasi, T. Hussain, Effects of integrated use of organic and inorganic nutrient sources with effective microorganisms (EM) on seed cotton yield in Pakistan, Bioresour. Technol. (2006). https://doi.org/10.1016/j.biortech.2005.05.002.
[321] N.M. Leys, L. Bastiaens, W. Verstraete, D. Springael, Influence of the carbon/nitrogen/phosphorus ratio on polycyclic aromatic hydrocarbon degradation by Mycobacterium and Sphingomonas in soil, Appl. Microbiol. Biotechnol. 66 (2005) 726–736. https://doi.org/10.1007/s00253-004-1766-4.
[322] B.. Chang, L.. Shiung, S.. Yuan, Anaerobic biodegradation of polycyclic

aromatic hydrocarbon in soil, Chemosphere. 48 (2002) 717–724. https://doi.org/10.1016/S0045-6535(02)00151-0.
[323] R. Crisafully, M.A.L. Milhome, R.M. Cavalcante, E.R. Silveira, D. De Keukeleire, R.F. Nascimento, Removal of some polycyclic aromatic hydrocarbons from petrochemical wastewater using low-cost adsorbents of natural origin, Bioresour. Technol. (2008). https://doi.org/10.1016/j.biortech.2007.08.041.
[324] E.Y. Hwang, W. Namkoong, J.S. Park, Recycling of remediated soil for effective composting of diesel-contaminated soil, Compost Sci. Util. (2001). https://doi.org/10.1080/1065657X.2001.10702028.
[325] APHA, Standard Methods for Examination of Water and Wastewater, 20th ed, 1998. https://doi.org/10.1016/j.jhazmat.2010.04.118.
[326] U.S. EPA, METHOD 1684 Total, Fixed and Volatile, Solids and Biosolids, Sci. Technol. (2001).
[327] PanReac AppliChem, Nitrogen Determination by Kjeldahl Method, 2017. https://doi.org/https://www.itwreagents.com/uploads/20180114/A173_EN.pdf.
[328] S. Volk, A. Gratzfeld-Huesgen, Analysis of PAHs in soil according to EPA 8310 method with UV and fluorescence detection, Agil. Technol. - Appl. Note. (2011).
[329] G. Dreschke, S. Papirio, D.M.G. Sisinni, P.N.L. Lens, G. Esposito, Effect of feed glucose and acetic acid on continuous biohydrogen production by Thermotoga neapolitana, Bioresour. Technol. (2019). https://doi.org/10.1016/j.biortech.2018.11.040.
[330] F. Madrid, M. Rubio-Bellido, J. Villaverde, M. Tejada, E. Morillo, Natural attenuation of fluorene and pyrene in contaminated soils and assisted with hydroxypropyl-β-cyclodextrin. Effect of co-contamination, Sci. Total Environ. (2016). https://doi.org/10.1016/j.scitotenv.2016.07.110.
[331] C.H. Li, Y.S. Wong, H.Y. Wang, N.F.Y. Tam, Anaerobic biodegradation of PAHs in mangrove sediment with amendment of NaHCO<inf>3</inf>, J. Environ. Sci. (China). (2015). https://doi.org/10.1016/j.jes.2014.09.028.
[332] R.C. Loehr, J.R. Smith, R.L. Corsi, VOC and SVOC Emissions from Slurry and Solid Phase Bioremediation Processes, Pract. Period. Hazardous, Toxic, Radioact. Waste Manag. (2002). https://doi.org/10.1061/(asce)1090-025x(2001)5:4(211).
[333] F. Lüers, T.E.M. Ten Hulscher, Temperature effect on the partitioning of polycyclic aromatic hydrocarbons between natural organic carbon and water, Chemosphere. (1996). https://doi.org/10.1016/0045-6535(96)00217-2.
[334] M.P. Coover, R.C. Sims, The Effect of Temperature on Polycyclic Aromatic Hydrocarbon Persistence in an Unacclimated Agricultural Soil, Hazard. Waste Hazard. Mater. (1987). https://doi.org/10.1089/hwm.1987.4.69.
[335] M. Kästner, M. Breuer-Jammali, B. Mahro, Impact of inoculation protocols, salinity, and pH on the degradation of polycyclic aromatic hydrocarbons (PAHs) and survival of PAH-degrading bacteria introduced into soil, Appl. Environ. Microbiol. (1998).
[336] M.D. Aitken, W.T. Stringfellow, R.D. Nagel, C. Kazunga, S.-H. Chen, Characteristics of phenanthrene-degrading bacteria isolated from soils

contaminated with polycyclic aromatic hydrocarbons, Can. J. Microbiol. (2011). https://doi.org/10.1139/w98-065.
[337] H.I. Atagana, R.J. Haynes, F.M. Wallis, Optimization of soil physical and chemical conditions for the bioremediation of creosote-contaminated soil, Biodegradation. (2003). https://doi.org/10.1023/A:1024730722751.
[338] T. Sayara, M. Čvančarová, T. Cajthaml, M. Sarrà, A. Sánchez, Anaerobic bioremediation of PAH-contaminated soil: assessment of the degradation of contaminants and biogas production under thermophilic and mesophilic conditions., Environ. Eng. Manag. J. 14 (2015).
[339] S. Thiele, W.G. Brümmer, Bioformation of polycyclic aromatic hydrocarbons in soil under oxygen deficient conditions, Soil Biol. Biochem. (2002). https://doi.org/10.1016/S0038-0717(01)00204-8.
[340] A.B. Patel, S. Singh, A. Patel, K. Jain, S. Amin, D. Madamwar, Synergistic biodegradation of phenanthrene and fluoranthene by mixed bacterial cultures, Bioresour. Technol. 284 (2019) 115–120. https://doi.org/10.1016/j.biortech.2019.03.097.
[341] J.D. Macrae, K.J. Hall, Comparison of methods used to determine the availability of polycyclic aromatic hydrocarbons in marine sediment, Environ. Sci. Technol. (1998). https://doi.org/10.1021/es980165w.
[342] P. Baumard, H. Budzinski, P. Garrigues, H. Dizer, P.D. Hansen, Polycyclic aromatic hydrocarbons in recent sediments and mussels (Mytilus edulis) from the Western Baltic Sea: Occurrence, bioavailability and seasonal variations, Mar. Environ. Res. (1999). https://doi.org/10.1016/S0141-1136(98)00105-6.
[343] A. Gielnik, Y. Pechaud, D. Huguenot, A. Cébron, J.M. Riom, G. Guibaud, G. Esposito, E.D. van Hullebusch, Effect of digestate application on microbial respiration and bacterial communities' diversity during bioremediation of weathered petroleum hydrocarbons contaminated soils, Sci. Total Environ. (2019). https://doi.org/10.1016/j.scitotenv.2019.03.176.
[344] T.D. Gauthier, E.C. Shane, W.F. Guerin, W.R. Seitz, C.L. Grant, Fluorescence Quenching Method for Determining Equilibrium Constants for Polycyclic Aromatic Hydrocarbons Binding to Dissolved Humic Materials, Environ. Sci. Technol. (1986). https://doi.org/10.1021/es00153a012.
[345] T. Kobayashi, H. Sumida, Effects of humic acids on the sorption and bioavailability of pyrene and 1,2-dihydroxynaphthalene, Soil Sci. Plant Nutr. (2015). https://doi.org/10.1080/00380768.2015.1024581.
[346] Y. Liang, D.W. Britt, J.E. McLean, D.L. Sorensen, R.C. Sims, Humic acid effect on pyrene degradation: Finding an optimal range for pyrene solubility and mineralization enhancement, Appl. Microbiol. Biotechnol. (2007). https://doi.org/10.1007/s00253-006-0769-8.
[347] G. Guo, F. Tian, K. Ding, L. Wang, T. Liu, F. Yang, Effect of a bacterial consortium on the degradation of polycyclic aromatic hydrocarbons and bacterial community composition in Chinese soils, Int. Biodeterior. Biodegrad. (2017). https://doi.org/10.1016/j.ibiod.2017.04.022.
[348] H.I. Owamah, S.O. Dahunsi, U.S. Oranusi, M.I. Alfa, Fertilizer and sanitary quality of digestate biofertilizer from the co-digestion of food waste and human excreta, Waste Manag. (2014). https://doi.org/10.1016/j.wasman.2014.01.017.

[349] J. Ariunbaatar, A. Panico, G. Esposito, F. Pirozzi, P.N.L. Lens, Pretreatment methods to enhance anaerobic digestion of organic solid waste, Appl. Energy. (2014). https://doi.org/10.1016/j.apenergy.2014.02.035.
[350] W. Parawira, M. Murto, J.S. Read, B. Mattiasson, Volatile fatty acid production during anaerobic mesophilic digestion of solid potato waste, J. Chem. Technol. Biotechnol. (2004). https://doi.org/10.1002/jctb.1012.
[351] A. Schievano, M. Pognani, G. D'Imporzano, F. Adani, Predicting anaerobic biogasification potential of ingestates and digestates of a full-scale biogas plant using chemical and biological parameters, Bioresour. Technol. (2008). https://doi.org/10.1016/j.biortech.2008.03.030.
[352] E. Panagiotis, K.O. William, Anaerobic acidogenesis of primary sludge: The role of solids retention time, Biotechnol. Bioeng. (1994).
[353] J.I. Horiuchi, T. Shimizu, K. Tada, T. Kanno, M. Kobayashi, Selective production of organic acids in anaerobic acid reactor by pH control, Bioresour. Technol. (2002). https://doi.org/10.1016/S0960-8524(01)00195-X.
[354] B.R. Sharak Genthner, G.T. Townsend, S.E. Lantz, J.G. Mueller, Persistence of polycyclic aromatic hydrocarbon components of creosote under anaerobic enrichment conditions, Arch. Environ. Contam. Toxicol. (1997). https://doi.org/10.1007/s002449900160.
[355] L. Feng, J. Chen, F. Wang, Y. Chen, J. Luo, Acidogenic Fermentation Facilitates Anaerobic Biodegradation of Polycyclic Aromatic Hydrocarbons in Waste Activated Sludge, ACS Sustain. Chem. Eng. (2019). https://doi.org/10.1021/acssuschemeng.8b06425.
[356] L. Su, H. Zhou, A. Zhao, G. Guo, Y. Zhao, Anaerobic Biodegradation of PAH in River Sediment Treated with Different Additives, Procedia Environ. Sci. (2012). https://doi.org/10.1016/j.proenv.2012.10.044.
[357] C.-M. Hung, C.-P. Huang, S.S. Lam, C.-W. Chen, C.-D. Dong, The removal of polycyclic aromatic hydrocarbons (PAHs) from marine sediments using persulfate over a nano-sized iron composite of magnetite and carbon black activator, J. Environ. Chem. Eng. 8 (2020) 104440. https://doi.org/10.1016/j.jece.2020.104440.
[358] X. Xu, H. Zhou, X. Chen, B. Wang, Z. Jin, F. Ji, Biodegradation potential of polycyclic aromatic hydrocarbons by immobilized Klebsiella sp. in soil washing effluent, Chemosphere. (2019). https://doi.org/10.1016/j.chemosphere.2019.01.196.
[359] S. Peng, W. Wu, J. Chen, Removal of PAHs with surfactant-enhanced soil washing: Influencing factors and removal effectiveness, Chemosphere. 82 (2011) 1173–1177. https://doi.org/10.1016/j.chemosphere.2010.11.076.
[360] G.F.C. Lama, A. Errico, S. Francalanci, L. Solari, F. Preti, G.B. Chirico, Evaluation of flow resistance models based on field experiments in a partly vegetated reclamation channel, Geosci. 10 (2020) 47. https://doi.org/10.3390/geosciences10020047.
[361] X. Bai, Y. Wang, X. Zheng, K. Zhu, A. Long, X. Wu, H. Zhang, Remediation of phenanthrene contaminated soil by coupling soil washing with Tween 80, oxidation using the UV/S2O82− process and recycling of the surfactant, Chem. Eng. J. (2019). https://doi.org/10.1016/j.cej.2019.03.116.

[362] J. Guo, X. Wen, J. Yang, T. Fan, Removal of benzo(a)pyrene in polluted aqueous solution and soil using persulfate activated by corn straw biochar, J. Environ. Manage. (2020). https://doi.org/10.1016/j.jenvman.2020.111058.
[363] A.B. Patel, S. Shaikh, K.R. Jain, C. Desai, D. Madamwar, Polycyclic Aromatic Hydrocarbons: Sources, Toxicity, and Remediation Approaches, Front. Microbiol. (2020). https://doi.org/10.3389/fmicb.2020.562813.
[364] A. El-Maradny, M.M. El-Sherbiny, M. Ghandourah, M. El-Amin Bashir, M. Orif, PAH bioaccumulation in two polluted sites along the eastern coast of the Red Sea, Saudi Arabia, Int. J. Environ. Sci. Technol. (2020). https://doi.org/10.1007/s13762-020-02929-0.
[365] A.S. Bisht, Commercial Surfactants for Remediation-Methodology, in: 2019: pp. 31–38. https://doi.org/10.1007/978-981-13-0221-3_6.
[366] X. Gong, X. Xu, Z. Gong, X. Li, C. Jia, M. Guo, H. Li, Remediation of PAH-contaminated soil at a gas manufacturing plant by a combined two-phase partition system washing and microbial degradation process, Environ. Sci. Pollut. Res. (2015). https://doi.org/10.1007/s11356-015-4466-y.
[367] A. Oliva, L.C. Tan, S. Papirio, G. Esposito, P.N.L. Lens, Effect of methanol-organosolv pretreatment on anaerobic digestion of lignocellulosic materials, Renew. Energy. 169 (2021) 1000–1012. https://doi.org/https://doi.org/10.1016/j.renene.2020.12.095.
[368] R. Andreozzi, M. Fabbricino, A. Ferrraro, S. Lerza, R. Marotta, F. Pirozzi, M. Race, Simultaneous removal of Cr(III) from high contaminated soil and recovery of lactic acid from the spent solution, J. Environ. Manage. (2020). https://doi.org/10.1016/j.jenvman.2020.110584.
[369] F. Moscoso, F.J. Deive, M.A. Longo, M.A. Sanromán, Technoeconomic assessment of phenanthrene degradation by Pseudomonas stutzeri CECT 930 in a batch bioreactor, Bioresour. Technol. (2012). https://doi.org/10.1016/j.biortech.2011.10.053.
[370] W. Chen, H. Zhang, M. Zhang, X. Shen, X. Zhang, F. Wu, J. Hu, B. Wang, X. Wang, Removal of PAHs at high concentrations in a soil washing solution containing TX-100 via simultaneous sorption and biodegradation processes by immobilized degrading bacteria in PVA-SA hydrogel beads, J. Hazard. Mater. (2020) 124533. https://doi.org/10.1016/j.jhazmat.2020.124533.
[371] C.L. Guo, H.W. Zhou, Y.S. Wong, N.F.Y. Tam, Isolation of PAH-degrading bacteria from mangrove sediments and their biodegradation potential, Mar. Pollut. Bull. 51 (2005) 1054–1061. https://doi.org/10.1016/j.marpolbul.2005.02.012.
[372] B. Gargouri, F. Karray, N. Mhiri, F. Aloui, S. Sayadi, Application of a continuously stirred tank bioreactor (CSTR) for bioremediation of hydrocarbon-rich industrial wastewater effluents, J. Hazard. Mater. (2011). https://doi.org/10.1016/j.jhazmat.2011.02.057.
[373] F. Cazals, D. Huguenot, M. Crampon, S. Colombano, S. Betelu, N. Galopin, A. Perrault, M.-O. Simonnot, I. Ignatiadis, S. Rossano, Production of biosurfactant using the endemic bacterial community of a PAHs contaminated soil, and its potential use for PAHs remobilization, Sci. Total Environ. 709 (2020) 136143. https://doi.org/10.1016/j.scitotenv.2019.136143.

[374] T.A. Oyehan, A.A. Al-Thukair, Isolation and characterization of PAH-degrading bacteria from the Eastern Province, Saudi Arabia, Mar. Pollut. Bull. (2017). https://doi.org/10.1016/j.marpolbul.2016.11.007.
[375] Q. Cai, B. Zhang, B. Chen, Z. Zhu, W. Lin, T. Cao, Screening of biosurfactant producers from petroleum hydrocarbon contaminated sources in cold marine environments, Mar. Pollut. Bull. 86 (2014) 402–410. https://doi.org/10.1016/j.marpolbul.2014.06.039.
[376] C. Muangchinda, A. Rungsihiranrut, P. Prombutara, S. Soonglerdsongpha, O. Pinyakong, 16S metagenomic analysis reveals adaptability of a mixed-PAH-degrading consortium isolated from crude oil-contaminated seawater to changing environmental conditions, J. Hazard. Mater. 357 (2018) 119–127. https://doi.org/10.1016/j.jhazmat.2018.05.062.
[377] M.L.B.B. Da Silva, P.J.J.J. Alvarez, Effects of Ethanol versus MTBE on Benzene, Toluene, Ethylbenzene, and Xylene Natural Attenuation in Aquifer Columns, J. Environ. Eng. 128 (2002) 862–867. https://doi.org/10.1061/(asce)0733-9372(2002)128:9(862).
[378] S.C. Wilson, K.C. Jones, Bioremediation of soil contaminated with polynuclear aromatic hydrocarbons (PAHs): A review, Environ. Pollut. 81 (1993) 229–249. https://doi.org/10.1016/0269-7491(93)90206-4.
[379] C.-Y. Wang, F. Wang, T. Wang, X.-L. Yang, Y.-R. Bian, F.O. Kengara, Z.-B. Li, X. Jiang, Effects of Autoclaving and Mercuric Chloride Sterilization on PAHs Dissipation in a Two-Liquid-Phase Soil Slurry, Pedosphere. 21 (2011) 56–64. https://doi.org/10.1016/S1002-0160(10)60079-3.
[380] K. Queenan, C.H. Burton, C. Bechir, Development of a centrifuge-based procedure to analyse agricultural effluents for total and volatile suspended solids, Bioresour. Technol. 57 (1996) 259–263. https://doi.org/10.1016/S0960-8524(96)00077-6.
[381] S. Matassa, S. Papirio, G. Esposito, F. Pirozzi, Ammonia stripping from buffalo manure digestate for future nitrogen upcycling into bio-based products, in: 2020 IEEE Int. Work. Metrol. Agric. For. MetroAgriFor 2020 - Proc., 2020. https://doi.org/10.1109/MetroAgriFor50201.2020.9277623.
[382] APAT, IRSA-CNR, Agenzia per la Protezione dell'Ambiente e per i Servizi Tecnici (APAT), Istituto di Ricerca sulle Acque del Consiglio Nazionale delle Ricerche (IRSA-CNR). 2003, Manuali e Linee Guid. 29 (2003).
[383] A. Monballiu, K. Ghyselbrecht, L. Pinoy, B. Meesschaert, Phosphorus reclamation by end-of-pipe recovery as calcium phosphate from effluent of wastewater treatment plants of agroindustry, J. Environ. Chem. Eng. 8 (2020) 104280. https://doi.org/https://doi.org/10.1016/j.jece.2020.104280.
[384] L. Ke, Y.-S. Wong, N.F.-Y. Tam, Determination of Polycyclic Aromatic Hydrocarbons in Mangrove Sediments: Comparison of Two Internal Standard Surrogate Methods and Quality-Control Procedures, Int. J. Environ. Anal. Chem. 84 (2004) 661–675. https://doi.org/10.1080/03067310410001684547.
[385] S. Claassen, E. du Toit, M. Kaba, C. Moodley, H.J. Zar, M.P. Nicol, A comparison of the efficiency of five different commercial DNA extraction kits for extraction of DNA from faecal samples, J. Microbiol. Methods. (2013). https://doi.org/10.1016/j.mimet.2013.05.008.

[386] M. Aryal, M. Liakopoulou-Kyriakides, Biodegradation and Kinetics of Phenanthrene and Pyrene in the Presence of Nonionic Surfactants by Arthrobacter Strain Sphe3, Water, Air, Soil Pollut. 224 (2013) 1426. https://doi.org/10.1007/s11270-012-1426-8.
[387] B. Gupta, S. Puri, I.S. Thakur, J. Kaur, Comparative evaluation of growth kinetics for pyrene degradation by Acinetobacter pittii NFL and Enterobacter cloacae BT in the presence of biosurfactant, Bioresour. Technol. Reports. (2020). https://doi.org/10.1016/j.biteb.2019.100369.
[388] G.N. Tenea, D. Olmedo, C. Ortega, Peptide-based formulation from lactic acid bacteria impairs the pathogen growth in ananas comosus (pineapple), Coatings. (2020). https://doi.org/10.3390/COATINGS10050457.
[389] M.J. McFarland, R.C. Sims, Thermodynamic Framework for Evaluating PAH Degradation in the Subsurface, Groundwater. (1991). https://doi.org/10.1111/j.1745-6584.1991.tb00576.x.
[390] S.H. Woo, B.E. Rittmann, Microbial energetics and stoichiometry for biodegradation of aromatic compounds involving oxygenation reactions, Biodegradation. (2000). https://doi.org/10.1023/A:1011162830401.
[391] R. Iturbe, C. Flores, C. Chavez, G. Bautista, L.G. Torres, Remediation of contaminated soil using soil washing and biopile methodologies at a field level, J. Soils Sediments. (2004). https://doi.org/10.1007/bf02991055.
[392] P.A. Johnston, H. Zhou, A. Aui, M.M. Wright, Z. Wen, R.C. Brown, A lignin-first strategy to recover hydroxycinnamic acids and improve cellulosic ethanol production from corn stover, Biomass and Bioenergy. (2020). https://doi.org/10.1016/j.biombioe.2020.105579.
[393] A.G.M. Ibrahim, A.M. Rashad, I. Dincer, Exergoeconomic analysis for cost optimization of a solar distillation system, Sol. Energy. (2017). https://doi.org/10.1016/j.solener.2017.05.020.
[394] R. Mansour, S. Rioual, B. Lescop, P. Talbot, M. Abboud, W. Farah, G. Tanné, Development of a resonant microwave sensor for sediment density characterization, Sensors (Switzerland). (2020). https://doi.org/10.3390/s20041058.
[395] R.K. Rai, V.P. Singh, A. Upadhyay, Soil Analysis, in: Plan. Eval. Irrig. Proj., Elsevier, 2017: pp. 505–523. https://doi.org/10.1016/B978-0-12-811748-4.00017-0.
[396] G.F.C. Lama, M. Crimaldi, V. Pasquino, R. Padulano, G.B. Chirico, Bulk Drag Predictions of Riparian Arundo donax Stands through UAV-Acquired Multispectral Images, Water. 13 (2021) 1333. https://doi.org/10.3390/w13101333.
[397] A. Chiavola, R. Baciocchi, R. Gavasci, Biological treatment of PAH-contaminated sediments in a Sequencing Batch Reactor, J. Hazard. Mater. (2010). https://doi.org/10.1016/j.jhazmat.2010.08.010.
[398] A. Pedetta, K. Pouyte, M.K. Herrera Seitz, P.A. Babay, M. Espinosa, M. Costagliola, C.A. Studdert, S.R. Peressutti, Phenanthrene degradation and strategies to improve its bioavailability to microorganisms isolated from brackish sediments, Int. Biodeterior. Biodegradation. 84 (2013) 161–167. https://doi.org/10.1016/j.ibiod.2012.04.018.

[399] K. Sun, J. Liu, Y. Gao, L. Jin, Y. Gu, W. Wang, Isolation, plant colonization potential and phenanthrene degradation performance of the endophytic bacterium Pseudomonas sp. Ph6-gfp, Sci. Rep. 4 (2015) 5462. https://doi.org/10.1038/srep05462.
[400] A. Janbandhu, M.H. Fulekar, Biodegradation of phenanthrene using adapted microbial consortium isolated from petrochemical contaminated environment, J. Hazard. Mater. 187 (2011) 333–340. https://doi.org/10.1016/j.jhazmat.2011.01.034.
[401] F. Moscoso, I. Teijiz, F.J. Deive, M.A. Sanromán, Efficient PAHs biodegradation by a bacterial consortium at flask and bioreactor scale, Bioresour. Technol. (2012). https://doi.org/10.1016/j.biortech.2012.05.095.
[402] E.W. Low, H.A. Chase, Reducing production of excess biomass during wastewater treatment, Water Res. (1999). https://doi.org/10.1016/S0043-1354(98)00325-X.
[403] M.L.B. Da Silva, P.J.J. Alvarez, Enhanced anaerobic biodegradation of benzene-toluene-ethylbenzene-xylene- ethanol mixtures in bioaugmented aquifer columns, Appl. Environ. Microbiol. (2004). https://doi.org/10.1128/AEM.70.8.4720-4726.2004.
[404] I. Mozo, G. Lesage, J. Yin, Y. Bessiere, L. Barna, M. Sperandio, Dynamic modeling of biodegradation and volatilization of hazardous aromatic substances in aerobic bioreactor, Water Res. (2012). https://doi.org/10.1016/j.watres.2012.07.014.
[405] J. Chen, M.H. Wong, Y.S. Wong, N.F.Y. Tam, Multi-factors on biodegradation kinetics of polycyclic aromatic hydrocarbons (PAHs) by Sphingomonas sp. a bacterial strain isolated from mangrove sediment, Mar. Pollut. Bull. (2008). https://doi.org/10.1016/j.marpolbul.2008.03.013.
[406] S. Guha, P.R. Jaffé, Biodegradation kinetics of phenanthrene partitioned into the micellar phase of nonionic surfactants, Environ. Sci. Technol. (1996). https://doi.org/10.1021/es950385z.
[407] E.M. Rodrigues, A.V.N. de Carvalho Teixeira, D.E. Cesar, M.R. Tótola, Strategy to improve crude oil biodegradation in oligotrophic aquatic environments: W/O/W fertilized emulsions and hydrocarbonoclastic bacteria, Brazilian J. Microbiol. (2020). https://doi.org/10.1007/s42770-020-00244-x.
[408] M.S. Reddy, B. Naresh, T. Leela, M. Prashanthi, N.C. Madhusudhan, G. Dhanasri, P. Devi, Biodegradation of phenanthrene with biosurfactant production by a new strain of Brevibacillus sp., Bioresour. Technol. (2010). https://doi.org/10.1016/j.biortech.2010.04.054.
[409] D. Zhang, L. Zhu, F. Li, Influences and mechanisms of surfactants on pyrene biodegradation based on interactions of surfactant with a Klebsiella oxytoca strain, Bioresour. Technol. (2013). https://doi.org/10.1016/j.biortech.2013.05.077.
[410] S. Mallick, S. Chatterjee, T.K. Dutta, A novel degradation pathway in the assimilation of phenanthrene by Staphylococcus sp. strain PN/Y via meta-cleavage of 2-hydroxy-1-napthoic acid: Formation of trans-2,3-dioxo-5-(2′-hydroxyphenyl)-pent-4-enoic acid, Microbiology. (2007). https://doi.org/10.1099/mic.0.2006/004218-0.

[411] S. Demanèche, C. Meyer, J. Micoud, M. Louwagie, J.C. Willison, Y. Jouanneau, Identification and functional analysis of two aromatic-ring-hydroxylating dioxygenases from a Sphingomonas strain that degrades various polycyclic aromatic hydrocarbons, Appl. Environ. Microbiol. (2004). https://doi.org/10.1128/AEM.70.11.6714-6725.2004.
[412] X.Q. Tao, G.N. Lu, Z. Dang, X.Y. Yi, C. Yang, Isolation of phenanthrene-degrading bacteria and characterization of phenanthrene metabolites, World J. Microbiol. Biotechnol. (2007). https://doi.org/10.1007/s11274-006-9276-4.
[413] J. Zhong, L. Luo, B. Chen, S. Sha, Q. Qing, N.F.Y. Tam, Y. Zhang, T. Luan, Degradation pathways of 1-methylphenanthrene in bacterial Sphingobium sp. MP9-4 isolated from petroleum-contaminated soil, Mar. Pollut. Bull. (2017). https://doi.org/10.1016/j.marpolbul.2016.11.020.
[414] B. Zhao, H. Wang, X. Mao, R. Li, Biodegradation of phenanthrene by a halophilic bacterial consortium under aerobic conditions, Curr. Microbiol. (2009). https://doi.org/10.1007/s00284-008-9309-3.
[415] D. Ghosal, J. Chakraborty, P. Khara, T.K. Dutta, Degradation of phenanthrene via meta-cleavage of 2-hydroxy-1-naphthoic acid by Ochrobactrum sp. strain PWTJD, FEMS Microbiol. Lett. (2010). https://doi.org/10.1111/j.1574-6968.2010.02129.x.
[416] S. Mallick, T.K. Dutta, Kinetics of phenanthrene degradation by Staphylococcus sp. strain PN/Y involving 2-hydroxy-1-naphthoic acid in a novel metabolic pathway, Process Biochem. 43 (2008) 1004–1008. https://doi.org/https://doi.org/10.1016/j.procbio.2008.04.022.
[417] J. Wang, H. Xu, M. An, G. Yan, Kinetics and characteristics of phenanthrene degradation by a microbial consortium, Pet. Sci. (2008). https://doi.org/10.1007/s12182-008-0012-6.
[418] A.A. Pourbabaee, M.H. Shahriari, H. Garousin, Biodegradation of phenanthrene as a model hydrocarbon: Power display of a super-hydrophobic halotolerant enriched culture derived from a saline-sodic soil, Biotechnol. Reports. (2019). https://doi.org/10.1016/j.btre.2019.e00388.
[419] M. Lin, X. Hu, W. Chen, H. Wang, C. Wang, Biodegradation of phenanthrene by Pseudomonas sp: BZ-3, isolated from crude oil contaminated soil, Int. Biodeterior. Biodegrad. (2014). https://doi.org/10.1016/j.ibiod.2014.07.011.
[420] B. Wang, X. Xu, X. Yao, H. Tang, F. Ji, Degradation of phenanthrene and fluoranthene in a slurry bioreactor using free and Ca-alginate-immobilized Sphingomonas pseudosanguinis and Pseudomonas stutzeri bacteria, J. Environ. Manage. (2019). https://doi.org/10.1016/j.jenvman.2019.109388.
[421] Y.M. Kim, C.K. Ahn, S.H. Woo, G.Y. Jung, J.M. Park, Synergic degradation of phenanthrene by consortia of newly isolated bacterial strains, J. Biotechnol. (2009). https://doi.org/10.1016/j.jbiotec.2009.09.021.
[422] J. Ma, W. Zhang, Y. Chen, S. Zhang, Q. Feng, H. Hou, F. Chen, Spatial variability of PAHs and microbial community structure in surrounding surficial soil of coal-fired power plants in Xuzhou, China, Int. J. Environ. Res. Public Health. (2016). https://doi.org/10.3390/ijerph13090878.
[423] B. Chen, R. He, K. Yuan, E. Chen, L. Lin, X. Chen, S. Sha, J. Zhong, L. Lin, L. Yang, Y. Yang, X. Wang, S. Zou, T. Luan, Polycyclic aromatic hydrocarbons

(PAHs) enriching antibiotic resistance genes (ARGs) in the soils, Environ. Pollut. (2017). https://doi.org/10.1016/j.envpol.2016.11.047.
[424] D. Huang, Z. Zhang, M. Sun, Z. Feng, M. Ye, Characterization and ecological function of bacterial communities in seabed sediments of the southwestern Yellow Sea and northwestern East China Sea, Western Pacific, Sci. Total Environ. (2020). https://doi.org/10.1016/j.scitotenv.2020.143233.
[425] L.K. Redfern, C.M. Gardner, E. Hodzic, P.L. Ferguson, H. Hsu-Kim, C.K. Gunsch, A new framework for approaching precision bioremediation of PAH contaminated soils, J. Hazard. Mater. (2019). https://doi.org/10.1016/j.jhazmat.2019.120859.
[426] S. Storey, M.M. Ashaari, N. Clipson, E. Doyle, A.B. De Menezes, Opportunistic bacteria dominate the soil microbiome response to phenanthrene in a microcosm-based study, Front. Microbiol. (2018). https://doi.org/10.3389/fmicb.2018.02815.
[427] F. Thomas, E. Corre, A. Cébron, Stable isotope probing and metagenomics highlight the effect of plants on uncultured phenanthrene-degrading bacterial consortium in polluted soil, ISME J. (2019). https://doi.org/10.1038/s41396-019-0394-z.
[428] J. Wang, X. Song, Q. Li, H. Bai, C. Zhu, B. Weng, D. Yan, J. Bai, Bioenergy generation and degradation pathway of phenanthrene and anthracene in a constructed wetland-microbial fuel cell with an anode amended with nZVI, Water Res. (2019). https://doi.org/10.1016/j.watres.2018.11.075.
[429] J. Wang, H. Xu, S. Guo, Isolation and characteristics of a microbial consortium for effectively degrading phenanthrene, Pet. Sci. (2007). https://doi.org/10.1007/s12182-007-0012-y.
[430] N.A.F. Mohd-Kamil, N.H. Hussain, M.B. Mizad, S. Abdul-Talib, Enhancing Performance of Sphingobacterium spiritivorum in Bioremediation Phenanthrene Contaminated Sand, Remediation. (2014). https://doi.org/10.1002/rem.21398.
[431] A. Pugazhendi, H. Qari, J.M. Al-Badry Basahi, J.J. Godon, J. Dhavamani, Role of a halothermophilic bacterial consortium for the biodegradation of PAHs and the treatment of petroleum wastewater at extreme conditions, Int. Biodeterior. Biodegrad. (2017). https://doi.org/10.1016/j.ibiod.2017.03.015.
[432] F. Bücker, C.S. Barbosa, P.D. Quadros, M.K. Bueno, P. Fiori, C. te Huang, A.P.G. Frazzon, M.F. Ferrão, F.A. de Oliveira Camargo, F.M. Bento, Fuel biodegradation and molecular characterization of microbial biofilms in stored diesel/biodiesel blend B10 and the effect of biocide, Int. Biodeterior. Biodegradation. 95 (2014) 346–355. https://doi.org/10.1016/j.ibiod.2014.05.030.
[433] N. González-Benítez, L.F. Bautista, R. Simarro, C. Vargas, A. Salmerón, Y. Murillo, M.C. Molina, Bacterial diversity in aqueous/sludge phases within diesel fuel storage tanks, World J. Microbiol. Biotechnol. 36 (2020) 180. https://doi.org/10.1007/s11274-020-02956-6.
[434] T.M. Lozano, A.L. McCutchan, M.J. Krzmarzick, Hydraulic fracturing fluid compositions induce differential enrichment of soil bacterial communities, Environ. Eng. Sci. (2019). https://doi.org/10.1089/ees.2018.0271.

[435] Y.T. Chang, C.H. Hung, H.L. Chou, Effects of polyethoxylate lauryl ether (Brij 35) addition on phenanthrene biodegradation in a soil/water system, J. Environ. Sci. Heal. - Part A Toxic/Hazardous Subst. Environ. Eng. (2014). https://doi.org/10.1080/10934529.2014.951228.
[436] K. Furtak, K. Gawryjołek, A. Gałązka, J. Grządziel, The Response of Red Clover (Trifolium pratense L.) to Separate and Mixed Inoculations with Rhizobium leguminosarum and Azospirillum brasilense in Presence of Polycyclic Aromatic Hydrocarbons, Int. J. Environ. Res. Public Health. 17 (2020) 5751. https://doi.org/10.3390/ijerph17165751.
[437] M. Viñas, J. Sabaté, M.J. Espuny, A.M. Solanas, Bacterial community dynamics and polycyclic aromatic hydrocarbon degradation during bioremediation of heavily creosote-contaminated soil, Appl. Environ. Microbiol. (2005). https://doi.org/10.1128/AEM.71.11.7008-7018.2005.
[438] S. Gao, J.S. Seo, J. Wang, Y.S. Keum, J. Li, Q.X. Li, Multiple degradation pathways of phenanthrene by Stenotrophomonas maltophilia C6, Int. Biodeterior. Biodegrad. (2013). https://doi.org/10.1016/j.ibiod.2013.01.012.
[439] M. Xiao, X. Yin, H. Gai, H. Ma, Y. Qi, K. Li, X. Hua, M. Sun, H. Song, Effect of hydroxypropyl-B-cyclodextrin on the cometabolism of phenol and phenanthrene by a novel Chryseobacterium sp., Bioresour. Technol. (2019). https://doi.org/10.1016/j.biortech.2018.10.087.
[440] V. Parab, M. Phadke, Co-biodegradation studies of naphthalene and phenanthrene using bacterial consortium, J. Environ. Sci. Heal. Part A. 55 (2020) 912–924. https://doi.org/10.1080/10934529.2020.1754054.
[441] F. Wang, C. Li, H. Wang, W. Chen, Q. Huang, Characterization of a phenanthrene-degrading microbial consortium enriched from petrochemical contaminated environment, Int. Biodeterior. Biodegrad. (2016). https://doi.org/10.1016/j.ibiod.2016.08.028.
[442] J. Liang, S. Gao, Z. Wu, H.H.M. Rijnaarts, T. Grotenhuis, DNA-SIP identification of phenanthrene-degrading bacteria undergoing bioaugmentation and natural attenuation in petroleum-contaminated soil, Chemosphere. (2020) 128984. https://doi.org/10.1016/j.chemosphere.2020.128984.
[443] M.D. Jones, E.A. Rodgers-Vieira, J. Hu, M.D. Aitken, Association of growth substrates and bacterial genera with benzo[a]pyrene mineralization in contaminated soil, Environ. Eng. Sci. (2014). https://doi.org/10.1089/ees.2014.0275.
[444] Sakshi, A.K. Haritash, A comprehensive review of metabolic and genomic aspects of PAH-degradation, Arch. Microbiol. 202 (2020) 2033–2058. https://doi.org/10.1007/s00203-020-01929-5.
[445] X.Q. Tao, J.P. Liu, G.N. Lu, X. Guo, H.P. Jiang, G.Q. Sun, Biodegradation of phenanthrene in artificial seawater by using free and immobilized strain of Sphingomonas sp. GY2B, African J. Biotechnol. 9 (2010) 2654–2660. https://doi.org/10.5897/AJB2010.000-3084.
[446] H.P. Zhao, L. Wang, J.R. Ren, Z. Li, M. Li, H.W. Gao, Isolation and characterization of phenanthrene-degrading strains Sphingomonas sp. ZP1 and Tistrella sp. ZP5, J. Hazard. Mater. (2008). https://doi.org/10.1016/j.jhazmat.2007.08.008.

[447] V.M. León, I. García, C. Martínez-Gómez, J.A. Campillo, J. Benedicto, Heterogeneous distribution of polycyclic aromatic hydrocarbons in surface sediments and red mullet along the Spanish Mediterranean coast, Mar. Pollut. Bull. (2014). https://doi.org/10.1016/j.marpolbul.2014.07.049.
[448] A. Yadu, B.P. Sahariah, J. Anandkumar, Novel Bioremediation Approach for Treatment of Naphthalene, Ammonia-N and Sulphate in Fed-batch Reactor, J. Environ. Chem. Eng. (2019). https://doi.org/10.1016/j.jece.2019.103388.
[449] C.E. Schaefer, X. Yang, O. Pelz, D.T. Tsao, S.H. Streger, R.J. Steffan, Anaerobic biodegradation of iso-butanol and ethanol and their relative effects on BTEX biodegradation in aquifer materials, Chemosphere. 81 (2010) 1104–1110. https://doi.org/10.1016/j.chemosphere.2010.09.002.
[450] X.Y. Lu, T. Zhang, H.H.P. Fang, Bacteria-mediated PAH degradation in soil and sediment, Appl. Microbiol. Biotechnol. (2011). https://doi.org/10.1007/s00253-010-3072-7.
[451] G. Li, G. Lan, Y. Liu, C. Chen, L. Lei, J. Du, Y. Lu, Q. Li, G. Du, J. Zhang, Evaluation of biodegradability and biotoxicity of surfactants in soil, RSC Adv. (2017). https://doi.org/10.1039/c7ra02105d.
[452] C. Liu, C.I. Olivares, A.J. Pinto, C. V. Lauderdale, J. Brown, M. Selbes, T. Karanfil, The control of disinfection byproducts and their precursors in biologically active filtration processes, Water Res. (2017). https://doi.org/10.1016/j.watres.2017.07.080.
[453] S. Fan, Z. Xiao, M. Li, S. Li, Pervaporation membrane bioreactor with permeate fractional condensation and mechanical vapor compression for energy efficient ethanol production, Appl. Energy. (2016). https://doi.org/10.1016/j.apenergy.2016.07.060.
[454] W. Chen, H. Li, Cost-Effectiveness Analysis for Soil Heavy Metal Contamination Treatments, Water. Air. Soil Pollut. (2018). https://doi.org/10.1007/s11270-018-3784-3.
[455] I. Gabriele, M. Race, S. Papirio, G. Esposito, Phytoremediation of pyrene-contaminated soils: A critical review of the key factors affecting the fate of pyrene, J. Environ. Manage. 293 (2021) 112805. https://doi.org/10.1016/j.jenvman.2021.112805.
[456] I. Gdara, I. Zrafi, C. Balducci, A. Cecinato, A. Ghrabi, Seasonal Distribution, Source Identification, and Toxicological Risk Assessment of Polycyclic Aromatic Hydrocarbons (PAHs) in Sediments from Wadi El Bey Watershed in Tunisia, Arch. Environ. Contam. Toxicol. 73 (2017) 488–510. https://doi.org/10.1007/s00244-017-0440-7.
[457] M. Cheng, G. Zeng, D. Huang, C. Yang, C. Lai, C. Zhang, Y. Liu, Advantages and challenges of Tween 80 surfactant-enhanced technologies for the remediation of soils contaminated with hydrophobic organic compounds, Chem. Eng. J. 314 (2017) 98–113. https://doi.org/10.1016/j.cej.2016.12.135.
[458] O. Iglesias, M.A. Sanromán, M. Pazos, Surfactant-Enhanced Solubilization and Simultaneous Degradation of Phenanthrene in Marine Sediment by Electro-Fenton Treatment, Ind. Eng. Chem. Res. 53 (2014) 2917–2923. https://doi.org/10.1021/ie4041115.
[459] E.V. dos Santos, C. Sáez, P. Cañizares, D.R. da Silva, C.A. Martínez-Huitle,

M.A. Rodrigo, Treatment of ex-situ soil-washing fluids polluted with petroleum by anodic oxidation, photolysis, sonolysis and combined approaches, Chem. Eng. J. 310 (2017) 581–588. https://doi.org/10.1016/j.cej.2016.05.015.
[460] F. Moscoso, I. Teijiz, M.A. Sanromán, F.J. Deive, On the Suitability of a Bacterial Consortium To Implement a Continuous PAHs Biodegradation Process in a Stirred Tank Bioreactor, Ind. Eng. Chem. Res. 51 (2012) 15895–15900. https://doi.org/10.1021/ie3021736.
[461] M. Lu, L.P. Gu, W.H. Xu, Treatment of petroleum refinery wastewater using a sequential anaerobic-aerobic moving-bed biofilm reactor system based on suspended ceramsite, Water Sci. Technol. 67 (2013) 1976–1983. https://doi.org/10.2166/wst.2013.077.
[462] J. Li, C. Luo, D. Zhang, X. Cai, L. Jiang, X. Zhao, G. Zhang, Diversity of the active phenanthrene degraders in PAH-polluted soil is shaped by ryegrass rhizosphere and root exudates, Soil Biol. Biochem. 128 (2019) 100–110. https://doi.org/10.1016/j.soilbio.2018.10.008.
[463] J. Li, D. Zhang, B. Li, C. Luo, G. Zhang, Identifying the Active Phenanthrene Degraders and Characterizing Their Metabolic Activities at the Single-Cell Level by the Combination of Magnetic-Nanoparticle-Mediated Isolation, Stable-Isotope Probing, and Raman-Activated Cell Sorting (MMI–SIP–RACS), Environ. Sci. Technol. 56 (2022) 2289–2299. https://doi.org/10.1021/acs.est.1c04952.
[464] R. Hasanzadeh, B. Abbasi Souraki, A. Pendashteh, G. Khayati, F.R. Ahmadun, Application of isolated halophilic microorganisms suspended and immobilized on walnut shell as biocarrier for treatment of oilfield produced water, J. Hazard. Mater. 400 (2020) 123197. https://doi.org/10.1016/j.jhazmat.2020.123197.
[465] E.J.T.M. Leenen, V.A.P. Dos Santos, K.C.F. Grolle, J. Tramper, R. Wijffels, Characteristics of and selection criteria for support materials for cell immobilization in wastewater treatment, Water Res. 30 (1996) 2985–2996. https://doi.org/10.1016/S0043-1354(96)00209-6.
[466] A. Rombel, P. Krasucka, P. Oleszczuk, Sustainable biochar-based soil fertilizers and amendments as a new trend in biochar research, Sci. Total Environ. (2021) 151588. https://doi.org/10.1016/j.scitotenv.2021.151588.
[467] P. Godlewska, A. Siatecka, M. Kończak, P. Oleszczuk, Adsorption capacity of phenanthrene and pyrene to engineered carbon-based adsorbents produced from sewage sludge or sewage sludge-biomass mixture in various gaseous conditions, Bioresour. Technol. 280 (2019) 421–429. https://doi.org/10.1016/j.biortech.2019.02.021.
[468] L. Song, X. Niu, N. Zhang, T. Li, Effect of biochar-immobilized Sphingomonas sp. PJ2 on bioremediation of PAHs and bacterial community composition in saline soil, Chemosphere. 279 (2021) 130427. https://doi.org/10.1016/j.chemosphere.2021.130427.
[469] B. Chen, M. Yuan, L. Qian, Enhanced bioremediation of PAH-contaminated soil by immobilized bacteria with plant residue and biochar as carriers, J. Soils Sediments. 12 (2012) 1350–1359. https://doi.org/10.1007/s11368-012-0554-5.
[470] S. Liu, C. Guo, W. Lin, F. Wu, G. Lu, J. Lu, Z. Dang, Comparative transcriptomic evidence for Tween80-enhanced biodegradation of

phenanthrene by Sphingomonas sp. GY2B, Sci. Total Environ. 609 (2017) 1161–1171. https://doi.org/10.1016/j.scitotenv.2017.07.245.
[471] S. Liu, C. Guo, X. Liang, F. Wu, Z. Dang, Nonionic surfactants induced changes in cell characteristics and phenanthrene degradation ability of Sphingomonas sp. GY2B, Ecotoxicol. Environ. Saf. 129 (2016) 210–218. https://doi.org/10.1016/j.ecoenv.2016.03.035.
[472] Y. Tao, H. Huang, H. Zhang, Remediation of Cu-phenanthrene co-contaminated soil by soil washing and subsequent photoelectrochemical process in presence of persulfate, J. Hazard. Mater. 400 (2020) 123111. https://doi.org/10.1016/j.jhazmat.2020.123111.
[473] A. Siatecka, K. Różyło, Y.S. Ok, P. Oleszczuk, Biochars ages differently depending on the feedstock used for their production: Willow- versus sewage sludge-derived biochars, Sci. Total Environ. 789 (2021) 147458. https://doi.org/10.1016/j.scitotenv.2021.147458.
[474] A.K. Jaiswal, O. Frenkel, L. Tsechansky, Y. Elad, E.R. Graber, Immobilization and deactivation of pathogenic enzymes and toxic metabolites by biochar: A possible mechanism involved in soilborne disease suppression, Soil Biol. Biochem. 121 (2018) 59–66. https://doi.org/10.1016/j.soilbio.2018.03.001.
[475] B. Tomczyk, A. Siatecka, K. Jędruchniewicz, A. Sochacka, A. Bogusz, P. Oleszczuk, Polycyclic aromatic hydrocarbons (PAHs) persistence, bioavailability and toxicity in sewage sludge- or sewage sludge-derived biochar-amended soil, Sci. Total Environ. 747 (2020) 141123. https://doi.org/10.1016/j.scitotenv.2020.141123.
[476] Q. Chen, J. Li, M. Liu, H. Sun, M. Bao, Study on the biodegradation of crude oil by free and immobilized bacterial consortium in marine environment, PLoS One. 12 (2017) e0174445. https://doi.org/10.1371/journal.pone.0174445.
[477] B. Guieysse, I. Bernhoft, B.E. Andersson, T. Henrysson, S. Olsson, B. Mattiasson, Degradation of acenaphthene, phenanthrene and pyrene in a packed-bed biofilm reactor, Appl. Microbiol. Biotechnol. 54 (2000) 826–831. https://doi.org/10.1007/s002530000442.
[478] E. Fenibo, 2.2-Diphenic Acid: A Reliable Biomarker Of Phenanthrene Biodegradation, Sci. Prepr. (2021). https://doi.org/10.14293/S2199-1006.1.SOR-.PPP4HD5.v1.
[479] D. ASTM, Standard test method for ash in the analysis sample of coal and coke from coal, ASTM Int. West Conshohocken, PA. (2008).
[480] J.M. Novak, I. Lima, B. Xing, J.W. Gaskin, C. Steiner, K.C. Das, M. Ahmedna, D. Rehrah, D.W. Watts, W.J. Busscher, Characterization of designer biochar produced at different temperatures and their effects on a loamy sand, Ann. Environ. Sci. 3 (2009) 195–206.
[481] A. Siatecka, P. Oleszczuk, Mechanism of aging of biochars obtained at different temperatures from sewage sludges with different composition and character, Chemosphere. 287 (2022) 132258. https://doi.org/10.1016/j.chemosphere.2021.132258.
[482] M.I. Al-Wabel, A. Al-Omran, A.H. El-Naggar, M. Nadeem, A.R.A. Usman, Pyrolysis temperature induced changes in characteristics and chemical composition of biochar produced from conocarpus wastes, Bioresour. Technol.

131 (2013) 374–379. https://doi.org/10.1016/j.biortech.2012.12.165.
[483] F. Iannacone, F. Di Capua, F. Granata, R. Gargano, G. Esposito, Shortcut nitrification-denitrification and biological phosphorus removal in acetate- and ethanol-fed moving bed biofilm reactors under microaerobic/aerobic conditions, Bioresour. Technol. 330 (2021) 124958. https://doi.org/10.1016/j.biortech.2021.124958.
[484] G.N. Tenea, T.D. Pozo, Antimicrobial Peptides from Lactobacillus plantarum UTNGt2 Prevent Harmful Bacteria Growth on Fresh Tomatoes, J. Microbiol. Biotechnol. 29 (2019) 1553–1560. https://doi.org/10.4014/jmb.1904.04063.
[485] A. Vera, F.P. Wilson, A.M. Cupples, Predicted functional genes for the biodegradation of xenobiotics in groundwater and sediment at two contaminated naval sites, Appl. Microbiol. Biotechnol. 106 (2022) 835–853. https://doi.org/10.1007/s00253-021-11756-3.
[486] F. Chen, Z. Luo, J. Ma, S. Zeng, Y. Yang, S. Zhang, Interaction of Cadmium and Polycyclic Aromatic Hydrocarbons in Co-contaminated Soil, Water, Air, Soil Pollut. 229 (2018) 114. https://doi.org/10.1007/s11270-018-3774-5.
[487] J.-L. Li, B.-H. Chen, Solubilization of model polycyclic aromatic hydrocarbons by nonionic surfactants, Chem. Eng. Sci. 57 (2002) 2825–2835. https://doi.org/10.1016/S0009-2509(02)00169-0.
[488] J. Liu, Y. Wang, H. Li, Synergistic Solubilization of Phenanthrene by Mixed Micelles Composed of Biosurfactants and a Conventional Non-Ionic Surfactant, Molecules. 25 (2020) 4327. https://doi.org/10.3390/molecules25184327.
[489] B. Czech, M. Kończak, M. Rakowska, P. Oleszczuk, Engineered biochars from organic wastes for the adsorption of diclofenac, naproxen and triclosan from water systems, J. Clean. Prod. 288 (2021) 125686. https://doi.org/10.1016/j.jclepro.2020.125686.
[490] Dong-ju Kim, Relation of microbial biomass to counting units for Pseudomonas aeruginosa, African J. Microbiol. Res. 6 (2012) 4620–4622. https://doi.org/10.5897/AJMR10.902.
[491] M. Amir, S. Mohsen, M. Afsaneh, Simultaneous Desorption and Desorption Kinetics of Phenanthrene, Anthracene, and Heavy Metals from Kaolinite with Different Organic Matter Content, Https://Doi.Org/10.1080/15320383.2017.1339666. 27 (2018) 200–220. https://doi.org/10.1080/15320383.2017.1339666.
[492] F. Gharibzadeh, R.R. Kalantary, M. Golshan, Optimization of Influencing Parameters on Phenanthrene Removal Efficiency in Soil Washing Process by Using Response Surface Methodology, Soil Sediment Contam. An Int. J. 27 (2018) 46–59. https://doi.org/10.1080/15320383.2017.1405381.
[493] B. Zhao, L. Zhu, W. Li, B. Chen, Solubilization and biodegradation of phenanthrene in mixed anionic–nonionic surfactant solutions, Chemosphere. 58 (2005) 33–40. https://doi.org/10.1016/j.chemosphere.2004.08.067.
[494] W. Zhou, J. Yang, L. Lou, L. Zhu, Solubilization properties of polycyclic aromatic hydrocarbons by saponin, a plant-derived biosurfactant, Environ. Pollut. 159 (2011) 1198–1204. https://doi.org/10.1016/j.envpol.2011.02.001.
[495] D. Grasso, K. Subramaniam, J.. Pignatello, Y. Yang, D. Ratté, Micellar desorption of polynuclear aromatic hydrocarbons from contaminated soil,

Colloids Surfaces A Physicochem. Eng. Asp. 194 (2001) 65–74. https://doi.org/10.1016/S0927-7757(01)00800-7.
[496] M. Saeedi, L.Y. Li, J.R. Grace, Desorption and mobility mechanisms of co-existing polycyclic aromatic hydrocarbons and heavy metals in clays and clay minerals, J. Environ. Manage. 214 (2018) 204–214. https://doi.org/10.1016/j.jenvman.2018.02.065.
[497] C. Kim, Y. Lee, S.K. Ong, Factors affecting EDTA extraction of lead from lead-contaminated soils, Chemosphere. 51 (2003) 845–853. https://doi.org/10.1016/S0045-6535(03)00155-3.
[498] R. López-Vizcaíno, C. Sáez, P. Cañizares, M.A. Rodrigo, The use of a combined process of surfactant-aided soil washing and coagulation for PAH-contaminated soils treatment, Sep. Purif. Technol. 88 (2012) 46–51. https://doi.org/10.1016/j.seppur.2011.11.038.
[499] M. Labib, S.S. Dukhin, Y. Tabani, Desorption kinetics during capillary flow, Colloids Surfaces A Physicochem. Eng. Asp. 354 (2010) 45–50. https://doi.org/10.1016/j.colsurfa.2009.11.028.
[500] P. Godlewska, A. Bogusz, J. Dobrzyńska, R. Dobrowolski, P. Oleszczuk, Engineered biochar modified with iron as a new adsorbent for treatment of water contaminated by selenium, J. Saudi Chem. Soc. 24 (2020) 824–834. https://doi.org/10.1016/j.jscs.2020.07.006.
[501] X. Zhan, M. Zhu, Y. Shen, L. Yue, J. Li, J.L. Gardea-Torresdey, G. Xu, Apoplastic and symplastic uptake of phenanthrene in wheat roots, Environ. Pollut. 233 (2018) 331–339. https://doi.org/10.1016/j.envpol.2017.10.056.
[502] S. Zhao, G. Huang, S. Mu, C. An, X. Chen, Immobilization of phenanthrene onto gemini surfactant modified sepiolite at solid/aqueous interface: Equilibrium, thermodynamic and kinetic studies, Sci. Total Environ. 598 (2017) 619–627. https://doi.org/10.1016/j.scitotenv.2017.04.120.
[503] A.A. Awe, B.O. Opeolu, O.S. Fatoki, O.S. Ayanda, V.A. Jackson, R. Snyman, Preparation and characterisation of activated carbon from Vitisvinifera leaf litter and its adsorption performance for aqueous phenanthrene, Appl. Biol. Chem. 63 (2020) 12. https://doi.org/10.1186/s13765-020-00494-1.
[504] S. Mohamadi, M. Saeedi, A. Mollahosseini, Desorption Kinetics of Heavy Metals (Lead, Zinc, and Nickel) Coexisted with Phenanthrene from a Natural High Buffering Soil, Int. J. Eng. 32 (2019) 1716–1725.
[505] X. Zheng, H. Lin, Y. Tao, H. Zhang, Selective adsorption of phenanthrene dissolved in Tween 80 solution using activated carbon derived from walnut shells, Chemosphere. 208 (2018) 951–959. https://doi.org/10.1016/j.chemosphere.2018.06.025.
[506] W.-J. Dai, P. Wu, D. Liu, J. Hu, Y. Cao, T.-Z. Liu, C.P. Okoli, B. Wang, L. Li, Adsorption of Polycyclic Aromatic Hydrocarbons from aqueous solution by Organic Montmorillonite Sodium Alginate Nanocomposites, Chemosphere. 251 (2020) 126074. https://doi.org/10.1016/j.chemosphere.2020.126074.
[507] M. Alkan, M. Doğan, Y. Turhan, Ö. Demirbaş, P. Turan, Adsorption kinetics and mechanism of maxilon blue 5G dye on sepiolite from aqueous solutions, Chem. Eng. J. 139 (2008) 213–223. https://doi.org/10.1016/j.cej.2007.07.080.
[508] A. Rein, I.K.U. Adam, A. Miltner, K. Brumme, M. Kästner, S. Trapp, Impact

of bacterial activity on turnover of insoluble hydrophobic substrates (phenanthrene and pyrene)—Model simulations for prediction of bioremediation success, J. Hazard. Mater. 306 (2016) 105–114. https://doi.org/10.1016/j.jhazmat.2015.12.005.
[509] Z. Liu, A.M. Jacobson, R.G. Luthy, Biodegradation of naphthalene in aqueous nonionic surfactant systems, Appl. Environ. Microbiol. 61 (1995) 145–151. https://doi.org/10.1128/aem.61.1.145-151.1995.
[510] P. Arulazhagan, K. Al-Shekri, Q. Huda, J.J. Godon, J.M. Basahi, D. Jeyakumar, Biodegradation of polycyclic aromatic hydrocarbons by an acidophilic Stenotrophomonas maltophilia strain AJH1 isolated from a mineral mining site in Saudi Arabia, Extremophiles. 21 (2017) 163–174. https://doi.org/10.1007/s00792-016-0892-0.
[511] M.T. Jamal, A. Pugazhendi, Isolation and characterization of halophilic bacterial consortium from seagrass, Jeddah coast, for the degradation of petroleum hydrocarbons and treatment of hydrocarbons-contaminated boat fuel station wastewater, Clean Technol. Environ. Policy. 23 (2021) 77–88. https://doi.org/10.1007/s10098-020-01957-1.
[512] D.T. Sponza, O. Gök, Effect of rhamnolipid on the aerobic removal of polyaromatic hydrocarbons (PAHs) and COD components from petrochemical wastewater, Bioresour. Technol. 101 (2010) 914–924. https://doi.org/10.1016/j.biortech.2009.09.022.
[513] Y. Zhang, X. Xiao, X. Zhu, B. Chen, Self-assembled fungus-biochar composite pellets (FBPs) for enhanced co-sorption-biodegradation towards phenanthrene, Chemosphere. 286 (2022) 131887. https://doi.org/10.1016/j.chemosphere.2021.131887.
[514] D. Cassidy, A comparison of CSTR and SBR bioslurry reactor performance, Water Res. 34 (2000) 4333–4342. https://doi.org/10.1016/S0043-1354(00)00211-6.
[515] S. Molaei, G. Moussavi, N. Talebbeydokhti, S. Shekoohiyan, Biodegradation of the petroleum hydrocarbons using an anoxic packed-bed biofilm reactor with in-situ biosurfactant-producing bacteria, J. Hazard. Mater. 421 (2022) 126699. https://doi.org/10.1016/j.jhazmat.2021.126699.
[516] H.W. Zhou, A.H.Y. Wong, R.M.K. Yu, Y.D. Park, Y.S. Wong, N.F.Y. Tam, Polycyclic Aromatic Hydrocarbon-Induced Structural Shift of Bacterial Communities in Mangrove Sediment, Microb. Ecol. 58 (2009) 153–160. https://doi.org/10.1007/s00248-008-9456-x.
[517] P. Wanapaisan, N. Laothamteep, F. Vejarano, J. Chakraborty, M. Shintani, C. Muangchinda, T. Morita, C. Suzuki-Minakuchi, K. Inoue, H. Nojiri, O. Pinyakong, Synergistic degradation of pyrene by five culturable bacteria in a mangrove sediment-derived bacterial consortium, J. Hazard. Mater. 342 (2018) 561–570. https://doi.org/10.1016/j.jhazmat.2017.08.062.
[518] A. Gottfried, N. Singhal, R. Elliot, S. Swift, The role of salicylate and biosurfactant in inducing phenanthrene degradation in batch soil slurries, Appl. Microbiol. Biotechnol. 86 (2010) 1563–1571. https://doi.org/10.1007/s00253-010-2453-2.
[519] M.J.J. Kotterman, H. Rietberg, A. Hage, J.A. Field, Polycyclic aromatic

hydrocarbon oxidation by the white-rot fungus Bjerkandera sp. strain BOS55 in the presence of nonionic surfactants, Biotechnol. Bioeng. 57 (1998) 220–227.
[520] O. Gok, D.T. Sponza, Effects of sludge retention time (SRTs) on the removals of polycyclic aromatic hydrocarbons (PAHs), chemical oxygen demand (COD), and toxicity in a petrochemical industry wastewater, Desalin. Water Treat. 26 (2011) 57–65. https://doi.org/10.5004/dwt.2011.2110.
[521] J. Zhang, D. Kumari, C. Fang, V. Achal, Combining the microbial calcite precipitation process with biochar in order to improve nickel remediation, Appl. Geochemistry. 103 (2019) 68–71. https://doi.org/10.1016/j.apgeochem.2019.02.011.
[522] C. Yin, W. Xiong, H. Qiu, W. Peng, Z. Deng, S. Lin, R. Liang, Characterization of the Phenanthrene-Degrading Sphingobium yanoikuyae SJTF8 in Heavy Metal Co-Existing Liquid Medium and Analysis of Its Metabolic Pathway, Microorganisms. 8 (2020) 946. https://doi.org/10.3390/microorganisms8060946.
[523] J.-L. Li, B.-H. Chen, Surfactant-mediated Biodegradation of Polycyclic Aromatic Hydrocarbons, Materials (Basel). 2 (2009) 76–94. https://doi.org/10.3390/ma2010076.
[524] J.-L. Li, B.-H. Chen, Effect of nonionic surfactants on biodegradation of phenanthrene by a marine bacteria of Neptunomonas naphthovorans, J. Hazard. Mater. 162 (2009) 66–73. https://doi.org/10.1016/j.jhazmat.2008.05.019.
[525] F. Li, L. Zhu, Effect of surfactant-induced cell surface modifications on electron transport system and catechol 1,2-dioxygenase activities and phenanthrene biodegradation by Citrobacter sp. SA01, Bioresour. Technol. 123 (2012) 42–48. https://doi.org/10.1016/j.biortech.2012.07.059.
[526] H. Zhong, G. ming Zeng, X.Z. Yuan, H. yan Fu, G.H. Huang, F.Y. Ren, Adsorption of dirhamnolipid on four microorganisms and the effect on cell surface hydrophobicity, Appl. Microbiol. Biotechnol. 77 (2007) 447–455. https://doi.org/10.1007/s00253-007-1154-y.
[527] R.A. Al-Tahhan, T.R. Sandrin, A.A. Bodour, R.M. Maier, Rhamnolipid-Induced Removal of Lipopolysaccharide from Pseudomonas aeruginosa : Effect on Cell Surface Properties and Interaction with Hydrophobic Substrates, Appl. Environ. Microbiol. 66 (2000) 3262–3268. https://doi.org/10.1128/AEM.66.8.3262-3268.2000.
[528] S. Liu, C. Guo, Z. Dang, X. Liang, Comparative proteomics reveal the mechanism of Tween80 enhanced phenanthrene biodegradation by Sphingomonas sp. GY2B, Ecotoxicol. Environ. Saf. 137 (2017) 256–264. https://doi.org/10.1016/j.ecoenv.2016.12.015.
[529] X. Yin, X. Liang, R. Zhang, L. Yu, G. Xu, Q. Zhou, X. Zhan, Impact of phenanthrene exposure on activities of nitrate reductase, phosphoenolpyruvate carboxylase, vacuolar H+-pyrophosphatase and plasma membrane H+-ATPase in roots of soybean, wheat and carrot, Environ. Exp. Bot. 113 (2015) 59–66. https://doi.org/10.1016/j.envexpbot.2015.02.001.
[530] E. Navrozidou, N. Remmas, P. Melidis, D.G. Karpouzas, G. Tsiamis, S. Ntougias, Biodegradation Potential and Diversity of Diclofenac-degrading Microbiota in an Immobilized Cell Biofilter, Processes. 7 (2019) 554.

https://doi.org/10.3390/pr7090554.
[531] S.Y. Zhang, Q.F. Wang, S.G. Xie, Molecular characterization of phenanthrene-degrading methanogenic communities in leachate-contaminated aquifer sediment, Int. J. Environ. Sci. Technol. 9 (2012) 705–712. https://doi.org/10.1007/s13762-012-0098-7.
[532] C.-M. Hung, C.-P. Huang, C.-W. Chen, C.-D. Dong, Degradation of organic contaminants in marine sediments by peroxymonosulfate over LaFeO3 nanoparticles supported on water caltrop shell-derived biochar and the associated microbial community responses, J. Hazard. Mater. 420 (2021) 126553. https://doi.org/10.1016/j.jhazmat.2021.126553.
[533] S. Jokanović, K. Kajan, S. Perović, M. Ivanić, V. Mačić, S. Orlić, Anthropogenic influence on the environmental health along Montenegro coast based on the bacterial and chemical characterization, Environ. Pollut. 271 (2021) 116383. https://doi.org/10.1016/j.envpol.2020.116383.
[534] B. Huang, H. Jia, X. Han, J. Gou, C. Huang, J. Wang, J. Wei, J. Wang, C. Zhang, Effects of biocontrol Bacillus and fermentation bacteria additions on the microbial community, functions and antibiotic resistance genes of prickly ash seed oil meal-biochar compost, Bioresour. Technol. 340 (2021) 125668. https://doi.org/10.1016/j.biortech.2021.125668.
[535] S. Siebielec, G. Siebielec, P. Sugier, M. Woźniak, J. Grządziel, A. Gałązka, T. Stuczyński, Activity and Diversity of Microorganisms in Root Zone of Plant Species Spontaneously Inhabiting Smelter Waste Piles, Molecules. 25 (2020) 5638. https://doi.org/10.3390/molecules25235638.
[536] M. Yi, L. Zhang, C. Qin, P. Lu, H. Bai, X. Han, S. Yuan, Temporal changes of microbial community structure and nitrogen cycling processes during the aerobic degradation of phenanthrene, Chemosphere. 286 (2022) 131709. https://doi.org/10.1016/j.chemosphere.2021.131709.
[537] J. Li, C. Luo, D. Zhang, M. Song, X. Cai, L. Jiang, G. Zhang, Autochthonous Bioaugmentation-Modified Bacterial Diversity of Phenanthrene Degraders in PAH-Contaminated Wastewater as Revealed by DNA-Stable Isotope Probing, Environ. Sci. Technol. 52 (2018) 2934–2944. https://doi.org/10.1021/acs.est.7b05646.
[538] J. Brzeszcz, P. Kapusta, T. Steliga, A. Turkiewicz, Hydrocarbon Removal by Two Differently Developed Microbial Inoculants and Comparing Their Actions with Biostimulation Treatment, Molecules. 25 (2020) 661. https://doi.org/10.3390/molecules25030661.
[539] Y. Qi, H. Liu, J. Wang, Y. Wang, Effects of different straw biochar combined with microbial inoculants on soil environment in pot experiment, Sci. Rep. 11 (2021) 14685. https://doi.org/10.1038/s41598-021-94209-1.
[540] D.-S. Li, J.-Q. Feng, Y.-F. Liu, L. Zhou, J.-F. Liu, B.-Z. Mu, S.-Z. Yang, J.-D. Gu, Enrichment and immobilization of oil-degrading microbial consortium on different sorbents for bioremediation testing under simulated aquatic and soil conditions, Appl. Environ. Biotechnol. 5 (2020) 1–11. https://doi.org/10.26789/AEB.2019.02.003.
[541] D. Garrido-Sanz, M. Redondo-Nieto, M. Guirado, O. Pindado Jiménez, R. Millán, M. Martin, R. Rivilla, Metagenomic Insights into the Bacterial

Functions of a Diesel-Degrading Consortium for the Rhizoremediation of Diesel-Polluted Soil, Genes (Basel). 10 (2019) 456. https://doi.org/10.3390/genes10060456.
[542] P. Dörr de Quadros, V.S. Cerqueira, J.C. Cazarolli, M. do C.R. Peralba, F.A.O. Camargo, A. Giongo, F.M. Bento, Oily sludge stimulates microbial activity and changes microbial structure in a landfarming soil, Int. Biodeterior. Biodegradation. 115 (2016) 90–101. https://doi.org/10.1016/j.ibiod.2016.07.018.
[543] N.A. ElNaker, M. Elektorowicz, V. Naddeo, S.W. Hasan, A.F. Yousef, Assessment of Microbial Community Structure and Function in Serially Passaged Wastewater Electro-Bioreactor Sludge: An Approach to Enhance Sludge Settleability, Sci. Rep. 8 (2018) 7013. https://doi.org/10.1038/s41598-018-25509-2.
[544] S. Geng, W. Cao, J. Yuan, Y. Wang, Y. Guo, A. Ding, Y. Zhu, J. Dou, Microbial diversity and co-occurrence patterns in deep soils contaminated by polycyclic aromatic hydrocarbons (PAHs), Ecotoxicol. Environ. Saf. 203 (2020) 110931. https://doi.org/10.1016/j.ecoenv.2020.110931.
[545] H. Bao, J. Wang, H. Zhang, J. Li, H. Li, F. Wu, Effects of biochar and organic substrates on biodegradation of polycyclic aromatic hydrocarbons and microbial community structure in PAHs-contaminated soils, J. Hazard. Mater. 385 (2020) 121595. https://doi.org/10.1016/j.jhazmat.2019.121595.
[546] J. Wu, H. Li, J. Zhang, Y. Gu, X. Zhou, D. Zhang, Y. Ma, S. Wang, X. Nian, W. Jin, R. Li, Z. Xu, Microbial diversity and function in response to occurrence and source apportionment of polycyclic aromatic hydrocarbons in combined sewer overflows, J. Clean. Prod. 279 (2021) 123723. https://doi.org/10.1016/j.jclepro.2020.123723.
[547] J. Chen, B. Fan, J. Li, X. Wang, W. Li, L. Cui, Z. Liu, Development of human health ambient water quality criteria of 12 polycyclic aromatic hydrocarbons (PAH) and risk assessment in China, Chemosphere. (2020). https://doi.org/10.1016/j.chemosphere.2020.126590.
[548] M.A. Primost, M. Commendatore, P.J. Torres, G. Bigatti, PAHs contamination in edible gastropods from north Patagonian harbor areas, Mar. Pollut. Bull. (2018). https://doi.org/10.1016/j.marpolbul.2018.08.021.
[549] M. Haimann, C. Hauer, M. Tritthart, D. Prenner, P. Leitner, O. Moog, H. Habersack, Monitoring and modelling concept for ecological optimized harbour dredging and fine sediment disposal in large rivers, Hydrobiologia. (2018). https://doi.org/10.1007/s10750-016-2935-z.
[550] V. Mymrin, J.C. Stella, C.B. Scremim, R.C.Y. Pan, F.G. Sanches, K. Alekseev, D.E. Pedroso, A. Molinetti, O.M. Fortini, Utilization of sediments dredged from marine ports as a principal component of composite material, J. Clean. Prod. (2017). https://doi.org/10.1016/j.jclepro.2016.10.035.
[551] S. Abel, I. Nybom, J. Akkanen, Carbon Amendments and Remediation of Contaminated Sediments, in: 2020. https://doi.org/10.1007/698_2020_512.
[552] M. Waqas, A.S. Aburiazaiza, R. Miandad, M. Rehan, M.A. Barakat, A.S. Nizami, Development of biochar as fuel and catalyst in energy recovery technologies, J. Clean. Prod. (2018).

https://doi.org/10.1016/j.jclepro.2018.04.017.
[553] S. Wang, L. Wu, X. Hu, L. Zhang, T. Li, S. Jiang, K.M. O'Donnell, C.E. Buckley, C.Z. Li, Changes in the Biochar Chemical Structure during the Low-Temperature Gasification of Mallee Biochar in Air as Revealed with Fourier Transform Infrared/Raman and X-ray Photoelectron Spectroscopies, Energy and Fuels. (2018). https://doi.org/10.1021/acs.energyfuels.8b02870.
[554] M. Kołtowski, I. Hilber, T.D. Bucheli, B. Charmas, J. Skubiszewska-Zięba, P. Oleszczuk, Activated biochars reduce the exposure of polycyclic aromatic hydrocarbons in industrially contaminated soils, Chem. Eng. J. (2017). https://doi.org/10.1016/j.cej.2016.10.065.
[555] S. Wongrod, S. Simon, E.D. van Hullebusch, P.N.L. Lens, G. Guibaud, Assessing arsenic redox state evolution in solution and solid phase during As(III) sorption onto chemically-treated sewage sludge digestate biochars, Bioresour. Technol. (2019). https://doi.org/10.1016/j.biortech.2018.12.056.
[556] N.A. Qambrani, M.M. Rahman, S. Won, S. Shim, C. Ra, Biochar properties and eco-friendly applications for climate change mitigation, waste management, and wastewater treatment: A review, Renew. Sustain. Energy Rev. (2017). https://doi.org/10.1016/j.rser.2017.05.057.
[557] L. Kong, Y. Gao, Q. Zhou, X. Zhao, Z. Sun, Biochar accelerates PAHs biodegradation in petroleum-polluted soil by biostimulation strategy, J. Hazard. Mater. (2018). https://doi.org/10.1016/j.jhazmat.2017.09.040.
[558] S. Matassa, S. Papirio, I. Pikaar, T. Hülsen, E. Leijenhorst, G. Esposito, F. Pirozzi, W. Verstraete, Upcycling of biowaste carbon and nutrients in line with consumer confidence: the "full gas" route to single cell protein, Green Chem. 22 (2020) 4912–4929. https://doi.org/10.1039/D0GC01382J.
[559] S. Sri Shalini, K. Palanivelu, A. Ramachandran, V. Raghavan, Biochar from biomass waste as a renewable carbon material for climate change mitigation in reducing greenhouse gas emissions—a review, Biomass Convers. Biorefinery. (2020). https://doi.org/10.1007/s13399-020-00604-5.
[560] M. Wang, Y. Zhu, L. Cheng, B. Andserson, X. Zhao, D. Wang, A. Ding, Review on utilization of biochar for metal-contaminated soil and sediment remediation, J. Environ. Sci. (China). (2018). https://doi.org/10.1016/j.jes.2017.08.004.
[561] N. Ni, D. Kong, W. Wu, J. He, Z. Shan, J. Li, Y. Dou, Y. Zhang, Y. Song, X. Jiang, The Role of Biochar in Reducing the Bioavailability and Migration of Persistent Organic Pollutants in Soil–Plant Systems: A Review, Bull. Environ. Contam. Toxicol. 104 (2020) 157–165. https://doi.org/10.1007/s00128-019-02779-8.
[562] J.E. Balmer, H. Hung, Y. Yu, R.J. Letcher, D.C.G. Muir, Sources and environmental fate of pyrogenic polycyclic aromatic hydrocarbons (PAHs) in the Arctic, Emerg. Contam. (2019). https://doi.org/10.1016/j.emcon.2019.04.002.
[563] D. Lorenzi, J.A. Entwistle, M. Cave, J.R. Dean, Determination of polycyclic aromatic hydrocarbons in urban street dust: Implications for human health, Chemosphere. (2011). https://doi.org/10.1016/j.chemosphere.2011.02.020.
[564] N. Wang, Y.P. Wang, X. Duan, J. Wang, Y. Xie, C. Dong, J. Gao, P. Yin, Controlling factors for the distribution of typical organic pollutants in the

surface sediment of a macrotidal bay, Environ. Sci. Pollut. Res. (2020). https://doi.org/10.1007/s11356-020-09199-w.
[565] J. Dachs, L. Méjanelle, Organic pollutants in coastal waters, sediments, and biota: A relevant driver for ecosystems during the anthropocene?, Estuaries and Coasts. (2010). https://doi.org/10.1007/s12237-009-9255-8.
[566] R.M. Cavalcante, F.W. Sousa, R.F. Nascimento, E.R. Silveira, G.S.S. Freire, The impact of urbanization on tropical mangroves (Fortaleza, Brazil): evidence from PAH distribution in sediments, J. Environ. Manage. 91 (2009) 328–335.
[567] N. Cardellicchio, A. Buccolieri, S. Giandomenico, L. Lopez, F. Pizzulli, L. Spada, Organic pollutants (PAHs, PCBs) in sediments from the Mar Piccolo in Taranto (Ionian Sea, Southern Italy), Mar. Pollut. Bull. (2007). https://doi.org/10.1016/j.marpolbul.2007.09.007.
[568] Q. Zeng, E. Jeppesen, X. Gu, Z. Mao, H. Chen, Distribution, fate and risk assessment of PAHs in water and sediments from an aquaculture- and shipping-impacted subtropical lake, China, Chemosphere. (2018). https://doi.org/10.1016/j.chemosphere.2018.03.031.
[569] Y. Meng, X. Liu, S. Lu, T. Zhang, B. Jin, Q. Wang, Z. Tang, Y. Liu, X. Guo, J. Zhou, B. Xi, A review on occurrence and risk of polycyclic aromatic hydrocarbons (PAHs) in lakes of China, Sci. Total Environ. (2019). https://doi.org/10.1016/j.scitotenv.2018.10.162.
[570] V. Bert, P. Seuntjens, W. Dejonghe, S. Lacherez, H.T.T. Thuy, B. Vandecasteele, Phytoremediation as a management option for contaminated sediments in tidal marshes, flood control areas and dredged sediment landfill sites, Environ. Sci. Pollut. Res. (2009). https://doi.org/10.1007/s11356-009-0205-6.
[571] G. Bortone, Sediment Treatment - a General Introduction, Sustain. Manag. Sediment Resour. (2007). https://doi.org/10.1016/S1872-1990(07)80013-4.
[572] M. Di Risio, D.F. Hayes, D. Pasquali, Marine Sediments: Processes, Transport and Environmental Aspects, J. Mar. Sci. Eng. (2020). https://doi.org/10.3390/jmse8040243.
[573] J. Kvasnicka, G.A. Burton Jr, J. Semrau, O. Jolliet, Dredging Contaminated Sediments: Is it Worth the Risks?, Environ. Toxicol. Chem. 39 (2020) 515.
[574] L. Cutroneo, M. Castellano, C. Carbone, S. Consani, F. Gaino, S. Tucci, S. Magrì, P. Povero, R.M. Bertolotto, G. Canepa, M. Capello, Evaluation of the boundary condition influence on PAH concentrations in the water column during the sediment dredging of a port, Mar. Pollut. Bull. (2015). https://doi.org/10.1016/j.marpolbul.2015.10.055.
[575] G.F. Birch, A review of chemical-based sediment quality assessment methodologies for the marine environment, Mar. Pollut. Bull. (2018). https://doi.org/10.1016/j.marpolbul.2018.05.039.
[576] W.F. Directive, Directive 2000/60/EC of the European Parliament and of the Council of 23 October 2000 establishing a framework for Community action in the field of water policy, Off. J. Eur. Communities. 22 (2000) 2000.
[577] J.C.G. Sousa, A.R. Ribeiro, M.O. Barbosa, M.F.R. Pereira, A.M.T. Silva, A review on environmental monitoring of water organic pollutants identified by EU guidelines, J. Hazard. Mater. (2018).

https://doi.org/10.1016/j.jhazmat.2017.09.058.
[578] M. Gavrilescu, Fate of pesticides in the environment and its bioremediation, Eng. Life Sci. (2005). https://doi.org/10.1002/elsc.200520098.
[579] P.K. Agrawal, R. Shrivastava, J. Verma, Bioremediation approaches for degradation and detoxification of polycyclic aromatic hydrocarbons, in: Emerg. Eco-Friendly Approaches Waste Manag., 2018. https://doi.org/10.1007/978-981-10-8669-4_6.
[580] N. Othman, M.I. Juki, N. Hussain, S.A. Talib, Bioremediation a potential approach for soil contaminated with polycyclic aromatic hydrocarbons: an overview, Int. J. Sustain. Constr. Eng. Technol. 2 (2011).
[581] M. Alexander, Biodegradation and Bioremediation, second ed., Acad. Press. San Diego, CA, USA. (1999). https://doi.org/10.1007/978-3-662-05794-0.
[582] R. Posada-Baquero, M.L. Martín, J.J. Ortega-Calvo, Implementing standardized desorption extraction into bioavailability-oriented bioremediation of PAH-polluted soils, Sci. Total Environ. (2019). https://doi.org/10.1016/j.scitotenv.2019.134011.
[583] J.A. Kumar, D.J. Amarnath, S. Sathish, S.A. Jabasingh, A. Saravanan, R. V. Hemavathy, K.V. Anand, P.R. Yaashikaa, Enhanced PAHs removal using pyrolysis-assisted potassium hydroxide induced palm shell activated carbon: Batch and column investigation, J. Mol. Liq. (2019). https://doi.org/10.1016/j.molliq.2019.01.121.
[584] G.N. Kim, Y.H. Jung, J.J. Lee, J.K. Moon, C.H. Jung, Development of electrokinetic-flushing technology for the remediation of contaminated soil around nuclear facilities, J. Ind. Eng. Chem. (2008). https://doi.org/10.1016/j.jiec.2008.05.001.
[585] A.N. Alshawabkeh, R.J. Gale, E. Ozsu-Acar, R.M. Bricka, Optimization of 2-D electrode configuration for electrokinetic remediation, Soil Sediment Contam. (1999). https://doi.org/10.1080/10588339991339504.
[586] C. Walgraeve, K. Demeestere, J. Dewulf, R. Zimmermann, H. Van Langenhove, Oxygenated polycyclic aromatic hydrocarbons in atmospheric particulate matter: Molecular characterization and occurrence, Atmos. Environ. (2010). https://doi.org/10.1016/j.atmosenv.2009.12.004.
[587] S. Lundstedt, B.A.M. Bandowe, W. Wilcke, E. Boll, J.H. Christensen, J. Vila, M. Grifoll, P. Faure, C. Biache, C. Lorgeoux, M. Larsson, K. Frech Irgum, P. Ivarsson, M. Ricci, First intercomparison study on the analysis of oxygenated polycyclic aromatic hydrocarbons (oxy-PAHs) and nitrogen heterocyclic polycyclic aromatic compounds (N-PACs) in contaminated soil, TrAC - Trends Anal. Chem. (2014). https://doi.org/10.1016/j.trac.2014.01.007.
[588] R.S. Baker, J. LaChance, G. Heron, In-pile thermal desorption of PAHs, PCBs and dioxins/furans in soil and sediment, L. Contam. Reclam. 14 (2006) 620–624.
[589] D.F. Mclaughlin, S. V Dighe, D.L. Keairns, N.H. Ulerich, Decontamination and Beneficial Reuse of Dredged Estuarine Sediment: the Westinghouse Plasma Vitrification Process, Proc. 19th West. Dredg. Assoc. Annu. Meet. (1999).
[590] R.J. Torres, D.M.S. Abessa, F.C. Santos, L.A. Maranho, M.B. Davanso, M.R.L. do Nascimento, A.A. Mozeto, Effects of dredging operations on sediment

quality: Contaminant mobilization in dredged sediments from the Port of Santos, SP, Brazil, J. Soils Sediments. (2009). https://doi.org/10.1007/s11368-009-0121-x.
[591] F. Tozzi, M. Del Bubba, W.A. Petrucci, S. Pecchioli, C. Macci, F. Hernández García, J.J. Martínez Nicolás, E. Giordani, Use of a remediated dredged marine sediment as a substrate for food crop cultivation: Sediment characterization and assessment of fruit safety and quality using strawberry (Fragaria x ananassa Duch.) as model species of contamination transfer, Chemosphere. (2020). https://doi.org/10.1016/j.chemosphere.2019.124651.
[592] P. Melgarejo, P. Legua, F. Pérez-Sarmiento, R. Martínez-Font, J.J. Martínez-Nicolás, F. Hernández, Effect of a new remediated substrate on fruit quality and bioactive compounds in two strawberry cultivars, J. Food Nutr. Res. 5 (2017) 579–586.
[593] P. Mattei, L.P. D'Acqui, F.P. Nicese, G. Lazzerini, G. Masciandaro, C. Macci, S. Doni, F. Sarteschi, L. Giagnoni, G. Renella, Use of phytoremediated sediments dredged in maritime port as plant nursery growing media, J. Environ. Manage. (2017). https://doi.org/10.1016/j.jenvman.2016.05.069.
[594] L. Bonomo, A. Careghini, S. Dastoli, L. De Propris, G. Ferrari, M. Gabellini, S. Saponaro, Feasibility studies for the treatment and reuse of contaminated marine sediments, Environ. Technol. (2009). https://doi.org/10.1080/09593330902990105.
[595] V. Cappuyns, V. Deweirt, S. Rousseau, Dredged sediments as a resource for brick production: Possibilities and barriers from a consumers' perspective, Waste Manag. (2015). https://doi.org/10.1016/j.wasman.2014.12.025.
[596] H. Beddaa, I. Ouazi, A. Ben Fraj, F. Lavergne, J.-M. Torrenti, Reuse potential of dredged river sediments in concrete: Effect of sediment variability, J. Clean. Prod. (2020) 121665.
[597] Z. Zhao, M. Benzerzour, N.E. Abriak, D. Damidot, L. Courard, D. Wang, Use of uncontaminated marine sediments in mortar and concrete by partial substitution of cement, Cem. Concr. Compos. (2018). https://doi.org/10.1016/j.cemconcomp.2018.07.010.
[598] W. Maherzi, M. Benzerzour, Y. Mamindy-Pajany, E. van Veen, M. Boutouil, N.E. Abriak, Beneficial reuse of Brest-Harbor (France)-dredged sediment as alternative material in road building: laboratory investigations, Environ. Technol. 39 (2018) 566–580.
[599] J. Gebert, C. Knoblauch, A. Gröngröft, Gas production from dredged sediment, Waste Manag. (2019). https://doi.org/10.1016/j.wasman.2018.12.009.
[600] L. Wang, L. Chen, D.C.W. Tsang, H.W. Kua, J. Yang, Y.S. Ok, S. Ding, D. Hou, C.S. Poon, The roles of biochar as green admixture for sediment-based construction products, Cem. Concr. Compos. (2019). https://doi.org/10.1016/j.cemconcomp.2019.103348.
[601] F. Todaro, C. Vitone, M. Notarnicola, Stabilization and recycling of contaminated marine sediments, in: E3S Web Conf., 2019. https://doi.org/10.1051/e3sconf/20199211004.
[602] F. Wang, Q. Bu, X. Xia, M. Shen, Contrasting effects of black carbon amendments on PAH bioaccumulation by Chironomus plumosus larvae in two

distinct sediments: Role of water absorption and particle ingestion, Environ. Pollut. (2011). https://doi.org/10.1016/j.envpol.2011.03.033.
[603] M. Shen, X. Xia, F. Wang, P. Zhang, X. Zhao, Influences of multiwalled carbon nanotubes and plant residue chars on bioaccumulation of polycyclic aromatic hydrocarbons by Chironomus plumosus larvae in sediment, Environ. Toxicol. Chem. (2012). https://doi.org/10.1002/etc.722.
[604] H. Jia, J. Li, Y. Li, H. Lu, J. Liu, C. Yan, The remediation of PAH contaminated sediment with mangrove plant and its derived biochars, J. Environ. Manage. 268 (2020) 110410. https://doi.org/10.1016/j.jenvman.2020.110410.
[605] J. Chi, H. Liu, Effects of biochars derived from different pyrolysis temperatures on growth of Vallisneria spiralis and dissipation of polycyclic aromatic hydrocarbons in sediments, Ecol. Eng. (2016). https://doi.org/10.1016/j.ecoleng.2016.05.036.
[606] J.L. Gomez-Eyles, C. Yupanqui, B. Beckingham, G. Riedel, C. Gilmour, U. Ghosh, Evaluation of biochars and activated carbons for in situ remediation of sediments impacted with organics, mercury, and methylmercury, Environ. Sci. Technol. (2013). https://doi.org/10.1021/es403712q.
[607] I. Jośko, P. Oleszczuk, J. Pranagal, J. Lehmann, B. Xing, G. Cornelissen, Effect of biochars, activated carbon and multiwalled carbon nanotubes on phytotoxicity of sediment contaminated by inorganic and organic pollutants, Ecol. Eng. (2013). https://doi.org/10.1016/j.ecoleng.2013.07.064.
[608] W. Yang, Y. Wang, P. Sharma, B. Li, K. Liu, J. Liu, M. Flury, J. Shang, Effect of naphthalene on transport and retention of biochar colloids through saturated porous media, Colloids Surfaces A Physicochem. Eng. Asp. (2017). https://doi.org/10.1016/j.colsurfa.2017.07.010.
[609] G. Ojeda, J. Patrício, S. Mattana, A.J.F.N. Sobral, Effects of biochar addition to estuarine sediments, J. Soils Sediments. (2016). https://doi.org/10.1007/s11368-016-1493-3.
[610] M. Ahmad, A.U. Rajapaksha, J.E. Lim, M. Zhang, N. Bolan, D. Mohan, M. Vithanage, S.S. Lee, Y.S. Ok, Biochar as a sorbent for contaminant management in soil and water: A review, Chemosphere. (2014). https://doi.org/10.1016/j.chemosphere.2013.10.071.
[611] S. Shabangu, D. Woolf, E.M. Fisher, L.T. Angenent, J. Lehmann, Techno-economic assessment of biomass slow pyrolysis into different biochar and methanol concepts, Fuel. (2014). https://doi.org/10.1016/j.fuel.2013.08.053.
[612] D. Pandey, A. Daverey, K. Arunachalam, Biochar: Production, properties and emerging role as a support for enzyme immobilization, J. Clean. Prod. (2020). https://doi.org/10.1016/j.jclepro.2020.120267.
[613] X. Hu, M. Gholizadeh, Biomass pyrolysis: A review of the process development and challenges from initial researches up to the commercialisation stage, J. Energy Chem. (2019). https://doi.org/10.1016/j.jechem.2019.01.024.
[614] X.J. Lee, H.C. Ong, Y.Y. Gan, W.H. Chen, T.M.I. Mahlia, State of art review on conventional and advanced pyrolysis of macroalgae and microalgae for biochar, bio-oil and bio-syngas production, Energy Convers. Manag. (2020). https://doi.org/10.1016/j.enconman.2020.112707.
[615] B.A. Oni, O. Oziegbe, O.O. Olawole, Significance of biochar application to the

environment and economy, Ann. Agric. Sci. (2019). https://doi.org/10.1016/j.aoas.2019.12.006.
[616] R.N. State, A. Volceanov, P. Muley, D. Boldor, A review of catalysts used in microwave assisted pyrolysis and gasification, Bioresour. Technol. (2019). https://doi.org/10.1016/j.biortech.2019.01.036.
[617] A. Sharma, V. Pareek, D. Zhang, Biomass pyrolysis - A review of modelling, process parameters and catalytic studies, Renew. Sustain. Energy Rev. (2015). https://doi.org/10.1016/j.rser.2015.04.193.
[618] S. You, Y.S. Ok, S.S. Chen, D.C.W. Tsang, E.E. Kwon, J. Lee, C.H. Wang, A critical review on sustainable biochar system through gasification: Energy and environmental applications, Bioresour. Technol. (2017). https://doi.org/10.1016/j.biortech.2017.06.177.
[619] H.A. Ruiz, M. Conrad, S.N. Sun, A. Sanchez, G.J.M. Rocha, A. Romaní, E. Castro, A. Torres, R.M. Rodríguez-Jasso, L.P. Andrade, I. Smirnova, R.C. Sun, A.S. Meyer, Engineering aspects of hydrothermal pretreatment: From batch to continuous operation, scale-up and pilot reactor under biorefinery concept, Bioresour. Technol. (2020). https://doi.org/10.1016/j.biortech.2019.122685.
[620] F. Motasemi, M.T. Afzal, A review on the microwave-assisted pyrolysis technique, Renew. Sustain. Energy Rev. (2013). https://doi.org/10.1016/j.rser.2013.08.008.
[621] Z. Zhang, Z. Zhu, B. Shen, L. Liu, Insights into biochar and hydrochar production and applications: A review, Energy. (2019). https://doi.org/10.1016/j.energy.2019.01.035.
[622] A. Kumar, K. Saini, T. Bhaskar, Hydochar and biochar: Production, physicochemical properties and techno-economic analysis, Bioresour. Technol. (2020) 123442.
[623] J. Li, J. Dai, G. Liu, H. Zhang, Z. Gao, J. Fu, Y. He, Y. Huang, Biochar from microwave pyrolysis of biomass: A review, Biomass and Bioenergy. (2016). https://doi.org/10.1016/j.biombioe.2016.09.010.
[624] Y. Zhang, P. Chen, S. Liu, P. Peng, M. Min, Y. Cheng, E. Anderson, N. Zhou, L. Fan, C. Liu, G. Chen, Y. Liu, H. Lei, B. Li, R. Ruan, Effects of feedstock characteristics on microwave-assisted pyrolysis – A review, Bioresour. Technol. (2017). https://doi.org/10.1016/j.biortech.2017.01.046.
[625] J. Wang, S. Wang, Preparation, modification and environmental application of biochar: A review, J. Clean. Prod. (2019). https://doi.org/10.1016/j.jclepro.2019.04.282.
[626] Y.-F. Huang, P.-T. Chiueh, S.-L. Lo, A review on microwave pyrolysis of lignocellulosic biomass, Sustain. Environ. Res. 26 (2016) 103–109. https://doi.org/10.1016/j.serj.2016.04.012.
[627] W. Kwapinski, C.M.P. Byrne, E. Kryachko, P. Wolfram, C. Adley, J.J. Leahy, E.H. Novotny, M.H.B. Hayes, Biochar from biomass and waste, Waste and Biomass Valorization. (2010). https://doi.org/10.1007/s12649-010-9024-8.
[628] S. Brick, S. Lyutse, Biochar: Assessing the promise and risks to guide US policy, Nat. Resour. Def. Counc. USA. Http//Www. Nrdc. Org/Energy/Files/Biochar_paper. Pdf. (2010).
[629] M.H. Duku, S. Gu, E. Ben Hagan, Biochar production potential in Ghana - A

review, Renew. Sustain. Energy Rev. (2011). https://doi.org/10.1016/j.rser.2011.05.010.
[630] X. xia Guo, H. tao Liu, J. Zhang, The role of biochar in organic waste composting and soil improvement: A review, Waste Manag. (2020). https://doi.org/10.1016/j.wasman.2019.12.003.
[631] H. Wu, X. Che, Z. Ding, X. Hu, A.E. Creamer, H. Chen, B. Gao, Release of soluble elements from biochars derived from various biomass feedstocks, Environ. Sci. Pollut. Res. (2016). https://doi.org/10.1007/s11356-015-5451-1.
[632] P.R. Yaashikaa, P. Senthil Kumar, S.J. Varjani, A. Saravanan, Advances in production and application of biochar from lignocellulosic feedstocks for remediation of environmental pollutants, Bioresour. Technol. (2019). https://doi.org/10.1016/j.biortech.2019.122030.
[633] S. Papari, K. Hawboldt, A review on the pyrolysis of woody biomass to bio-oil: Focus on kinetic models, Renew. Sustain. Energy Rev. (2015). https://doi.org/10.1016/j.rser.2015.07.191.
[634] G. Chang, Y. Huang, J. Xie, H. Yang, H. Liu, X. Yin, C. Wu, The lignin pyrolysis composition and pyrolysis products of palm kernel shell, wheat straw, and pine sawdust, Energy Convers. Manag. (2016). https://doi.org/10.1016/j.enconman.2016.07.038.
[635] Y. Lee, J. Park, C. Ryu, K.S. Gang, W. Yang, Y.K. Park, J. Jung, S. Hyun, Comparison of biochar properties from biomass residues produced by slow pyrolysis at 500°C, Bioresour. Technol. (2013). https://doi.org/10.1016/j.biortech.2013.08.135.
[636] S. Rangabhashiyam, P. Balasubramanian, The potential of lignocellulosic biomass precursors for biochar production: performance, mechanism and wastewater application-a review., Ind. Crops Prod. 128 (2019) 405–423.
[637] E.G. Pereira, M.A. Martins, R. Pecenka, A. de C.O. Carneiro, Pyrolysis gases burners: Sustainability for integrated production of charcoal, heat and electricity, Renew. Sustain. Energy Rev. (2017). https://doi.org/10.1016/j.rser.2016.11.028.
[638] H. Meng, S. Wang, L. Chen, Z. Wu, J. Zhao, Study on product distributions and char morphology during rapid co-pyrolysis of platanus wood and lignite in a drop tube fixed-bed reactor, Bioresour. Technol. (2016). https://doi.org/10.1016/j.biortech.2016.03.024.
[639] K.L. Yu, B.F. Lau, P.L. Show, H.C. Ong, T.C. Ling, W.H. Chen, E.P. Ng, J.S. Chang, Recent developments on algal biochar production and characterization, Bioresour. Technol. (2017). https://doi.org/10.1016/j.biortech.2017.08.009.
[640] J. Fan, Y. Li, H. Yu, Y. Li, Q. Yuan, H. Xiao, F. Li, B. Pan, Using sewage sludge with high ash content for biochar production and Cu(II) sorption, Sci. Total Environ. (2020). https://doi.org/10.1016/j.scitotenv.2020.136663.
[641] P. Cely, G. Gascó, J. Paz-Ferreiro, A. Méndez, Agronomic properties of biochars from different manure wastes, J. Anal. Appl. Pyrolysis. (2015). https://doi.org/10.1016/j.jaap.2014.11.014.
[642] P. Pariyar, K. Kumari, M.K. Jain, P.S. Jadhao, Evaluation of change in biochar properties derived from different feedstock and pyrolysis temperature for environmental and agricultural application, Sci. Total Environ. (2020) 136433.

[643] H. Cheng, R. Ji, Y. Bian, X. Jiang, Y. Song, From macroalgae to porous graphitized nitrogen-doped biochars – Using aquatic biota to treat polycyclic aromatic hydrocarbons-contaminated water, Bioresour. Technol. (2020). https://doi.org/10.1016/j.biortech.2020.122947.
[644] Z. Wang, L. Han, K. Sun, J. Jin, K.S. Ro, J.A. Libra, X. Liu, B. Xing, Sorption of four hydrophobic organic contaminants by biochars derived from maize straw, wood dust and swine manure at different pyrolytic temperatures, Chemosphere. (2016). https://doi.org/10.1016/j.chemosphere.2015.08.042.
[645] L. Wang, M. Chai, R. Liu, J. Cai, Synergetic effects during co-pyrolysis of biomass and waste tire: A study on product distribution and reaction kinetics, Bioresour. Technol. (2018). https://doi.org/10.1016/j.biortech.2018.07.153.
[646] P. Lu, Q. Huang, A.C. (Thanos) Bourtsalas, Y. Chi, J. Yan, Synergistic effects on char and oil produced by the co-pyrolysis of pine wood, polyethylene and polyvinyl chloride, Fuel. (2018). https://doi.org/10.1016/j.fuel.2018.05.072.
[647] M.J. Ahmed, B.H. Hameed, Insight into the co-pyrolysis of different blended feedstocks to biochar for the adsorption of organic and inorganic pollutants: A review, J. Clean. Prod. (2020). https://doi.org/10.1016/j.jclepro.2020.121762.
[648] Y. Sun, B. Gao, Y. Yao, J. Fang, M. Zhang, Y. Zhou, H. Chen, L. Yang, Effects of feedstock type, production method, and pyrolysis temperature on biochar and hydrochar properties, Chem. Eng. J. (2014). https://doi.org/10.1016/j.cej.2013.10.081.
[649] Y. Wang, Y. Hu, X. Zhao, S. Wang, G. Xing, Comparisons of biochar properties from wood material and crop residues at different temperatures and residence times, Energy and Fuels. (2013). https://doi.org/10.1021/ef400972z.
[650] R. Azargohar, S. Nanda, J.A. Kozinski, A.K. Dalai, R. Sutarto, Effects of temperature on the physicochemical characteristics of fast pyrolysis bio-chars derived from Canadian waste biomass, Fuel. (2014). https://doi.org/10.1016/j.fuel.2014.01.083.
[651] A. Tomczyk, Z. Sokołowska, P. Boguta, Biochar physicochemical properties: pyrolysis temperature and feedstock kind effects, Rev. Environ. Sci. Biotechnol. (2020). https://doi.org/10.1007/s11157-020-09523-3.
[652] A. Shaaban, S.M. Se, M.F. Dimin, J.M. Juoi, M.H. Mohd Husin, N.M.M. Mitan, Influence of heating temperature and holding time on biochars derived from rubber wood sawdust via slow pyrolysis, J. Anal. Appl. Pyrolysis. (2014). https://doi.org/10.1016/j.jaap.2014.01.021.
[653] X. He, Z. Liu, W. Niu, L. Yang, T. Zhou, D. Qin, Z. Niu, Q. Yuan, Effects of pyrolysis temperature on the physicochemical properties of gas and biochar obtained from pyrolysis of crop residues, Energy. (2018). https://doi.org/10.1016/j.energy.2017.11.062.
[654] Z. Ma, Y. Yang, Q. Ma, H. Zhou, X. Luo, X. Liu, S. Wang, Evolution of the chemical composition, functional group, pore structure and crystallographic structure of bio-char from palm kernel shell pyrolysis under different temperatures, J. Anal. Appl. Pyrolysis. (2017). https://doi.org/10.1016/j.jaap.2017.07.015.
[655] C. Wang, Y. Wang, H.M.S.K. Herath, Polycyclic aromatic hydrocarbons (PAHs) in biochar – Their formation, occurrence and analysis: A review, Org.

Geochem. (2017). https://doi.org/10.1016/j.orggeochem.2017.09.001.
[656] J.Y. Kim, S. Oh, Y.K. Park, Overview of biochar production from preservative-treated wood with detailed analysis of biochar characteristics, heavy metals behaviors, and their ecotoxicity, J. Hazard. Mater. (2020). https://doi.org/10.1016/j.jhazmat.2019.121356.
[657] J. Jin, Y. Li, J. Zhang, S. Wu, Y. Cao, P. Liang, J. Zhang, M.H. Wong, M. Wang, S. Shan, P. Christie, Influence of pyrolysis temperature on properties and environmental safety of heavy metals in biochars derived from municipal sewage sludge, J. Hazard. Mater. (2016). https://doi.org/10.1016/j.jhazmat.2016.08.050.
[658] A. Zielińska, P. Oleszczuk, The conversion of sewage sludge into biochar reduces polycyclic aromatic hydrocarbon content and ecotoxicity but increases trace metal content, Biomass and Bioenergy. 75 (2015) 235–244. https://doi.org/10.1016/j.biombioe.2015.02.019.
[659] P. Devi, A.K. Saroha, Effect of pyrolysis temperature on polycyclic aromatic hydrocarbons toxicity and sorption behaviour of biochars prepared by pyrolysis of paper mill effluent treatment plant sludge, Bioresour. Technol. (2015). https://doi.org/10.1016/j.biortech.2015.05.084.
[660] S. Xu, L. Zhang, S. Huang, G. Zeeman, H. Rijnaarts, Y. Liu, Improving the energy efficiency of a pilot-scale UASB-digester for low temperature domestic wastewater treatment, Biochem. Eng. J. (2018). https://doi.org/10.1016/j.bej.2018.04.003.
[661] H. Fu, C. Wei, X. Qu, H. Li, D. Zhu, Strong binding of apolar hydrophobic organic contaminants by dissolved black carbon released from biochar: A mechanism of pseudomicelle partition and environmental implications, Environ. Pollut. (2018). https://doi.org/10.1016/j.envpol.2017.09.053.
[662] K. Zhang, B. Chen, J. Mao, L. Zhu, B. Xing, Water clusters contributed to molecular interactions of ionizable organic pollutants with aromatized biochar via Π-PAHB: Sorption experiments and DFT calculations, Environ. Pollut. (2018). https://doi.org/10.1016/j.envpol.2018.04.083.
[663] X. Tan, Y. Liu, G. Zeng, X. Wang, X. Hu, Y. Gu, Z. Yang, Application of biochar for the removal of pollutants from aqueous solutions, Chemosphere. (2015). https://doi.org/10.1016/j.chemosphere.2014.12.058.
[664] R. Tareq, N. Akter, M.S. Azam, Biochars and biochar composites: Low-cost adsorbents for environmental remediation, in: Biochar from Biomass Waste Fundam. Appl., 2018. https://doi.org/10.1016/B978-0-12-811729-3.00010-8.
[665] X. Zhu, Y. Wang, Y. Zhang, B. Chen, Reduced bioavailability and plant uptake of polycyclic aromatic hydrocarbons from soil slurry amended with biochars pyrolyzed under various temperatures, Environ. Sci. Pollut. Res. (2018). https://doi.org/10.1007/s11356-018-1874-9.
[666] J. Tang, H. Lv, Y. Gong, Y. Huang, Preparation and characterization of a novel graphene/biochar composite for aqueous phenanthrene and mercury removal, Bioresour. Technol. 196 (2015) 355–363.
[667] J.H.F. de Jesus, G. da, E.M.C. Cardoso, A.S. Mangrich, L.P.C. Romão, Evaluation of waste biomasses and their biochars for removal of polycyclic aromatic hydrocarbons, J. Environ. Manage. (2017).

https://doi.org/10.1016/j.jenvman.2017.05.084.
[668] K. Sun, B. Gao, Z. Zhang, G. Zhang, Y. Zhao, B. Xing, Sorption of atrazine and phenanthrene by organic matter fractions in soil and sediment, Environ. Pollut. (2010). https://doi.org/10.1016/j.envpol.2010.08.022.
[669] G. Zhang, Q. Zhang, K. Sun, X. Liu, W. Zheng, Y. Zhao, Sorption of simazine to corn straw biochars prepared at different pyrolytic temperatures, Environ. Pollut. (2011). https://doi.org/10.1016/j.envpol.2011.06.012.
[670] P. Zhang, H. Sun, L. Yu, T. Sun, Adsorption and catalytic hydrolysis of carbaryl and atrazine on pig manure-derived biochars: Impact of structural properties of biochars, J. Hazard. Mater. (2013). https://doi.org/10.1016/j.jhazmat.2012.11.046.
[671] J. Jin, K. Sun, F. Wu, B. Gao, Z. Wang, M. Kang, Y. Bai, Y. Zhao, X. Liu, B. Xing, Single-solute and bi-solute sorption of phenanthrene and dibutyl phthalate by plant- and manure-derived biochars, Sci. Total Environ. (2014). https://doi.org/10.1016/j.scitotenv.2013.12.033.
[672] K. Yang, J. Yang, Y. Jiang, W. Wu, D. Lin, Correlations and adsorption mechanisms of aromatic compounds on a high heat temperature treated bamboo biochar, Environ. Pollut. (2016). https://doi.org/10.1016/j.envpol.2015.12.004.
[673] M. Keiluweit, M. Kleber, Molecular-level interactions in soils and sediments: The role of aromatic π-systems, Environ. Sci. Technol. (2009). https://doi.org/10.1021/es8033044.
[674] Z. Chen, J. Chen, X. Yang, C. Chen, S. Huang, H. Luo, Biochar as An Effective Material on Sediment Remediation for Polycyclic Aromatic Hydrocarbons Contamination, IOP Conf. Ser. Earth Environ. Sci. 281 (2019) 12016. https://doi.org/10.1088/1755-1315/281/1/012016.
[675] X.Y. Cui, F. Jia, Y.X. Chen, J. Gan, Influence of single-walled carbon nanotubes on microbial availability of phenanthrene in sediment, Ecotoxicology. (2011). https://doi.org/10.1007/s10646-011-0684-3.
[676] K.T. Ho, R.M. Burgess, M.C. Pelletier, J.R. Serbst, H. Cook, M.G. Cantwell, S.A. Ryba, M.M. Perron, J. Lebo, J. Huckins, J. Petty, Use of powdered coconut charcoal as a toxicity identification and evaluation manipulation for organic toxicants in marine sediments, Environ. Toxicol. Chem. (2004). https://doi.org/10.1897/03-407.
[677] G. Marchal, K.E.C. Smith, A. Rein, A. Winding, L. Wollensen De Jonge, S. Trapp, U.G. Karlson, Impact of activated carbon, biochar and compost on the desorption and mineralization of phenanthrene in soil, Environ. Pollut. (2013). https://doi.org/10.1016/j.envpol.2013.06.026.
[678] M.K. Männistö, E.S. Melin, J.A. Puhakka, J.F. Ferguson, Biodegradation of PAH mixtures by a marine sediment enrichment, Polycycl. Aromat. Compd. (1996). https://doi.org/10.1080/10406639608544646.
[679] J. Dai, X. Meng, Y. Zhang, Y. Huang, Effects of modification and magnetization of rice straw derived biochar on adsorption of tetracycline from water, Bioresour. Technol. (2020). https://doi.org/10.1016/j.biortech.2020.123455.
[680] J. Ifthikar, T. Wang, A. Khan, A. Jawad, T. Sun, X. Jiao, Z. Chen, J. Wang, Q. Wang, H. Wang, A. Jawad, Highly Efficient Lead Distribution by Magnetic

Sewage Sludge Biochar: Sorption Mechanisms and Bench Applications, Bioresour. Technol. (2017). https://doi.org/10.1016/j.biortech.2017.03.133.
[681] A.M.P. Oen, B. Beckingham, U. Ghosh, M.E. Kruså, R.G. Luthy, T. Hartnik, T. Henriksen, G. Cornelissen, Sorption of organic compounds to fresh and field-aged activated carbons in soils and sediments, Environ. Sci. Technol. (2012). https://doi.org/10.1021/es202814e.
[682] A. Balati, A. Shahbazi, M.M. Amini, S.H. Hashemi, Adsorption of polycyclic aromatic hydrocarbons from wastewater by using silica-based organic–inorganic nanohybrid material, J. Water Reuse Desalin. (2015). https://doi.org/10.2166/wrd.2014.013.
[683] Z. Xi, B. Chen, Removal of polycyclic aromatic hydrocarbons from aqueous solution by raw and modified plant residue materials as biosorbents, J. Environ. Sci. (China). (2014). https://doi.org/10.1016/S1001-0742(13)60501-X.
[684] Y.S. Ho, G. McKay, Sorption of dye from aqueous solution by peat, Chem. Eng. J. (1998). https://doi.org/10.1016/S1385-8947(98)00076-X.
[685] M.D. Johnson, T.M. Keinath, W.J. Weber, A Distributed Reactivity Model for Sorption by Soils and Sediments. 14. Characterization and Modeling of Phenanthrene Desorption Rates, Environ. Sci. Technol. 35 (2001) 1688–1695. https://doi.org/10.1021/es001391k.
[686] B.H. Hameed, A.T.M. Din, A.L. Ahmad, Adsorption of methylene blue onto bamboo-based activated carbon: Kinetics and equilibrium studies, J. Hazard. Mater. (2007). https://doi.org/10.1016/j.jhazmat.2006.07.049.
[687] S. Kang, J. Jung, J.K. Choe, Y.S. Ok, Y. Choi, Effect of biochar particle size on hydrophobic organic compound sorption kinetics: Applicability of using representative size, Sci. Total Environ. (2018). https://doi.org/10.1016/j.scitotenv.2017.11.129.
[688] Z. Wang, J. Zhao, L. Song, H. Mashayekhi, B. Chefetz, B. Xing, Adsorption and desorption of phenanthrene on carbon nanotubes in simulated gastrointestinal fluids, Environ. Sci. Technol. (2011). https://doi.org/10.1021/es200790x.
[689] Y. Fei, K.M.Y. Leung, X. Li, Adsorption and desorption behaviors of selected endocrine disrupting chemicals in simulated gastrointestinal fluids, Mar. Pollut. Bull. 85 (2014) 363–369.
[690] H. Zhang, K. Lin, H. Wang, J. Gan, Effect of Pinus radiata derived biochars on soil sorption and desorption of phenanthrene, Environ. Pollut. 158 (2010) 2821–2825. https://doi.org/10.1016/j.envpol.2010.06.025.
[691] X. Liu, R. Ji, Y. Shi, F. Wang, W. Chen, Release of polycyclic aromatic hydrocarbons from biochar fine particles in simulated lung fluids: Implications for bioavailability and risks of airborne aromatics, Sci. Total Environ. (2019). https://doi.org/10.1016/j.scitotenv.2018.11.294.
[692] K.E.C. Smith, G.J. Oostingh, P. Mayer, Passive dosing for producing defined and constant exposure of hydrophobic organic compounds during in vitro toxicity tests, Chem. Res. Toxicol. (2010). https://doi.org/10.1021/tx900274j.
[693] X. Yang, L. Yu, Z. Chen, M. Xu, Bioavailability of Polycyclic Aromatic Hydrocarbons and their Potential Application in Eco-risk Assessment and Source Apportionment in Urban River Sediment, Sci. Rep. (2016).

https://doi.org/10.1038/srep23134.
[694] X. Xia, X. Chen, X. Zhao, H. Chen, M. Shen, Effects of carbon nanotubes, chars, and ash on bioaccumulation of perfluorochemicals by chironomus plumosus larvae in sediment, Environ. Sci. Technol. (2012). https://doi.org/10.1021/es303024x.
[695] X. Cui, P. Mayer, J. Gan, Methods to assess bioavailability of hydrophobic organic contaminants: Principles, operations, and limitations, Environ. Pollut. (2013). https://doi.org/10.1016/j.envpol.2012.09.013.
[696] F. Verheijen, S. Jeffery, A.C. Bastos, M. Van Der Velde, I. Diafas, Biochar Application to Soils: A Critical Scientific Review of Effects on Soil Properties, Processes and Functions, 2010. https://doi.org/10.2788/472.
[697] P. Oleszczuk, M. Rycaj, J. Lehmann, G. Cornelissen, Influence of activated carbon and biochar on phytotoxicity of air-dried sewage sludges to Lepidium sativum, Ecotoxicol. Environ. Saf. (2012). https://doi.org/10.1016/j.ecoenv.2012.03.015.
[698] Z. Han, B. Sani, J. Akkanen, S. Abel, I. Nybom, H.K. Karapanagioti, D. Werner, A critical evaluation of magnetic activated carbon's potential for the remediation of sediment impacted by polycyclic aromatic hydrocarbons, J. Hazard. Mater. (2015). https://doi.org/10.1016/j.jhazmat.2014.12.030.
[699] K. Sakaya, D.A. Salam, P. Campo, Assessment of crude oil bioremediation potential of seawater and sediments from the shore of Lebanon in laboratory microcosms, Sci. Total Environ. (2019). https://doi.org/10.1016/j.scitotenv.2019.01.025.
[700] F.S. Lang, J. Destain, F. Delvigne, P. Druart, M. Ongena, P. Thonart, Biodegradation of Polycyclic Aromatic Hydrocarbons in Mangrove Sediments Under Different Strategies: Natural Attenuation, Biostimulation, and Bioaugmentation with Rhodococcus erythropolis T902.1, Water. Air. Soil Pollut. (2016). https://doi.org/10.1007/s11270-016-2999-4.
[701] Y. He, J. Chi, Pilot-scale demonstration of phytoremediation of PAH-contaminated sediments by Hydrilla verticillata and Vallisneria spiralis, Environ. Technol. (United Kingdom). (2019). https://doi.org/10.1080/09593330.2017.1398783.
[702] Y. Cao, B. Zhang, Z. Zhu, X. Song, Q. Cai, B. Chen, G. Dong, X. Ye, Microbial eco-physiological strategies for salinity-mediated crude oil biodegradation, Sci. Total Environ. (2020) 138723.
[703] P. Wang, H. Wang, L. Wu, H. Di, Y. He, J. Xu, Influence of black carbon addition on phenanthrene dissipation and microbial community structure in soil, Environ. Pollut. (2012). https://doi.org/10.1016/j.envpol.2011.09.038.
[704] A.H. Rhodes, L.E. McAllister, R. Chen, K.T. Semple, Impact of activated charcoal on the mineralisation of 14C-phenanthrene in soils, Chemosphere. (2010). https://doi.org/10.1016/j.chemosphere.2010.01.032.
[705] P. Wu, Z. Wang, H. Wang, N.S. Bolan, Y. Wang, W. Chen, Visualizing the emerging trends of biochar research and applications in 2019: a scientometric analysis and review, Biochar. (2020). https://doi.org/10.1007/s42773-020-00055-1.
[706] P. Oleszczuk, I. Jośko, M. Kuśmierz, B. Futa, E. Wielgosz, S. Ligeza, J.

Pranagal, Microbiological, biochemical and ecotoxicological evaluation of soils in the area of biochar production in relation to polycyclic aromatic hydrocarbon content, Geoderma. (2014). https://doi.org/10.1016/j.geoderma.2013.08.027.
[707] E.M.L. Janssen, Y. Choi, R.G. Luthy, Assessment of nontoxic, secondary effects of sorbent amendment to sediments on the deposit-feeding organism neanthes arenaceodentata, Environ. Sci. Technol. (2012). https://doi.org/10.1021/es204066g.
[708] X.Y. Lu, B. Li, T. Zhang, H.H.P. Fang, Enhanced anoxic bioremediation of PAHs-contaminated sediment, Bioresour. Technol. (2012). https://doi.org/10.1016/j.biortech.2011.10.011.
[709] M. Xu, Z. He, Q. Zhang, J. Liu, J. Guo, G. Sun, J. Zhou, Responses of Aromatic-Degrading Microbial Communities to Elevated Nitrate in Sediments, Environ. Sci. Technol. (2015). https://doi.org/10.1021/acs.est.5b03442.
[710] B. Louvel, A. Cébron, C. Leyval, Root exudates affect phenanthrene biodegradation, bacterial community and functional gene expression in sand microcosms, Int. Biodeterior. Biodegrad. (2011). https://doi.org/10.1016/j.ibiod.2011.07.003.
[711] J. Heider, G. Fuchs, Microbial anaerobic aromatic metabolism, Anaerobe. (1997). https://doi.org/10.1006/anae.1997.0073.
[712] F. Meng, J. Huang, H. Liu, J. Chi, Remedial effects of Potamogeton crispus L. on PAH-contaminated sediments, Environ. Sci. Pollut. Res. (2015). https://doi.org/10.1007/s11356-015-4280-6.
[713] H. Liu, F. Meng, Y. Tong, J. Chi, Effect of plant density on phytoremediation of polycyclic aromatic hydrocarbons contaminated sediments with Vallisneria spiralis, Ecol. Eng. (2014). https://doi.org/10.1016/j.ecoleng.2014.09.084.
[714] L. Beesley, E. Moreno-Jiménez, J.L. Gomez-Eyles, E. Harris, B. Robinson, T. Sizmur, A review of biochars' potential role in the remediation, revegetation and restoration of contaminated soils, Environ. Pollut. (2011). https://doi.org/10.1016/j.envpol.2011.07.023.
[715] M.I. Rakowska, D. Kupryianchyk, J. Harmsen, T. Grotenhuis, A.A. Koelmans, In situ remediation of contaminated sediments using carbonaceous materials, Environ. Toxicol. Chem. (2012). https://doi.org/10.1002/etc.1763.
[716] E.M.L. Janssen, B.A. Beckingham, Biological responses to activated carbon amendments in sediment remediation, Environ. Sci. Technol. (2013). https://doi.org/10.1021/es401142e.
[717] K. Zhang, J. Mao, B. Chen, Reconsideration of heterostructures of biochars: Morphology, particle size, elemental composition, reactivity and toxicity, Environ. Pollut. (2019). https://doi.org/10.1016/j.envpol.2019.113017.
[718] H. Zheng, X. Liu, G. Liu, X. Luo, F. Li, Z. Wang, Comparison of the ecotoxicological effects of biochar and activated carbon on a marine clam (Meretrix meretrix), J. Clean. Prod. (2018). https://doi.org/10.1016/j.jclepro.2018.01.115.
[719] M.P.R. Lima, A.M.V.M. Soares, S. Loureiro, Combined effects of soil moisture and carbaryl to earthworms and plants: Simulation of flood and drought scenarios, Environ. Pollut. (2011). https://doi.org/10.1016/j.envpol.2011.03.029.

[720] I. Nybom, D. Werner, M.T. Leppänen, G. Siavalas, K. Christanis, H.K. Karapanagioti, J.V.K. Kukkonen, J. Akkanen, Responses of lumbriculus variegatus to activated carbon amendments in uncontaminated sediments, Environ. Sci. Technol. (2012). https://doi.org/10.1021/es303430j.
[721] C. Zhang, B. Shan, S. Jiang, W. Tang, Effects of the pyrolysis temperature on the biotoxicity of Phyllostachys pubescens biochar in the aquatic environment, J. Hazard. Mater. (2019). https://doi.org/10.1016/j.jhazmat.2019.05.010.
[722] O. Malev, M. Contin, S. Licen, P. Barbieri, M. De Nobili, Bioaccumulation of polycyclic aromatic hydrocarbons and survival of earthworms (Eisenia andrei) exposed to biochar amended soils, Environ. Sci. Pollut. Res. (2016). https://doi.org/10.1007/s11356-015-5568-2.
[723] I.M. Voparil, R.M. Burgess, L.M. Mayer, R. Tien, M.G. Cantwell, S.A. Ryba, Digestive bioavailability to a deposit feeder (Arenicola marina) of polycyclic aromatic hydrocarbons associated with anthropogenic particles, in: Environ. Toxicol. Chem., 2004. https://doi.org/10.1897/03-357.
[724] C. Di Dong, C.W. Chen, C.M. Hung, Synthesis of magnetic biochar from bamboo biomass to activate persulfate for the removal of polycyclic aromatic hydrocarbons in marine sediments, Bioresour. Technol. (2017). https://doi.org/10.1016/j.biortech.2017.08.204.
[725] C. Di Dong, Y.C. Lu, J.H. Chang, T.H. Wang, C.W. Chen, C.M. Hung, Enhanced persulfate degradation of PAH-contaminated sediments using magnetic carbon microspheres as the catalyst substrate, Process Saf. Environ. Prot. (2019). https://doi.org/10.1016/j.psep.2019.03.011.
[726] C. Di Dong, C.W. Chen, C.M. Kao, C.C. Chien, C.M. Hung, Wood-biochar-supported magnetite nanoparticles for remediation of PAH-contaminated estuary sediment, Catalysts. (2018). https://doi.org/10.3390/catal8020073.
[727] B. Ranc, P. Faure, V. Croze, M.O. Simonnot, Selection of oxidant doses for in situ chemical oxidation of soils contaminated by polycyclic aromatic hydrocarbons (PAHs): A review, J. Hazard. Mater. (2016). https://doi.org/10.1016/j.jhazmat.2016.03.068.
[728] C. Di Dong, M.L. Tsai, C.W. Chen, C.M. Hung, Remediation and cytotoxicity study of polycyclic aromatic hydrocarbon-contaminated marine sediments using synthesized iron oxide–carbon composite, Environ. Sci. Pollut. Res. (2018). https://doi.org/10.1007/s11356-017-9354-1.
[729] J. Yan, L. Han, W. Gao, S. Xue, M. Chen, Biochar supported nanoscale zerovalent iron composite used as persulfate activator for removing trichloroethylene, Bioresour. Technol. (2015). https://doi.org/10.1016/j.biortech.2014.10.103.
[730] A.L. Teel, M. Ahmad, R.J. Watts, Persulfate activation by naturally occurring trace minerals, J. Hazard. Mater. (2011). https://doi.org/10.1016/j.jhazmat.2011.09.011.
[731] C. Liang, H.W. Su, Identification of sulfate and hydroxyl radicals in thermally activated persulfate, Ind. Eng. Chem. Res. (2009). https://doi.org/10.1021/ie9002848.
[732] Z. Ma, Y. Yang, Y. Jiang, B. Xi, T. Yang, X. Peng, X. Lian, K. Yan, H. Liu, Enhanced degradation of 2,4-dinitrotoluene in groundwater by persulfate

activated using iron–carbon micro-electrolysis, Chem. Eng. J. (2017). https://doi.org/10.1016/j.cej.2016.11.083.
[733] L.W. Matzek, K.E. Carter, Activated persulfate for organic chemical degradation: A review, Chemosphere. (2016). https://doi.org/10.1016/j.chemosphere.2016.02.055.
[734] K. Nam, W. Rodriguez, J.J. Kukor, Enhanced degradation of polycyclic aromatic hydrocarbons by biodegradation combined with a modified Fenton reaction, Chemosphere. (2001). https://doi.org/10.1016/S0045-6535(01)00051-0.
[735] M. Usman, K. Hanna, S. Haderlein, Fenton oxidation to remediate PAHs in contaminated soils: A critical review of major limitations and counter-strategies, Sci. Total Environ. (2016). https://doi.org/10.1016/j.scitotenv.2016.06.135.
[736] N.B. Weston, A.E. Giblin, G.T. Banta, C.S. Hopkinson, J. Tucker, The effects of varying salinity on ammonium exchange in estuarine sediments of the Parker River, Massachusetts, Estuaries and Coasts. (2010). https://doi.org/10.1007/s12237-010-9282-5.
[737] L. Lu, Y. Lin, Q. Chai, S. He, C. Yang, Removal of acenaphthene by biochar and raw biomass with coexisting heavy metal and phenanthrene, Colloids Surfaces A Physicochem. Eng. Asp. (2018). https://doi.org/10.1016/j.colsurfa.2018.08.057.
[738] H. Sun, W. Wu, L. Wang, Phenanthrene partitioning in sediment-surfactant-fresh/saline water systems, Environ. Pollut. (2009). https://doi.org/10.1016/j.envpol.2009.03.012.
[739] G. Abate, J.C. Masini, Influence of pH and ionic strength on removal processes of a sedimentary humic acid in a suspension of vermiculite, Colloids Surfaces A Physicochem. Eng. Asp. (2003). https://doi.org/10.1016/S0927-7757(03)00418-7.
[740] Y. Qian, T. Posch, T.C. Schmidt, Sorption of polycyclic aromatic hydrocarbons (PAHs) on glass surfaces, Chemosphere. (2011). https://doi.org/10.1016/j.chemosphere.2010.11.002.
[741] J. Chen, W. Chen, D. Zhu, Adsorption of nonionic aromatic compounds to single-walled carbon nanotubes: Effects of aqueous solution chemistry, Environ. Sci. Technol. (2008). https://doi.org/10.1021/es801412j.
[742] J. Chen, D. Zhu, C. Sun, Effect of heavy metals on the sorption of hydrophobic organic compounds to wood charcoal, Environ. Sci. Technol. (2007). https://doi.org/10.1021/es062113+.
[743] Z. Han, B. Sani, W. Mrozik, M. Obst, B. Beckingham, H.K. Karapanagioti, D. Werner, Magnetite impregnation effects on the sorbent properties of activated carbons and biochars, Water Res. (2015). https://doi.org/10.1016/j.watres.2014.12.016.
[744] T.J. McGenity, Halophilic Hydrocarbon Degraders, in: Handb. Hydrocarb. Lipid Microbiol., 2010. https://doi.org/10.1007/978-3-540-77587-4_142.
[745] L. Ping, Y. Luo, L. Wu, W. Qian, J. Song, P. Christie, Phenanthrene adsorption by soils treated with humic substances under different pH and temperature conditions, Environ. Geochem. Health. (2006). https://doi.org/10.1007/s10653-

005-9030-0.
[746] D. Caniani, S. Calace, G. Mazzone, M. Caivano, I.M. Mancini, M. Greco, S. Masi, Removal of Hydrocarbons from Contaminated Soils by Using a Thermally Expanded Graphite Sorbent, Bull. Environ. Contam. Toxicol. (2018). https://doi.org/10.1007/s00128-018-2395-4.
[747] X.D. Huang, Y. El-Alawi, D.M. Penrose, B.R. Glick, B.M. Greenberg, A multi-process phytoremediation system for removal of polycyclic aromatic hydrocarbons from contaminated soils, Environ. Pollut. (2004). https://doi.org/10.1016/j.envpol.2003.09.031.
[748] Y. Wu, Y.M. Cho, R.G. Luthy, K. Kim, J. Jung, W.R. Gala, Y. Choi, Assessment of hydrophobic organic contaminant availability in sediments after sorbent amendment and its complete removal, Environ. Pollut. (2017). https://doi.org/10.1016/j.envpol.2017.08.117.
[749] Y. Tao, S. Zhang, Z. Wang, R. Ke, X.Q. Shan, P. Christie, Biomimetic accumulation of PAHs from soils by triolein-embedded cellulose acetate membranes (TECAMs) to estimate their bioavailability, Water Res. (2008). https://doi.org/10.1016/j.watres.2007.08.006.
[750] J.W. Gaskin, R.A. Speir, K. Harris, K.C. Das, R.D. Lee, L.A. Morris, D.S. Fisher, Effect of peanut hull and pine chip biochar on soil nutrients, corn nutrient status, and yield, Agron. J. (2010). https://doi.org/10.2134/agronj2009.0083.
[751] S.E. Hale, J.E. Tomaszewski, R.G. Luthy, D. Werner, Sorption of dichlorodiphenyltrichloroethane (DDT) and its metabolites by activated carbon in clean water and sediment slurries, Water Res. (2009). https://doi.org/10.1016/j.watres.2009.06.031.
[752] L. Leng, H. Huang, H. Li, J. Li, W. Zhou, Biochar stability assessment methods: A review, Sci. Total Environ. (2019). https://doi.org/10.1016/j.scitotenv.2018.07.402.
[753] C.H. Cheng, J. Lehmann, Ageing of black carbon along a temperature gradient, Chemosphere. (2009). https://doi.org/10.1016/j.chemosphere.2009.01.045.
[754] B. Sun, F. Lian, Q. Bao, Z. Liu, Z. Song, L. Zhu, Impact of low molecular weight organic acids (LMWOAs) on biochar micropores and sorption properties for sulfamethoxazole, Environ. Pollut. (2016). https://doi.org/10.1016/j.envpol.2016.04.017.
[755] F. Ding, L. Van Zwieten, W. Zhang, Z. (Han) Weng, S. Shi, J. Wang, J. Meng, A meta-analysis and critical evaluation of influencing factors on soil carbon priming following biochar amendment, J. Soils Sediments. (2018). https://doi.org/10.1007/s11368-017-1899-6.
[756] K. Břendová, J. Száková, M. Lhotka, T. Krulikovská, M. Punčochář, P. Tlustoš, Biochar physicochemical parameters as a result of feedstock material and pyrolysis temperature: predictable for the fate of biochar in soil?, Environ. Geochem. Health. (2017). https://doi.org/10.1007/s10653-017-0004-9.
[757] Z. Liu, F.S. Zhang, J. Wu, Characterization and application of chars produced from pinewood pyrolysis and hydrothermal treatment, Fuel. (2010). https://doi.org/10.1016/j.fuel.2009.08.042.
[758] X. Zhang, P. Zhang, X. Yuan, Y. Li, L. Han, Effect of pyrolysis temperature

and correlation analysis on the yield and physicochemical properties of crop residue biochar, Bioresour. Technol. (2020). https://doi.org/10.1016/j.biortech.2019.122318.
[759] H. Li, R. Qu, C. Li, W. Guo, X. Han, F. He, Y. Ma, B. Xing, Selective removal of polycyclic aromatic hydrocarbons (PAHs) from soil washing effluents using biochars produced at different pyrolytic temperatures, Bioresour. Technol. (2014). https://doi.org/10.1016/j.biortech.2014.04.042.
[760] W. Zheng, M. Guo, T. Chow, D.N. Bennett, N. Rajagopalan, Sorption properties of greenwaste biochar for two triazine pesticides, J. Hazard. Mater. (2010). https://doi.org/10.1016/j.jhazmat.2010.04.103.
[761] U. Ghosh, R.G. Luthy, G. Cornelissen, D. Werner, C.A. Menzie, In-situ sorbent amendments: A new direction in contaminated sediment management, Environ. Sci. Technol. (2011). https://doi.org/10.1021/es102694h.
[762] L. Goswami, N.A. Manikandan, J.C.R. Taube, K. Pakshirajan, G. Pugazhenthi, Novel waste-derived biochar from biomass gasification effluent: preparation, characterization, cost estimation, and application in polycyclic aromatic hydrocarbon biodegradation and lipid accumulation by Rhodococcus opacus, Environ. Sci. Pollut. Res. (2019). https://doi.org/10.1007/s11356-019-05677-y.
[763] D. Mohan, A. Sarswat, Y.S. Ok, C.U. Pittman, Organic and inorganic contaminants removal from water with biochar, a renewable, low cost and sustainable adsorbent - A critical review, Bioresour. Technol. (2014). https://doi.org/10.1016/j.biortech.2014.01.120.
[764] A.P. Philipse, G.H. Koenderink, Sedimentation-diffusion profiles and layered sedimentation of charged colloids at low ionic strength, Adv. Colloid Interface Sci. (2003). https://doi.org/10.1016/S0001-8686(02)00078-7.
[765] Y. Yang, Y. Chun, G. Shang, M. Huang, pH-dependence of pesticide adsorption by wheat-residue-derived black carbon, Langmuir. (2004). https://doi.org/10.1021/la049363t.
[766] Y.W. Choi, K. Kim, J.Y. Kim, Y. Lee, D. Sohn, Adsorption mechanism of a weak polyelectrolyte, PAH, onto carboxylate PS particles, Colloids Surfaces A Physicochem. Eng. Asp. (2008). https://doi.org/10.1016/j.colsurfa.2007.07.002.
[767] W. Zhang, J. Niu, V.L. Morales, X. Chen, A.G. Hay, J. Lehmann, T.S. Steenhuis, Transport and retention of biochar particles in porous media: Effect of pH, ionic strength, and particle size, Ecohydrology. (2010). https://doi.org/10.1002/eco.160.
[768] A.G. Rombolà, D. Fabbri, S. Baronti, F.P. Vaccari, L. Genesio, F. Miglietta, Changes in the pattern of polycyclic aromatic hydrocarbons in soil treated with biochar from a multiyear field experiment, Chemosphere. (2019). https://doi.org/10.1016/j.chemosphere.2018.11.178.
[769] W. Chen, L. Duan, L. Wang, D. Zhu, Adsorption of hydroxyl- and amino-substituted aromatics to carbon nanotubes, Environ. Sci. Technol. (2008). https://doi.org/10.1021/es8013612.
[770] S. Kuppusamy, P. Thavamani, M. Megharaj, Y.B. Lee, R. Naidu, Isolation and characterization of polycyclic aromatic hydrocarbons (PAHs) degrading, pH tolerant, N-fixing and P-solubilizing novel bacteria from manufactured gas

plant (MGP) site soils, Environ. Technol. Innov. (2016). https://doi.org/10.1016/j.eti.2016.04.006.